DEPOSITIONAL PROCESSES OF A PLACER GOLD DEPOSIT, DOMINION CREEK, KLONDIKE, YUKON

By

Tara Michelle Christie

A THESIS SUBMITTED IN PARTIAL FULFILLMENT OF
THE REQUIREMENTS FOR THE DEGREE OF
BACHELOR OF APPLIED SCIENCE

in

GEOLOGICAL ENGINEERING

Department of Earth and Ocean Sciences

We accept this thesis as conforming

to the required standard

.....

.....

.....

.....

THE UNIVERSITY OF BRITISH COLUMBIA
April, 1996

ABSTRACT

Dominion Creek, part of the unglaciated Klondike Goldfield of west-central Yukon, has been placer mined since the gold rush of 1898, but the surficial geology, sedimentology and paleodepositional environment are poorly understood. There is evidence of two major depositional events that formed the White Channel terrace deposits followed by the younger valley-bottom deposits. After the White Channel was deposited, stream rejuvenation up to the time of Reid Glaciation resulted in the deepening of Dominion Creek valley (>30m). Since the more recent McConnell Glaciation the valley has been relatively stable. Recent work focused on field observation and collection of sixteen 160-190 kg samples from the basal units, which were all similar looking massive disorganized quartz gravels, from a 610 meter mine cut face. A long-tom was used to preconcentrate gold thereby reducing nugget effects in the -0.425 mm samples submitted for FA-AAS analysis.

Grain size distributions calculated for -0.053 mm to +200 mm size fractions identified two sediment populations on cumulative probability plots: a matrix infilling (A), and a coarse framework (B). An additional fine sand-silt (C) population was found in nine samples which were designated as trimodal. Sediment and gold correlations (-0.053 mm to 0.150 mm) showed a positive relation between gold and sediment 2-4 size fractions larger, indicating hydraulic and transport equivalence processes were likely involved in the formation of the basal units. Deposition of the basal unit was in high flow aggrading braided streams, with associated mass wasting. The proposed Dominion Creek paleodepositional model is similar to other deposits in the Klondike, with the valley-bottom gravels deposited in Pliocene-Pleistocene interglacial periods. Differences in the correlation matrices and probability plots suggest that units designated as

bimodal and trimodal, despite similarities in appearance and structure, were formed under slightly different depositional regimes.

TABLE OF CONTENTS

LIST OF TABLES

LIST OF FIGURES

LIST OF PLATES

ACKNOWLEDGMENTS

Thanks to my advisor Dr. W.K. Fletcher for all of his advice, patience, and support. Funding for the chemical analyses and for a lab assistant was provided through Dr. Fletcher's research grant. Gimlex Gold Mines also contributed to this project by supplying field assistants, equipment, and freight costs.

I am grateful to my field assistants Terry Henning and Dave McDonald and to my lab assistant Melissa Spencer. Also, a thank-you to Dr. Church for the use of field equipment.

Dr. A.J. Sinclair provided insight into the use and "misuse" of probability plots in analysis of sediments.

Thank-you to Kersti Livingstone for brining me a smile, and diner, when I felt I would never finish and for proof-reading. I am grateful to Rob Steves for fixing my computer problems, helping with making figures and proof-reading.

Finally, I would like to thank my family, especially my parents, Jim and Dagmar Christie. Their love and support has helped me to endure the four long years to finish this degree.

Dedicated with love to Elisabeth Catherine Christie.

1.0 INTRODUCTION

The Klondike District of the west-central Yukon Territory is a well known placer gold camp, where mining has flourished since the gold discovery of 1896, and is still the leading gold producing district in the Yukon. Production in 1995 was 127,333 crude ounces, valued at over $54 million dollars (Burke, 1995), with annual production averaging around 100,000 crude ounces. Although there has been extensive placer mining on the numerous gold bearing creeks of the Klondike, until recently there has been very little sedimentological investigation of the deposits, except for Morison (1985, 1991, 1994). Present day mining continues to provide new exposures of gold bearing gravel and bedrock, and the opportunity to study the depositional environments and the origin of these placer deposits.

The study was designed to examine new exposures, created during 1995, at a placer mine site on the left limit of Dominion Creek about 2 km downstream of the confluence of Gold Run Creek. Dominion Creek was mined by hand during the 1898 Gold Rush, dredged in later years and then reworked with modern mining machinery in the last 15 years. The paystreak occurs in the paleochannel of Dominion Creek, which is in the order of 300 meters wide and 12 - 18 meters below the present surface. The richest deposits occurred in the deepest parts of this channel along the right limit of the valley (right hand side looking downstream, to the northwest), and was the focus of past mining. Current mining is along the left limit (south side) of the paleochannel some 2 meters higher than the deepest part. From drilling results, gold values are known to drop off as bedrock rises in a southerly direction. The present study examined the distribution of gold finer than 0.425 mm in the basal units of the deposit, which are believed to have formed under similar conditions. The paleodepositional environment, and the interrelationships between textural data and gold

concentrations, is also considered. An outline of the methodology, procedures and potential problems with determining the grain size distribution and the gold distribution in a placer gold deposit is discussed. The effectiveness of the long-tom (sluice run) as a preconcentration device and its applicability to sedimentological studies of gold occurrences is also considered.

The aim was to use the sedimentological data and gold grain size distribution to determine the paleodepositional processes, which were active in the formation and concentration of gold in the placer deposit, at the grain scale and apply this to the interpretation of the larger scale placer formation processes and distribution. Understanding the placer forming mechanisms and depositional environments will aid in predicting the gold distribution and potential grades for future lode and placer exploration and mining in the Klondike.

1.1 PROPERTIES OF GOLD

Pure gold has a very high specific gravity of 19.3, but natural gold, due to solid solution with elements such as silver, copper, or mercury, has a specific gravity ranging from 15 to 19. Gold tends to be mechanically dispersed and concentrated from lode sources and residual soils. Placer deposits in streams show a wide range of gold morphologies, due to gold's high ductility and malleability. Typical shapes include flakes, cylinders and dust (flour gold). During transport and concentration, gold tends to be flattened and rounded due to hammering and rolling along the beds, and may be comminuted to very fine particles due to abrasion. Controversy exists as to whether very fine "flour" gold is actually due to

comminution during transport, derivation from epithermal sources of finely disseminated gold or precipitation of gold from solution (Boyle, 1979).

High fineness gold is typically found as rims around placer gold. These rims are not found on relatively young placers suggesting either that this effect is due to post-depositional changes of the gold or removal by abrasion during transport. Proposed rim sources are: the chemical precipitation of aqueous gold onto pre-existing detrital grains or the preferential leaching of Ag from the surface of gold grains due to Ag's greater solubility in aqueous solutions. Post - depositional remobilization of gold occurs because of gold's low solubility in most natural waters. Gold has been found in both soil solutions and stream waters and will preferentially precipitate around a nucleus formed by a pre-existing gold grain (Boyle, 1979). Migration of gold and silver in solution has been documented to be high in areas where humic (organics) substances are high and also has been found to occur in permafrost. Evidence of transport and redeposition of gold in placer deposits due to ground waters is as follows (Boyle, 1979):

1.) Gold and silver are constituents of most natural waters, in high concentrations near primary gold and silver deposits.

2.) The habit of gold nuggets is typically mammillary suggesting chemical accretion.

3) Crystals and crystal faces, and delicate protuberance of gold are common in placers, but typically rare in primary sources and destroyed by hammering and attrition during transport and concentration.

4) Gold nuggets may have a rind of higher purity gold, suggesting chemical accretion of gold or preferential leaching of silver.

5.) Fineness of gold flakes and nuggets tends to increase with distance from the source

1.2 PLACER DEPOSITS

Placer deposits are defined as deposits which have been concentrated by a mechanical agent including water, wind, and gravity over a period of time. Concentration by fluvial processes have produced the most economically significant placer deposits (Slingerland, 1986). Minerals which form placer deposits have high specific gravity and resistance to weathering; such as gold, diamond, platinum, cassiterite and magnetite. Placer gold is typically found with a suite of heavy, resistant minerals including: magnetite, garnet, scheelite, and barite. Coarse grained gold tends to be found close to the source, with particle size decreasing away from the source. In situ chemical depositional and leaching processes may alter placer deposits during and after deposition (Boyle, 1979).

There are many different types of fluvial depositional environments and processes which can produce concentrations of heavy minerals on a variety of scales. Three scales of placer formation have been identified (Slingerland, 1984): the system scale (10^4m), which refers to regional deposits such as, heads of alluvial fans, exit points of high land rivers onto a plain and regional unconformities; the bar scale (10^2m), which refers to geomorphic landform size deposits such as, heads of mid-channel bars, bedrock riffles, scour holes, concave sides of sharp bends and convex bends of meanders; and the bed scale (10^0m), which refers to deposits in individual bedforms, such as winnowed tops of gravel bars, scoured bases of trough cross-strata sets, dune crests and forset beds, and plane parallel laminae. In order to understand the formation and distribution paleoplacers, the grain and bed scale process which leads to the concentration and deposition of heavy minerals must be discussed and understood.

Heavy minerals, such as gold are selectively sorted at the grain scale by size and density. Due to their high densities, they are often concentrated in the beds of streams by fluvial processes. Most commonly the greatest concentrations are found in the lower part of the alluvial section and in cracks and depressions on the bedrock surface. Gold may be concentrated at other sites in a stream such as on the lee side of boulders or islands, on meander bends, at the heads of point and channel bars, and areas where turbulence prevents low density particles from being deposited, while selectively depositing gold particles. (Similarly, gold is concentrated due to turbulent flow and the creation of vortices over the bed of a sluice box). Turbulence may be created at stream and alluvial fan junctions, or when the stream is forced against a bank or around an obstruction. Important local variables controlling sediment movement and deposition in a stream bed are: the settling velocity distribution of the local populations of heavy and light minerals, the long-term flow hydraulics and energy of the site, the average roughness size of the bed, and the volume of material processed through time (Slingerland, 1984). Four hydraulic mechanisms for sorting are: settling (hydraulic equivalence), entrainment and transport by flowing water, shear or dispersive sorting and interstitial trapping (Slingerland, 1984).

Settling of grains is a function of their shape, size, and density. Stoke's Law can be used to determine terminal settling velocity and to predict that small (small surface area) high density particles would settle in the same environment as large less dense particles. The concept of hydraulic equivalence, or particles with the same settling behavior in a hydraulic regime, is based on calculations of settling-velocity from theoretical formulae, such as, Stokes Law and from empirically derived formulae from settling tube-data (Reid and Frostick, 1985). Figure 1.1a shows particles of different density which would settle with the

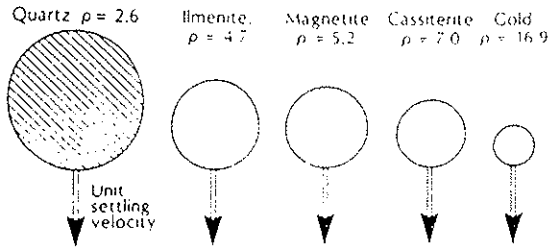

Figure 1.1a

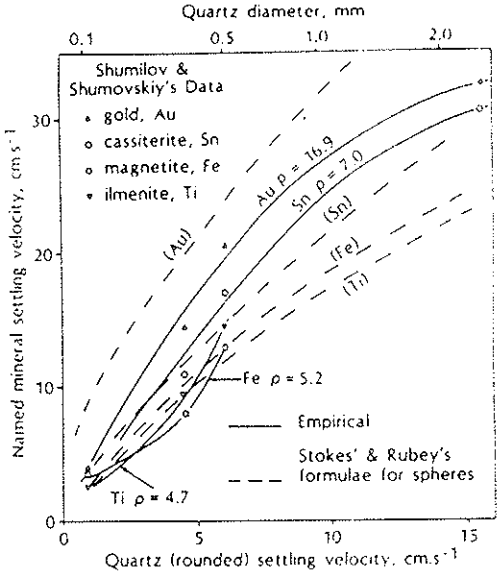

Figure 1.1b

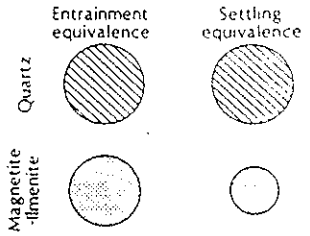

Figure 1.1c

Figure 1.1 Hydraulic and Settling Equivalents
a) Spheres of selected minerals (densities shown) that have the hydraulic or settling equivalence of a quartz particle.
b) Comparison of empirical settling velocities for natural placer minerals and derived settling velocities from Stokes' and Rubey's equations.
c) Comparison of relative size of particles demonstrating settling and entrainment equivalence
(From Reid and Frostick, 1985)

same unit settling velocity (under controlled conditions). Similarly, Figure 1.1b shows comparisons of empirical and theoretical predictions of settling velocity for various minerals.

Entrainment occurs when the forces which tend to hold a particle to the stream bed are overcome by the forces tending to incorporate it into the stream flow. Particles of low density, and high surface area are selectively winnowed, leaving a denser lag (Slingerland, 1986). Under a given flow, heavy minerals will have a lower probability of being entrained, while particles with a high surface area, which protrude into the stream flow will preferentially become entrained. This mechanism separates grains into distinct populations by size, shape and density due to differential pick-up off a bed; however, particles which settled together on a stream bed will not necessarily be entrained together. A comparison of particles with entrainment equivalence and those with settling equivalence is shown in Figure 1.1c. Important variables determining the probability of entrainment of a particle are density, friction velocity U^*, grain diameter d, grain density p, and bottom roughness k (Reid and Frostick, 1985). Bed roughness is defined as the sediment size at which 65 percent of the bed material is finer, by mass. Entrainment is most effective for particles slightly larger than the bed roughness, k, where frictional resistance is minimal. Frictional resistance is greater for particles less than k and also increases for particles larger than the size of minimal frictional resistance to entrainment.Entrainment of particles which are trapped, deposited, on the bed may be prevented by larger clasts hidding smaller clasts. Particles of a diameter one quarter to one third of the median size of the bed may be fully hidden and proctected from entrainment.

In interstitial trapping small dense particles are deposited between larger clasts where they are protected from entrainment in the stream flow. This mechanism is most effective in concentrating heavy minerals during high flow (flood) events when abnormally high flow rates remobilize the large clasts in the stream bed, and small dense particles in the bed. The coarse material forms a frame work and fine matrix material, including small particles of heavy minerals, then filters into the voids between the large clasts. (Reid and Frostick, 1985).

In dispersive or shear sorting, grains in a concentrated granular dispersion are separated by size and density into different horizons. Grain collisions result in dispersive pressures proportional to particle size and density, which force larger or denser grains upwards towards a free surface (Slingerland, 1984). If two grains (x and y) of different density come to rest in the same horizon, then the ratio of size to density of the two particles will be given by (Slingerland, 1984; after Sallenger 1979):

$$D_x/D_y = (\rho_y/\rho_x)^{\frac{1}{2}}$$

Dispersive sorting also includes the process of kinetic sieving where smaller or denser particles fall between larger grains, resulting in a coarse lag of low density particles at the surface. The large particles at the surface protrude into the stream flow and have a greater probability of becoming entrained and removed from the bed (Slingerland, 1984).

Formation of placer deposits probably involves all of the above mechanisms and processes interacting in varying degrees, with each other in a very dynamic alluvial environment. In order to understand how natural deposits are formed, the interaction between these processes and the resultant particle motion on the stream bed, with different sediment sources and flow conditions, must be quantified. An attempt at this is to define the concept of virtual velocity.

The virtual velocity of a particle is the average net transport velocity of a particle, which is a function of the frequency of entrainment, average velocity while in motion and the settling velocity. Density, shape and size will affect the virtual velocity by changing the entrainment and settling velocities of particles. Virtual velocity will also be affected by change in flow conditions, which changes the frequency of entrainment, the average velocity in motion and the settling of particles (Fletcher, 1991).

Recently, the concept of transport equivalence has been developed as an improved explanation of the natural size and density distributions found in stream beds. Particles with transport equivalence will travel with the same average net transport velocity, despite differences in particle size, density and flow conditions Transport equivalent particles will be found in the same relative concentration (constant ratio), despite changes in sediments and flow conditions over time, as long as, virtual velocities remain the same. (Fletcher, 1991) Transport equivalence might be used in modelling "spatial and temporal evolution of placer deposit" by quantifying the relative importance of settling and entrainment for light and heavy minerals (Fletcher, 1991). Calculations to determine the transport equivalence involve calculating the coefficient of variation (See statistical review in Appendix I for calculation of coefficient of variation, CV) for the concentration of each size fraction of gold in each sediment size fraction. The minimum CV for a gold size fraction over all the sediment size fractions is considered to represent the sediment particle which has the most nearly constant relative rate of transport, or its transport equivalent, with the gold particle.

Gold deposits may be formed from complex cycles of transportation, deposition and weathering of pre-existing gold deposits. Interpretation of polycyclic placer deposits may be

difficult, particularly if a deposit contains gold from several sources and there is no field evidence of earlier deposits. An example may be a deposit with locally derived, monocyclic gold, and paleoplacer derived, polycyclic gold. Polycyclic deposits are difficult to interpret due to: an apparent absence of hydrodynamic equilibrium, immaturity of the placer, the presence of a wide variety of gold morphologies and/or chemical or hydrothermal activity producing new gold grains or coatings on particles(Giusti, 1986).

1.3 SAMPLING PROBLEMS

Sampling for minerals, such as gold, diamond and cassiterite, which tend to occur as rare grains, must be done in such a way that representative subsamples are obtained for analysis. Gold has unique properties which may make sampling difficult. There are two areas of concern that need to be addressed with respect to potential sampling problems.

1. Gold occurs as rare discrete particles and therefore particle size and concentration are critical factors in designing sampling programs to ensure samples contain sufficient numbers of gold particles to be representative of the material being sampled.
2. Mechanical concentration of gold, while reducing rare grain effects, will result in some losses and errors in data. In addition to mechanical losses, gold may also be lost in processing due to the hydrophobicity of gold and the inability of processing techniques to adequately separate gold particles from clays and clasts to which they adhere.

These two principle sources of errors associated with sampling for gold will be discussed in further detail below. However, first the general statistical distribution for sampling rare grains must be considered.

1.3.1 Statistical Sampling Distributions

The distribution of very rare grains in a soil, sediment or rock sample can be described by the Poisson Distribution. The definition of the Poisson Distribution is:

$$P(n) = \mu^n e^{-\mu}/n!$$

Where P(n) is the probability of n particles in the sample and μ is the expected number (or mean) of particles in the population. As n becomes large and p becomes very small the Poisson Distribution approaches the Binomial distribution; therefore, the Poisson Distribution can be used to describe low probability events of the binomial distribution (Koch and Link, 1970).

Results obtained in a geochemical survey for a mineral which occurs as rare grains will be dependent on both the size of analytical subsample, as well as, the size of particles (size fraction) in the sample analyzed. The number of particles of gold in the subsample is a function of both of these factors. The size of the subsample governs the probability of a particle occurring in the subsample (i.e. the rare grain effect), while the size of particles in the sample analyzed governs the number of particles present in a sample for a given concentration and weight of gold.

1.3.2 Rare Grain (Nugget) Effects

The results of geochemical analysis for elements which occur as rare grains are often erratic and are irreproducible, due to the low abundance and mode of occurrence. The number of rare grains present in a sample may be insufficient to give representative analytical results. A sample which is too small to contain a statistically representative number of rare grains may result in non-reproducible results and the concentrations of gold reported may be either anomalously high or low. If a large number of samples is taken, a majority of samples will contain too few rare grains and will yield values less than the true concentration, while a small percentage of the samples yield anomalously high values. Elevated gold values, due to the random inclusion of a single gold particle within a sample is called the "nugget effect (Ingamells, 1981).

The nugget effect can be demonstrated with an example. Consider 300 gram samples with an initial average concentration of 500 ppb Au. The 300 gram sample then contains 150 μg of gold, which if assumed to be spheres of pure gold (ρ=19.3 g/cm^3) of radius 150 μm, then the sample contains on average 2.12 particles of mass 70.7 μg. The 30 gram sample taken as an analytical portion then will contain an average of 0.212 particles of gold. Using the Poisson Distribution, the probability that a sample will contain zero particles of gold is p(0)=0.912 or 91.2 % of the samples will have zero particles of gold. In 8.8 % of the samples the subsample contains one particle of gold resulting in an anomalously high gold concentration of 2360 ppb, which is almost 5 times higher than the actual average gold concentration.

Errors associated with sampling populations which can be modelled with the Poisson Distribution can be estimated to be $\pm 100/\sqrt{n}$, where n is the number of or particles in the sample. At low numbers of particles in a sample, less than 20 particles, the error bounds on the Poisson Distribution become asymmetric and calculations become more complicated (Zarr, 1984). The asymmetric Poisson Distribution will be discussed in Chapter 5, in determining the error bounds on the results of gold analyses.

1.3.3 Effects of Size Fraction Analyzed

The size fraction analyzed, or the grain size distribution in the sample, also effects the number of particles in a subsample. To illustrate this, consider samples of uniform spheres which contain a fixed mass of gold, but with a different particle diameter in each sample. As the gold particle size increases, there will be fewer gold grains present in the sample. Thus, if the size of gold particles increases, with sample size remaining constant, the Poisson probability of zero particles occurring in the sample increases. Therefore, to obtain representative samples, as the size of gold particles in a sample increases, the size of the subsample analyzed must also increase. In determining the size of subsample to analyze, the critical factor is the number of particles of gold which occur in the sample. Clifton (1969) determined that the minimum sample size for meaningful gold analysis is a sample which contains 20 particles of gold, to yield a precision of ±50% at the 95% confidence level.

1.3.4 Other Physical Sampling Problems

Pure gold, Au, is hydrophobic and is not easily wetted; because of this fine grained gold, particularly flakey, disc-shaped particles, may float in the processing of samples. Natural gold is commonly in solid solution with other, more easily wetted elements such as Ag which decreases gold's susceptibility to flotation.(Note, hereinafter pure gold shall be referred to as Au while gold refers to solid solutions of elemental Au, with other elements such as Ag, Hg, and Cu) However, silver tends to be preferentially leached from the surface of placer gold particles, producing high purity rims around the gold particles. Gold particles coated with a Au-Hg amalgam also tend to be more susceptible to flotation than Au-Ag alloys (Wang and Poling, 1983). The hydrophobicity of gold can cause a problem when using mechanical processes with water to concentrate gold, as visable gold can often be seen floating on the surface of the water. Consequently, finer microscopic particles are also then susceptible to flotation. Impurities in water such as petroleum products (i.e. oil from heavy equipment, hand lotion when panning) introduced in the water increases the susceptibility of flotation of gold particles. This problem is reduced by adding a surface active agent (i.e. detergent) to the water.

Another physical sampling problem with gold particles, is that fine, flakey gold tends to adhere to pebbles and bedrock fracture surfaces. During processing, some types of decomposed bedrock and highly weathered materials, may form sticky clay balls that adhere to rocks and are difficult to break-up. Consequently, fine gold may be not be adequately represented in processed samples. Also, any preconcentration technique will inherently result in the loss of some gold due to mechanical sampling and processing errors.

1.4 OBJECTIVES OF STUDY

The objectives and rationale for this study are to describe the sedimentology and the relationship between the sediments and the distribution of placer gold in the Dominion Creek deposit. Data compiled from field observations, sediment texture and mineralogy, and gold grain size distribution are used to examine paleodepositional models for the Dominion Creek gold deposit. In addition, data on the recovery of gold using the long-tom will be reported.

CHAPTER 2: DESCRIPTION OF STUDY LOCATION

2.1 LOCATION, ACCESS AND SITE SELECTION

The study area is located in the Central Yukon on the Kondike Plateau, 1:50000, Granville map sheet , NTS 115-O-10, at latitude 63°42' N and longitude 138°43' W, bounded by the Dawson Range to the South and the Tintina Trench and Ogilive Mountains to the North. (Figure 2.1) The site is in the southeastern part of a district referred to as the Klondike Goldfield, which lies between the Indian River and Klondike River Drainage Basins. The site is accessible from Dawson City by 70 kilometers of good gravel road, and driving time is approximately 1.5 hours.

2.2 REGIONAL GEOLOGY

The Yukon is comprised of the ancient North American Margin on to which more than fifty exotic terranes were accreted during the Mesozoic. (Figure 2.2). A major Tertiary dextral strike slip fault , the Tintina Fault, trends to the Northwest and has accommodated approximately 450 km of movement (Templeman-Kluit, 1981). Active since mid-Cretaceous, the Tintina Fault is recognized as the Northwestern extension of the Rocky Mountain Trench (Gabrielse, 1991) and is one of two major strike slip fault systems in the Yukon. The Klondike Plateau is underlain by the Yukon Cataclastic Complex, an accreted terrane of the North American Craton. The study area is primarily underlain by Pericratonic Terranes -

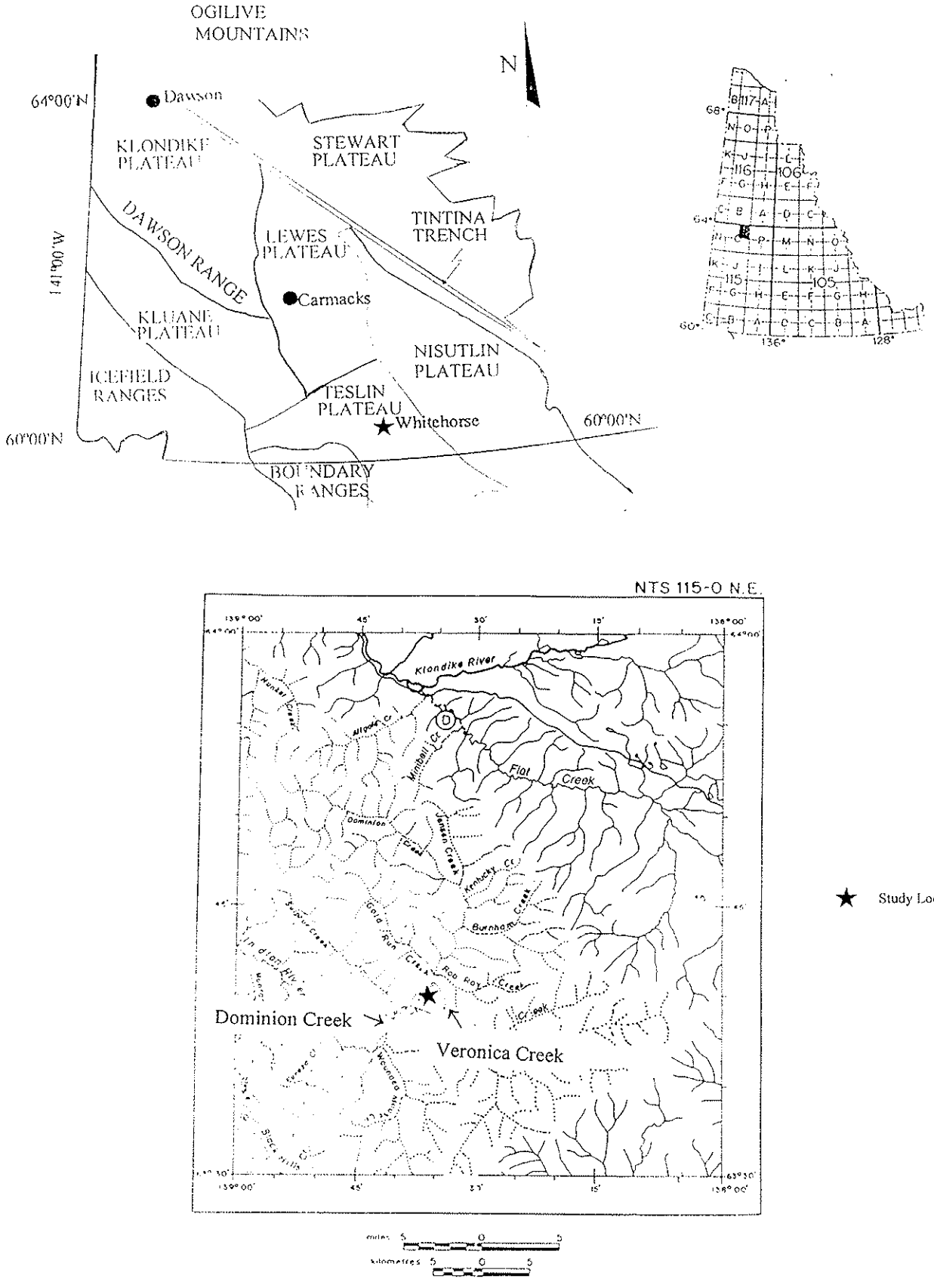

Figure 2.1 Study location map, Dominion Creek, Yukon
(From Yukon Placer Authorization, 1992 and LeBarge, 1995)

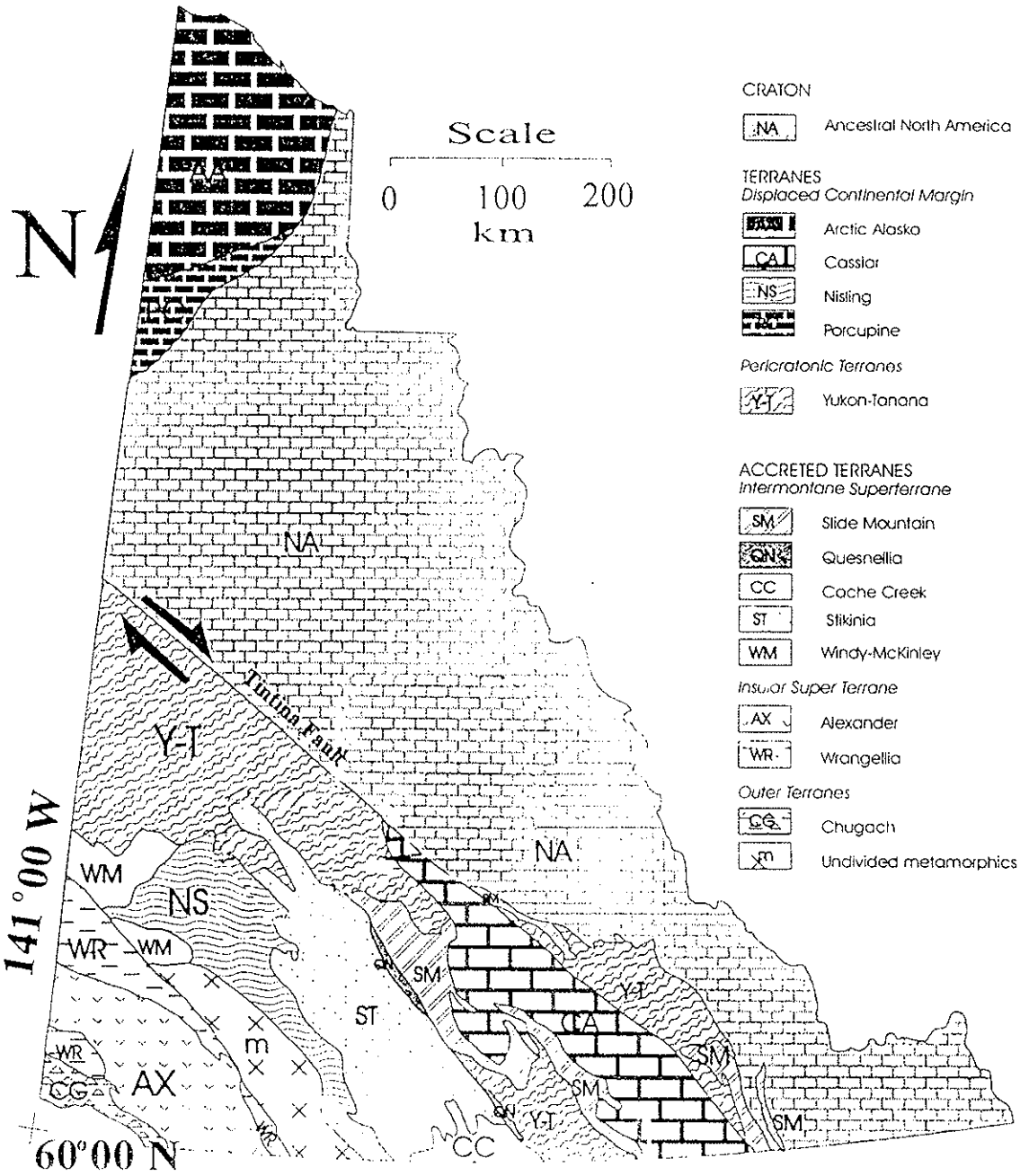

Figure 2.2 Yukon Tectonic Assemblages
(From LeBarge, 1995, after Wheeler and McFeely, 1991)

Yukon-Tanana (LeBarge, 1995), which is composed of schistose metamorphic rocks, greenstones and ultramaific rocks, undeformed intrusive rocks and young volcanic and sedimentary rocks (Knight et. al., 1992). In the Klondike, this terrane is represented by the chloritic and felsic schists collectively referred to as the Klondike schist. Most of the placer deposits within the Yukon are located on rocks of the Yukon Tanana on the Klondike Plateau.

The Klondike Plateau was unaffected by the Pleistocene Cordilleran glaciations (Figure 2.3), but surrounding areas, including the Dawson range, were glaciated. Morison (1985) described the Klondike Plateau as a mature, uplifted Tertiary erosional surface, characterized by dissected, rolling terrain with accordant ridges. Extensive subaerial erosion, with dominant drainage to the southwest, ended in the Miocene, and resulted in a mature subdued landscape. Rejuvenation by differential uplift began in the Pliocene and continued to the Pleistocene. During and prior to differential uplift the White Channel sediments were deposited. Aggredation of White Channel deposition was accelerated by local uplift and ended as pre-Reid glacial activity and deposition of the glaciofluvial Klondike gravels commenced in early Pleistocene.

The pre-Reid glacial activity is given a minimum age of 1.22 Ma by radiometric dating of the Mosquito Creek tephra, which formed after the deposition of the Klondike gravel. Downcutting and incision in the Pleistocene, due to uplift, resulted in the present drainage patterns. Two phases of downcutting and uplift are believed to have occurred: the first resulting in the White Channel deposits preserved as terrace gravel and the second resulting in the present-day valley-bottom stream deposits.

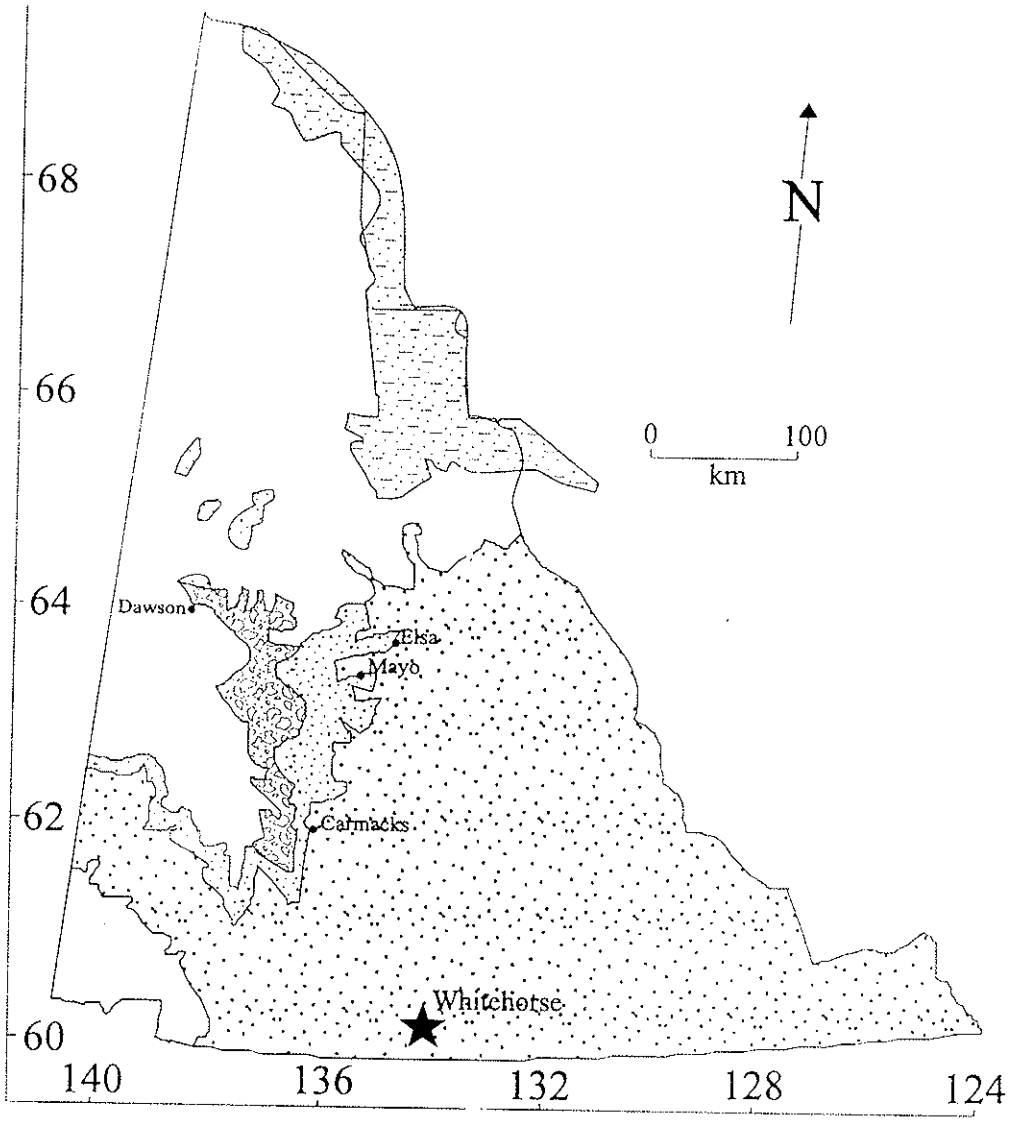

Unglaciated Terrain

Undifferentiated nonglacial deposits

Glaciated Terrain

McConnell glacial deposits

Reid glacial deposits

pre-Reid glacial deposits

Hungry Creek or Buckland glacial deposits

Icefield glaciers

Figure 2.3 Limits of Glacial Activity - Cordilleran Ice Sheet (LeBarge, 1995, after Hughes, 1987).

The earliest geological work in the Dawson Area was by R.G. McConnell (1905, 1907) who described and classified the gold bearing gravels into four categories: White Channel gravel, stream gravel, terrace gravel and high level river gravel (Figure 2.4). Geologic work on the stratigraphy of the White Channel deposit in the Klondike has been undertaken by Naldrett (1981) and Milner (1976) and further sedimentology has been conducted by Morison (1985, 1991). These studies have led to an interpreted paleodepositional environment of the White Channel as a proximal braided environment in a confined upland valley similar to the "scott-type system" (Miall, 1978) The unit is a poorly sorted, massive gravel. White Channel deposits are believed to have been extensive and Morison (1985) has also documented similarities between Klondike White Channel Deposits and easterly deposits at Clear Creek. The high level terraces of Plio-pleistocene White Channel Gravel, were previously divided into 2 distinct units by McConnell (1905, 1907), the white and the yellow units. However, Morison (1985) found no distinct break in sedimentation and concluded that the yellow gravel is the stained equivalent of the white unit. Staining is believed to have been caused by weathering and seepage of meteoric waters. Paleocurrent directions determined by a-axis imbrications plotted on rose diagrams from the White Channel indicate the fluvial system drained to the North. (While this coincides with the direction of many of the other major placer streams, such as Hunker and Bonanza, it is opposite to the present trend of Dominion Creek).

A schematic diagram of Morisons' interpreted paleodepositional environment for the White Channel gravels is shown in Figure 2.5. Morison (1985), has identified 14 lithofacies types in the White Channel gravel deposits which range from laminated silt and clay to massive and disorganized boulder gravel. The deposits are believed to have formed in a glaciofluvial

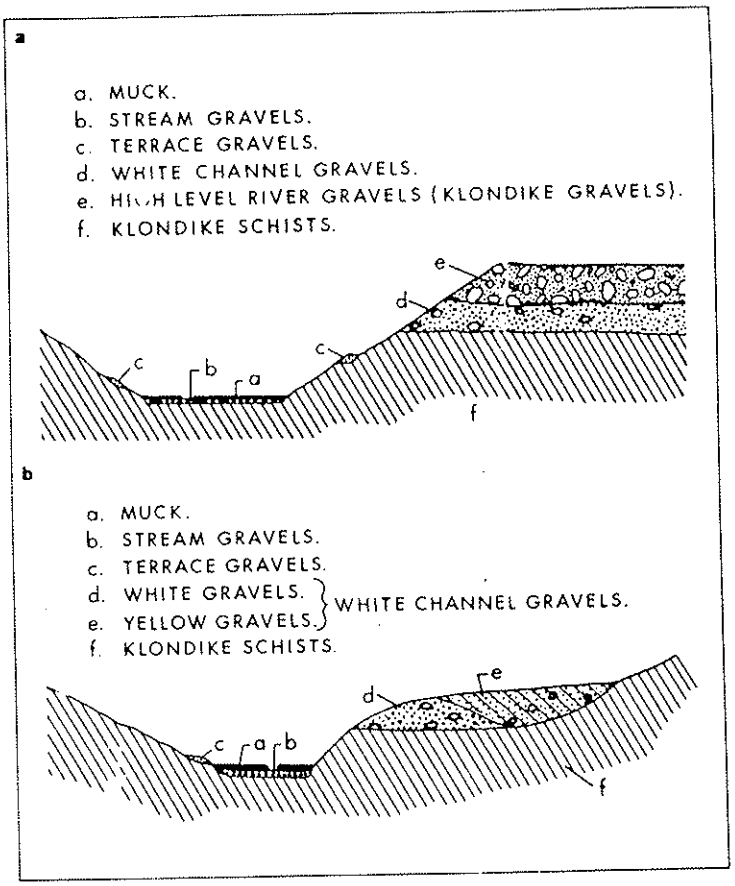

Figure 2.4 Schematic sketch of Pliocene - Recent Stratigraphy in the Klondike Area, Yukon Territory (from McConnell, 1907)

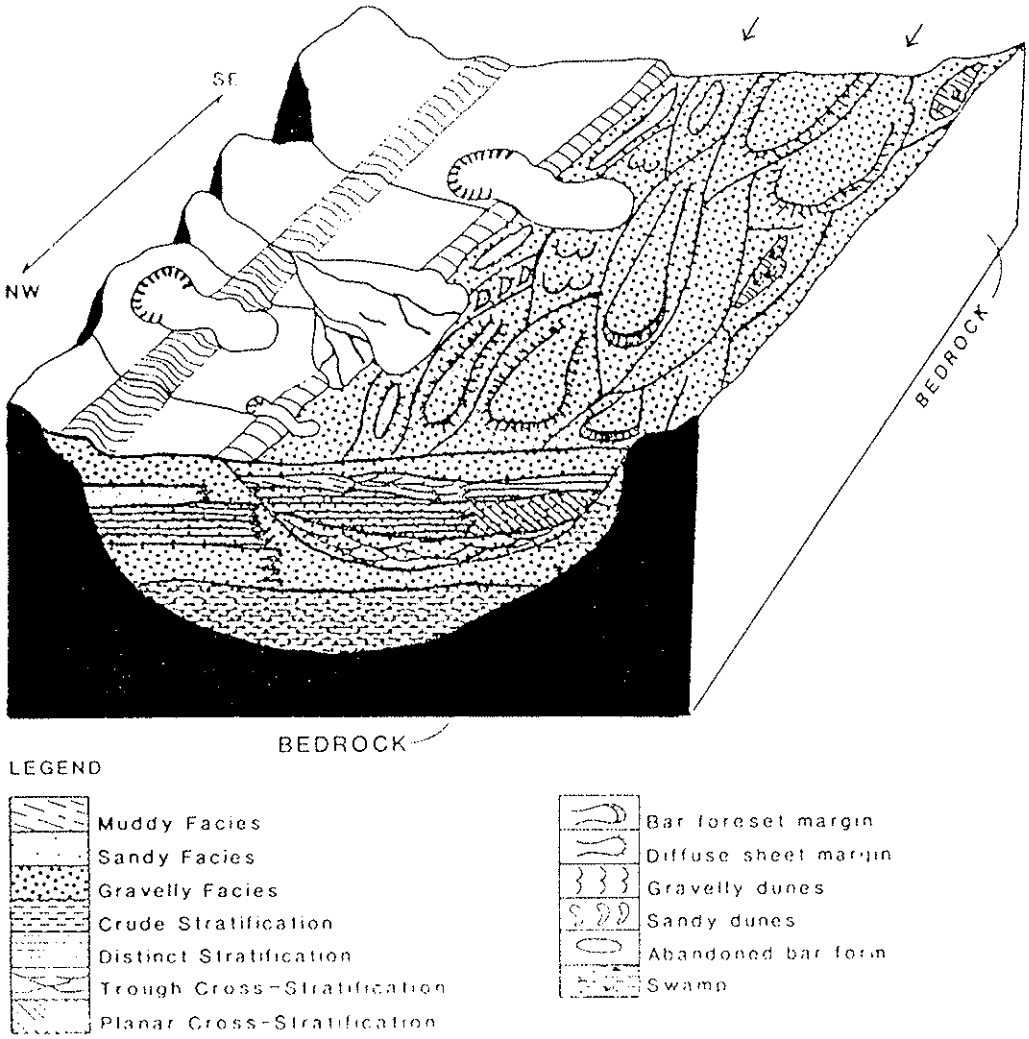

Figure 2.5 Morison's Interpreted Paleoenvironment for the White Channel Deposit in the Klondike Area, Yukon Territory. A gravelly braided river flanked by alluvial fans and slump or slide deposits from colluvial slopes. Note: lower parts of the valley-fill sequence shown in cross section are crudely stratified and massive or disorganized; gravels further upsection show improved sorting, distinct stratification and crossbedding. This reflects an initial stage of infill by a poorly developed braided channel system which, through time, becomes more fully developed into a mature braidplain with many channels, some floored with gravelly dunes, pools, low relief bars, bars with forsets, and interchannel areas with overbank and swamps (from Morison, 1987).

braided river environment which included three components as follows (Morison and Hein, in press):

1. A main valley proximal setting dominated by high discharge or flood channels in a crudely braided system with few main channels.
2. Main valley medial to distal settings which formed well defined braided sequences of channels and low relief unit bars.
3. Valley wall debris flows in association with either tributary alluvial fan sequences or as independent gravity flows.

According to Morison (1985), the proximal main valley settings, with high discharge and flood conditions resulted in very rapid rates of deposition, under highly erosive sediment-laden flows. Large clasts are transported during high flows as bedload and interstices are filled with finer particles when the flood levels wane. Units are clast-supported, matrix in-filled and are characterized by scoured bases due to channelized flows of sediment-laden gravelly flows, which contained large amounts of suspended sediment (possible hyperconcentrated flood flows). In this setting aggradation exceeds progradation and resulting units lack defined bedforms and structures. Medial to distal main valley settings, show channel bedform sedimentation, ripples and trough cross-stratification. Units range from clast supported, matrix-filled gravel to pebbly sands and gravels, and contacts between units are typically flat and slightly scoured. Along the steep sloped valley walls with and near tributary drainages of the main valley, coarse, massive gravelly beds were deposited as sediment gravity flows independent of the main valley setting. Often these debris and sediment-gravity flows are covered with a thin veneer of stratified gravels (to open work gravel) which indicates they may have been accompanied by subsequent alluvial fan

sedimentation or may have slumped into the main valley braidplain for subsequent reworking. Debris flows were initiated by high seasonal flood runoff on unstable weathered slopes with movement downslope, perpendicular to the main valley.

Figure 2.6 shows typical stratigraphic sections from Trail and Lovett Hills, with descriptions of the units. In general, in the lower part of the White Channel deposit the facies tend to be coarse grained, poorly sorted and disorganized with sorting and stratification improving upsection. Thus, the role of fluvial sorting mechanisms improve upsection, and corresponding increases in gold concentration upsection would be expected. However, gold concentrations decrease upsection and the highest concentrations of gold are found in the lower units within a few meters and on bedrock. This indicates that lode/placer sources were available for reworking and erosion in the initial stages of White Channel deposition and as aggregation continued the sources were depleted and corresponding gold concentrations in the deposit decreased (Morison, 1985).

Hydrothermal alteration of White Channel sediments and underlying bedrock was first noted by Templeman-Kluit (1982) and is characterized by the development of secondary clay minerals. This alteration has resulted in clast becoming soft and disintegrating, and sedimentary structures being destroyed or masked (Morison, 1987). On Dago Hill, Morison has identified alteration to a thickness of 20-25 meters and extending 5-10 meters into bedrock. Evidence that this alteration is due to hydrothermal process is cited as the presence of a distinct boundary between overlying sediments and altered sediments, across which crystalline secondary minerals are developed (Morison, 1987). It has also been suggested that hydrothermal gold mineralization may be a factor in addition to placer mineralization (Templeman- Kluit, 1982, Morison, 1987).

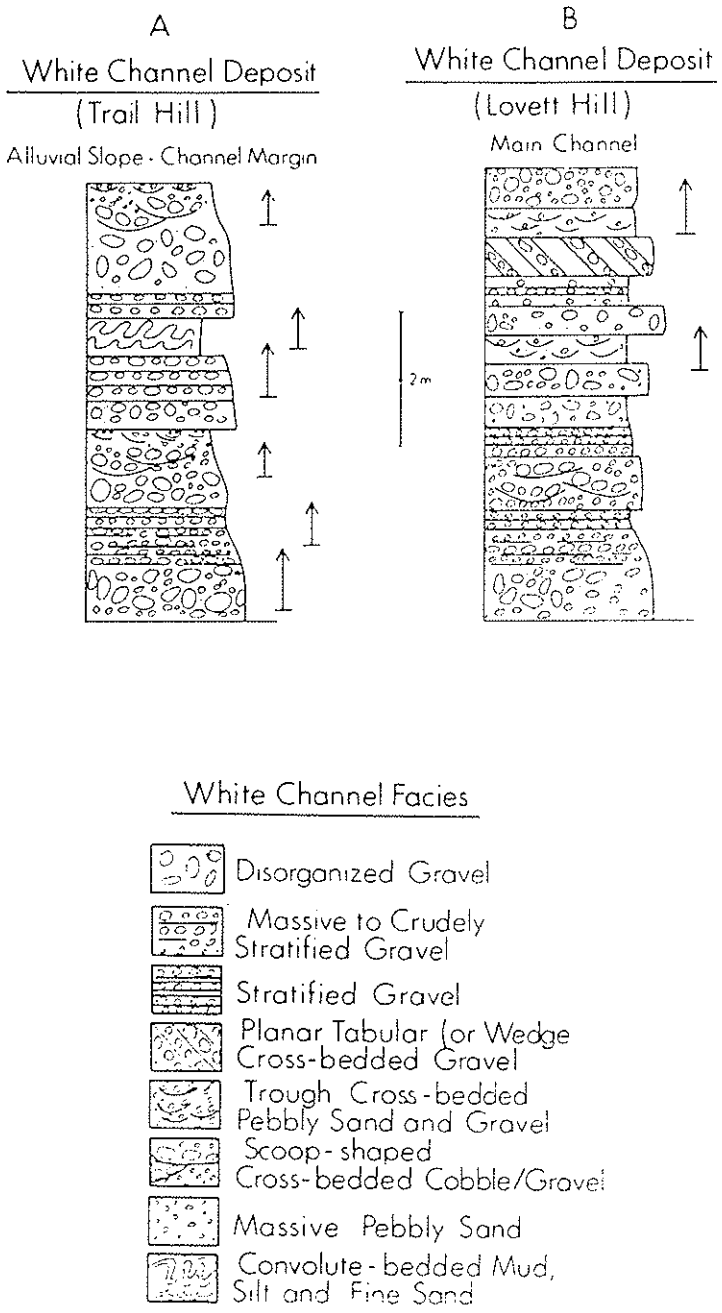

Figure 2.6 Preferred facies trend of the White Channel Gravel at (A) Trail Hill and (B) Lovett Hill. (Morison 1987)

2.3 KLONDIKE PLACER DEPOSITS (SOURCE)

The sources of Klondike placer gold remain unknown, this topic is contentious and highly debated. Extensive exploration for lode sources has identified several small bedrock sources of gold in the Klondike, however, no source of sufficient size to account for the enormous amount of gold recovered has been identified. Potential sources of the Klondike gold have traditionally been hypothesized as one of the following (Knight et. al., 1994):

1.) Undiscovered or completely eroded mesothermal gold-bearing quartz veins within metamorphic rocks

2.) Epithermal gold-bearing veins and alteration zones associated with Eocene quartz-feldspar porphyry bodies.

3.) Gold disseminated in pyritic, felsic schists

4.) Epithermal gold bearing veins and alteration zones within White Channel gravels and underlying bedrock (low temperature)

5.) *in situ* growth of gold in alluvial and/or colluvial deposits (Quaternary)

Knight et. al. (1994) determined that the geochemical signature of most Klondike gold was typical of "mesothermal" vein systems, with the exception of the very low fineness deposits. Epithermal gold is not considered to be a viable source for the placer gold of the Klondike, as the gold from epithermal systems is very fine grained and is not characteristic of the coarse gold which is recovered in the Klondike placer mines (However, current placer mining methods would not likely recover fine grained epithermal gold). Currently there is no evidence to support the growth of gold crystals or precipitation of gold on the rims of pre-

existing gold particles in the "White Channel" sediments. Consequently, Knight et. al., (1994) concluded that most if not all of the Klondike placer gold was derived from mesothermal quartz veins which may have been of considerable vertical extent, which are now either completely eroded or yet undiscovered. The shape and composition of most placer gold in the Klondike is detrital and from low fineness sources. Gold in most creeks has a distinct geochemical signature that allows the point of entry into the stream and links to lode sources to be determined (Knight et. al, 1994). While potential gold-bearing lodes have been identified none of sufficient size to be the source of the large quantity of Klondike gold have been located.

2.4 PERMAFROST

The study area is situated within the discontinuous permafrost zone, with an annual mean daily temperature in the area is -5.5°C (Whal, 1987). Locally, permafrost is known to be present to, at least, depths of 100m. Drill hole data from Keno Hill, in Mayo indicates the thickness of permafrost is 135 m (Brown, 1978). The maximum depth of permafrost in the local area is unknown. Permafrost is defined as ground (soils or rock) which remains at or below 0 degrees C for at least 2 years, and does not depend on the presence or absence of ice. The surface active layer, which thaws each summer, is approximately 0.5 meters thick in the area. The peat and moss, which are characteristic in the valleys of the Klondike, have a very high insulating potential and prevents the formation of a deeper active layer. Where the ground is not covered by organic material the surface active layer tends to be thicker. Also,

the active layer tends to be thinner on the North facing slopes and sides of valleys, than on the opposite slopes, where the active layer may be as deep as 2m.

Ground ice is present in the thick colluvial deposits of silty organic mud characteristic of valley floors in the Klondike as relict (Pleistocene) ice wedges (Naldrett, 1982) and buried snow banks (French and Pollard, 1986). These ice masses have been preserved largely due to the insulating capacity of the thick peat and moss surface layer. Ice wedge casts form at the top of the permafrost boundary and record cyclic freezing and thawing. An ice wedge cast was found 1.5 meters above bedrock in the Dominion Creek pit. In the White Channel sediments ice wedges are found about half way up the section, and record a previous permafrost boundary. Work by Morison (1985), has suggested that this paleo-permafrost level may coincide with climatic cooling at the Pliocene - Pleistocene boundary.

Thermokarst features produced by the melting of ground ice are present in the form of progressive thaw slumps. As ice rich, permafrost sediments and soils are exposed along river banks, or devegetated areas (such as forest fire areas), in the summer months the ice is progressively melted. In steep headwall slopes, the soil may liquefy and flow forming a disorganized deposit. The process continues indefinitely or until an insulating layer covers the face (Burn, 1987).

2.5 LOCAL GEOLOGY OF STUDY AREA

The study area is located on the left limit (south side) of the broad Dominion Creek valley (Figure 2.1) High concentrations of gold are found at the confluence of Dominion with its

right limit tributary, Gold Run and along the right limit of Dominion Creek (Figure 2.1). Both areas have been heavily worked over the last one hundred years. Recently a high grade placer deposit was discovered on Veronica Creek, a small left limit tributary of Dominion directly across from Dominion's Confluence with Gold Run and also gold-bearing quartz gravels were discovered on high terraces of Dominion Creek. Figure 2.7 shows a schematic cross-section of the deposits of the Dominion Valley.

2.5.1 SEDIMENTOLOGY

The site is covered with a frozen organic/moss layer about 2 meters thick lying on 2 -5 meters of dark gray silty mud. Beneath the mud layers 1-2 meters of rusty sand may be present grading downwards to rusty brown pebbly sand or gravel. At a depth of about 8 meters from surface the rusty gravels are underlain by medium to dark gray gravels which contain the bulk of the economic placer deposit. The paystreak occurs in the paleochannel of Dominion Creek, which is in the order of 300 meters wide and 12 - 18 meters below the present surface. The richest deposits occurred in the deepest parts of this channel along the right limit of the valley (right hand side looking downstream, to the Southwest), and was the focus of past mining. Bedrock is at an average depth of 12 meters below the surface, and the upper 0.5 meters of bedrock is also part of the placer deposit. Permafrost extends from surface to an unknown depth.

Gold is know to occur throughout all of the gravel units, with the greatest concentrations being found near bedrock, but with significant amounts in the lower gray gravels 2- 2.5 meters (6-8 feet) above bedrock. Contacts between beds most frequently are scoured, and less commonly are planar or gradational. Organic debris, mud lenses and open work gravel

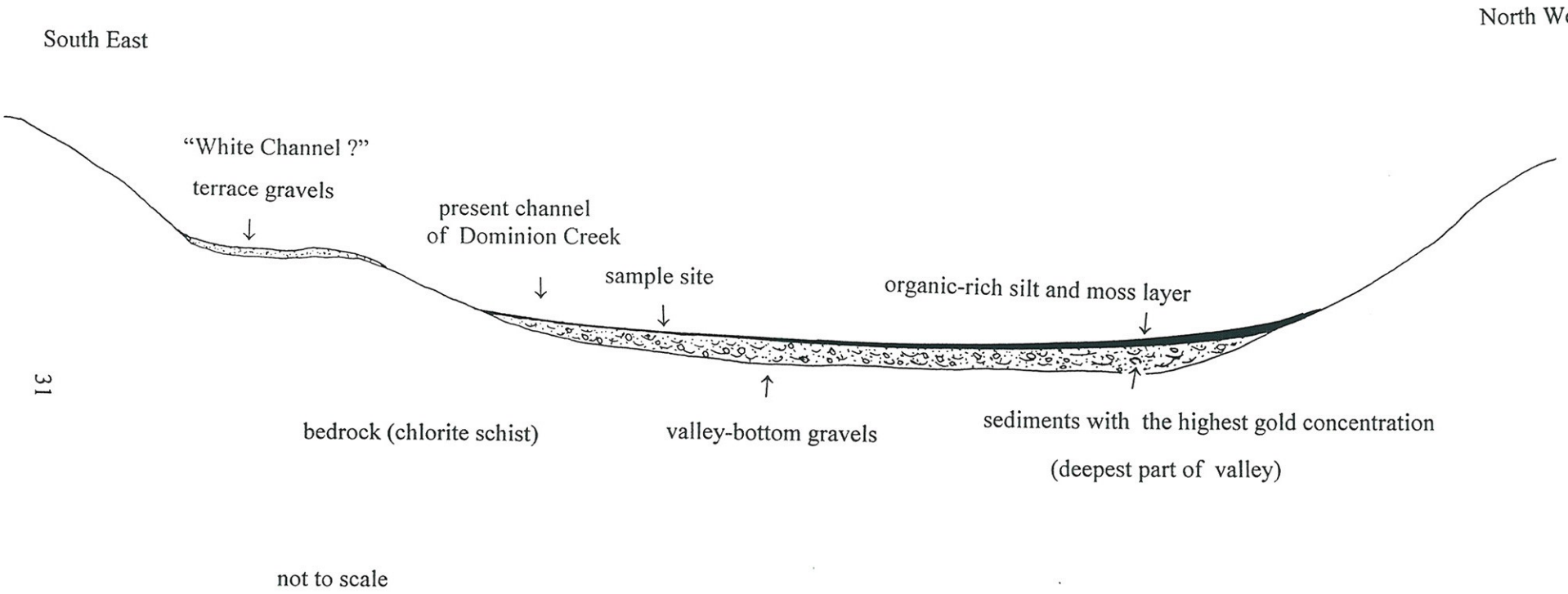

Figure 2.7 Schematic cross-section of the Dominion Creek Valley Deposits. In the valley, the richest deposits occurred in the deepest parts of this channel along the right limit of the valley. Terrace, gold-bearing, quartz gravels are located 30 m (100ft) above the valley floor on the left limit of Dominion Creek. The sample site is located on the left limit of the valley and the present stream course is to the south (into the page).

and sand are interbeded in the deposit. Units in the gray gravel vary from a clast supported matrix filled, slightly imbricated gravel to a disorganized to massive gravel, which contains between 0 - 35 % of angular bedrock and a high content of fine matrix material. The orientation of bedrock clasts is often planar or dipping slightly into the valley. Beds range in thickness from 0.1 m to 0.75 m. A generalized stratigraphic section is depicted in Figure 2.8. Stratigraphic sections cannot be used to connect units between sample locations as the units are not laterally continuous in the cut faces and represent multiple deposition sequences. (The sample locations are presented in Figure 3.2 of the next section.)

The unit sampled is a massive to disorganized pebble-boulder clast supported gravel directly overlying bedrock which varies from 0.3 - 1m thick. (Plate 2.1) Clasts are approximately 80 % rounded to sub-rounded quartz, 10 % sub-angular felsic clasts and varying amounts of angular, friable bedrock. The unit lacks sedimentary structures and often appears disorganized, which made measuring pebble imbrication difficult. A Rose Diagram of the thirty measurements, taken from small gravel lenses and occasional pebble-cobble units, was insufficient to yield a paleocurrent direction and is therefore not presented.

The lack of sedimentary structures typical of fluvial deposits and the planar to slightly inclined (toward the center of the valley) orientation of bedrock clasts indicates that this unit may be a result of mass wasting, potentially in combination with fluvial reworking processes. Units with a high percentage of locally derived bedrock and highly scoured basal contacts, are believed to have been formed by debris flow. The proximity of the site to the valley walls and the potential input from tributary alluvial fans support this hypotheses. Massive units, with lower bedrock contents, and less scoured basal contacts are suspected to have been deposited by the main channel by rapid deposition and aggredation during high

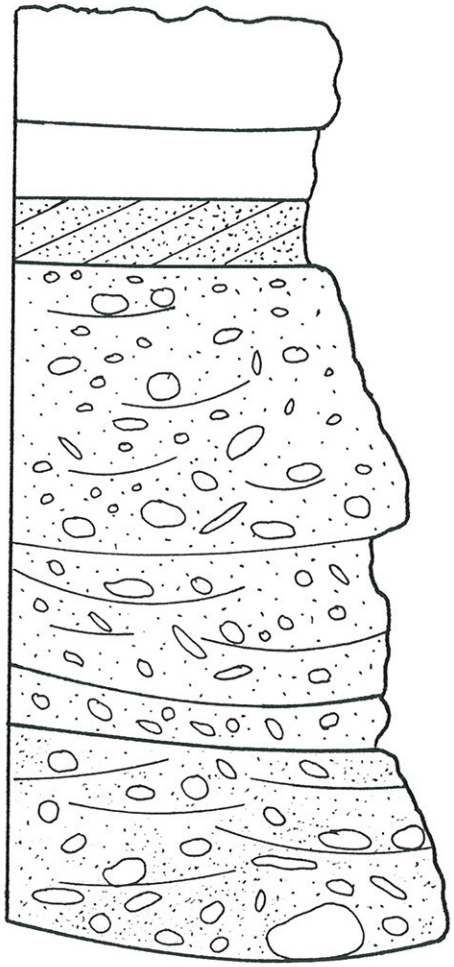

1-2 m Peat, moss and organic rich soil

2 m Dark gray silt

1-2 m Rusty massive to cross bedded sand

5-7 m Rusty, massive to crudely stratified, clast supported, matrix-filled, quartz, pebble-cobble gravel. Beds are 0.1m-0.75 m thick, with small interbedded lenses of openwork pebble-sand and silt. Contacts are gradational to slightly scoured.

3-5 m Gray, massive to disorganized, clast-supported, matrix-filled, quartz gravel with scoured basal contacts between units. Bed are 0.1m -0.5 m thick and the locally derived bedrock content varies from 0-35 %.

Figure 2.8 Generalized stratigraphic section of deposits on the left limit of Dominion Creek

Plate 2.1 Representative photograph of unit sampled from site T-5.

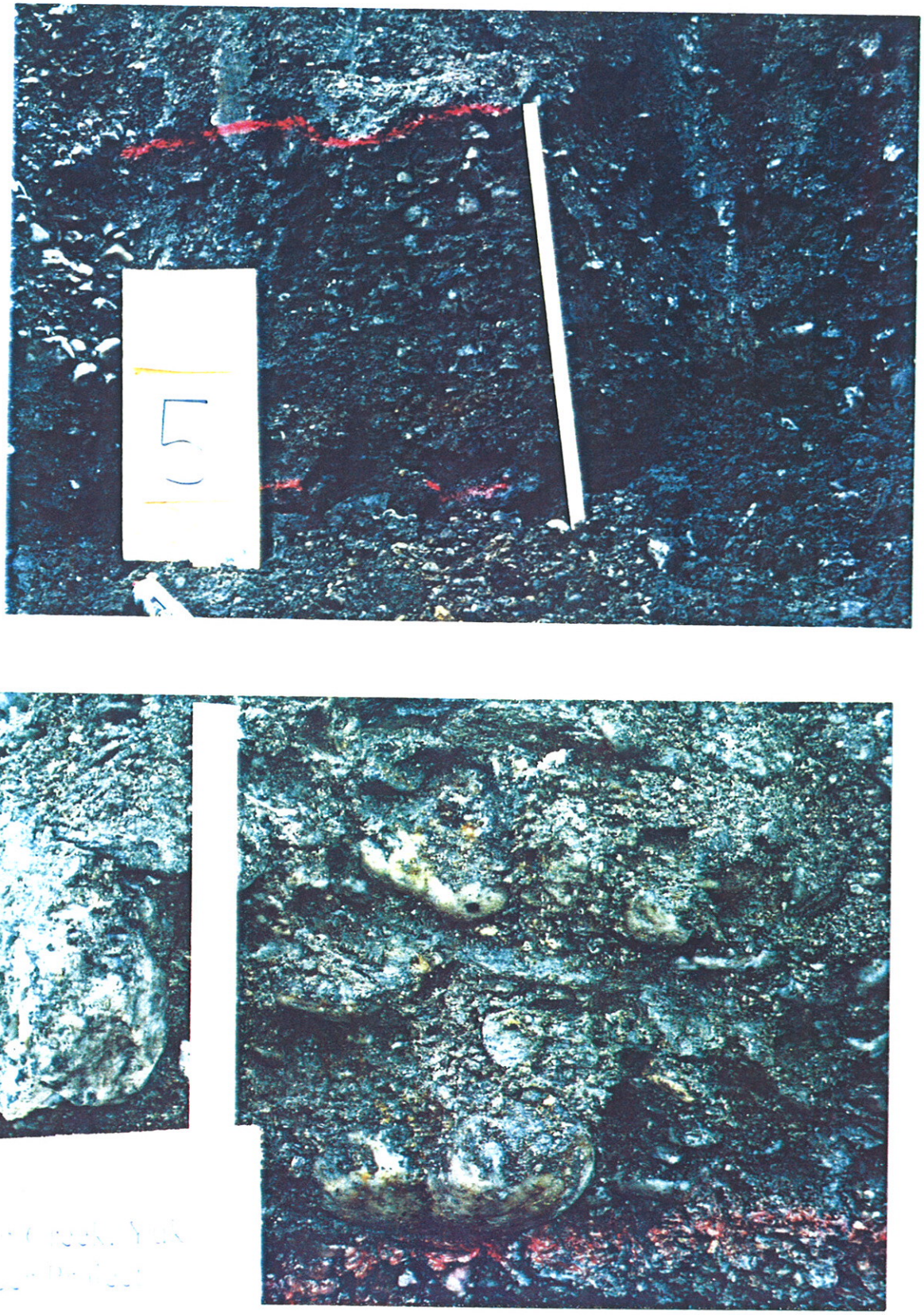

water flows, which accounts for the lack of defined bars, channels and bedding. However, arid environments with seasonal major flood events may also result in the accumulation of sediments with a high percentage of fine matrix material, from mass wasting events. The fine material in these sediments may have been reworked and removed from the deposit due to low water volume and energy throughout the rest of season (Fletcher, per. com.)

The Dominion Creek bench gravels were re-discovered by J.S. Christie in 1993. There are a number of "old timers" shafts in the area. These bench deposits were not part of the current sedimentological study and are included here only on account of being new information pertinent to the interpretation of the surficial geology. About 50 backhoe trenches were examined in 2 separate areas north and south of the Rob Roy Creek, a tributary of Dominion, which has bisected the terrace. The quartz gravels are so much as 11.5 meters thick with the base of the gravels (bedrock surface) about 30 m above the floodplain of Dominion Creek. It is believed that these quartz gravels are remnant at the ancestral bed of Dominion Creek, the remainder of which have been eroded, re-worked and incorporated into the present day valley-bottom deposits of Dominion, which are the focus of current work.

Gravels on the terraces of Dominion Creek grade downwards from mature (clean) to massive and disorganized, quartz gravel. Sediments on the benches are more mature than those sampled from the valley bottom deposits sampled and the content of locally derived bedrock is low (approximately 5 %). Testing has produced only fine grained gold; no coarse nuggets have been recovered. At present gold prices, the deposit is of marginal economic grade to mine. Bedrock clasts are highly weathered in the bench deposits and are obvious in frozen material but disintegrate when thawed. The matrix is also strongly weathered and when sampled and sluiced these materials generate a lot of suspended silt and clay which

turns the sluice water milky. The presence of these highly weathered deposits on dissected terraces 30 m above the valley floor, confirm it is an older unit than the valley bottom deposits. The thickness of the unit indicates that the terrace gravels were extensive at one time and are remnants of the bed of a higher level ancestral Dominion Creek. These high level terrace gravels are postulated to be contemporaneous with or to be White Channel.

2.5.2 BEDROCK GEOLOGY

The area is underlain by friable chlorite, muscovite, and biotite schists which may contain coarse pyrite and garnet porphyroblasts. Foliation in the schist trends approximately 150 °/ 50°W and the gross bedrock slope is at less than 1% to the southwest parallel to the present stream course direction. In the mining pit, the bedrock also rises significantly towards the southeast wall, where the samples were taken, and continues to rise into the adjacent hillslope, at approximately 3 %. This sharp rise in bedrock appears to coincide with the left limit of the paleochannel and is the limit of the economic placer deposit. The bedrock-gravel contact is highly undulatory, with large scour holes up to 0.5 meters deep in some locations. The upper 0.3 meters of bedrock is often highly decomposed to a green-gray, plastic, clay-rich cap. Fresh bedrock during mechanical processing breaks down easily into a range of sizes from: smaller pebble sized fragments to silt size, individual minerals.

Some quartz veining is present in the schist, however, these veins are not gold bearing. Minor supergene enrichment of gold in the schist bedrock appears to have occurred in the area; but, preliminary drilling, sampling and investigation by Christie has indicated that the

zone of enrichment does not extend beyond 2 meters into bedrock. Placer gold is found in bedrock cracks and foliation to depths of approximately 0.5 meters.

Pyrite crystals in the bedrock range from finely disseminated to 2-3 mm. Upstream approximately 1 km, at another mine site, the chlorite schist bedrock contains larger cubic pyrite crystals up to 1 cm in width. Faulting is also evident in this area as there are clear offsets within the schist sequence along well defined gougy fault surfaces. Offset may also be seen between stratigraphic layers in some locations.

2.6 CHARACTER OF GOLD IN THE STUDY AREA

The gold in the study area typically occurs as discrete particles, usually as flakes, rods or cylinders, with 85 % finer than 1.68 mm (passing a ASTM # 12 sieve). Assays on gold bars shipped from the mine average 85% pure gold with silver being the principal impurity. While some gold appears slightly crystalline and has a delicate structure other flakes and scales appear to have been ductily deformed and are folded and hammered. Hammering and abrasion have been found to be the dominant mechanisms in fluvial environments to decrease particle size (removal and breakage), flatten particles and increase roundness. Approximately 5% of Dominion Creek gold is found attached to quartz due to hammering and smearing of gold onto or around quartz grains. Klondike gold characteristically has high fineness rims which have been caused by leaching of Ag, not precipitation of Au (Knight et. al., 1994 Klondike placer gold morphology and fineness have been studied and described by Knight et. al., (1994), to determine a relationship between shape, texture and distance from a

potential lode source for gold the 0.2 to 1.5 mm range. Knight et. al., (1994) concluded that the Dominion Creek system could be treated as a simple system with the lode source at the headwaters of Dominion Creek based on gold compositions studies. However, no major lode source has been identified at the headwaters of Dominion Creek despite extensive trenching, drilling and the excavation of an adit

Heavy minerals associated with gold in the Dominion gravels are garnet, kyanite, pyrite and small amounts of magnetite and zircon. Pyrite cubes derived from the local decomposed bedrock are locally abundant. Approximately 25 % of gold from this mine is coated to some degree with a dark gray, manganese oxide coating, which can be removed with nitric acid.

Gold particles from the Dominion deposit can be described as primarily disc shaped with a small proportion of rod like and spheroid shapes. However, as a portion of this study was to accurately determine numbers of particles of gold and gold concentrations, a means of quantifying the shape of particles was needed. A method of characterizing the shape of particles in calculations is to use Corey Grain Shape factors, which relate the particle shape to a sphere with the sample diameter as the long axis of the gold particle. Twenty particles from the 0.212-0.425 mm size fraction were selected and the 3 axis were measured with a microscope. It is impractical to attempt to measure smaller size fractions with an petrographic microscope and measuring the three axes became impossible below 0.212 mm. The Corey Grain Shape Factor was Calculated using the following formula:

$$\text{Corey Shape Factor} = (\text{Thickness}) / (\text{length} * \text{width})^{1/2}$$

The values obtained were found to vary from a maximum of 0.25 to minimum of 0.12, with a mean value of 0.19. As a small number of particles was measured and the method of measuring was not very accurate, particularly for the thickness of the particles , the values calculated are only an approximation.

Knight et. al., (1994) analyzed gold particles from the Klondike and determined Corey grain shape factors for locations further downstream, on Dominion and Indian River (which Dominion is a tributary) (refer to Figure 2.1). Their samples were taken approximately 5 km below the site sampled in this study, before the confluence of Dominion with its major tributary Sulphur Creek. At this location the Corey grain shape factor was determined to be 0.15 , based on 56 particles between .2 mm and .15 mm, mounted and viewed under a reflected light microscope. A further 5 km downstream below the confluence of Dominion with Australia creek, Wounded Moose and several smaller creeks the stream is known as Indian River. At this site Knight et al. collected 86 particles of the same size fraction and determined a Corey Grain shape factor of .175. These values for grain shape factors are close to the values calculated for the gold in this study. However, as grain size factors generally decrease as particle size increase the assumed CSF for gold finer than .425, is larger than these determined CSF to account for larger grain size. A CSF of 0.20 was adopted for calculations within this study. A visual estimation of a limited number of gold particles confirm that approximately 80 % of gold particles in Dominion creek occur as flakes with the remainder occurring as spheres, rods or irregular shapes including folded and ductily deformed shapes.

Giusuti (1986) found that the average Corey grain shape factor (CSF) of gravity recovered gold increases as the particle size decreases. Gold lost to the tailings givers very low average

shape factors (i.e. high degree of flattening). Thus, the apparent increase in the CSF for the smallest fractions recovered with a mechanical concentration method is likely due to flaky gold particles being more difficult to recover that more spherical ones.

2.7 SUMMARY

The depositional process and environment in which the Dominion Creek gold deposit was formed are poorly understood. Information from mineralogy, sediment texture and gold grain size distribution may be useful, in conjunction with the field observations, in understanding the paleodepositional environment which formed the Dominion Creek gold deposit.

3.0 SAMPLING AND ANALYTICAL METHODS

3.1 INTRODUCTION

The field work for this study was conducted progressively thorough the months of June, July and August, 1995, as mining advanced and new exposures were created. Sixteen 160 -190 kilogram samples were collected along the mine cut face and stratigraphic sections compiled. Samples were concentrated in a long-tom (sluice run) set up at a stable, permanent location where the process could be carried out under controlled conditions. For each sample the long-tom concentrate, a portion of the tailings and a split of the original sample were retained for analysis. Laboratory procedures included wet sieving and fire assay, atomic absorption spectroscopy. Figure 3.1 shows a summary flow chart of sample preparation and analysis.

3.2 FIELD TECHNIQUES

3.2.1 Data Collection and Stratigraphic Sections

Sites to be sampled were carefully selected at regular intervals along a 610 meter long vertical wall running 050° as shown on Figure 3.2. About 130 meters of the total wall length was inaccessible because of waste piles which pre-dated the sampling. Sites were selected so that samples could be taken from a basal gravel unit lying directly on bedrock; that was sufficiently large to sample (over 20 cm thick), contained no interbedded sands, mud or organic debris, appeared uniform and to represent a single phase of deposition (i.e. a single

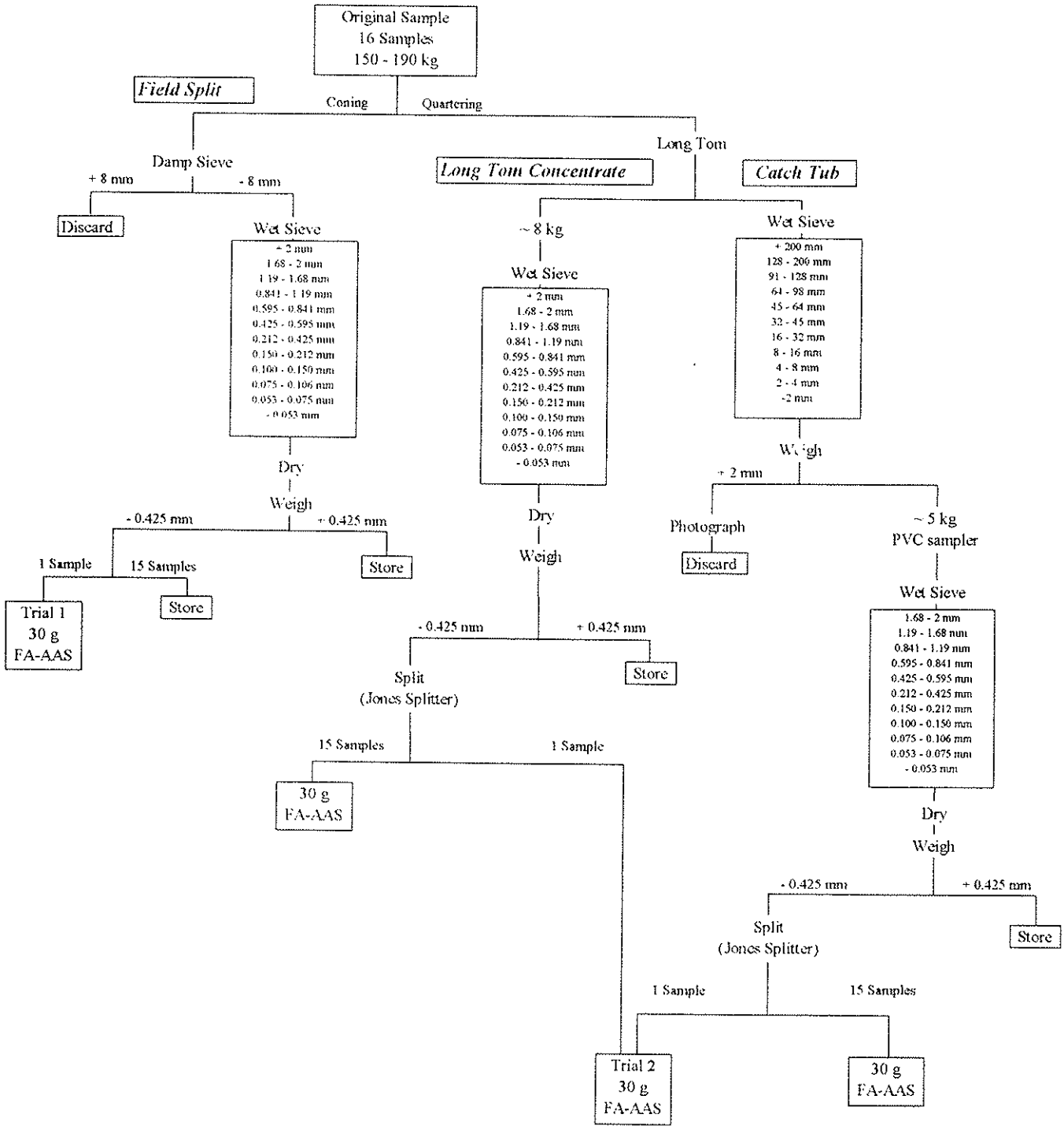

Figure 3.1 Summary Flow Chart for Sample Preparation and Analysis

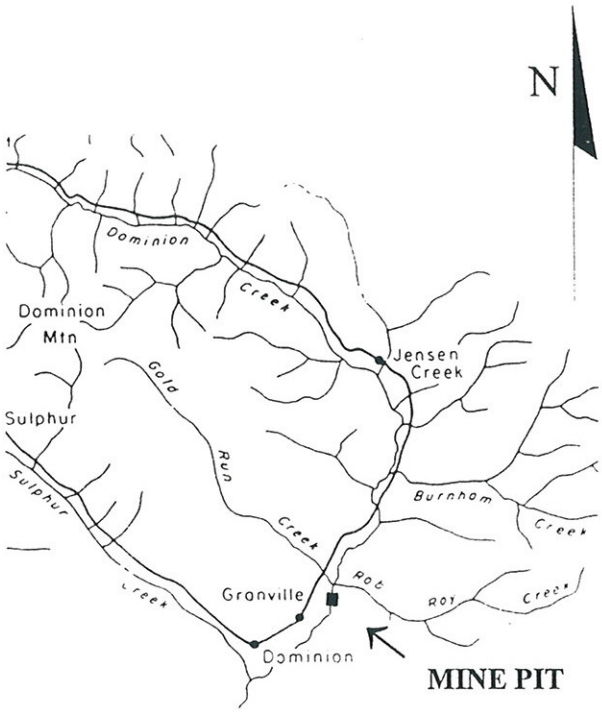

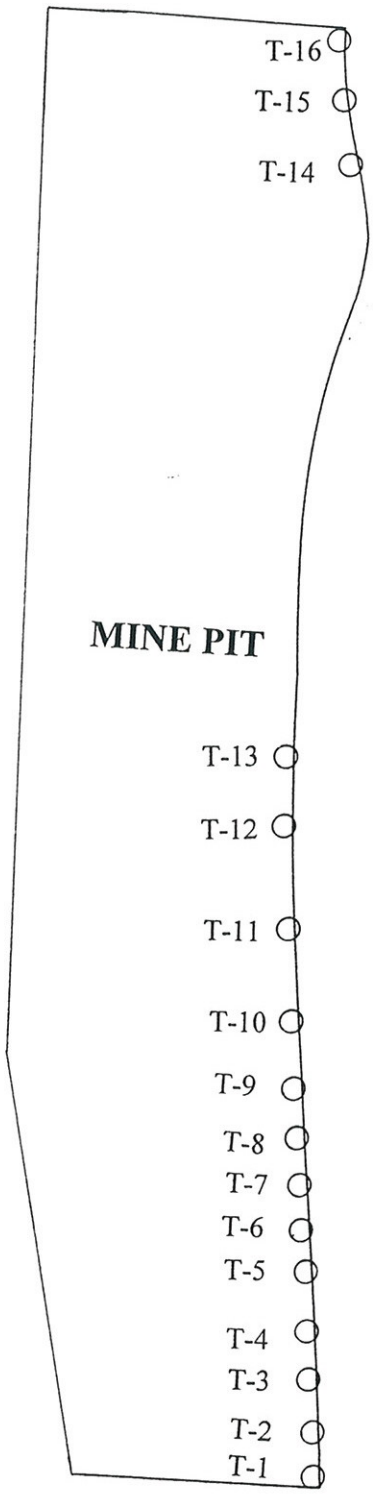

Figure 3.2 Sample Sites in Mine Pit

unit). A hand level and hip chain were used to survey the sites and determine the relative elevations of bedrock. At each site a stratigraphic section was drawn and the section was described. Plate 3.1 shows a typical vertical section of the deposit

3.2.2 Sample Collection

Samples weighing 150- 190 kilograms were taken from each of the 16 sites shown on Figure 3.2. In order to obtain a sample it was necessary to wait about 2 weeks after the completion of mining to allow permafrost to thaw. The site was prepared by first clearing away all debris, sloughed from the upper units, to reveal a clean face of the deposit. Bedrock in front of the sample was cleaned and a layer of washed orange-brown sand was spread to form a pad on which to put the sample and mark the bottom of the sample. The sample material was extracted as a panel from a clean face by scraping with the bucket of a Cat 235 excavator[1]. (Plate 3.2) The sample was pulled forward onto the prepared orange sand pad which distinguished it from the underlying bedrock of the pit floor.

The sample was manually shoveled into 6 standard 20 liter (5 gallon) pails, each weighing an average of 35 kg (78 pounds). Pails were weighed, wet, in the pit on a small platform scale to give a rough weight. The samples had high water content when removed from the pit wall, due to permafrost meltwater, but rain and sample size precluded air drying and more accurate weighing at the pre-sluicing stage. The sample was then transferred to large (+ 20 liter) labelled bags, sealed with twist ties and flagged for easy identification. All sample bags

[1] The backhoe bucket was enhanced with 5 hardened steel teeth, which are required to penetrate into permafrost.

a)

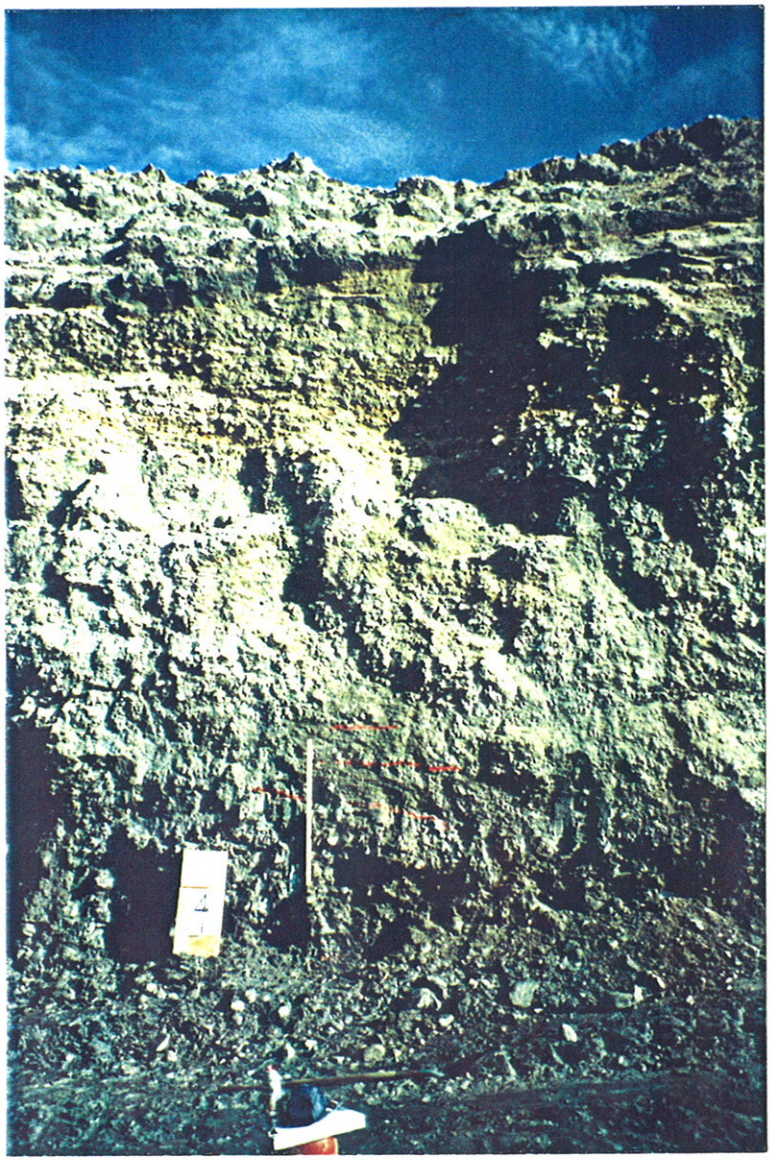

b)

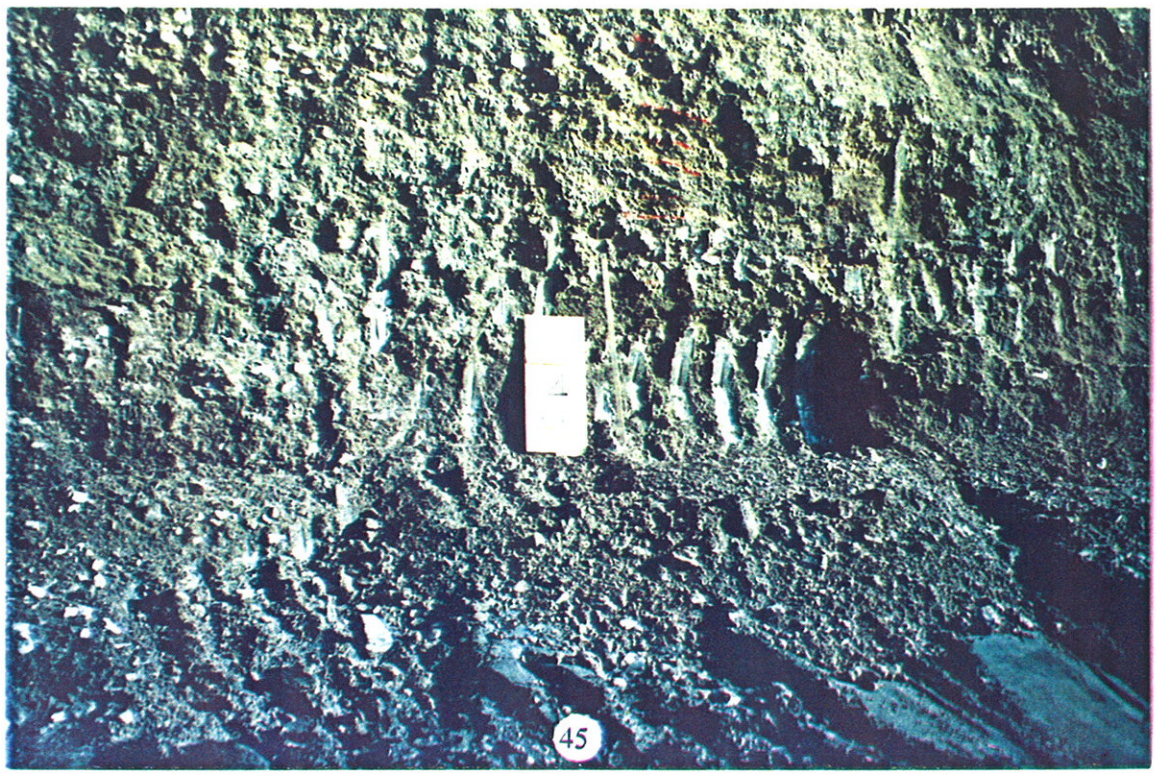

Plate 3.1 Vertical section of pit wall at sample site T14. (a) Shows section of pit face (upper peat and some mud have been removed). (b) Shows a closer view of the bottom units of the deposit.

Plate 3.2. Sampling equipment (Cat 235 backhoe, buckets, shovels)

Plate 3.3. Long-tom and catch-tub setup

from a sample site were stored together on a single pallet and covered with tarps until moved to the processing area.

3.2.3 Processing Samples

3.2.3.1 Mixing Sample and Splitting

A field split control sample was taken to determine the amount of fine size fractions which would be lost by sluicing so that an accurate size frequency distribution could be reconstructed for the fine size fractions. Each of the 6 bags of sample were individually poured out onto a piece of plywood, mixed with a shovel and were then cone and quartered twice. The material remaining from all of the bags was then further cone and quartered until approximately half a bucket of material was selected. The remaining 5.5 bags of sample were put aside for sluicing. The piece of plywood was swept clean between samples.

The damp field split sample was then sieved in an 8 mm sieve onto a tarp supported by a piece of plywood. The less than 8 mm control sample was placed in a plastic sample bag, labelled and stored. Material coarser than 8 mm was discarded. The sieve was cleaned between samples with a wire brush and the tarp and plywood was also swept clean.

3.2.3.2 Sluicing Sample

Equipment used to sluice the sample consisted of a large steel dump box, a steel long-tom (sluice) and a large steel tailings collection tub(Plates 3.3 and 3.4). The dump box consists of a 6 x 4 foot 16.5 inch deep metal tub placed on a 2:1 incline with a 4 inch drain/cleanout at the lowermost corner. Within the dump box a 2 x 3 foot metal screen was placed on an

a)

b)

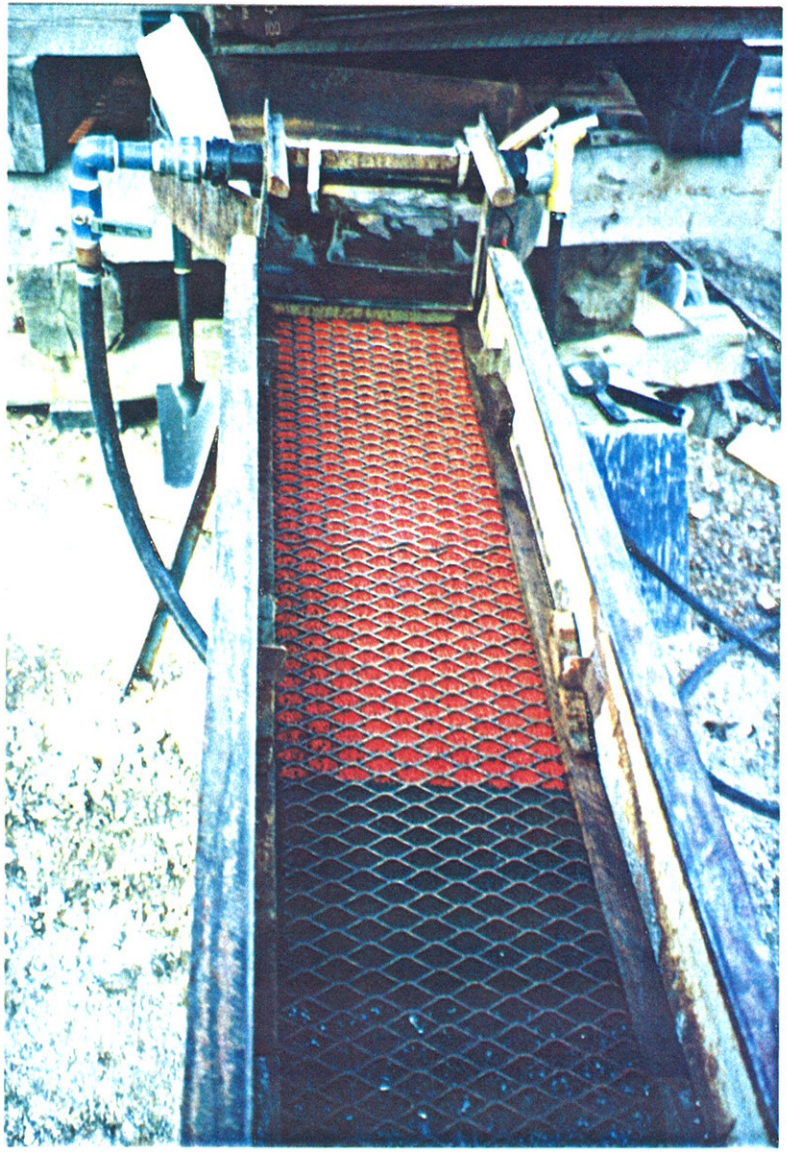

Plate 3.4. a)Long-tom setup and catch-tub. b) long-tom setup showing matting and orientation of expanded metal.

incline to act as a grizzly to separate large rocks. The grizzly prevents large rocks from entering the long-tom where they could potentially plug up the run.

The long-tom consists of a shallow 2 x 3 foot dump box joined to an 8 x 1 foot sluice run set on a 1 (vertical) to 2 (horizontal) slope. A spray bar at the throat of the dump box controls the flow of material into the run and provides the necessary water for sluicing. The run was lined with 8 - 1 x 1 foot pieces of unbacked 3M Nomad rubber matting overlain by 4 - 1 x 2 foot pieces of light expanded metal riffles held firmly to the mats with wooden side pieces and wedges. The expanded metal was oriented as shown on Plate 3.4b such that vortices would be created close to the matting and would drive heavy particles into the mats where they become trapped (Clarkson ,1990).

The tailings collection tub was of similar size to the dump box and has water drain plugs at the 2 and 12 inch levels as well as a 4 inch drain/cleanout at floor level.

After the separation of the control sample, the remaining 5.5 bags of sample were sluiced. The sample was washed with garden hoses through the screen in the dump box and the clean cobbles and boulders were picked off by hand and placed in buckets for later size grading. When all of the sample was washed, the screen was lifted and the entire dump box and screen were cleaned.

The material passing through the screen drained out of the dump box into the smaller dump box of the long-tom run where a spray bar further washed the material and prevented surging of material into the run. The amount of water coming out of the spray bar and from the

garden hoses was kept constant for all samples. During sluicing, the run was kept free of rocks and pebbles by hand picking to minimize scouring of the riffles.

Upon completion of sluicing the supply water was turned off except for one garden hose which was used to clean out the run. All of the concentrate was washed into a 24 x 12 inch aluminum bin under the end of the run as the sluice was cleaned. The wedges and the wood holding down the expanded metal were removed and rinsed with the hose in the run. The mats were then placed in the aluminum bin and the entire run was thoroughly rinsed. Then , the aluminum bin was removed from the bottom of the sluice, placed on the ground and filled with water. Each of the mats was gently shaken and rinsed in the bin until clean. After carefully decanting the water, the bin of concentrate was placed in the sun to dry. Unfortunately, the weather precluded complete air drying of the samples. The semi-dry concentrate was scooped into sample bag using a metal spatula. Material remaining in the tub was placed in the sun until dry, after which it could be removed by gentle banging on the sides of the tub and finally by the use of a new clean paint brush to sweep the material into a sample bag. The sluicing of each sample took approximately 45 minutes to an hour. During sluicing and cleaning of the long-tom, detergent was added to the water to prevent gold floating on the surface of the water and subsequently being lost.

During sluicing, an Imhoff cone sample was taken from the overflow of the tailings tub, to determine the amount of settleable solids being lost. The test involves sampling one liter of water in a graduated plastic cone. The sample was allowed to settle for 1 hour before a reading was taken. The average reading taken for the samples was 2.1 ml per liter of water. This reading indicates that a significant amount of fine material is washing over the top of the tailings collection-tub. While this number can not be directly converted to grams of

sediments - due to variability in the amount of water used in each sample, the variation in the fine content of the material being processed at any time, and the variation of the amount of sediment in the sluicing water over time - can be used for an estimate. An approximation of the amount of fines lost in sluicing would be in the order of 300 grams, based on rough calculations

3.2.3.3 Collection of tailings and sieving for grain size analysis

The sluice water and tailings were collected in the large tailings collection tub, and upon completion of sluicing, the suspended solids were allowed 15 minutes to settle before the water was carefully drained. The tub was placed at a slight incline, so that all of the water could drain out of the tub. The tailings were shovelled up to the high side of the tub in a large pile in preparation for wet sieving through three nested square metal 1.5 foot sieve boxes shown on Plate 3.5.

The boxes contained 16 mm, 8 mm and 4 mm screens which were placed in the lower portion of the large metal tub containing the tailings. A flat shovel was used to scrape the tailings off the bottom of the tub and place it in the sieves. Two standard 1/2 inch garden hoses, powered by a four horsepower Honda pump were used to wash the material through the sieves. The sieves were also rocked back and forth by tilting them on their edges for 1 minute and then turned ninety degrees and rocked back and forth until the material appeared clean. The material which remained in each of the sieves was collected in separate buckets, but the material from the 16 mm screen was washed through over an additional 32 mm screen, which was laid over the top of the bucket. Thus the plus 32 mm material could be removed and was set aside for further grain size grading.

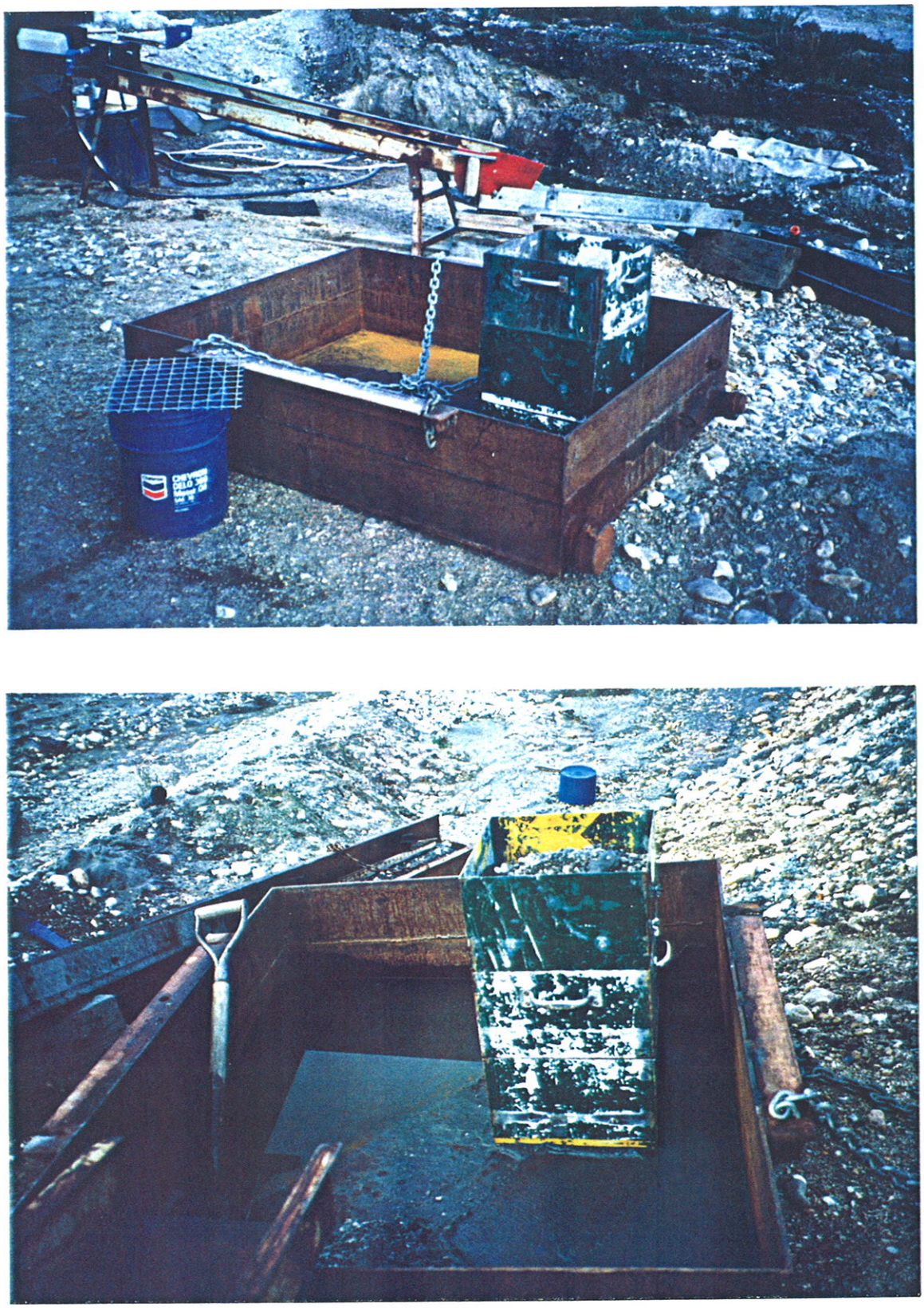

Plate 3.5. Equipment used to sieve the material in the catch-tub.

The buckets used were 20 liter pails cut in half, so that they would easily slide into a cradle, constructed of a milk crate, which could be suspended from a scale. The bottoms of all of the buckets were drilled with appropriately sized holes to facilitate drainage while preventing the loss of material through the openings. During sieving the drainage plugs in the tub were closed to prevent the loss of fine material. The water collected in the tub was also helpful for the 4 mm sieve, which after the removal of the 16 mm and the 8 mm sieves could be directly sieved into the tub. The process usually required two people, one person to shovel the sample and rock the sieves, while the other person held the hoses and cleaned the sieves into the appropriate containers.

After the box sieving was complete, only the minus 4 mm fraction remained in the tailings collection tub. The upper drainage plugs were removed and the excess water drained off. Then the bottom, large plug was removed and the material was washed with the hoses out of the drain and through the 12 inch circular plastic 2 mm sieve. The material that was less than 2 mm was caught in a 24" square, water filled tub placed under the drain so that the sieve could be agitated under water. The 2-4 mm material was poured out of the sieve into a bucket with drainage holes less than 2 mm. The less than 2 mm material was left in the tub and the clean excess water was carefully decanted from the surface after particulate matter settled. Liquid detergent (biodegradable) was added to all water used in the sieving process in an attempt to prevent the loss of gold due to flotation. The different size fractions were placed in the basket of the scale, their weight recorded, and the percentage of quartz, bedrock and other clasts visually estimated. Each size fraction was then spread out on a piece of plywood, labelled with sample number and size classification and photographed for future reference. Plate 3.6 shows sediments for the 16-32 mm size fraction from two samples.

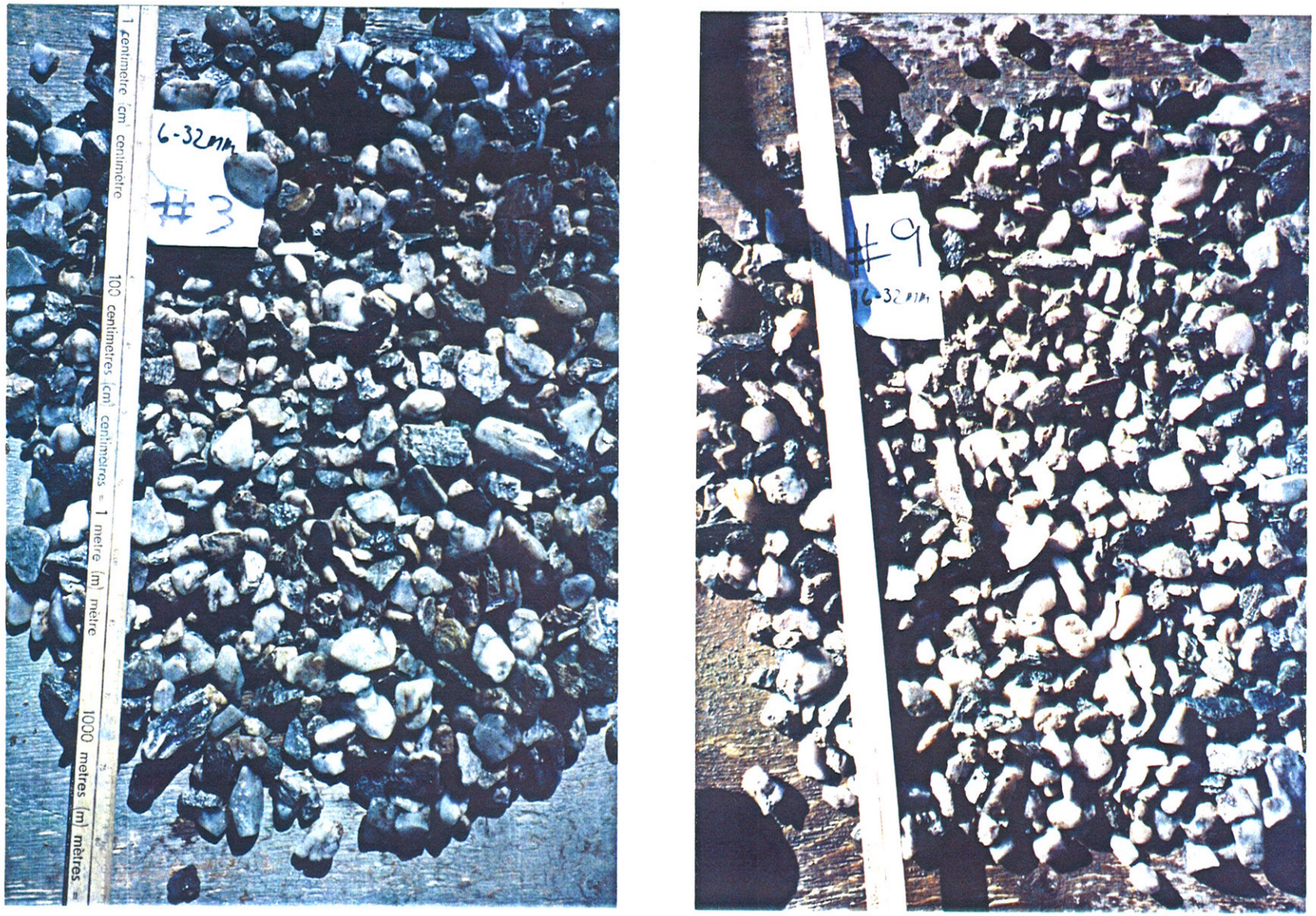

Plate 3.6 Photographs of the 16-32 mm size fractions for samples T-5 (#3 in photo) and T-11 (#9 in photo).

Material larger than the 32 mm screen from both the box sieving of the tailings and the material screened off by the grizzly was hand sized using an aluminum template into the following size fractions: 32-45 mm, 45-64 mm, 64-91 mm, 91- 128 mm , +128 mm. The coarser material was then sorted into lithological categories, quartz, bedrock and other smaller categories such as chert and sandstone. Each size category of +32 mm, was weighed for each different lithology. Thus the weight percent of each lithology could be determined. Weights of the coarse size fractions and estimated percentages of each lithology are in Appendix A. The entire grading and sieving process took approximately four hours per sample.

3.2.3.4 Transport and Storage of Samples

The samples were placed in plastic bags and firmly sealed with metal ties, packed into a wood crate and sent by freight truck to U.B.C. The samples arrived in good condition and bags were all intact.

3.3 LABORATORY PROCESSING

3.3.1 Sieving

All of the samples including the field split control sample and the long-tom concentrate were wet sieved through a series of eleven sieves using the apparatus shown in Figure 3.3. The sieve stack was mounted on a standard 23 liter pail through a specially cut hole in the lid. A thick rim of silicone seal held the sieves firmly in place and prevented any material spilt

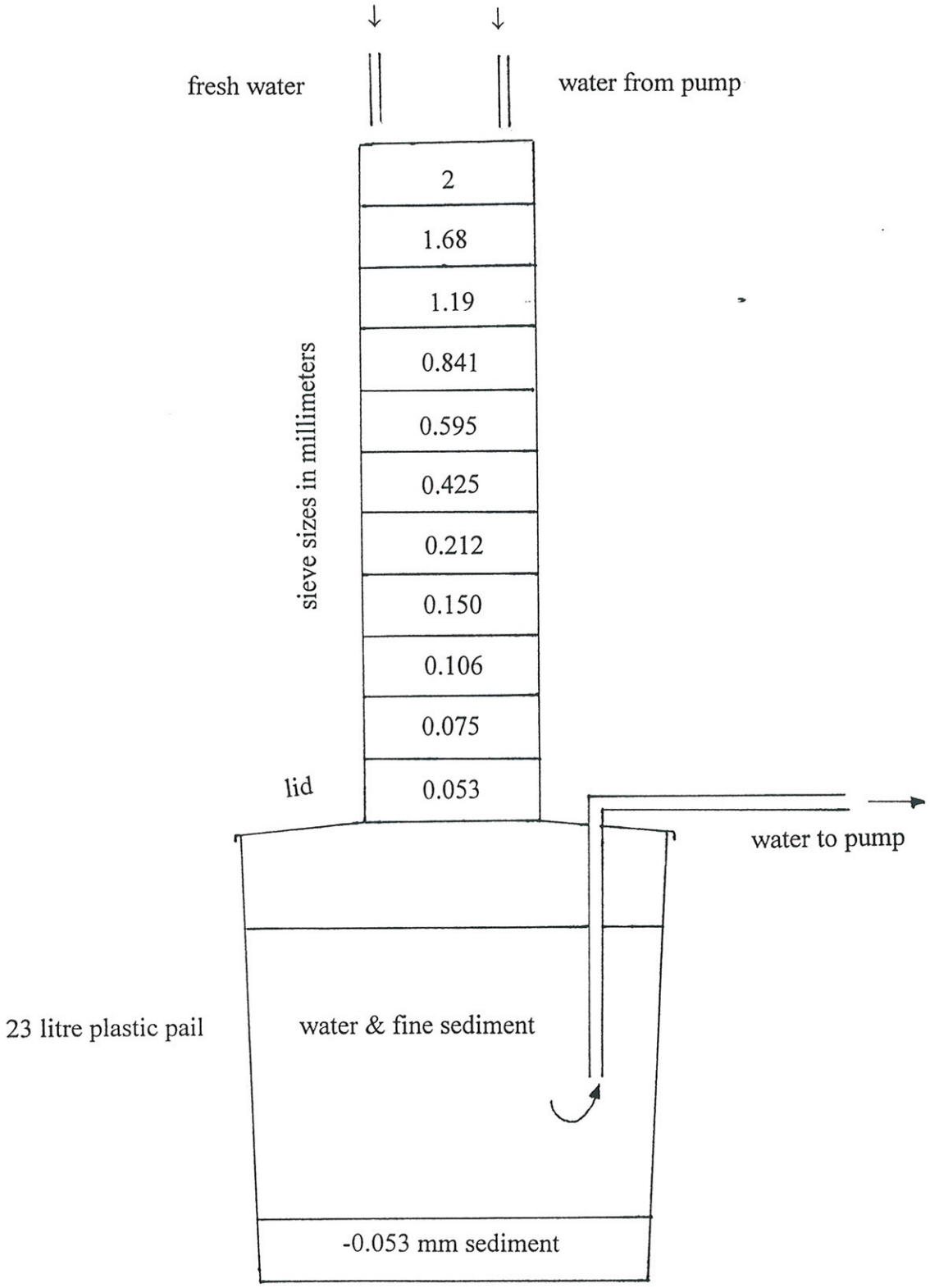

Figure 3.3 Wet Sieving Apparatus (After Day, 1985)

from entering the pail. Most of the samples weighed about 5 kg and these were all washed through the sieve stack in approximate 400 gram batches. With the help of a small hose and clean fingers the samples were gently disaggregated and worked through the top sieve until the material was visibly clean. The top sieve was then removed and the contents were rinsed into a labelled drying tray. The sample was washed through each successive sieve and the material from each sieve was rinsed into a separate glass tray. The end of the hose and the hands were carefully washed between sieves to avoid contamination of the size fractions. Material and water passing through the final 0.053 mm sieve collected in the 23 liter pail. The process was repeated until the entire sample was separated into the 12 size fractions: the procedure took between 4- 6 hours per sample.

Occasionally a sieve, particularly for the finer fractions, would become clogged and water and fine sediments would leak out from the joints between sieves. The hole in the lid of the pail fitted snugly to the bottom sieve and prevented overflow from contaminating the fine (-0.053 mm) size fraction collecting in the pail. Fresh water was used to wash the sample until the collection pail was approximately three-quarters full, and then a pump was used to recirculate the water from the pail to prevent loss of fines which would occur if the water were to overflow the pail. After the entire sample was processed the pail was labelled, and sealed with a lid and the -0.053 mm size fraction was allowed to settle for at least 48 hours or until the water was clear. The water was then decanted and discarded, while the sediment was washed into a glass-drying tray.

All of the samples in glass trays were oven dried at approximately 150°-200°C and then were carefully weighed and transferred to plastic sample bags.

Between samples the sieves were thoroughly cleaned with a stiff bristle brush, a tooth brush and water until the screens were visibly clean. Any breakage in the screens found during cleaning or sieving were sealed immediately with epoxy.

3.4 SAMPLE PREPARATION FOR CHEMICAL ANALYSIS

Prior to being sent for chemical analysis, samples weighing more than 30 grams had to be reduced. A large Jones Splitter was used to bring samples down to 100 - 200 grams, and a smaller Jones Splitter further reduced the sample size to 30 - 45 grams, by repetitive splitting when necessary. The samples were placed in randomly numbered, pre-weighted plastic vials. Samples less than 30 grams were transferred directly from the plastic sample bags to the randomly numbered plastic vials. Between samples the Jones Splitters were cleaned with compressed air.

On drying the -0.053 mm size fractions solidified and had to be disaggregated with a mortar and pestle prior to splitting. Splitting was required for a few of the tailings catch tub - 0.053 mm samples, but most were less than 30 grams and did not require splitting. The mortar and pestle were thoroughly cleaned with tissue paper and then with compressed air between samples.

3.5 GEOCHEMICAL ANALYSIS

Geochemical analysis was done by standard fire assay - atomic absorption spectrometry (FA-AAS), by Chemex Labs, North Vancouver. 30 gram subsamples, approximately one assay ton, were submitted where enough material existed. Samples or size fractions with less than 30 grams were completely analyzed by FA-AAS. Analysis of 30 gram samples was selected over 10 grams samples to reduce potential "nugget" effects and increase the probability of the sample to contain a statistically representative number of particles. Larger analytical portions for FA-AAS are not commonly available as 30 grams is an upper, practical limit, for samples in this technique . The detection limit for FA-AAS is 5 ppb.

Trial analysis was undertaken on two small batches of samples prior to sending them in, to determine if representative gold values could be obtained from the field split samples. However, if nugget and sample size effects were significant in the trial analysis then both the catch-tub and long-tom concentrate samples would have to be analyzed, at considerable more expense.

3.5.1 Trial Analysis 1 and 2: FA-AAS

The purpose of trial 1 was to determine if analysis of the field splits would give sufficient precision for meaningful gold analysis. The concentration of gold in the samples was estimated to be 1 ppm (Conversion factors in Appendix I) or less in a given sample based on average gold grades at the mine. Estimates from Clifton (Figure 3.4), showed that the 30 gram subsamples could potentially give meaningful gold results for the finer size fractions at concentrations of 1 ppm gold. Using the assumption that the gold particles were present as

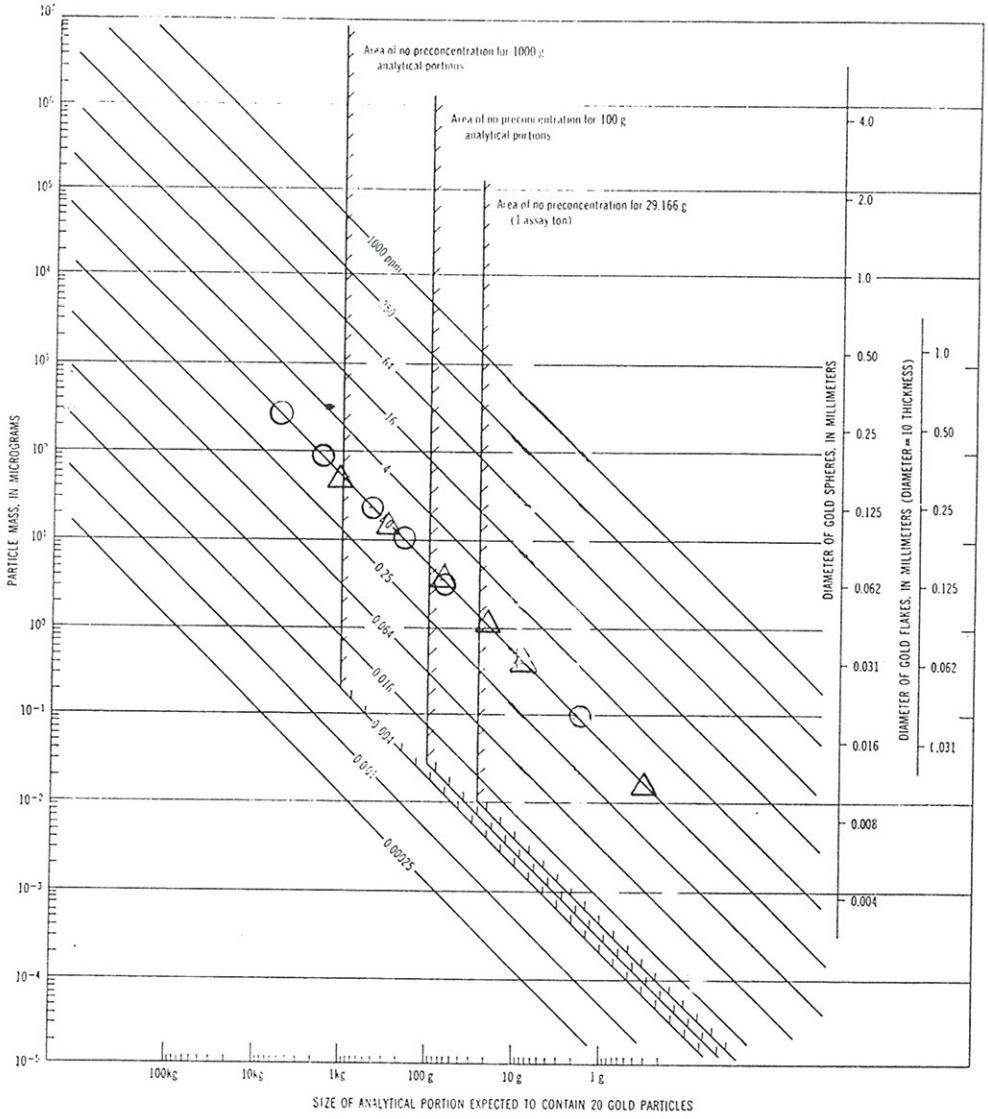

Figure 3.4 This chart from Clifton (1969), showing the relation of gold grain size and grade to preconcentration requirements was used to estimate whether meaningful gold values will result from analysis of Field Split samples. If the gold particles are assumed to be spheres (circles on the chart), the analytical results for a 30 gram sample would only be meaningful without preconcentration for the -0.053 mm size fraction. If it was assumed that the gold particles occurred as flakes with a diameter to thickness ratio of 1:10, then three size fractions, -0.053 mm, 0.053-0.075 mm and 0.075-0.106 mm, were predicted to give meaningful gold results. The concentration of gold in the sample was estimated at 1 ppm.

spheres with a diameter equal to the logarithmic average of the bounding sieve openings, Clifton's charts predicted that analytical results would only be meaningful for the -0.053 mm size fraction. However, if it was assumed that the gold particles occurred as flakes with a diameter to thickness ratio of 1:10, then the size fractions, -0.053 mm, 0.053-0.075 mm and 0.075-0.106 mm, were predicted to give meaningful gold results.

Eight samples of the 6 finest sieve size fractions (0.212 - 0.425 mm, 0.150 - 0.212 mm, 0.106 - 0.150 mm, 0.075 - 0.106 mm, 0.053 - 0.075 mm, and -0.053 mm) from sample T-5, were sent in randomly numbered vials and included two duplicate samples of the two coarser (0.150 - 0.212 mm and 0.212 - 0.425 mm) size fractions. The results, presented in Table 3.1a, showed that reproducibility of gold values in the coarser size fractions of the field splits was very poor, and the "nugget" effect was clearly evident. The finer size fractions also showed erratic gold values with three results below the detection limit of 5 ppb. The number of particles of gold in the analytical portion of the field split samples was calculated, based on the assumption that gold occurs as flakes (1:5 thickness to diameter), and are presented in Table 3.2a. (The method of calculating the number of particles of gold is presented in Chapter 5) Significantly fewer particles of gold, than the 20 particles of gold recommended by Clifton for meaningful gold analysis, were calculated to be in the field split analytical portions.

Due to the concern that gold concentrations in field splits might be less than the detection limit and the prominent "nugget" effect in the coarser size fractions, it was determined that analysis of the long-tom concentrate and the catch-tub samples would be a better alternative. It was necessary to also analyze the catch-tub sample to determine the amount of gold which is not recovered in the long-tom. Results for the long-tom concentrate and the catch-tub

Table 3.1a Analytical results from trial 1: field split samples.

Size Fraction	Logarithmic Average Size	Analytic Results Field Split
millimeters	*millimeters*	*ppb*
0.212-0.425	0.300	7140
		<5
0.150-0.212	0.178	2150
		1050
0.106-0.150	0.126	<5
0.075-0.106	0.089	145
0.053-0.075	0.063	<5
-0.053	0.020	45

Table 3.1b Analytical results from trail 2: long-tom and catch-tub samples.

Size Fraction	Logarithmic Average Size	Analytic Results Long-Tom	Catch-Tub
millimeters	*millimeters*	*ppb*	*ppb*
0.212-0.425	0.300	3460	<5
		4260	<5
0.150-0.212	0.178	3400	5
		1180	90
0.106-0.150	0.126	10	885
0.075-0.106	0.089	1810	860
0.053-0.075	0.063	1790	1040
-0.053	0.020	510	90

Table 3.2a Number of particles of gold in the field split samles: trial 1.

Size Fraction	Logarithmic Average Size	# of Au Particles in Analytical Portion
millimeters	*millimeters*	Field Split
0.212-0.425	0.300	0.56 0.0002
0.150-0.212	0.178	0.8 0.39
0.106-0.150	0.126	0.002
0.075-0.106	0.089	0.43
0.053-0.075	0.063	0.02
-0.053	0.020	11.8

Table 3.2b Number of particles of gold in the long-tom and catch-tub samples: trial 2.

Size Fraction	Logarithmic Average Size	# of Au Particles in Analytical Portion	
millimeters	*millimeters*	Long Tom	Catch Tub
0.212-0.425	0.300	0.27 0.33	0.0002 0.0002
0.150-0.212	0.178	1.26 0.44	0.002 0.033
0.106-0.150	0.126	1.69	0.001
0.075-0.106	0.089	2.76	0.01
0.053-0.075	0.063	11.5	0.03
-0.053	0.020	150	9.7

would then have to be combined to estimate the total gold in the original sample. These analyses would also provide data to evaluate the effectiveness of the long-tom as a method of pre-concentrating gold.

Prior to submitting the samples for the second trial, rough estimates of potential concentration factors were done. The calculations were based on an idealized situation, where the concentration of gold is increased by the factor of the total mass of sediments sluiced to the mass of heavy concentrate retained in the long-tom. In these calculations the incorrect assumption that only heavy minerals are recovered in the long-tom must be made. While these calculations are not accurate, they do suggest that heavy minerals could potentially be concentrated by 5 - 40 times the original concentration. The large variability in these concentration factors is due to uncertainty in: the "true" concentration of gold in any size fraction, and the proportion of heavy minerals to light minerals retained in the long-tom. The concentration factors did not predict that analytical portions from the long-tom would all contain greater than 20 particles of gold. However, the increase in concentration of samples, was considered to be sufficient to obtain potentially meaningful gold results. The second trial was conducted to confirm that long-tom concentrate samples returned more significant gold results, before committing to the high cost of analyzing all the samples.

A total of 16 subsamples, from sample T-5, were sent in the second trial; a sample for each of the six size fractions -0.425 mm, from both the long-tom concentrate and the catch-tub, and duplicate samples for the 0.150 mm-0.212 mm and 0.212mm-0.425mm size fractions. The results of the second trial are presented in Table 3.1b, with the results from the first trial (Table 3.1a). In the results of the long-tom concentrate analyses, the "nugget effect" was less prominent than in the field split results and all samples returned a concentration greater than

the detection limit. Some results for the catch-tub were below the detection limit and the "nugget effect" was evident in duplicate samples. Also, the concentration of -0.106 mm gold in the long-tom concentrate was only marginally larger than the concentration of gold in the catch tub, suggesting that recovery of fine gold in the long-tom is poor. The average number of particles in the analytical portions of the long-tom concentrate and the catch-tub were calculated, based on particles of gold occuring as flakes (Section 5), and are presented in Table 3.2b with the results from the field split, Table 3.2a, for comparison.

3.5.2 Results of Analysis of sample data

From the two preliminary trials it was determined that analytical portions from both the long-tom and the catch-tub would have to be analyzed to alleviate sampling problems. A total of 200 samples were submitted to Chemex in December of 1995. The certified certificates from Chemex and a key to the results can be found in Appendix F. In order to determine the errors which may have accrued with sampling and analysis, a program to monitor both analytical accuracy and precision was implemented.

3.5.3 Monitoring Analytical Accuracy

In order to have an estimate of the accuracy of the FA-AAS results, three Reference Standards were included. Table 3.3 shows the concentration of gold in the standard samples and the results from FA-AAS analysis. The results from FA-AAS appear to closely correspond with the concentrations of gold in the standard samples and are close to the accuracy which can be attributed to preparation of the standards. The Nevada Bureau of

Table 3.3 Analytical results compared to standard samples

Name	Gold Content of Standard oz/ton	ppb	Analytical Results ppb
Nevada Bureau of Mines NBM - 1c	0.468	16000 +/- 1100	17600
Gold Ore MA-2	0.0542	1860	1730
Nevada Bureau of Mines- Limestone	0.228	7810	8320

Mines reference standard NBM -1c , prepared with a gold concentration of 16.0 ± 1.1 ppm, gave the analytical results a value of 17.6 ppm. Results from the Nevada Bureau of Mines, limestone, returned values of 8320 ppb, with the mean concentration of the standard at 7810 ppb, while the Gold Ore MA-2, with a mean of 1860 ppb, returned an analytical value of 1730 ppb. From this we can infer that the probability of analytical error in accuracy is low in these samples.

3.5.4 Monitoring of Analytical Precision

An estimate of the precision of the analysis was obtained from duplicate samples submitted for analysis. Twenty duplicates were sent in the third batch and results obtained are plotted in Figure 3.5. (Duplicate results for the first and second trials are also plotted.) The results of duplicate analysis showed poor reproducibility of gold values and are rather imprecise, with over half of the duplicate pairs falling out of the ± 50 % precision bounds at the 95 % confidence level. This effect may be attributed to the "nugget effect" previously discussed in this paper.

3.6 EFFICIENCY OF LONG-TOM

Concentrations of gold in most soils and sediments are relatively low, which makes obtaining samples with enough particles of gold to be representative and to be above the detection limit of the analytical method, problematic. Preconcentration methods such as sluicing are often used to increase the number of particles of gold in the sample. Mechanical preconcentration

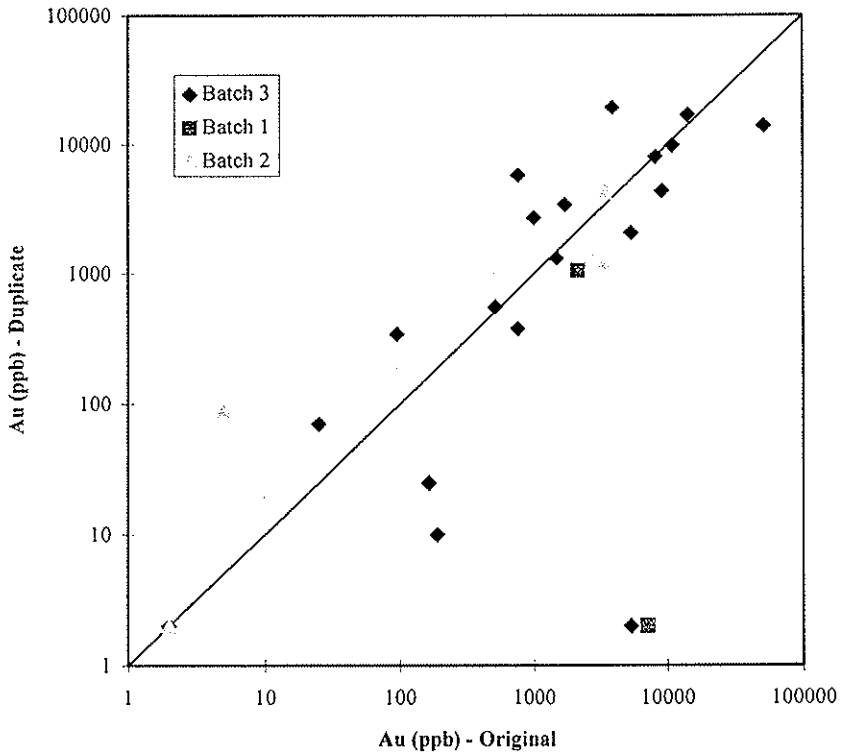

Figure 3.5 Comparison of duplicate analyses for the 1st, 2nd and 3rd batches of analytical results. Solid line represents the x=y line. Dashed lines represent the ± 50 % analytical precision limits.

methods invariably result in the loss of gold, particularly the fine gold. As the finer size fractions are frequently the most reliable in determining gold concentrations, evaluating trends and calculating transport equivalences, the loss of gold can have serious implications in sedimentological studies.

There are many types of sluices and long-toms. The principle variables in any sluice system which have an effect upon gold recovery are: dimensions of sluice run (length, width, height of sides); type of matting used to catch concentrate (principle types are Coconut matting and rubber matting (primarily 3M Nomad matting)); type of riffles, expanded metal (weight, orientation, position sitting); screen or grading device to restrict grain size passing through sluice; volume of water used; method used to clean long-tom; slope (influences velocity of water and sediments transported); water/ solids ratio.

Gold may be lost in sluicing due to incorrect combinations of these variables. Also, gold tends to occur as flakes or rods with large surface area to weight ratio. High turbidity in a sluice run prevents flakes of gold from being trapped in the matting and riffles of the long-tom. Large cobbles, pebbles and angular rocks in the long-tom will tend to knock gold out of the riffles Also, gold may also be trapped in clays adhering to cobbles which is not adequately washed or able to be washed in the sluicing process. Flotation of gold, during processing, due to contamination with oils or grease is also known to cause fine gold to be lost.

The effectiveness of the long-tom in recovering gold, was considered by analyzing samples from the tailings, collected in the catch-tub for gold concentration and comparing the results with the concentration of gold in the long-tom. The percentage of gold recovered in the

long-tom was calculated by dividing the calculated mass of gold in the long-tom, by the calculated mass of gold in the total sample (the sum of gold in the long-tom and in the catch tub). Calculation for the mass of gold in the long-tom, catch-tub and the total sample are presented in section 5. In this study, the percentage of gold recovered by the long-tom increases with increasing gold grain size and is erratic for all size fractions less than 212 microns (Table 3.4).

Concentration factors were calculated based on the increase in the number of particles of gold (as flakes of gold) which would be present in the analytical portion from the long-tom concentrate compared to one taken from an unprocessed field sample. The long-tom was found to concentrate the number of gold particles (flakes) in the sample significantly, with concentration factors ranging for 9 to 139 (Table 3.5). The concentration factor for the 212-425 is Although only the 0.053-0.075 mm and -0.053 mm size fractions in the long-tom concentrate have greater than 20 particles of gold, as specified by Clifton to obtain a precision of ± 50 %, the overall increase in gold particles in a 30 gram analytical portion is significantly increased. The average increase in number of particles in the analytical portion for the long-tom is 48 times the number of particles in the field-split. From this it is evident that better analytical results could be obtained for the coarser size fractions if larger samples were processed through the long-tom. For the coarser size fractions, 0.150 - 0.212 mm and 0.212 - 0.425 mm, in order to get better accuracy in the analytical results, the samples would have to be twenty times as large; approximately 4 tonnes.

In summary, while the use of the long-tom is effective as preconcentration method, the user should be aware of the limitations and potential errors which may arise from any mechanical

Table 3.4 Recovery of Gold in the long-tom. Calculations are based on the percentage ofthe total mass (long-tom + catch tub) of gold retained in the long-tom.

Size Fraction (microns)	Mean Recovery %	Median Recovery %
212-425	98.1	99.8
150-212	74.5	80.0
106-150	77.2	95.5
75-106	75.5	78.1
53-75	60.5	63.6
<53	39.6	21.5

Table 3.5 Number of gold particles in a 30 gram subsample from the long-tom concentrate and the field split. Concentration factors were calculated on the basis of the increase in the number of gold particles (flakes), which would be present in an analytical portion from the long-tom concentrate compared to one taken from an unprocessed field sample.

Size Fraction Microns	# of Gold Particles in 30 gram subsample taken from the Long-Tom Concentrate	# of Gold Particles in 30 gram subsample taken from the Field Split	Concentration Factor
212-425	1.00	0.01 *	159.1
150-212	1.43	0.16	9.1
106-150	5.22	0.22	23.3
75-106	11.84	0.31	38.3
53-75	32.02	1.28	25.1
<53	912.67	6.87	132.9

*The calculated number of particles in this sample is likely lower than the actual number of particles, as the Poisson Distribution underestimates at low numbers of particles. Therefore, this factor is likely not representative of the actual concentration factor of this size fraction.

processing method. The effects of these errors should be considered and , if possible, quantified, when reconstructing gold concentrations in the original sample. A more detailed description of the long-tom process and efficiency of gold recovery in this study can be found in Appendix H.

4.0 GRAIN SIZE DATA AND ANALYSIS

In this chapter, the field and laboratory techniques used to determine the grain size distribution of the samples are presented and justified. Cumulative probability plots were used for comparative textural analysis and interpretation of results. Trial runs had indicated that a loss of fine material in the catch-tub overflow during sluicing would preclude accurate determination of the grain size distribution. To compensate, 5-10 kg field splits of each sample were taken for later laboratory analysis of the finer grain sizes. The recovery of fine material in the catch-tub will be considered first, to justify the method used to reconstruct the grain size distribution.

4.1 RECOVERY OF FINES IN CATCH TUB

During sluicing, sediment from the fine fractions suspended in the overflow water of the catch tub is lost and in order to compensate for this loss, a field split was taken for controlled laboratory analysis. The data from the field split and the data from the catch-tub can be used to quantify the fine fractions lost during sluicing. The procedure for this involves constructing a graph of $M_{(FS)i+1} / M_{(FS)i}$ versus $M_{(CT)i+1} / M_{(CT)i}$, where $M_{(FS)i}$ is the mass of sediment size fraction i in the field split and $M_{(CT)i}$ is the mass of the same sediment size fraction i in the catch tub (figure 4.1).

Graphs are plotted for each size fraction. If there is no loss of a size fraction during sluicing, then the data points should all fall on the x=y line of the graph. Points lying below

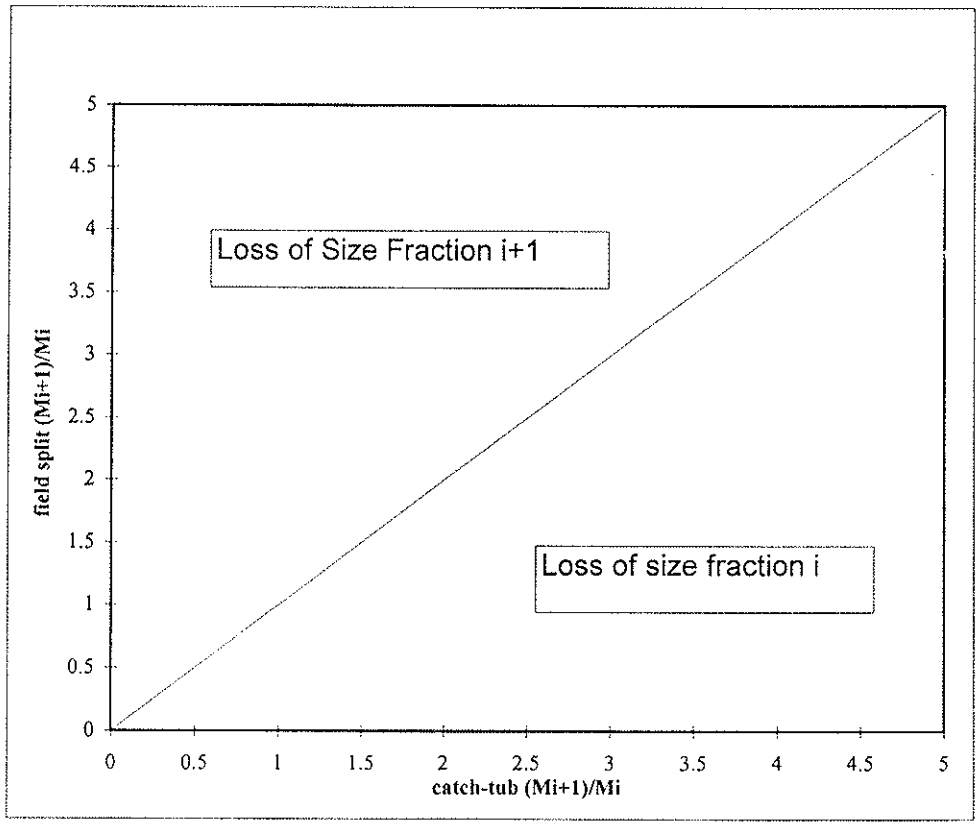

Figure 4.1 Example: Plot of recovery of fine sediment sizes in the catch-tub. The line, x=y, represents equal ratios of sediment in the catch tub and the field split. Below the line when sediment of size fraction i is lost from the catch tub, above the line when sediment of size fraction i+1 is lost and on the line when there are no losses of either size fraction or both size fractions have lost material such the proportion of the two size fractions is still the same.

the x=y line suggest that sediment in size fraction i is being lost, while points lying above the x=y line suggest that sediment in size fraction i+1 is being lost. Caution must be used when interpreting these graphs because the results are dependent on the relative depletion of size fraction i and of i+1. Thus, if equal proportions of sediment size i and i+1 are lost, then the data will plot on the x=y line, erroneously suggesting that no fine fractions have been lost.

This method does not yield conclusive results but can be use to determine which size fraction may experience losses during sluicing. All fine size intervals must be considered where the loss of size fractions is suspected. One assumption in this method is that the loss of fine sediments during the laboratory processing of the field-split was negligable. This assumption is reasonable since a recirculating pump was used during sieving of the sample and the losses during processing, drying and bagging were likely small. Another assumption, that the field split sample is representative of the fine fractions in the whole sample, must also be made.

The grain size data from the catch tub and field split was plotted for i less than 1.68 mm. These graphs are presented in figures 4.2 and 4.3. Graphs for sediment size fractions between 0.425 mm and 1.68 mm plotted close to the x=y line, suggesting that losses from the catch-tub during sluicing for these size fractions was minimal. However, for all size fractions less than 0.425 mm, losses of fine sediment during sluicing are suspected. In figure 4.3, sediments of the size fractions -0.053 mm, 0.053-0.075 mm, 0.106-0.150 mm and 0.212-0.425 mm are clearly depleted in the catch tub, compared with the sediment one size fraction larger. This indicates that a portion of these size fractions was suspended in the overflow water and lost from the catch-tub. However, two size fractions, 0.075-0.106 mm and 0.150-0.212 mm, are plotted close to the x=y line. It is suspected that this phenomenon is due to

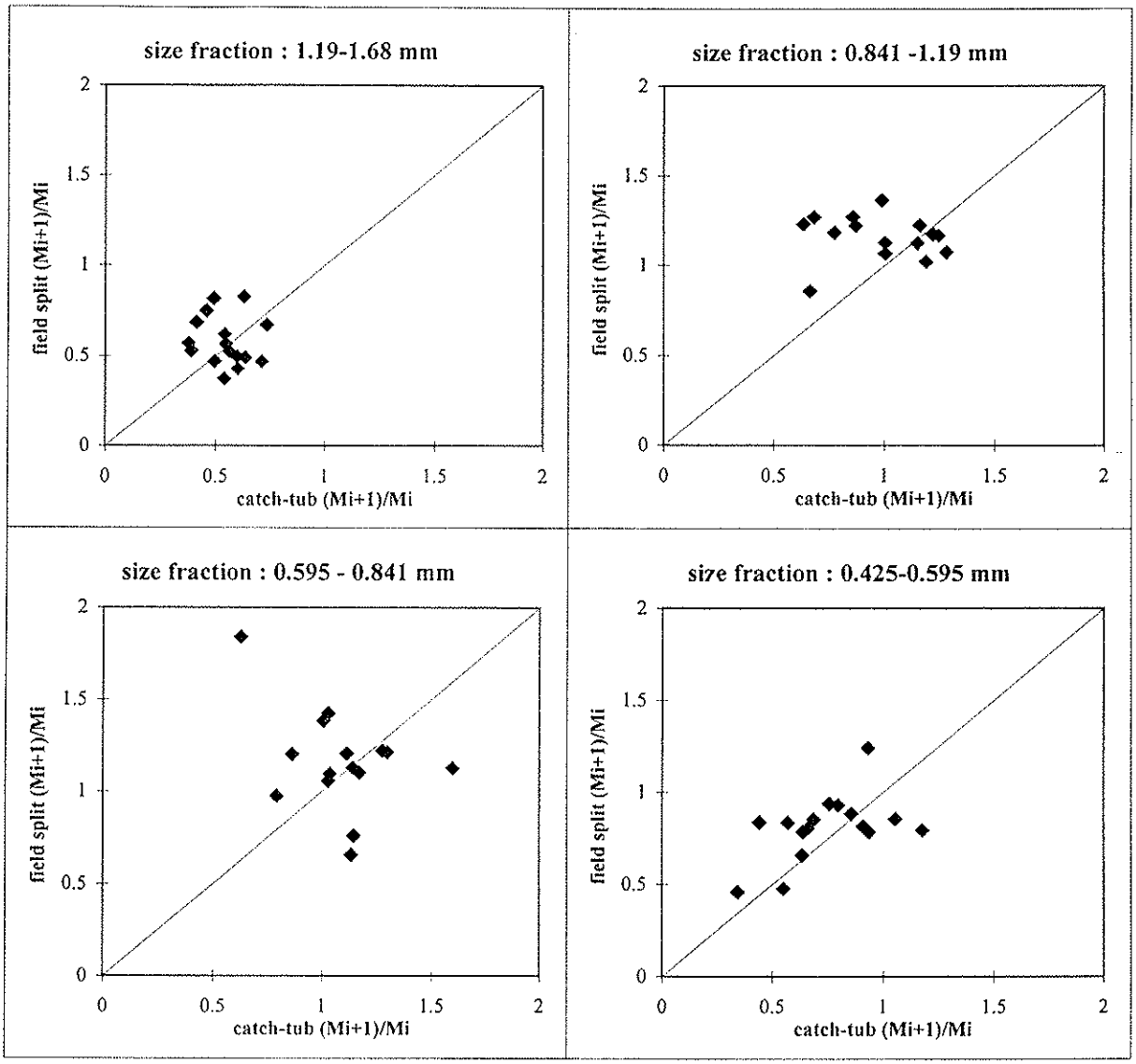

Figure 4.2 Plots of sediment size recovery in the field split versus in the catch tub for size fractions from 0.495-1.68 mm. Note that the data fall on close to the x=y line, indicating no losses of these sediment size fractions from the catch tub.

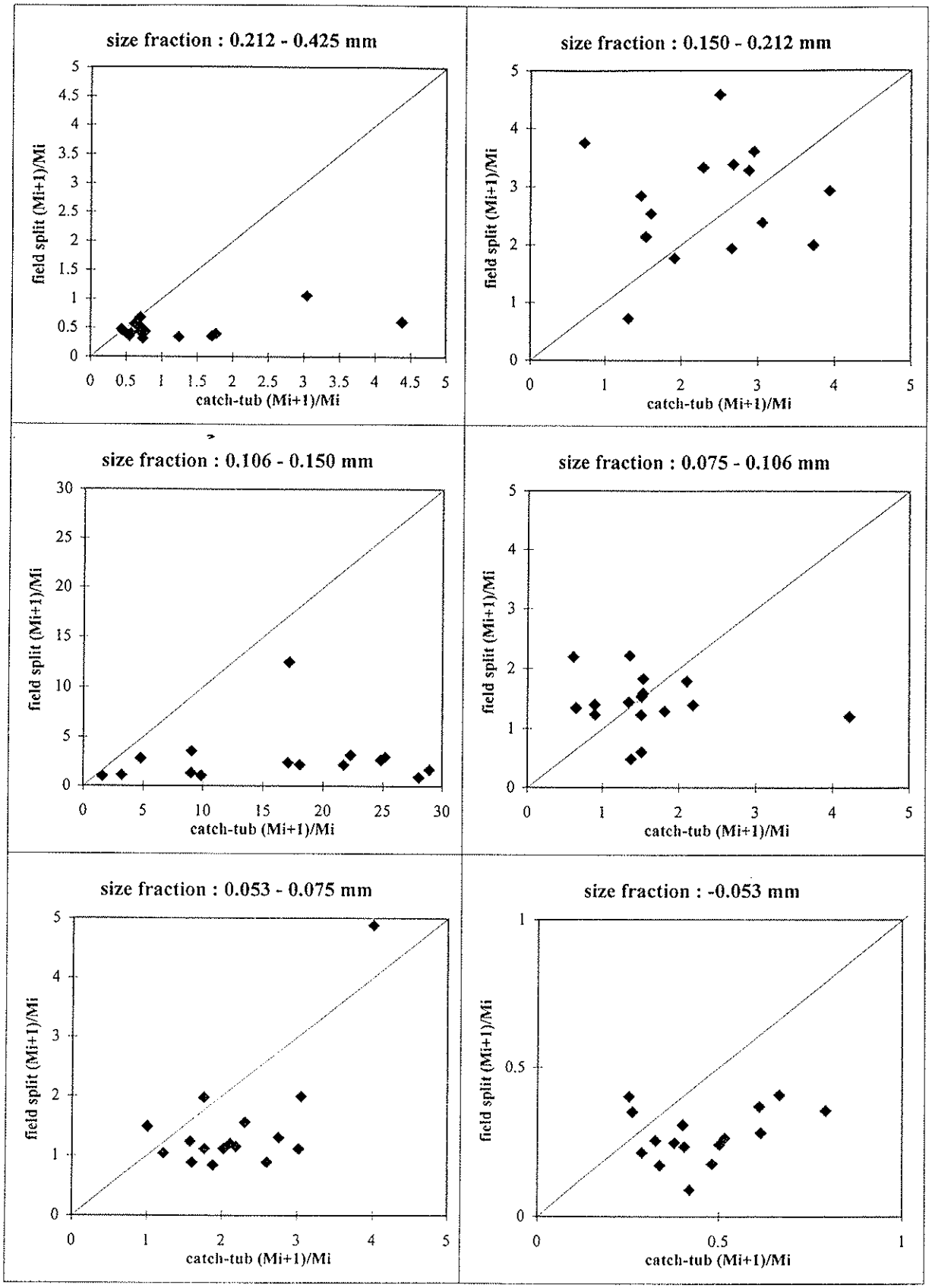

Figure 4.3 Plots of sediment size recovery in the field split versus in the catch tub for size fractions from -0.053 to 0.425 mm. The size fractions -0.053 mm, 0.053-0.075 mm, 0.075-0.106 mm, 0.106-0.150mm and 0.212-0.425 mm are depleted in the catch tub, compared to the sediment one size fraction larger. This indicates that a portion of these size fractions was suspended in the overflow water from the catch-tub. However, two size fractions, 0.075-0.106 mm and 0.150-0.212 mm, plotted close to the x=y line. This phenomenon is due to equal loss of material from these sediment sizes, as from the sediment size fractions one interval larger. Note the changes in scales between graphs.

equal loss of material from these sediment sizes and from the sediment size fractions one interval larger.

These plots confirm the initial hypotheses that accurate grain size distributions for the fine size fraction could not be obtained from the material collected in the catch-tub. These results clearly show that losses of sediment from the fine size fractions, less than 0.425mm, are significant and thus the collection of a field split sample to reconstruct the grain size distribution is necessary. When the field split samples were taken, it was also uncertain as to which sizes might be selectively removed from the catch-tub in suspension. Thus, it was uncertain how coarse a field split sample was required to allow for these effects in the grain size distribution. The field split was used to reconstruct sediment sizes less than 2 mm in the total grain size distribution. As size fractions between 0.425 mm and 0.168 mm showed no apparent loss of sediment from the catch-tub, while size fractions less than 0.425 mm clearly did; the selection of 2 mm as the boundary to reconstruct the grain size distribution should remove any effects of material being washed out of the catch-tub from the grain size distribution.

4.2 CALCULATION OF GRAIN SIZE DISTRIBUTIONS

Grain size distribution of is useful for correlation with other field and lab data; however, the distribution could not be obtained directly owing to the preconcentration method selected. The mass of sediments in the catch-tub represented a large proportion of the total grain size distribution, but as discussed in the preceeding section, sluicing the sample through the long-

tom resulted in material being retained in the long-tom and a portion of the finer fractions becoming suspended and lost from the sample when water overflowed the catch-tub.

The calculations to reconstruct the total grain size distribution for 20 size fractions from +200 mm to -0.053 mm and the variables used are described below.

$Ms_{(FS)i}$ - Mass of sediment in field split of size fraction i
$Ms_{(LT)i}$ - Mass of sediment in long-tom of size fraction i
$Ms_{(CT)i}$ - Mass of sediment in catch-tub of size fraction i
$Ms_{(tot)i}$ - Mass of sediment of size fraction i in the total reconstructed grain size distribution

For the sediments + 2 mm the sediment grain size distribution can be reconstructed directly by adding the mass of each size fraction in the catch-tub and in the long-tom.

$$Ms_{(tot)i} = Ms_{(CT)i} + Ms_{(LT)i} \text{ (for } i > 2 \text{ mm)}$$

For the sediments -2 mm, the reconstruction of the grain size distribution is more complex. The principal assumption in this step is that the mass of the less than two millimeter fraction in the catch-tub is representative of the total mass of -2 mm sediments in the sample and is directly proportional to the less than 2 mm fractions in the field split. This calculation assumes that the mass of the suspended material that overflowed the catch-tub is insignificant compared with the bulk wet weight of the total material collected in the catch-tub less than 2 millimeters. This was calculated with the following formula:

$$Ms_{(tot)i} = Ms_{(FS)i} \times (Ms_{(CT)<2\text{ mm}} + Ms_{(LT)<2\text{ mm}}) / Ms_{(FS)<2\text{ mm}} \quad \text{(for } i < 2 \text{ mm)}$$

The sediment size fractions were then converted from diameters expressed in millimeters to phi values using the Udden-Wentworth scale or the logarithmic Phi Scale proposed by Krumbein in 1934 where:

$$\phi = - \log_2 S$$

ϕ = Phi size
S = sediment grain size in millimeters

This scale is particularly useful as it expresses grain size data in units of equal value, which enables meaningful plotting of data and statistical calculations. In this grain size scale, large sediment sizes have negative values and silt and clay sizes have progressively larger positive phi values.

Data tables with the calculated masses and mass percentage of total samples can be found in Appendix C (expressed in both millimeter sizes and phi size), followed by cumulative grain size curves for each of the samples. Figure 4.4 shows the cumulative grain size curve for the arithmetic average sample for grain sizes in phi and in millimeters. When these curves were compared with similar grain size curves for gravel streams, there were no apparent differences in the shape of the curves and the distribution of sediments. In-situ, the unit appeared to have an unusually high content of fine material, but the proportions of fines in the samples did not appear to differ from those in typical gravel stream environments.

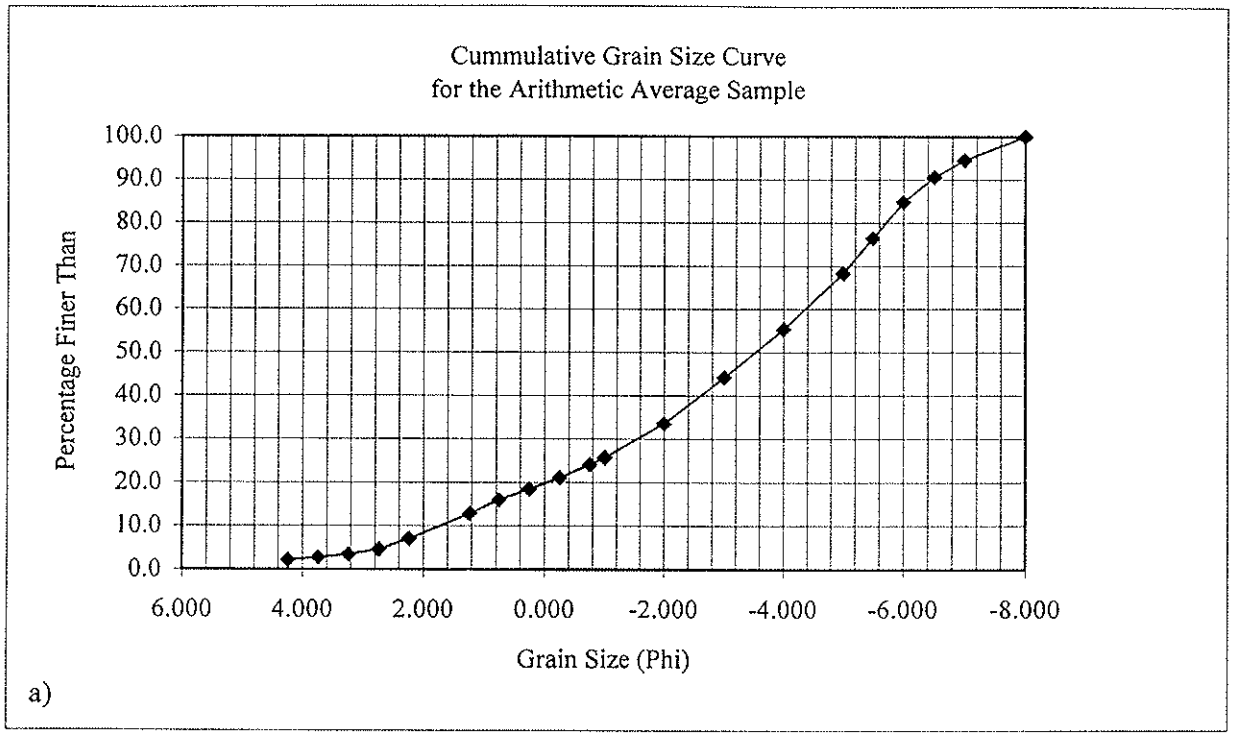

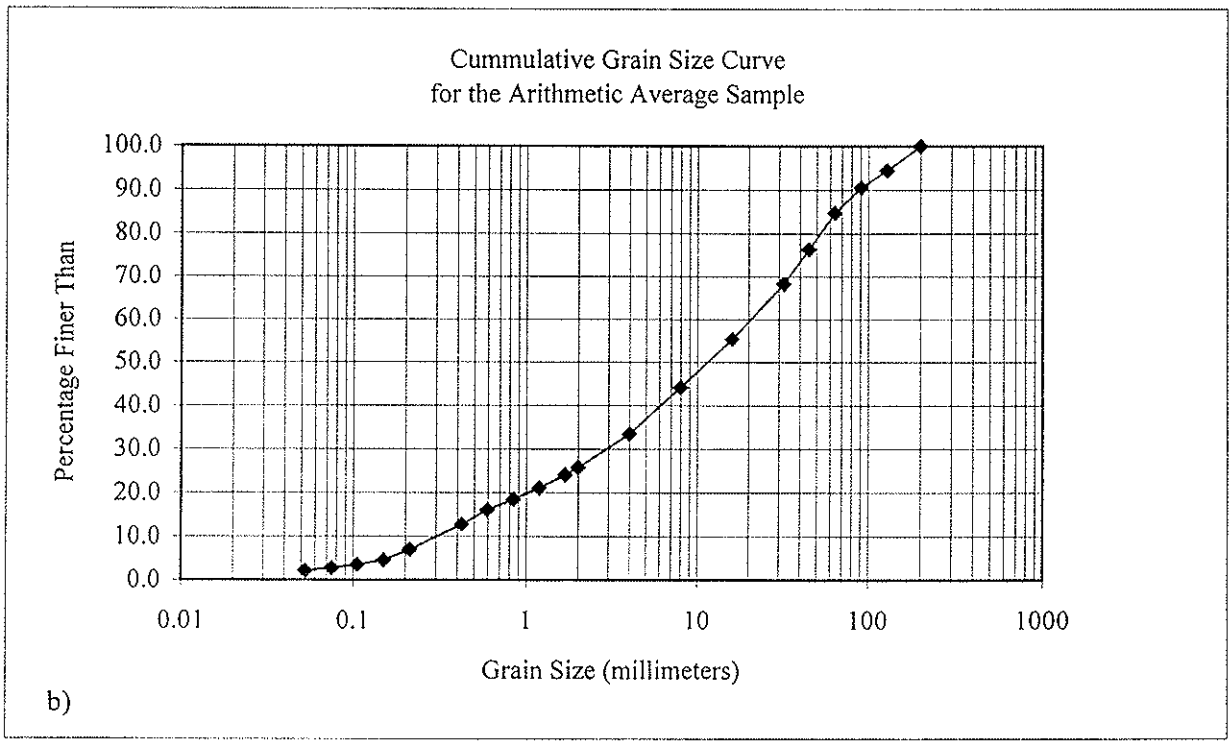

Figure 4.4 Cummulative grain size curve for the arithmetic average sample. The same data is plotted in both graphs but the grain size scale of a) is phi and of b) is millimeters.

4.3 TEXTURAL ANALYSIS OF SEDIMENT

A complete grain size distribution was obtained for size fractions between -.053 mm to 200 mm, a range of 12 ϕ ,by combining the data from the wet field and laboratory sieving as described in the preceeding section. Textural analysis involved plotting the data on cumulative phi-probability plots to determine the size frequency distribution. Differences in texture between samples might indicate different hydraulic or depositional regimes, which were responsible for forming the deposit.

On cumulative probability plots, a single log-normal population will form a straight line. When the data do not form a single line, a "best-fit" model curve can be drawn and it is assumed that populations overlap to form the curve. The following formula can be used to partition the mixture of populations represented by the model curve into its component curves.

$$P_M = f_A P_A + f_B P_B + f_C P_C$$

Where P_M represents the cumulative probability of the mixture of populations, which is represented by the model curve and is the sum of the products of f_A , f_B and f_C, the fractions of each population in the modeled curve, and P_A,P_B, and P_C, the cumulative probability of each component. The fraction of each component in the modal mixture is determined by finding the positive inflection points of the graph, which are considered the points of modal

overlap. The above formula is valid for mixtures comprised of three populations, however, the technique can be used for mixtures of 2 or more populations. When using real data sampling error must be considered and accounted for by selecting a "best fit" curve which models the data. To check the model curve after partitioning into component populations, the populations should be recombined in the estimated proportions (Sinclair, 1976 and per. com. 1996).

4.4 MODEL FITTING SAMPLE DATA

The grain size distribution data for the sixteen samples were plotted on cumulative log-probability plots (Appendix E). Interpretation of the graphs was necessary to determine the number of inflection points and the model that best fits the graphs. Seven samples clearly showed only one inflection point and could be interpreted as bimodal. However, the data from nine of the samples could be interpreted as having one or two inflection points. Consequently, these samples could be interpreted as being bimodal or trimodal. Figure 4.5 shows sample T-12 interpreted as bimodal and trimodal. Schematic representations of the normal distributions that correspond with bimodal and trimodal samples are shown in figure 4.6. Partitioning of these curves identified two populations present in all samples: a fine sediment population designated A and a coarse sediment population designated B. A third population, C, was identified as potentially existing in nine of the sixteen samples.

Population A is dominantly composed of the sand size fractions, is poorly sorted and is interpreted as matrix material. Slightly different proportions of population A are present in

Figure 4.5. Interpretation of data set from sample T-12 as bimodal and trimodal. Sample data are represented by '+', construction points for partitioning are designated by circles. The straight lines indicate the populations A, B and C partitioned from the model curve. Triangles are points from recombining the component populations in the mixture as a test of the model curve.

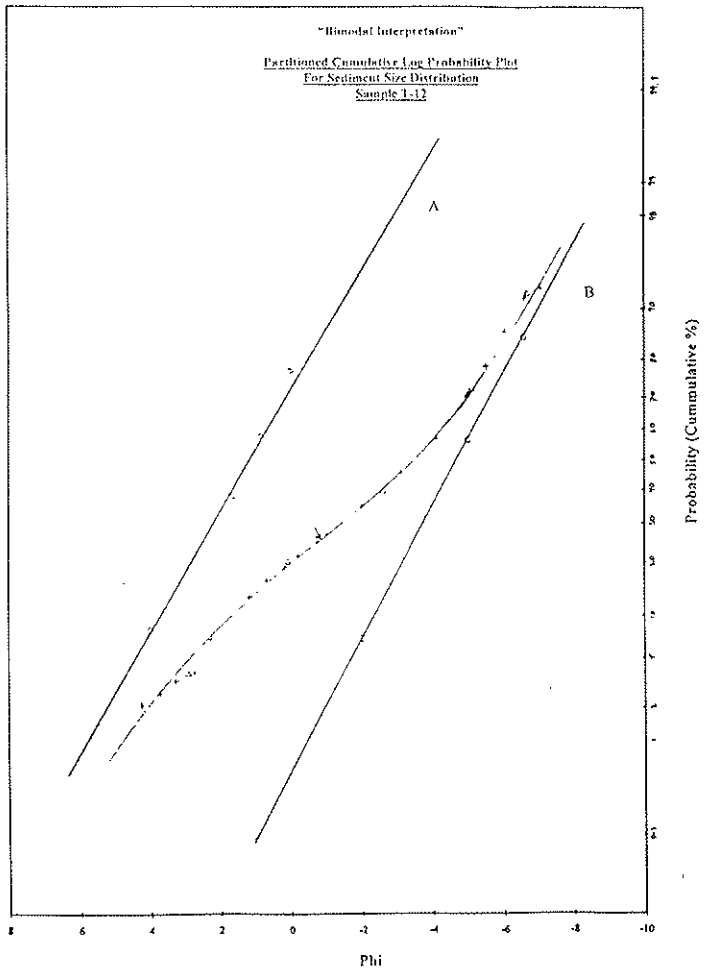

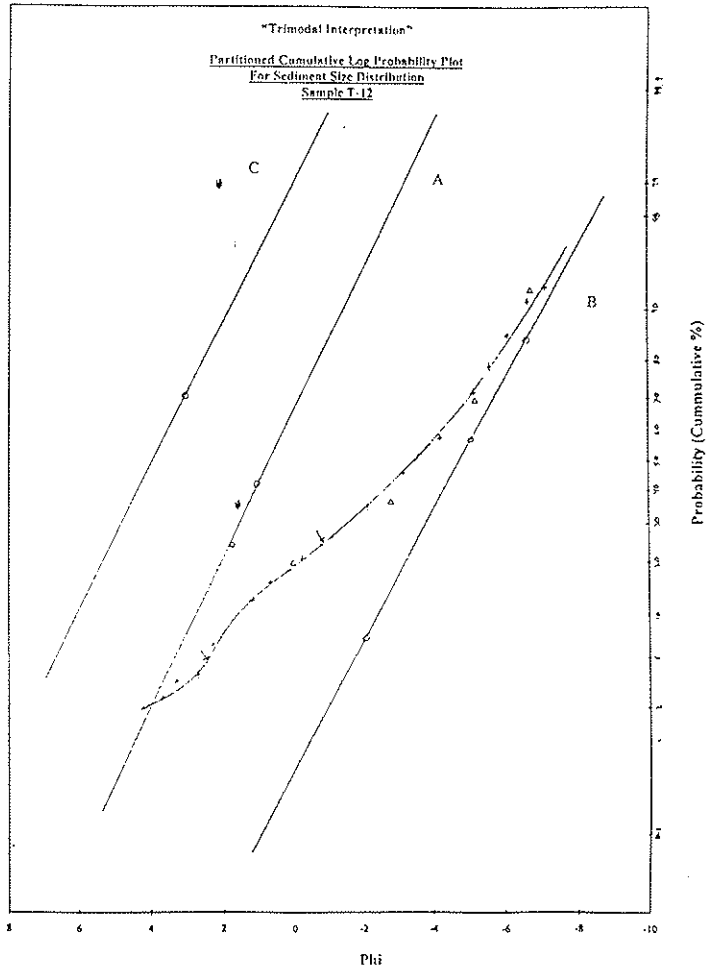

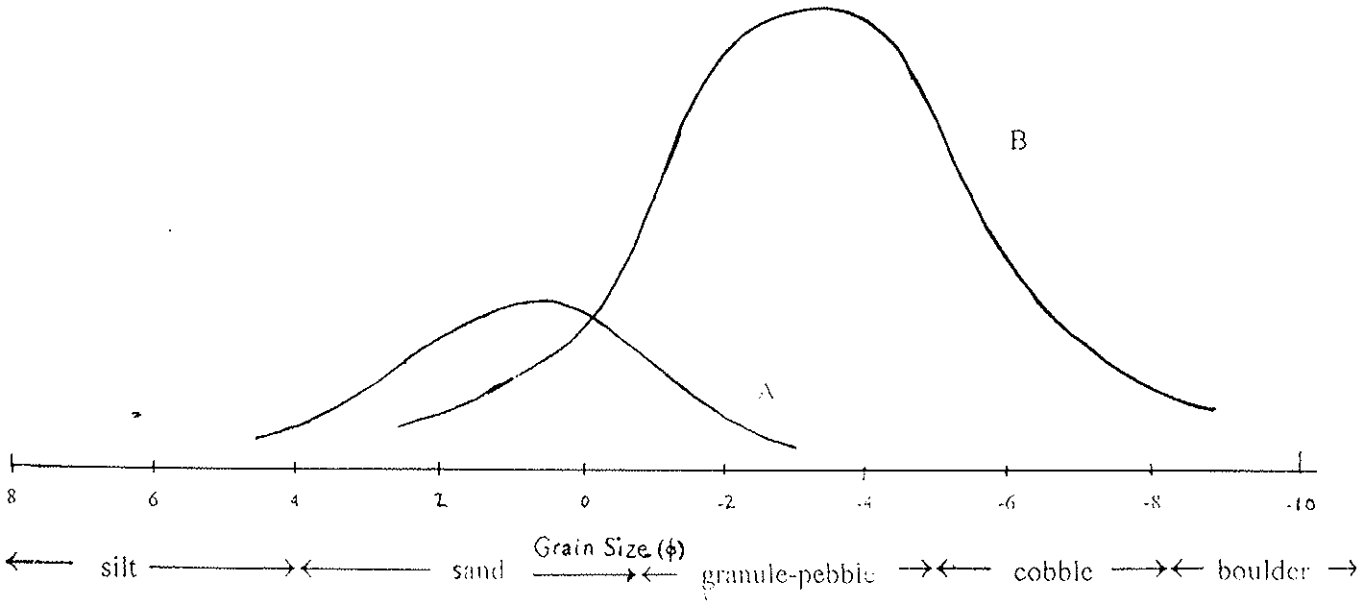

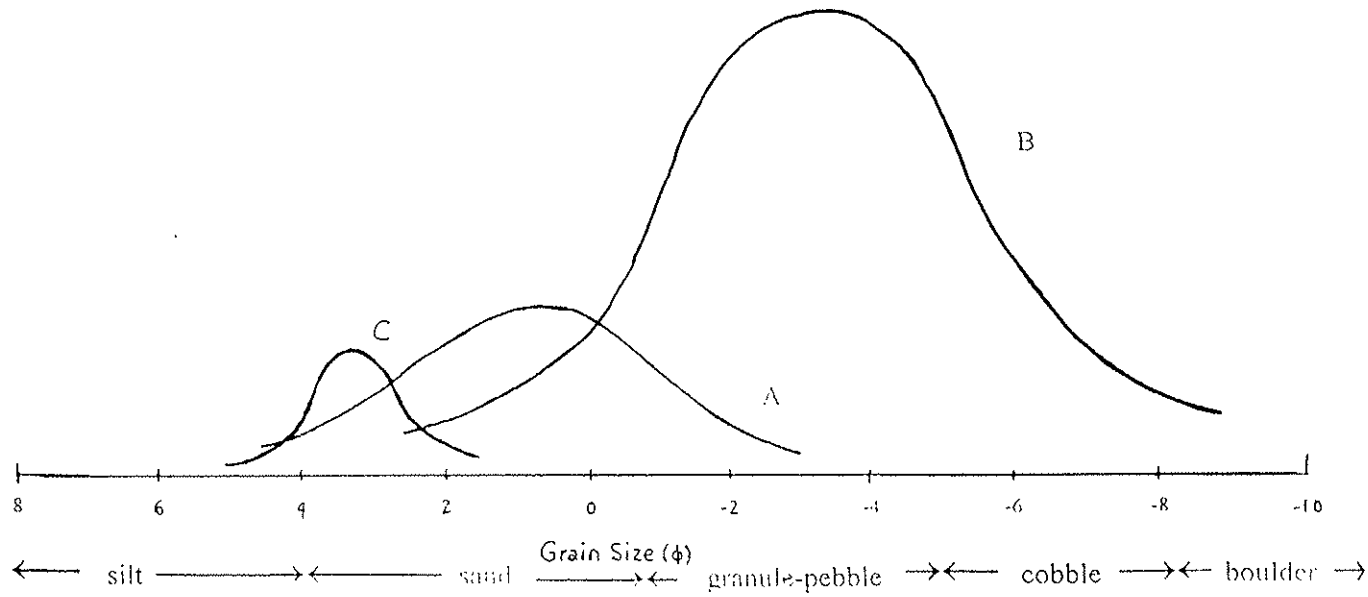

Figure 4.6 Schematic representation of the bimodal and trimodal model. Population A is dominantly composed of the sand size fraction and is interpreted as matrix material, while population B represents the coarse gravel matrix. The third potential population, C, is poorly defined and is found in the silt size fractions.

the samples interpreted as bimodal and trimodal (figure 4.7). The median grain size (D_{50}) of population A in bimodal samples is 1.0ϕ or 0.6 mm and 1.7ϕ or 0.3 mm in the trimodal samples. Population A, on average, comprises 31%, by weight of bimodal samples, and 20%, by weight of trimodal samples.

Population B is the most well defined population and likely represents the coarse gravel framework. It is poorly sorted, σ (standard deviation) = 1.7 (bimodal) - 2.0 (trimodal) with a median grain size (D_{50}) of -5.0 ϕ (31.1 mm) and -4.6 ϕ (24.9 mm), for bimodal and trimodal samples respectively. However, these differences between bimodal and trimodal samples may not be statistically significant. The population forms 69-74 % of the samples by weight. This population is primarily composed of the pebble - cobble size fractions, with a small amount of silt and clay. Boulders may also be present, as is represented by the steepening of the probability curve near the coarse sediment end. The top of the B populations appears to be slightly truncated in the coarse size fractions in approximately 75 % of the samples. It is unknown whether this effect is due to natural processes or to sampling error, although a conscious effort was made to take representative samples and to include all material from large boulders to fine fractions. One large boulder, from the area where there is slight truncation, may weigh between 10-25 kg; a substantial percentage (up to 15 %) of the 150-190 kg samples collected. Such boulders are characteristic of the basal gravels, a feature that is used by miners to identify the "paystreak". Considerable sampling error could have resulted from a single large clast being overlooked or from sampling sites chosen not to include the relatively rare, randomly distributed boulders. Larger samples would be required to construct a grain size distribution in which the coarse size fraction was

Bimodal Samples					
population	average % in mixture	average size which 50 % is finer phi	mm	average standard deviation phi	mm
A	31	1	0.6	2.1	0.23
B	69	-5	31.1	1.7	0.31

Trimodal Samples					
population	average % in mixture	average size which 50 % is finer phi	mm	average standard deviation phi	mm
A	20	1.7	0.3	1.3	0.41
B	74	-4.6	24.9	2	0.25
C	6	2.5	0.18	1.4	0.38

Figure 4.7 Data for populations in the bimodal and trimodal samples. Note the median grain size of the sediments in Populations A and B is less in trimodal samples than is bimodal samples.

represented accurately at the coarse end; therefore, the apparent truncation of the data curves is likely an artificial effect due to non-representative sampling.

Population C forms 6%, on average, of the samples interpreted as trimodal and is characterized by a median grain size (D_{50}) of 2.5ϕ (0.18 mm). The standard deviation , σ_1, of this population is 1.4ϕ, which would also indicate that this population is poorly sorted. Nine out of the 16 samples appear to contain population C. This population shows a lot of variability in its location on the cumulative probability plots. As population C occupies a very small proportion by weight of the overall sample, there are very few data points which characterize this population. Therefore, extrapolation of a model curve for population C on the probability plots is difficult. Thus assumptions must be made for the tail end of the distribution by extrapolating the curve beyond known data points. This may be one reason for the great variability in population C.

Fluvial gravel deposits are typically bimodal with a coarse framework and a finer matrix or infilling material. Consequently, bimodal samples are an expected result in a fluvial environment; however, the trimodal samples require further explanation.

Four potential explanations for the existence of an apparent third population (C) include: (1) an artificial effect on a bimodal sample due to errors in sampling and determination of the grain size distribution, (2) different depositional environments or mechanisms between bimodal and trimodal samples, (3) winnowing of a size fraction from the bimodal population or (4) the apparent addition of a population to the bimodal samples due to weathering and breakdown. These four possibilities are discussed in detail below.

If the graphs that are identified as potentially trimodal are modeled as bimodal samples, without a third population C, the greatest departure of the data from the model curve occurs in the sand and silt size fractions less than ϕ=0.5 (0.7 mm). (Refer to figure 4.5 where sample T-12 was interpreted as bimodal and trimodal) One potential explanation for this deviation from the model curve is that this effect is due to sampling, processing and/or weighing errors. These fine fractions are easily lost in processing and occupy a small mass percentage of the sample. Thus minor losses of material in these size fractions may result in apparently large errors and deviation from a normal distribution when the data are plotted. Alternatively, the deviation from the model curve may have resulted from error in recalculating the total grain size distribution (section 2.2). However, if this were the case, the greatest error or break in the grain size distribution would be expected in the 1.68-2 mm size fraction, which was the size interval where the total grain size distribution was based on the sediment distribution in the field split. The greatest apparent departure from the model curve occurs at values less than 0.7 mm, which is three size fraction interval less than the interval at which the catch-tub and field split distributions were combined. Thus, the interpretation that the samples are bimodal with departure from the model curve in the fine fractions due to errors in sampling or processing is not considered a sufficient explanation for the apparent third population.

When the data are interpreted as trimodal, model curves can be drawn to better fit the data points. Defining the line for the third population C is difficult because there are very few data points in the silt sizes. Thus, the slope of the line was estimated and then the model was tested by recombining the mixture with three proposed populations. If necessary the slope of

population C was adjusted to better fit the model. In general, the recombined trimodal models were found to fit the data.

Different depositional environments, mechanisms or sources are not suspected to have caused the appearance of the third population, since the samples all appeared to be of similar structure. The units were massive and disorganized, with no imbrication or stratification. Lithologies, determined by estimates from photographs of sieved size fractions and from field notes taken during sampling (Appendix A), did not appear to vary significantly between the bimodal and trimodal samples. As the deposit appears massive and disorganized, both rapidly aggrading stream and debris flow events are possible sources for the initial deposit. A debris flow event in the Dominion Valley might have resulted in gravels from high level terraces of "White Channel" mixing with varying amounts of the underlying bedrock before being deposited in the valley. These deposits may have become bimodal or potentially trimodal, owing to the debris flow of a pre-existing fluvial deposit incorporating a third population from another fluvial deposit or incorporation of bedrock in the flow. However, estimated bedrock contents of the samples were not proportional to the percentages of the C population in the samples.

The third possible source of population C is the winnowing of a particle size fraction after deposition from a bimodal deposit. Fluvial reworking of either the entire unit or of the surface portion of each unit may have lead to a selective size fraction being winnowed from the deposit. This effect can be represented by a narrow size fraction that is subtracted from two normal populations (figure 4.8a). Trials to confirm this potential source of the C population were conducted by using a probability plot to remove a size fraction or narrow

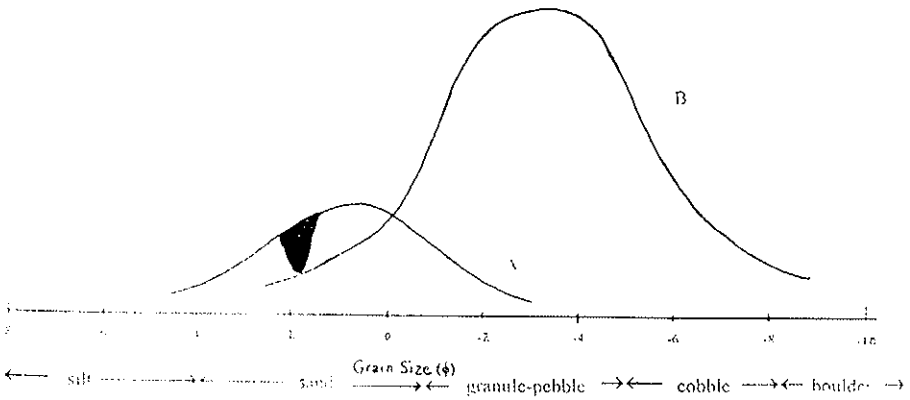

Figure 4.8a

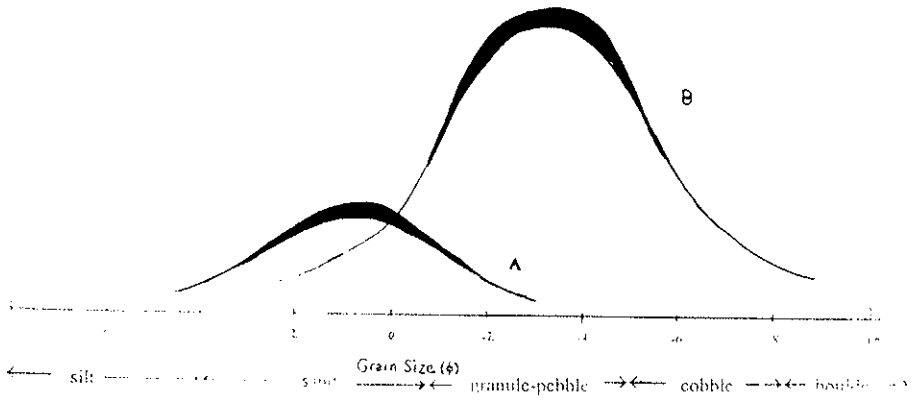

Figure 4.8b

Figure 4.8 Schematic representations of potential origins of population C in the samples. Figure 4.8a shows selectively winnowing a size fraction from a population and figure 4.8b shows weathering of the two populations resulting. The shaded portions of the curves represent the portion of the populations which would be removed in (a) or broken down into finer size fractions in (b).

population "W" from "idealized" A and B populations. This can be represented by the formula:

$$f_A P_{A(ideal)} + f_B P_{B(ideal)} - f_w P_w \Rightarrow f_A P_A + f_B P_B + f_C P_C$$

Plots using this formula were found to model the data and the trimodal interpretation. A problem with this interpretation is that the unit is massive and disorganized, showing little evidence of fluvial reworking. The unit appears to contains a higher percentage of fines than would be expected from fluvial reworking, but comparison of the grain distribution curves with similar curves for gravel stream beds showed that the content of fines in the deposit was not abnormally high.

Population C could also be an apparent population, due to the weathering and breakdown of both populations, A and B, into finer particulate (potentially to as fine as silt sizes). A schematic representation of Population C and modified A and B populations, termed population A' and B', resulting from the breakdown of ideal Populations A and B is shown in figure 4.8b and can be represented by the following formula:

$$f_A P_{A(ideal)} + f_B P_{B(ideal)} + \text{weathering} \Rightarrow f_{A'} P_{A'} + f_{B'} P_{B'} + f_C P_C$$

However, modeling this potential effect was very difficult due to uncertainty in the total amount of weathering and/or breakdown, the size fractions affected and the potential difference between weathering in populations A and B. In situ weathering and breakdown due to mechanical processing during sampling and sieving may also be factors Sediments at

the sampling site are older than 1.22 million years (Morison, 1985). The extensive time period and the lack of glaciation have allowed ample opportunity for chemical and physical weathering of the deposit to occur. Chemical action is evidenced by the oxidation of the upper sediments to an orange color. Cyclic freeze-thaw events have resulted in the growth of ice wedge casts. Decomposed relicts of clasts are present in the deposit and when removed from the wall they quickly break down into finer size fractions. These sediments were mechanically broken down further during sluicing and sieving. Angular bedrock fragments in the deposit are a friable chlorite- muscovite schist, which tends to break down significantly during mechanical processing; the sluicing water turns a gray-green. Consequently, population C may be due to weathering and mechanical processing of the samples and is not a reflection of a true sedimentological population. Potential evidence to support this hypothesis is that the median grain size of the sediments in Populations A and B is less in trimodal samples than it is in bimodal samples (figure 4.7). The median grain size can be expected to decrease in this model as larger sediments break down into smaller size fractions. However, the difference between the median grain sizes of populations A and B in the trimodal and bimodal samples is not sufficiently large to be statistically significant.

4.5 DISCUSSION OF TEXTURE

Basal units sampled in this study appear massive and disorganized with no apparent textural differences between sample locations. However, grain size distributions suggested that sedimentolgical differences might exist within the deposits of the basal unit. Seven samples were identified as being bimodal, while nine were identified as being potentially trimodal The three sediment populations identified were designated A and B, present in all samples,

and C. Population C did not appear to correspond to a particular type of lithology, either from pebble counts nor from visual estimation of percentage of clasts, including estimation of the percentage of bedrock in the sample. As there was no apparent reworking of the deposit by water on the surface or throughout, the selective removal of a particular size fraction due to winnowing is not suspected. The most probable explanation for the apparent presence of a third silt sized population is weathering and breakdown of populations A and B insitu and during processing of the samples. This hypothesis, however, can not be confirmed at this time since none of the explanations in the preceding section are conclusive. Further investigation is required to ascertain the origin of population C in the basal units of the Dominion Creek deposit.

5.0 GOLD GRAIN SIZE DISTRIBUTION

Gold analysis by FA-AAS was done for six size fractions from -53μm to 425μm for both the long-tom concentrate samples and the catch-tub samples. This chapter discusses how the gold concentration values from the two samples were recombined in proportion to reconstruct the mass and concentration of gold in the original sample. The total gold in the sample can then be represented by either the relative concentration of gold or by the weight of gold. Error bounds on the gold concentration were calculated with the Poisson Distribution by determining the number of particles of gold in the analytical portions.

5.1 CALCULATION OF GOLD GRAIN SIZE DISTRIBUTION

The total mass of gold in the field samples was determined by assuming that it was the sum of the mass of gold in the long-tom concentrate and the mass of the gold in the catch-tub. It was further assumed that the gold concentrations in the analytical portions were representative of the gold concentrations in the long-tom concentrate and the catch-tub samples (i.e. splitting of samples was representative; nugget effects are ignored). For most samples in the size fractions less than 0.212 mm, the analytical portion was sufficiently large to analyze the entire sample Therefore, it is a valid assumption that by analyzing both the long-tom and catch-tub samples, the total gold content of the original sample can be

obtained. Where duplicate gold analyses exist, the mean of the two duplicates was taken as the "true" concentration and where analytical results returned a value of <5ppb, a value of 2 ppb was assigned.

The formulae and definitions of variables for these calculations are as follows:

$Mg_{(LT)i}$ - Mass of gold in long-tom of size fraction i
$Mg_{(CT)i}$ - Mass of gold in catch-tub of size fraction i
$Mg_{(tot)i}$ - Mass of gold of size fraction i in the total sample
$Ms_{(LT)i}$ - Mass of sediment in long-tom of size fraction i
$Ms_{(CT)i}$ - Mass of sediment in catch-tub of size fraction i
$Ms_{(tot)i}$ - Mass of sediment of size fraction i in the total reconstructed grain size distribution in the sample
$Cg_{(LT)i}$ - Concentration of gold in long-tom samples
$Cg_{(CT)i}$ - Concentration of gold in catch-tub
$Cg_{(tot)ii}$ - Concentration of gold of size fraction i in sediments of size fraction i in the sample

The total mass of gold in the sample is calculated by:

$$Mg_{(tot)i} = Mg_{(CT)i} + Mg_{(LT)i} \text{ (for } i < 0.425 \text{ mm)}$$

$$[mg] = [mg] + [mg]$$

where

$$Mg_{(LT)i} = Cg_{(LT)i} \times Ms_{(LT)i} \times 10^{-6}$$

$$[mg] = [ppb] \times [g] \times 10^{-6}$$

$$Mg_{(CT)i} = Cg_{(CT)i} \times Ms_{(CT)i} \times 10^{-3}$$

$$[mg] = [ppb] \times [kg] \times 10^{-3}$$

The mass of gold in each size fraction can then be converted to the concentration of gold in that fraction by the formula:

$$Cg_{(tot)ii} = Mg_{(tot)i} \times 10^{-3} / Ms_{(tot)i}$$

$$[ppb] = [mg] \times 10^{-3} / [kg]$$

The concentration of a certain size fraction of gold in the whole sample can be found by:

$$Cg_{(tot)i} = Mg_{(tot)i} \times 10^{-3} / Ms_{(tot)\ all\ sizes}$$

$$[ppb] = [mg] \times 10^{-3} / [kg]$$

The concentration of gold with grain sizes less than 0.595 mm in the whole sample can be found by the formula:

$$Cg_{(tot)i} = Mg_{(tot),\ 0.595mm} \times 10^{-3} / Ms_{(tot)\ all\ sizes}$$

$$[ppb] = [mg] \times 10^{-3} / [kg]$$

5.2 DETERMINING ERROR BOUNDS IN GOLD ANALYSES

Determining error bounds on gold concentrations is essential in ascertaining if variation in gold concentrations between samples is due to natural variation, or to analytical errors. In this study, gold concentrations were calculated by combining the results of the long-tom and

the catch-tub samples analyses. Combining the error from these two analytical results poses a problem. The total variance in gold concentration can be attributed to three sources: the natural variation between samples due to variability in gold content in the deposit; the variation due to sampling and geochemical analysis of the long-tom samples, and the variation due to sampling and geochemical analysis of the catch-tub samples.

$$\sigma^2 = \sigma^2 \text{ (natural)} + \sigma^2 \text{ (long-tom)} + \sigma^2 \text{ (catch-tub)}$$

Thus, to evaluate the natural variation among samples, knowing the total variation in the analytical results, the variation for the long-tom and the catch-tub results must be estimated.

As gold content of each size fraction is calculated by proportionally combining the values of gold recovered in the long-tom concentrate and catch-tub, the error on the total gold values must also be calculated by proportionally combining the errors from the two gold sources. Generally, the long-tom has a higher concentration of gold than the catch-tub; therefore, the absolute error expected from the long-tom analytical results should be greater than the error from the catch-tub analytical results. However, the relative error in the catch-tub is expected to be higher than in the long-tom, due to the "nugget" effect from the low number of gold particles. In both samples, the number of particles of gold in the analytical portion is the principle source of error in the analytical results. An estimation of the combined error can be found by determining the hypothetical number of particles, which would be in an analytical portion of the original sample. The number of particles in the original sample can be approximated by converting the concentrations of gold from the analytical results to the number of particles of gold in the analytical portions for both the catch-tub and long-tom

concentrate and finding the sum . The asymmetric Poisson Distribution can then be used to find the error bounds based on the number of particles which would be in a sub-sample of the original sample.

For samples less than 0.150 mm, where the sample was sufficiently small that the whole size fraction could be analyzed, the calculated error is an estimate of whether the original sample was large enough to obtain representative gold analyses. The two coarser size fractions, however, required splitting and subsampling to obtain 30 gram analytical portions. Error bounds determined for these size fractions (0.150-0.495 mm) are affected by both subsampling and the size of the original sample. Differentiating and proportioning the error to these sources in order to evaluate the size of the original sample is not possible.

5.2.1 Calculation of the Number of Particles of Gold

Prior to calculating the number of particles of gold in each size fraction, it was necessary to make several key assumptions. Gold had to be assumed to occur as discrete particles within the sample (not attached to other rocks and minerals). Based on this assumption, further assumptions regarding the shape and size of the gold particles could be made.

Gold in Dominion Creek is typically found as flakes, but may also be found as rods or spheroids. In section 2, the Corey Grain Shape Factor, CSF, was presented as a means to quantitatively characterize the shape of a non-spherical particle in relation to a sphere. Data from another study in the locality and rough data from coarse gold from this study suggested

a CSF value of 0.2 to be reasonable. This implies that the average particle has a volume of 0.2 times that of a sphere of equivalent diameter (refer to section 2 for calculations of CSF).

Following assumptions about the shape of particles, a size for gold particles within the size fraction had to be estimated. The average particle diameter, d, for a given size fraction is the logarithmic average of the bounding sieve sizes.

$$\log d = (\log (US) + \log (LS)) / 2$$

US = Upper boundary sieve size

LS = Lower boundary sieve size

For the size fraction less than 0.053 mm, there was no lower bounding sieve to calculate an average. A diameter of 0.020 mm was selected arbitrarily as the average diameter for this size range (Day, 1988). For the purposes of this study, the density of gold is assumed to be 17 g/cm^3 . This value was based on an average assay purity of 85% Au from the producing mine at this location, with silver as the principle impurity.

Variables used in the calculation:

$Cg_{(LT)i}$ - Concentration of gold in long-tom samples
$Cg_{(CT)i}$ - Concentration of gold in catch-tub
CSF - Corey Grain Shape Factor (Assumed: 0.2)
d - logarithmic average gold grain diameter
$Mg_{(LT)i}$ - Mass of gold in long-tom of size fraction i
$Mg_{(CT)i}$ - Mass of gold in catch-tub of size fraction i
$Mg_{(tot)i}$ - Mass of gold of size fraction i in the total sample
$Ma_{(LT)i}$ - Mass of analytical portion for long-tom of size fraction i
$Ma_{(CT)i}$ - Mass of analytical portion for catch-tub of size fraction
$Pg_{(CT)i}$ - Number of particles of gold in the analytical portion of the catch-tub
$Pg_{(LT)i}$ - Number of particles of gold in the analytical portion of the long-tom
$Pg_{(tot)i}$ - Number of particles of gold in analysis of the long-tom and catch-tub
ρ_g - density of gold (Assumed : 17 g/cm^3)

To find the number of particles of gold in the long tom analytical portions:

$$Pg_{(LT)i} = Cg_{(LT)i} \times Ma_{(LT)i} \times 10^{-12} / \rho_g \times (4/3 \times CSF \times \pi (d/2)^3)$$

$$[\text{unitless}] = [\text{ppb}] \times [\text{g}] \times 10^{-12} / [\text{g/cm}^3] \times [\text{mm}^3]$$

Similarly, to find the number of particles of gold in the catch tub analytical portions:

$$Pg_{(CT)i} = Cg_{(CT)i} \times Ma_{(CT)i} \times 10^{-12} / \rho_g \times (4/3 \times CSF \times \pi (d/2)^3)$$

The combined number of particles in the two analytical portions is given by:

$$Pg_{(tot)i} = Pg_{(LT)i} + Pg_{(CT)i}$$

Table 5.1 shows the results of these calculations and the number of particles of gold in the long-tom and catch-tub samples. However, these calculations can be greatly influenced by changes in the assumed shape and size of the gold particles in the analytical portion. The CSF is used to account for the non-spherical nature of particles in the calculations. For the Dominion Creek gold the exact value is uncertain and may vary. The significance of changing the grain shape factor is illustrated in Table 5.2, where the number of particles of gold in a subsample of the long-tom concentrate is calculated for several CSF's and for spheres. From this table it is evident that the shape factor for particles of gold greatly influences the results of these calculations. If particles are considered to be discs with a width to diameter ratio of 1:5 rather than spheres, then the number of gold particles in the

Table 5.1 Number of particles of gold in the long-tom, catch-tub and in the original sample (combined results of the long-tom and the catch tub) sample.

	0.212-0.425 mm			0.150-0.212 mm			0.106-0.150 mm			0.075-0.106 mm			0.053-0.075 mm		
Sample #	LT+ CT	LT	CT	LT+ CT	LT	CT	LT+ CT	LT	CT	LT+ CT	LT	CT	LT+ CT	LT	CT
1	0.83	0.83	0.0019	3.49	2.62	0.8692	2.36	2.34	0.0189	6.14	6.12	0.0222	10.03	9.52	0.5124
2	1.08	1.07	0.0004	0.04	0.04	0.0000	4.86	4.86	0.0010	4.09	4.04	0.0516	11.79	11.68	0.1086
3	0.21	0.21	0.0004	0.24	0.23	0.0093	1.69	1.69	0.0011	2.77	2.76	0.0097	11.55	11.51	0.0307
4	1.26	1.26	0.0002	2.72	2.70	0.0130	0.02	0.01	0.0105	5.43	5.38	0.0508	9.08	8.92	0.1542
5	0.30	0.30	0.0004	0.93	0.85	0.0817	7.12	7.11	0.0105	11.07	11.03	0.0474	49.31	49.16	0.1498
6	0.81	0.81	0.0002	0.95	0.92	0.0241	2.29	1.60	0.6933	11.03	5.51	5.5130	11.43	5.91	5.5130
7	0.23	0.23	0.0002	0.50	0.47	0.0279	7.43	7.43	0.0003	12.39	12.39	0.0012	21.60	21.60	0.0016
8	1.39	1.39	0.0002	1.26	1.22	0.0353	3.14	3.04	0.1051	5.98	5.91	0.0638	10.15	9.68	0.4775
9	0.91	0.91	0.0002	0.65	0.65	0.0037	22.00	21.96	0.0434	63.32	63.30	0.0171	66.24	65.89	0.3467
10	0.71	0.71	0.0008	3.87	3.86	0.0037	2.63	2.29	0.3358	5.55	4.78	0.7602	11.17	10.85	0.3157
11	1.79	1.74	0.0409	4.32	3.53	0.7949	2.45	2.44	0.0124	6.18	6.12	0.0608	17.62	17.61	0.0098
12	2.55	2.55	0.0002	0.97	0.96	0.0178	8.53	8.53	0.0056	18.52	18.49	0.0318	48.92	48.91	0.0025
13	0.78	0.78	0.0002	2.26	2.25	0.0093	6.12	6.11	0.0032	14.51	14.50	0.0059	32.03	32.02	0.0055
14	2.08	2.08	0.0000	1.06	0.85	0.2106	3.01	3.00	0.0093	1.22	1.17	0.0483	12.24	12.19	0.0570
15	0.51	0.51	0.0019	0.37	0.37	0.0056	5.65	5.64	0.0053	15.71	15.69	0.0211	58.38	58.24	0.1419
16	0.67	0.67	0.0002	1.63	1.39	0.2377	5.53	5.41	0.1258	12.44	12.22	0.2163	37.06	36.41	0.6549
Average	1.01	1.00	0.0030	1.58	1.43	0.15	5.30	5.22	0.09	12.27	11.84	0.43	26.16	25.63	0.5301

Table 5.2 The effects of considering gold particles as flakes, with various Corey Shape Factors (CSF), compared to considering them as spheres, in calculations for the number of particles in the average analytical portion. From this table it can be seen that the calculated number of particles increase by 6 times for calculations using flakes, rather than spheres. The number of particles calculated also changes greatly for small changes in the CSF.

	Number of Particles in the Average Analytical Portion			
	For the Value of Corey Shape Factor			For
Size Fraction	0.15	0.2	0.25	spheres
0.212 - 0.425 mm	1.3	1.0	0.8	0.2
0.150 - 0.212 mm	1.9	1.4	1.2	0.29
0.106 - 0.150 mm	7.2	5.4	4.3	1.1
0.075 - 0.106 mm	16.3	12.2	9.8	2.4
0.053 -0.075 mm	48.5	36.4	29.1	7.3
-0.053 mm	1333.3	1000.0	800.0	200

analytical portion will increase by as much as six times. A change in the CSF of 0.05 can appreciably change the calculated number of particles.

The calculation of the number of particles was also based on the assumption that the diameter of gold particles was equal to the logarithmic mean of the bounding sieve openings for each size fraction. However, trial calculations (Table 5.3) showed that the diameter used greatly affected the results. Calculations showed that changing the particle diameter from the upper to the lower bounding sieve produced results differing by approximately 300 % for particle sizes above 0.053 mm. From these results it is obvious that shape and grain diameter of gold particles greatly effects the results of these calculations. Appendix G contains tables used in the calculations of these results.

Table 5.3. The effects of changing the assumed gold grain size diameter on the calculated number of particles in the analytical portion. Calculations using the particle diameter of the upper and lower bounding sieve increases the calculated number of gold particles by approximately 300 %, for particle sizes above 0.053 mm. Number of particles are based on the average number of particles in each size fraction

Size Fraction	Average Concentration (ppb)	Number of Particles in the Average Analytical Portion For different particle diameters		
		Upper Size	Average (log)	Lower Size
0.212 - 0.425 mm	1889	0.4	1.0	2.9
0.150 - 0.212 mm	934	0.9	1.4	2.4
0.106 - 0.150 mm	512	3.2	5.4	9.1
0.075 - 0.106 mm	281	7.3	12.2	20.5
0.053 -0.075 mm	191	21.6	36.4	61.3
-0.053 mm	199	18.9	1000.0	-

5.2.2 Calculation of Error Bounds with the Asymmetric Poisson Distribution

In the Poisson Distribution, the variance, σ^2, equals the mean, μ ($\mu = \sigma^2$). This property can be used to estimate confidence limits on a population. The upper (L_2) and lower (L_1) confidence limits are asymmetric around a parameter ($L_1 \leq \mu \leq L_2$), and can be estimated using the standard deviation, σ, calculated with the Poisson distribution for the 1-α confidence level by the following formulae (Zarr, 1984):

L_1 : Lower 1-α Confidence Limit

$$L_1 = \chi^2_{(1-\alpha/2),\nu}/2 \ ; \ \text{where} \ \nu = 2X$$

L_2 : Upper 1-α Confidence Limit

$$L_2 = \chi^2_{(\alpha/2),\nu}/2 \ ; \ \text{where} \ \nu = 2(X+1)$$

where:

X = number of particles in the combined analytical portions

$\chi^2_{\alpha,\nu}$ = The value of the Chi-Squared Distribution which has α probability of being exceeded, with ν degrees of freedom.

If the combined number of particles is considered to be the mean number of particles in a sample at that location, then it can be assumed to be the mean of a Poisson distribution which can then be used to estimate the sampling error. Table 5.4 shows the calculated upper and lower limits for the number of gold particles in the sample. These confidence limit calculations can be found in Appendix G. The upper and the lower limits were then

Table 5.4 Results of calculations of the upper and lower error bounds in terms of particles of gold using the asymmetric Poisson Distribution. (units ppm)

	212-425			150-212			106-150			75-106			53-75			<53		
	LT+CT	LL	UL	LT+CT	LL	UL	LT+CT	LL	UL	LT+CT	LL	UL	LT+CT	LL	UL	LT+CT	LL	UL
1	19.1	32.0	45.7	16.9	12.2	13.5	4.0	1.0	4.3	2.4	0.6	1.3	1.4	0.3	0.6	1.2	0.1	0.1
2	24.8	40.0	50.3	0.2	6.7	8.4	6.3	1.7	4.1	1.7	0.5	1.3	1.0	0.2	0.4	0.7	0.1	0.1
3	4.8	32.0	40.0	1.2	6.7	8.4	2.2	0.5	3.0	1.1	0.3	1.1	0.8	0.2	0.3	0.7	0.1	0.1
4	29.2	40.0	50.3	13.2	11.4	12.9	0.0	0.1	2.2	2.2	0.6	1.3	0.9	0.2	0.4	0.8	0.1	0.1
5	7.0	32.0	40.0	4.5	6.7	9.6	12.2	3.1	6.2	6.2	1.4	2.4	5.1	0.6	0.8	0.8	0.1	0.1
6	18.7	32.0	45.7	4.6	6.7	9.6	3.9	1.0	4.3	6.0	1.4	2.3	2.3	0.5	0.9	0.1	0.0	0.0
7	5.3	32.0	40.0	2.4	6.7	8.4	12.7	3.1	6.2	6.4	1.4	2.3	3.2	0.6	0.8	1.6	0.1	0.1
8	32.0	40.0	50.3	6.1	8.4	10.6	3.0	0.9	2.7	2.2	0.5	1.2	1.2	0.3	0.5	1.3	0.1	0.1
9	21.0	32.0	45.7	3.2	6.7	9.6	37.7	6.5	9.5	32.9	3.7	4.6	6.7	0.7	0.9	44.0	0.2	0.2
10	16.5	32.0	45.7	18.7	12.9	14.1	3.6	1.0	3.6	2.3	0.6	1.4	0.8	0.2	0.3	1.7	0.1	0.1
11	41.3	45.7	54.4	21.0	13.5	14.7	3.0	0.7	3.1	2.8	0.7	1.6	2.0	0.4	0.6	2.7	0.2	0.1
12	58.9	54.4	61.3	4.7	6.7	9.6	10.8	2.6	4.9	7.4	1.4	2.1	4.5	0.6	0.7	2.5	0.1	0.2
13	18.0	32.0	45.7	10.9	10.6	12.2	7.1	1.9	4.0	5.6	1.1	1.8	3.9	0.6	0.8	2.4	0.1	0.1
14	48.1	50.3	58.0	5.1	8.4	10.6	4.2	1.2	3.8	0.7	0.1	1.3	1.7	0.4	0.6	0.8	0.1	0.1
15	11.9	32.0	45.7	1.8	6.7	8.4	6.3	1.7	3.7	5.8	1.1	1.8	6.9	0.8	1.0	5.5	0.2	0.1
16	15.4	32.0	45.7	7.9	9.6	11.4	9.5	2.6	5.7	4.8	1.0	1.7	5.1	0.7	1.0	4.5	0.1	0.1
Average	23.2	36.9	47.8	7.6	8.8	10.7	7.9	1.9	4.5	5.7	1.0	1.8	3.0	0.5	0.7	4.5	0.1	0.1

converted from the number of particles of gold to concentrations of gold and the error bounds were plotted (figure 5.1 and 5.2). As expected, the error bounds decrease as the gold grain size decreases and the average number of particles in the analytical portion increases. This is due to error in the measurement of gold concentration decreasing as the number of particles in the analytical portion increases. As the proportion of variability attributed to sampling and analytical error decreases, the natural variability between samples becomes more apparent. From these graphs it is clear that the error bounds on the 0.212-0.425 mm and 0.150-0.212 mm size fractions are sufficiently large that natural variability between sample sites is likely masked by the analytical error. The error bounds on the -0.150 mm size fractions are smaller than the apparent variability between samples. Therefore, meaningful correlations and comparisons of data will likely result only from the gold values for sediment fractions -0.150 mm.

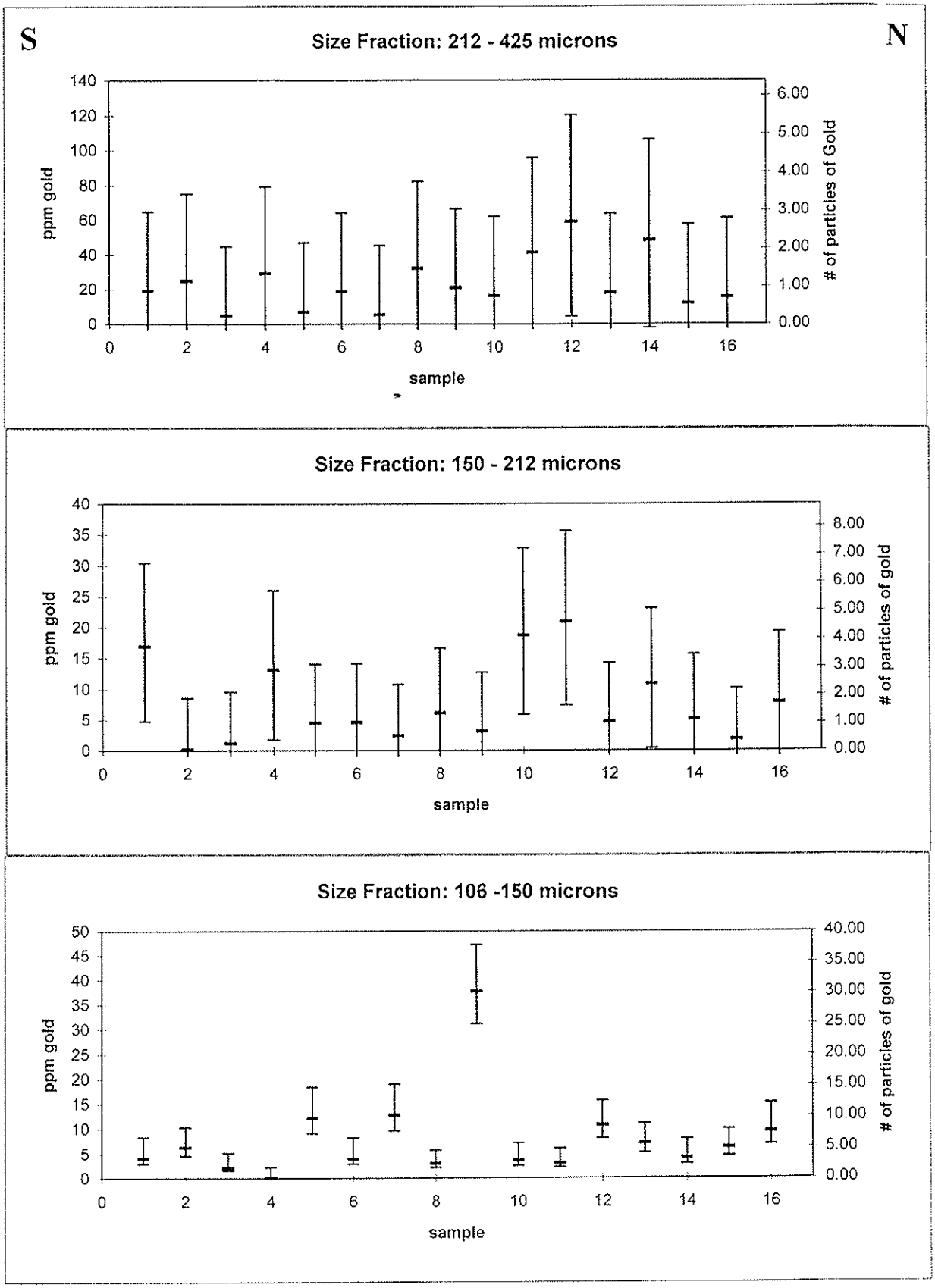

Figure 5.1 Graphs of gold concentration versus samples for the 0.212-0.425 mm, 0.150-0.212 mm, and 0.106 -0.150 mm size fractions, showing asymmetric Poisson error bounds on gold concentrations calculated from combined analytical results for the long-tom and catch tub. Note the change of concentration scale for each graph. The left axis is the number of particles of gold for the average concentration. The limits of the error bounds are not accurately represented by this axis.

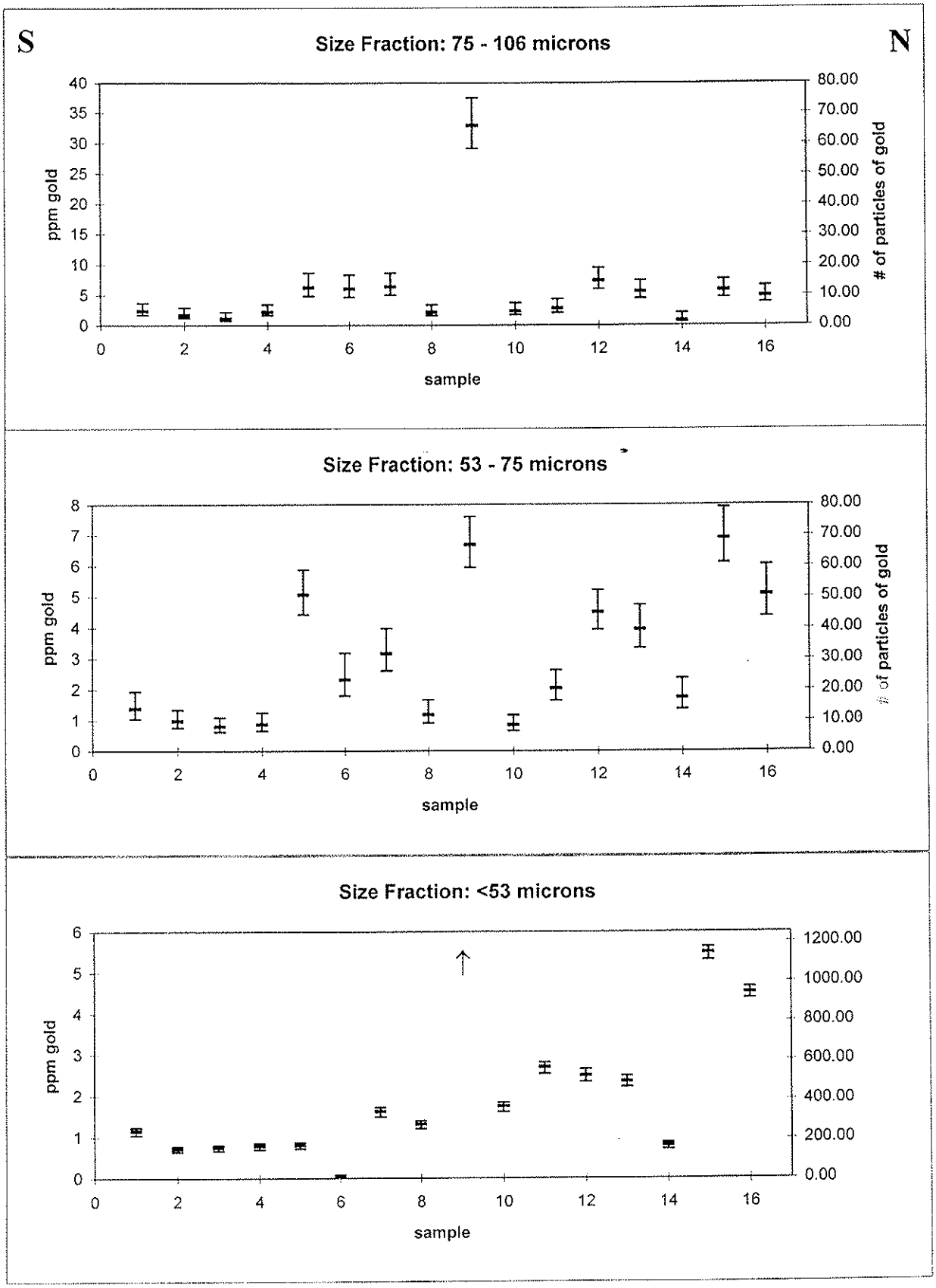

Figure 5.2 Graphs of gold concentration versus samples for the 0.075-106 mm, 0.053-0.075 mm, and -0.053 mm size fractions, showing asymmetric Poisson error bounds on gold concentrations calculated from combined analytical results for the long-tom and catch tub. Note the change of concentration scale for each graph. The left axis is the number of particles of gold for the average concentration. The limits of the error bounds are not accurately represented by this axis. Arrows represent concentrations exceeding limits of axis scale.

6.0 RELATIONSHIPS BETWEEN GOLD CONCENTRATIONS, TEXTURE AND SAMPLING SITES

After reconstruction of gold concentrations for the samples and the determination of whether natural variability between samples could be distinguished from analytical and sampling errors, other relationships among gold values, texture and sampling locations and among the sample descriptions were sought. Relations among these factors and gold values might give insight into the depositional environment and origin of this gold deposit. Gold concentrations from analysis of the size fractions greater than 0.150 mm were not considered, as error bounds were found to mask natural variability. Thus, only four size fractions were considered in these relations: -0.053 mm, 0.053-0.075 mm, 0.075-0.106 mm, and 0.106-0.150 mm.

6.1 GOLD TRENDS ALONG THE CUT WALL

Total concentrations of gold in the samples and the concentrations of gold for each size fraction were plotted for the location of the sample along the cut wall (Figure 6.1). The results showed high variability along the section, with no consistent increasing or decreasing trends for total gold in the sample or for gold in any particular size fraction. An anomalously high gold concentration for all size fractions was returned for sample site T-9, at 170 meters. This sample location is adjacent to a portion of the pit that was found to be "high grade" during mining.

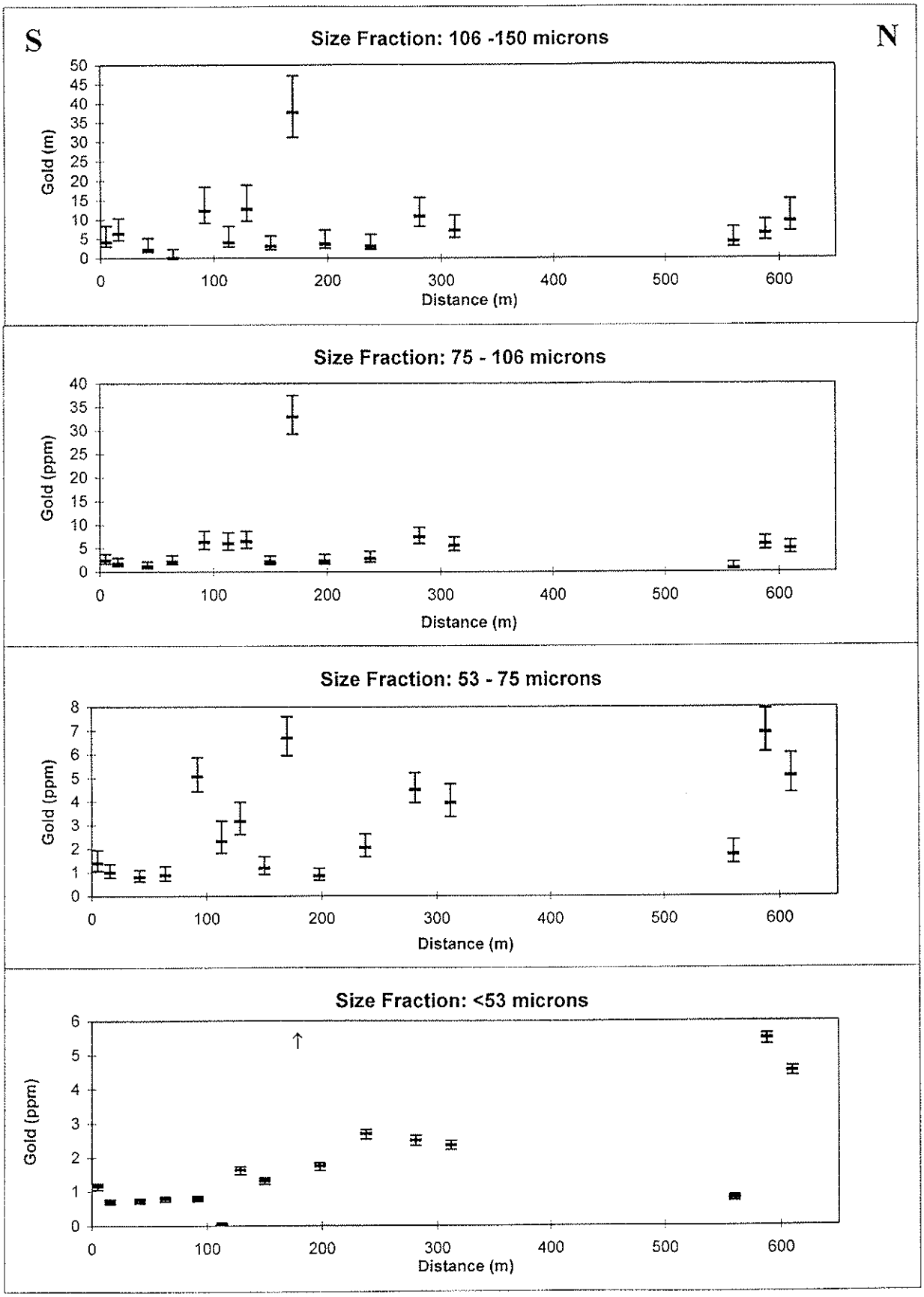

Figure 6.1 Profile of gold concentrations for various size fractions versus distance upstream. Note the graphs have different concentration scales and arrows represent concentrations exceeding limits of axis scale.

6.2 CORRELATION VALUES

Correlations between sediment size fractions and gold size fractions may give an indication of processes involved in the formation of the deposit. However, prior to using linear correlation as a tool in data analysis, the associated problems must be considered. Linear correlation expresses the tendency of two variables to form a straight line; therefore, outliers have a significant effect on correlation values. Spurious data may also result when using a closed data set, such as the data set in this study, where variables are expressed as percentages.

For each size fraction the gold concentrations were correlated with the percent mass of sediment for each size fraction. Positive and negative statistically significant correlations, at the 90 % confidence level, were found to exist within all samples, within the group of samples determined to be bimodal and within the group of samples determined to be trimodal. Table 6.1 shows the correlations, with the statistically significant correlations highlighted. The degrees of freedom for each group of samples and the corresponding value of the correlation constant, r, at the 90% confidence level are also found in Table 6.1.

On the corrrelations matrices three prominent features are evident. First, positive statistically significant correlations exist for gold size fractions and the abundance of sediments 2-4 size fractions larger, while negative correlations exist between gold size fractions and the abundance of sediment of the same size. These correlations are present for gold size fractions between 0 - 0.150 mm in the correlation matrices of all of the samples, the bimodal samples and the trimodal samples. They are most prominent in the matrix of trimodal samples where high positive correlations exist for sediments 3 sizes larger than gold particles and large

Table 6.1 Correlations between concentration of gold in size fractions less than 0.150 mm and percentage of sediment size fractions in the total samples. Strong correlations are shaded and correlations between a sediment size and the same gold size are boxed. Correlations were calculated for all of the samples together, and for the divisions of bimodal and trimodal samples established in textural analysis.

ALL SAMPLES

Correlations at the 90 % significance level, r = 0.4

Degrees of Freedom = 16

Sediment	Gold Size Fractions (Microns)			
Sizes (mm)	106-150	75-106	053-75	-53
(+128)	0.226	0.204	-0.250	-0.481
91 - 128	-0.281	-0.265	-0.092	0.166
64 - 91	0.260	0.183	-0.019	0.117
45 - 64	-0.050	0.103	-0.370	0.429
32 - 45	-0.185	-0.344	0.299	-0.013
16 - 32	-0.212	-0.130	0.190	0.349
(8 - 16)	-0.164	-0.042	0.479	0.450
(4 - 8)	-0.363	-0.191	0.341	0.205
(2 - 4)	-0.102	-0.228	0.169	-0.376
1.68-2	-0.197	0.039	-0.042	0.378
1.19-1.68	-0.021	-0.020	-0.273	-0.025
.841-1.19	0.284	0.173	-0.141	0.024
.595-.841	0.357	0.158	-0.112	-0.164
.425-.595	0.585	0.455	-0.013	-0.224
.212-.425	0.507	0.548	-0.101	0.095
.15-.212	-0.072	-0.271	0.459	-0.285
.106-150	-0.261	-0.147	-0.348	0.435
.075-.106	-0.341	-0.338	-0.227	0.152
.053-.075	-0.098	-0.109	-0.388	0.249
0-.053	0.269	0.032	-0.030	-0.114

BIMODAL SAMPLES

Correlations at the 90 % significance level, r = 0.582

Degrees of Freedom = 7

Sediment	Gold Size Fractions (Microns)			
Sizes (mm)	A-106-150	A-75-106	A-053-75	A-53
(+128)	0.424	0.038	0.231	-0.614
91 - 128	-0.376	-0.415	-0.091	-0.048
64 - 91	0.770	0.388	0.631	0.005
45 - 64	0.706	0.779	0.570	0.306
32 - 45	0.091	0.141	-0.029	0.152
16 - 32	-0.334	-0.001	-0.050	0.733
(8 - 16)	-0.162	0.361	0.208	0.804
(4 - 8)	-0.775	-0.603	-0.699	0.013
(2 - 4)	-0.612	-0.865	-0.684	-0.461
1.68-2	0.042	0.568	0.245	0.277
1.19-1.68	0.020	0.288	-0.128	-0.251
.841-1.19	0.036	0.402	0.018	0.048
.595-.841	0.463	0.679	0.265	-0.097
.425-.595	0.366	0.641	0.249	-0.036
.212-.425	0.352	0.505	0.132	0.178
.15-.212	-0.340	-0.429	0.601	-0.261
.106-150	-0.081	0.101	0.000	0.277
.075-.106	-0.340	-0.254	-0.309	0.017
.053-.075	-0.110	-0.049	0.002	0.024
0-.053	0.468	0.200	0.347	-0.375

TRIMODAL SAMPLES

Correlations at the 90 % significance level, r = 0.521

Degrees of Freedom = 9

Sediment	Gold Size Fractions (Microns)			
Sizes (mm)	A-106-150	A-75-106	A-053-75	A-53
(+128)	0.165	0.221	-0.420	-0.550
91 - 128	-0.240	-0.203	0.039	0.513
64 - 91	0.059	0.284	-0.230	-0.014
45 - 64	-0.364	-0.064	0.667	0.520
32 - 45	-0.361	-0.615	0.461	-0.249
16 - 32	-0.138	-0.156	0.418	-0.281
(8 - 16)	-0.160	-0.174	0.638	0.076
(4 - 8)	-0.314	-0.149	0.544	0.755
(2 - 4)	0.108	-0.114	0.516	0.146
1.68-2	-0.329	-0.186	-0.170	0.622
1.19-1.68	-0.047	-0.109	-0.364	0.238
.841-1.19	0.351	0.119	-0.192	0.028
.595-.841	0.337	0.068	-0.223	-0.233
.425-.595	0.637	0.404	-0.138	-0.387
.212-.425	0.579	0.579	-0.223	0.051
.15-.212	-0.021	-0.264	0.672	-0.350
.106-150	-0.448	-0.232	-0.396	0.636
.075-.106	-0.517	-0.561	0.101	-0.138
.053-.075	-0.006	-0.052	-0.468	0.266
0-.053	0.395	0.083	0.076	-0.214

negative correlations exist for a sediment size and the same gold size fraction. In the matrix of the bimodal samples, this feature is still evident but it is less prominent.

The second feature apparent in the correlation matrices is that there are several distinctly different patterns of negative and positive correlations for the bimodal and trimodal samples. In addition, the coarser size fractions show different correlation patterns between the trimodal and bimodal samples.

The third feature in the correlation matrix is that in the coarse size fractions a poorly defined pattern with both positive and negative correlations is evident. In the bimodal samples, strong negative correlations exist for gold size fractions form 0.053-0.150 mm and sediment sizes between 2-8 mm. For coarser sediments (45-91 mm) correlations become positive and then negative for sediments 91- +128 mm. These correlations approximate positive and negative bands of correlations across the matrix for the coarse sediment sizes. In the trimodal samples the pattern of positive and negative correlations forms a more complex chevron shape.

The correlations can be interpreted to yield information regarding the depositional environments of all of the samples and to examine the potential for sedimentological differences between the bimodal and trimodal samples.

The most prominent feature on the correlation matrix, the existence of positive statistically significant correlations between gold sizes and sediments 2-4 size fractions larger and negative correlations for gold and the same size fraction, is strong evidence of hydraulic mechanisms active in the depositional environment of the deposit. Concepts such as

hydraulic equivalence and transport equivalence (refer to section 1.2) may explain these trends where coarser light particles are found in a bed with smaller, denser particles. The concept of hydraulic equivalence and its potential applicability here can be illustrated with an example.

If we assume a simple environment where particles with the same settling velocity will be deposited on the bed of a stream, Dietrich's (1982) version of Stoke's Law can be used to predict the sizes of gold and sediment that will be deposited in the same hydraulic regime. Consider a flake of gold with a thickness to width ratio of 1:5 (CSF = 0.2) and a specific gravity of 17 and a spherical sediment particle with a specific gravity of 2.7. If the gold flake has a diameter of 0.106 mm, then Dietrich's version of Stoke's Law predicts a settling velocity 3.1 cm/s. Then the diameter of a sediment with the same settling velocity is 0.250 mm. Thus, in this environment gold is deposited in the same environment as sediment of 2 size fractions larger. Thus, hydraulic equivalence, and potentially transport equivalence, are plausible explanations for this feature seen in the correlation matrices.

Inverse correlations existing between gold size fractions and the same size fraction of sediment may also be due to hydraulic or transport equivalence. Small, low density particles will be entrained from a stream bed where more dense gold particles of the same size are being deposited. Thus, lighter particles may be selectively removed from the bed, while heavier particles of the same size will be concentrated on the bed.

The correlation matrices indicated that these correlations were stronger and more defined in the trimodal samples than in the bimodal samples. This suggests that fluvial sorting processes may have been greater in the depositional environment for the trimodal samples than the

bimodal samples. Also noted was the difference in correlation patterns between the bimodal and trimodal samples for coarse size fractions. These two factors suggest that there may be a significant difference in the depositional environment of gold in the trimodal and bimodal samples. The presence of the third population, C, may be related to this difference.

Interpretation of the correlation patterns noted in the correlation matrices for the coarser sediment sizes is speculative, but these patterns are thought to be related to energy, bed roughness and/or plugging effects. Energy and bed roughness of the depositional environment control the material that becomes trapped on the stream bed. Larger sediment sizes are deposited in high energy environments with high water velocities and volumes. Any particle smaller than one third of the median grain size of the bed is fully hidden and is protected from entrainment by turbulent flow. Thus, the trends in the correlation matrices may reflect changes in the energy of the depositional environments. Similarly, plugging may account for some of the trends on the correlation matrices. The effect of plugging is analogous to the effect of riffle spacing for optimal concentration of gold in a sluice box. If riffles are placed too close together, the riffles become plugged with fine sediments and gold can not be concentrated. When riffles are too far apart, large vortices are created and the space between the riffles becomes badly scoured. While these theories to explain the patterns in the matrices are speculative, a similar potential trend was noticed by Fletcher in Harris Creek and may give an indication of the energy of the environment in which the gold was deposited. (Fletcher, per. com. 1996). As the sediment and gold relations which result from the interaction of these processes are poorly understood, an interpretation of the matrices based on these concepts has not been attempted.

Interpretation of the patterns in the correlation matrices and the understanding of the differences between the bimodal and trimodal samples may improve if the origin of the third population C is understood. However, correlation data clearly shows that the two groups of samples were likely formed in slightly different depositional environments, which have resulted in basal units of apparently similar structure.

6.3 TRANSPORT EQUIVALENCES

On a stream bed, transport equivalent particles are always found in the same relative concentration, despite differences in the size and density of the particle and changing flow conditions (Fletcher, 1991). Transport equivalence between gold and the sediment size fraction with the most nearly constant relative rate of transport is estimated by the minimum coefficient of variation, CV, for a gold size fraction over all of the sediment size fractions (Fletcher, 1991). The coefficients of variation (CV) were calculated for each of the 16 relative concentrations over the 16 samples for each of the 6 gold size fractions. The minimum CV over the 16 sediment size fractions indicates the corresponding sediment size that had the most nearly constant relative rate of transport with the gold size fraction. The results of the CV calculations are presented in Table 6.2. The minimum CV for each of the 6 gold size fractions is in bold, italic print. The potential transport equivalences were calculated for all samples together - the group of bimodal samples and the group of trimodal samples.

Table 6.2 Potential transport equivalents calculated with the coefficient of variation. Minimum coefficients of variation are shaded.

All Populations

Sediment Sizes	Gold Size Fractions			
	+.106, - .150	+.075, -.106	+.053, -.075	-.053
+128 mm	218.5	144.7	170.6	117.2
+91, -128	101.2	109.3	84.4	124.6
+64, -91	95.5	86.7	69.6	79.9
+45, - 32	88.3	109.2	95.8	114.9
+32, -45	86.6	84.7	71.1	85.9
+16, -32	88.6	97.3	70.1	75.3
+8, -16	92.9	103.3	71.4	76.9
+4, -8	88.4	100.1	83.8	93.0
+2, -4	120.5	109.8	74.5	114.1
+1.68, -2	98.6	92.9	70.2	71.8
+1.19, -1.68	84.7	87.9	69.9	73.8
+.841, -1.19	86.7	87.5	67.4	74.8
+.595, -.841	84.2	91.3	67.6	78.4
+.425, -.595	93.1	91.1	71.2	81.8
+.212, -.425	82.5	87.4	72.5	79.5
+.150, -.212	78.5	89.0	70.4	80.1
+.106, - .150	95.4	106.9	85.8	100.3
+.075, -.106	95.7	109.0	76.6	88.3
+.053, -.075	86.7	107.6	97.0	116.8
-.053	80.4	94.6	59.0	77.3

Bimodal Samples

Sediment Sizes	Gold Size Fractions			
	+.106, - .150	+.075, -.106	+.053, -.075	-.053
+128 mm	204.6	159.6	160.4	114.4
+91, -128	107.1	128.5	96.4	138.5
+64, -91	92.5	62.7	58.4	74.3
+45, - 32	87.3	84.7	64.6	92.5
+32, -45	75.7	66.0	62.9	80.4
+16, -32	69.3	60.1	55.2	75.3
+8, -16	77.9	69.2	58.9	81.1
+4, -8	70.1	60.5	80.9	93.1
+2, -4	113.2	115.4	71.5	102.6
+1.68, -2	102.1	71.8	72.6	76.6
+1.19, -1.68	86.8	60.1	72.5	70.4
+.841, -1.19	84.4	59.4	65.8	69.8
+.595, -.841	82.9	61.7	65.9	72.4
+.425, -.595	85.8	62.4	65.6	72.6
+.212, -.425	76.5	59.0	71.0	74.6
+.150, -.212	59.6	63.2	61.9	75.4
+.106, - .150	87.3	101.5	70.4	109.4
+.075, -.106	75.5	85.1	58.3	94.9
+.053, -.075	89.1	93.2	69.5	96.8
-.053	74.6	73.0	54.7	83.1

Trimodal Samples

Sediment Sizes	Gold Size Fractions			
	+.106, - .150	+.075, -.106	+.053, -.075	-.053
+128 mm	113.3	123.5	128.5	119.8
+91, -128	81.0	79.3	65.0	79.6
+64, -91	70.2	92.4	67.7	86.7
+45, - 32	81.8	126.3	117.5	148.6
+32, -45	76.5	94.5	70.6	72.3
+16, -32	82.7	109.1	55.5	58.2
+8, -16	82.5	117.4	52.4	55.3
+4, -8	84.9	120.3	58.8	56.6
+2, -4	71.0	99.8	54.7	103.3
+1.68, -2	72.1	107.6	62.4	70.8
+1.19, -1.68	74.8	106.8	77.9	88.1
+.841, -1.19	75.4	104.1	71.1	83.1
+.595, -.841	73.8	108.3	73.1	85.7
+.425, -.595	81.8	109.4	76.4	88.6
+.212, -.425	80.9	103.6	83.3	94.4
+.150, -.212	79.6	105.2	78.5	78.0
+.106, - .150	64.6	102.0	85.4	107.7
+.075, -.106	90.9	119.6	58.7	65.2
+.053, -.075	93.2	116.4	109.4	140.1
-.053	83.4	113.9	57.5	67.5

Coefficients of variation all correspond to very large sediment sizes, 9-13 size fractions larger, despite very fine gold sizes. No major reduction in variation for a particular size fraction is evident and minimum coefficients of variation appear random. This suggests the processes that result in transport equivalence are not distinguishable in the data set for the sediments of the Dominion Creek deposit. Transport equivalents be masked by the break down of clasts due to weathering and further augmented by processing the samples in sluicing and sieving.

7.0 DISCUSSION

The study focused on a detailed examination of the basal unit of a gold bearing quartz gravel deposit near the left limit (Southeast side) of the paleochannel of Dominion Creek. Sampling followed the course of placer mining over the 1995 season as a 610 meter long cut face was exposed, parallel to the length of the channel. Sampling of the basal unit was selected as drilling, sampling and observation in the mine pits had identified the highest gold concentration to be within the lower 0.5 meters of gravel and the upper 0.5 meters of bedrock. The basal unit is a massive, disorganized, pebble-boulder, clast supported gravel, lacking stratification and imbrication, which varies from 0.3 - 1 meters thick. Commonly the unit contains scattered boulders, up to 1.0 meter in diameter, that are not found in higher parts of the section . The processes and environment in which the gold bearing basal units of this deposit formed have been poorly understood. The principle aim of this study was to develop textural relations and statistical correlations for the sediments and gold concentrations of the basal unit.

Correlation matrices of sediment abundance and gold concentrations showed trends that are indicative of the types of processes involved in the deposition of the basal units. A positive correlation was found for gold sizes and sediments, 2-4 size fractions larger, which is consistent with the sediment-gold particle relations predicted by the concepts of hydraulic and transport equivalence. These correlations suggest that dense gold particles will be found on a bed with coarse, less dense particles. An inverse correlation was also found for gold size fractions and the same sized sediment, suggesting that environment in which the deposit

formed favored the deposition and concentration of small dense particles of gold, while less dense sediments of the same size were entrained.

In the field, sampling sites were selected where the basal unit was uniform and similar in appearance, thickness and structure. Although efforts were made to select sample sites at which the basal units were visually similar to each other, textural studies have shown that there are differences in grain size distributions among the samples. On cumulative probability plots, samples were identified to all contain two principle populations: (A) a matrix infilling and (B) a coarse framework. Nine of the sixteen samples also contained a third, fine sand-silt population (C) and were designated as trimodal. Field observations, mineralogy and gold concentrations of the units did not define any significant differences between the units sampled and the groups of samples identified as bimodal and trimodal

Differences in the correlation matrices and the probability plots between the bimodal and trimodal samples suggest that the depositional regime (processes and environment) of the two groups of basal units was different. The positive correlations between gold size fractions and sediments 2-4 size fractions larger and the inverse relation between gold sizes and the same sediment size, were stronger and more defined in the trimodal samples than in the bimodal samples. These differences suggest that fluvial sorting processes that were involved in the concentration of gold in the deposit may have been more significant in the samples identified as trimodal. Further investigation into the origin of population (C) may facilitate determining the differences between the bimodal and trimodal samples.

The correlation matrices also showed differences in the patterns of positive and negative correlations for the fine gold and coarse sediment sizes, which may be indicative of the

energy of the depositional environment, however, these features are not understood. Further statistical analysis of the data set may identify other relations between the sediments, gold and depositional processes.

While the origins of all the patterns seen in the correlation data cannot be fully explained within this study, they are consistent with the characteristics of modern day streams, where processes such as hydraulic equivalence and transport equivalence are active. Similarly, textural data suggests that the sediment grain size distribution is also like those found in fluvial gravel deposits. Comparison of grain size distribution curves with showed no distinct differences between the sediments of modern gravel streams and the sediments examined in the basal unit. The lack of developed structure, except for very crude sub-horizontal fabric of flat pebbles and cobbles, in the otherwise massive and disorganized unit, suggests rapid deposition.

From all the textural, gold grain size distribution and field observations, the depositional environment of the basal unit is thought to have been that a high flow aggrading braided stream or alluvial fan deposit. Mass wasting of saturated sediments and bedrock may also have been a component in the deposition of this unit.

7.1 DOMINION CREEK STRATIGRAPHY AND CORRELATION

The basal units of the valley-bottom gravels and other units comprising the lower 2-3 meters of the section are all fairly homogeneous massive gray quartz gravels that lack stratification and are made up of overlapping successions of poorly defined tabular lensoid units, with

scoured contact surfaces. It is impossible to trace individual units between sites, and contacts are only obvious where coarse and fine gravels are in contact. Visually this lower part of the section appears similar, but there are important differences in the basal unit that are not apparent at individual sample sites. Not apparent is the common occurrence of scattered boulders on bedrock and in the bottom 1 meter of the section, which is very evident in the mine cuts as they are progressively deepened. Also not apparent is the higher gold concentration in the basal 0.5 meters of gravel and upper bedrock, and the elevated gold content in the overlying 2-3 meters of massive gravel.

A few kilometers northeast of the study area, a large remnants of a quartz gravel terrace has been recently found on an old bedrock surface some 30 meters higher than the Dominion Creek floodplain. These highly weathered remnants reach a thickness of 11.5 meters and are similar to the present day valley-bottom deposits, but are generally cleaner more mature, quartz gravels, and have much larger quartz boulders on bedrock. These deposits also become better stratified and sorted upwards and include some very mature pure quartz gravels in the upper parts of the section.

Morison (1985) correlated the Dominion Creek valley-bottom gravels with the White Channel gravels because of their close similarity, but at that time the occurrence of the higher level terrace deposits on Dominion were not known. These terrace deposits are cleaner more mature quartz gravels, and are more like the classic White Channel in composition and relative stratigraphic position, but at present only a tentative correlation can be made.

7.2 DEPOSITIONAL ENVIRONMENT - DOMINION CREEK

The deposition of the valley-bottom gravels followed a period of uplift and renewed erosion during which the valley was deepened by more than 30 meters. The basal units studied were deposited along the left limit of the paleochannel which was in the order of 300 meters wide and 2 or more meters deeper in the mid-channel (totally mined in the past and maximum depth unknown), than at the sample sites. This paleochannel is believed to have been formed by a degrading stream during a time when flow rates were much higher than at present and were sufficient to transport most of the sediment entering the drainage. Boulders and concentrations of gold probably existed in this channel prior to deposition of the basal unit studied.

Deposition of the basal units is believed to have occurred shortly after there had been a sudden change in stream hydrology from a degrading to an aggrading condition, as a result of accelerated erosion and increased stream flow. Greatly increased precipitation is the most likely reason for the high flow rates which gave rise to the deposit: there is no evidence of glaciation in the valley, thus ice meltwater is not a factor. The sources of sediment are believed to have been the pre-existing higher level gravel terraces, tributary stream alluvial fan deposits and gravity flow (mass wasting) deposits off adjacent water saturated slopes. Upon reaching the stream, these materials were re-worked and mixed into the aggrading valley deposits.

The transition from degrading to an aggrading condition is visualized to have occurred quickly. As water levels rose to extreme flood levels the existing stream bed remobilized and

pre-existing alluvium, boulders and gold became mixed with newly supplied sediment as the channel bottom was scoured. The influx of new sediment quickly increased as Dominion basin became water saturated. The mass wasting of the slopes and cut banks of the tributary creeks combined to produce an overload of sediment into the main stream. Gold and boulders remained concentrated at the bottom of the channel as the stream began to aggrade forming the basal units of the deposits. As the stream continued to aggrade it probably became braided, with the main channel continually shifting and scouring higher parts of the channel floor, such as the sample location, while the paleochannel continued to fill with sediments. Pre-existing placer gold concentrations and boulders remained near the bottom but were likely transported, to some degree, as bedload. While the lower 2-3 meters of the section was being deposited a supply of gold continued to be available. The source of gold may have been, in part, the older White Channel terrace deposits that were being eroded and re-worked as the stream aggraded, but gold was also probably derived from the scouring and re-working of sections of the main channel. Whatever the source, gold was deposited rapidly along with sediment with little opportunity to become concentrated in this rapidly aggrading fluvial environment. A relatively uniform distribution of gold values resulted and is the reason that an unusually thick 2-2.5 meter gravel section is of sufficient grade to mine.

Dominion Creek continued to aggrade for some time, but the supply of sediment diminished as precipitation began to drop off. The more stratified and better sorted upper parts of the deposit developed during this period, as flows returned to more normal levels. Eventually precipitation and stream flows diminished to current levels and the present day meandering stream was formed on the surface of the valley-bottom gravels. Numerous abandoned meander channels are buried under 2-3 meters of more recent overbank flood deposits of mud, silt and organic debris. Up to 2 meters of peat and moss cover the valley floor that has

slowly increased in thickness with annual moss growth in summer and upward encroachment of permafrost in winter.

7.3 REGIONAL PALEODEPOSITIONAL MODEL

The Klondike has been affected by extreme climatic and hydrological events associated with three Pliocene and Pleistocene glaciations, but has never been over ridden by glacial ice. The surficial geology therefore has been developing for a long period and the concentrating processes that give rise to placer deposits have had time to be effective. Two similar cycles of erosion and rapid deposition are envisioned as having formed the White Channel deposits and then the valley-bottom deposits.

In the early Pliocene a mature erosional surface was uplifted (Morison, 1985) and the current erosion cycle began. Placer gold concentrations and mature quartz gravels may have already existed on this old land surface from the previous erosion cycle, prior to the development of new topography. By the end of the Pliocene the streams and valleys had developed to be much like at the present, although narrower and not as deep. Erosion was in balance with stream flows and creeks were degrading. Placer gold deposits and some large boulders may have been present on the valley bottoms prior to the Pre-Reid glaciation. A large increase in precipitation caused flood conditions in the streams and rapid erosion in the stream basins. Initially the flood waters likely caused remobilization and scouring of the existing stream beds, but then as erosion of the water saturated slopes accelerated, overloads of sediment were delivered to the mainstreams, causing them to aggrade. The deposits of almost pure

quartz gravels that were formed during this period are named White Channel Gravels, and these accumulated rapidly in an environment which was described by Morison (1985) as a crudely to well -braided environment dominated by high discharges. Valley wall sediment gravity flow and tributary alluvial fans and/or slumps also resulted in deposits within the main valley braidplain. On Dominion Creek remnants of similar mature quartz gravels are preserved on terraces, and quartz rich terrace deposits are known elsewhere in the Klondike such as on Quartz Creek. The event that gave rise to the White Channel is believed to have had affected all the drainages of the Klondike and it has been dated at older than 1.22 million years. It seems unusual that mature quartz gravels were deposited at such an early stage in an erosion cycle which suggests they may be related in some way to a previous erosion cycle.

The upper section of the White Channel deposits is more stratified and graded than the lower massive portion. During deposition of the upper gravels the streams were still aggrading but the supply of sediment had started to diminish and continued to diminish until flows returned to normal levels. Thereafter, the streams may have immediately resumed degrading, or possibly later uplift caused the streams to be rejuvenated. Whatever the reason, a period of valley deepening followed deposition of the White Channel, accompanied by widening of some valleys by lateral migration of streams.

As the Klondike valleys deepened portions of the old stream beds and the White Channel gravels would have been eroded. Placer gold and boulders would therefore have been moved downward and been re-concentrated in the beds of the degrading streams as described in the previous section on Dominion Creek. Deepening of the Klondike area valleys is believed to have occurred near the time of the Reid glaciation (Morison, 1985).

A second period of extreme precipitation, accelerated erosion and high stream flows followed after the Reid glaciation, again causing the streams to aggrade. The deposits formed at this time are the present day valley-bottom deposits, such as described at Dominion Creek. They were deposited very rapidly and the sources of the sediment were the older White Channel terrace deposits, tributary stream alluvial fan deposits and deposits from mass wasting of the valley slopes. As in the earlier White Channel deposition, streams continued to aggrade for some time as precipitation and flows diminished, and the upper parts of the deposits become better stratified and sorted.

Wide valleys, such as Dominion, appear to have been stable since the McConnell glaciation and stream flows have been at relatively low levels. Overbank floodplain deposits of mud, silt and organics and thick moss-peat layers have developed above the gravels. Narrower and steeper streams and headwaters have continued to slowly degrade. Gold is believed to have been derived locally from prolonged weathering of the Klondike schists and has been concentrated and repeatedly reconcentrated on or near bedrock during every stage in the development of the streams in the Klondike Goldfield.

REFERENCES

Best, J.L., and Brayshaw, A.C., 1985. Flow Separation - A Physical Process for the Concentration of Heavy Minerals Within Alluvial Channels, J. Geol. Soc. London, 142, 747-755.

Boggs, s. Jr., 1988. Principles of Sedimentology and Stratigraphy, Merrill Publishing, Columbus, Ohio, 784 p.

Bostock, H.S., 1957. Yukon Territory, Selected Field Reports of the Geological Survey of Canada, 1898 to 1933, Geological Survey of Canada Memoir 284.

Boyle, R.W., 1987. Gold: History and Genesis of Deposits, Van Nostrand Reinhold, New York, 676 p.

Boyle, R.W., 1979. The Geochemistry of Gold and Its Deposits, Geological Survey of Canada, Bulletin 280, 584 p.

Brown, R.J.E., 1978. Permafrost: Plate 32. *In* Hydrological Atlas of Canada. Fisheries and Enviornment Canada, Ottawa, 34 plates.

Burn, C.R., 1987. Permafrost. *In* Guidebook to Quaternary Research in Yukon. *Edited by* S.R. Morison and C.A.S. Smith. XII INQUA Congress, Ottawa, Canada, pp 21-25.

Cass, T. 1973. Statistical Methods in Managements, Cassel and Co., London, 271 p.

Church, M. , J.F. Wolcott, and W.K. Fletcher, 1991. A Test of Equal Mobility in Fluvial Sediment Transport: Behaviour of the Sand Fraction, Water Reources Research, Vol. 27, No 11, pages 2941-2951.

Clarkson R., and O. Peer, 1990. An Analysis of Sluicbox Performance, New Era Engineering Corporation, Whitehorse, 31 p.

Clifton, H.E., Hunter, R.E., Swanson, F.J., and R.L. Phillips, 1969. Sample Size and Meaningful Gold Analysis: U.S. Geological Survey Professional Paper 625-C.

Darby, D.A., Whittecar, G.R., Garrett, J.R. and Barringer, R.A., 1988., Anomalous Heavy Mineral Size Relationships in a Humid Alluvial Fan, Columbia: Implications for Placer Formation, Economic Geology, 83, 1015-1025.

Day, S.J., and Fletcher, W.K., 1991. Concentration of Magnetite and Gold at Bar and Reach Scales in a Gravel-bed Stream, British Columbia, Canada, J. Sed. Petrol. **61**, 871-882.

Day, S. J., 1985. Sampling Stream Sediments for Gold In Mineral Exploration, Southern British Columbia, Unpub. M.Sc. Thesis, Department of Geological Sciences, University of British Columbia.

Darby, D.A, et. al., 1988. Anomalous Heavy Mineral Size Relationships in a Humid Alluvial Fan, Columbia: Implications for Placer Formation, Economic Geology, Vol 63, pp 1015-1025.

Dietrich, W.E., 1982. Settling Velocity of Natural Particles, Water Resources Research, Vol. 18, No 6, pages 1615-1626.

Diment, R., Brewery Creek Gold Deposit, *In* Yukon Exploration and Geology 1995,Exploration and Geological Services Division, Northern Affairs Program, Yukon. pp 57-63.

Einstein, H.A., 1964. Section 17-II, *in* Chow, V.T., ed., Handbook of Applied Hydrology, McGraw-Hill Book Company, New York.

Fletcher, W.K., 1994. Behaviour and Exploration Geochemistry of Cassiterite and Other Heavy Minerals in Streams, J.Southeast Asian Earth Science, 10, No 1/2, 5-10.

Fletcher, W.K., and Church, M., and Wolcott, J, 1992. Fluvial-Transport Equivalence of Heavy Minerals in the Sand Size Range, Can. J. Earth Sci., 29, 2017-2021.

Fletcher, W.K., 1990. Dispersion And Behaviour of Gold In Stream Sediments, Mineral Resources Division, Geological Survery Branch, Open File 1990-28.

Fletcher, W.K., 1981. Analytical Methods in Geochemical Prospecting. Elsevier, 255 pages.
Okkerman, J.A., 1984. Improved Methods of Ore Reserve Calculation for Detrital Tin Deposits, United Nations Development Programme, Document Number ROPEA - 132.

French, H.M. and W.H. Pollard, 1986. Ground Ice Investigations, Klondike District, Yukon Territory, Canadian Journal of Earth Sciences, 23, p. 550-560.

Giusti, L., 1986. The Morphology, Mineralogy, and Behaviour of "Fine Grained" Gold from Placer Deposits of Alberta: Sampling and Implications for Mineral Exploration, Can. J. Earth Sci., **23**, 1662-1672.

Hassan, M.A., M. Church, and A.P. Schick, 1991. Distance of Movement of Coarse Particles in Gravel Bed Streams, Water Resources Research, Vol. 27, No 4, pp 503-511.

Hughes, O.L., 1987. Quaternary Geology. *In* Guidebook to Quaternary Research in Yukon. *Edited by* S.R. Morison and C.A.S. Smith. XII INQUA Congress, Ottawa, Canada, p. 12-16.

Hughs, O.L., R.B. Cambell, J.E. Muller and J.O. Wheeler, 1969. Glacial Limits and Flow Patterms, Yukon Territory, South of 65 Degrees North Latitude, Geological Survey of Canada, Paper 68-34, 9p.

Ingamells, C.O, 1981. Evaluation of Skewed Exploration Data - The Nugget Effect, Geochim Cosmochim Acta, V. 45, p. 1209-1216.

Koch, G.S., and R.F. Link, 1970. Statistical Analysis of Geological Data, John Wiley and Sons, Inc. , New York, 375 p.

Knight, J.B., Mortensen, J.K., and S.R. Morison, 1994. Shape and Composition of Lode and Placer Gold From the Klondike District, Yukon, Canada, Exploration and Geological Services Division, Yukon Region, Bulletin 3, 142 p.

Krapez, B. 1985. The Ventersdorp Contact Placer: a Gold-Pyrite Placer of Stream and Debris-Flow Origins from the Archean Witwatersrand Basin of South Africa, Sedimentology, **32**, 223-234.

Laurus, K.A., 1995. Gold Distribution in Glacial Sediments and Soils at Spyder Lake, Hope Bay, Greenstone Belt, NWT; and the Effects of a Permafrost Environment, M.Sc. Thesis, University of British Columbia, Vancouver, British Columbia, 226 p.

LeBarge, W.P., 1995. Sedimentology of Placer Gold Gravels Near Mt. Nansen, Central Yukon Territory, Exploration and Geological Services Division, Yukon, Region, Bulletin 4, 155 p.

Lowe, D.R., 1982. Sediment Gravity Flows: II. Depostional Models With Special Reference to the Deposits of High-Density Turbidity Currents, p. 277-295

Miall, A.D., 1978. Lithofacies Types and Vertical Profile Models in Braided River Deposits: A Summary, *in* Miall, A.D., (ed.), Fluvial Sedimentology, Canadian Society of Petroleum Geologists, Memoir 5, p. 597-604.

Milner, N.W., 1976. Geomorphology of the Klondike Placer Goldfields, Department of Indian Affairs and Northern Development, Exploration and Geological Services Division, Final Report, Contract OSV 5-0047, Whitehorse, 157 p.

Morison, S.R., 1989. Placer Deposits in Canada, Chapter 11, Quaternary Resources in Canada, *In* Fulton, R.J. (ed.), Quaternary Geology of Canada and Greenland; Geological Survey of Canada, Geology of Canada, No. 1, p. 687-697.

Morison, S.R., 1985. Sedimentology of White Channel Placer Deposits, Klondike Area, West-Central Yukon, M.Sc Thesis, University of Alberta, Edmonton, Alberta, 149 p.

Morison , S.R., and F.J. Hein, 1987. Sedimentology of White Channel Gravels, Klondike Areas, Yukon Terrritory: Fluvial Deposits of a Confined Valley. *In* Proc. Third International Fluvial Sedimentoloby Conference, Fort Collins, Colorado; S.E.P.M. Spec. Publ. In Press.

McConnell, R.G., 1907, Report on Gold Values in Klondike High Level Gravels. Geological Survey of Canada, Pub. no., 979, 34 p.

McConnell, R.G., 1905. Report on the Klondike Gold Fields, Geological Survey of Canada, Annual report, v. 14, 1901, Part B, pp 1B-71B.

Naldrett, D.N., 1982. Aspects of the Surficial Geology and Permafrost Conditions, Klondike Gold Fields and Dawson City, Yukon Territory. M.Sc. Thesis, University of Ottawa, Ottawa, Ontario, 150 p.

Paopongsawan, P. and Fletcher, W.K. 1993. Distribution and Dispersion of Gold in Point Bar and Pavement Sediments of the Huai Hin Laep, Loei, northeastern Thailand, J. Geochem. Explor. 41, 251-268.

Poling, G.W. and Hamilton, J.F., 1985, Fine Gold Recovery of Selected Sluicbox Configurations, University of British Columbia, Department of Mining and Mineral Process Engineering, 77 p.

Rachocki, A.H., and M. Church, editors, Alluvial Fans: A Field Approach, John Wiley and Sons, John Wiley and Sons, Chichester, England, 1990. 391 p.

Reid, I.and Frostick, L.E., 1985. Role of Settling , Entrainment and Dispersive Equivalence and of Interstice Trapping in Placer Formation. J. Geol. Soc. London. 142, 739-746.

Selby, M.J., 1985. Earth's Changing Surface: An Introduction to Geomorphology. Oxford University Press, New York. 607 pp.

Sinclair, A.J., 1976. Applications of Probabilty Graphs in Mineral Exploration, Association of Exploration Geochemists, Spec. Vol. No. 4, 95 p.

Slingerland, R., 1984. Role of Hydraulic Sorting in the Origin of Fluvial Placers. J. Sed. Petrol. **54**, 137-150.

Slingerland, R.L., 1977. The Effects of Entrainment on the Hydraulic Equivalence Relationships of Light and Heavy Minerals in Sands, J. Sed. Pet., 47, 753-770.

Slingerland, R. and Smith, N.D., 1986. Occurrence and Formation of Water-Laid Placers. Ann Rev. Earth Plandt Sci. 14, 113-147.

Stanely, C.R., 1987. Probplot, and Interactive Computer Program to Fit Mixtures of Normal (or Log-Normal) Distributions with Maximum Likelihood Optimization Procedures. Association of Exploration Geochemists Spec. Vol. 14.

Swan, A.R.H., and M. Sandilands, Introduction to Geological Data Analysis, Blackwell Science, Oxford, 1995. 446 p.

Templeman-Kluit, D.J., 1981. Geology and Mineral Deposits of Southern Yukon, *In* INAC (1981), Yukon Geology and Exploration 1979-1980, Explorationa nd Geological Services Division, Indian and Northern Affairs, Canada, p 7-31.

Walsh, D.E., and Rao, P.D., 1986. A Study of Factors Suspected of Influencing the Settling Velocity of Fine Gold Particles, Mineral Industry Research Laboratory, University of Alaska-Fairbanks.

Wang, W. and G.W. Poling, 1983. Methods for Recovering Fine Placer Gold, 76, 47-56.

Whal, H.E. and T.O. Goos, Climate, *In* Guidebook to Quaternary Research in Yukon. *Edited by* S.R. Morison and C.A.S. Smith. XII INQUA Congress, Ottawa, Canada, p. 7-12.

Yukon Placer Authorization, Government of Canada, Ottawa, June 1991.

Zarr, J.H, 1984. Biostatistical Analysis, 2nd ed., pp 402-411.

APPENDIX A

SUMMARY UNIT DESCRIPTIONS FOR SAMPLE SITES			
Sample #	**% bedrock**	**Description**	**Thickness (m)**
T-1	30	Massive, Pebble-Cobble gravel, clast supporte, poooly sorted	0.3
T-2	15	Poorly sorted, laterally continuous, clast supporte, matrix filled, boulder gravel	0.5
T-3	10	Boulder-cobble gravle, very scoured base, massive, planar bedding	0.45
T-4	15	Massive, grey-green, clast supporte boulder-cobble gravel	0.4
T-5	10	Moderately sorted, clast supporte planar bedding brown cobble-pebble gravel	0.95
T-6	20	Massive, clast supporte boulder-pebble-cobble gravel	0.5
T-7	15	Massive, continous, clast supporte, pebble-cobble gravel(no boulders)	0.8
T-8	25	Disorganized, clast supporte, greeen-grey, pebble, cobble gravel	0.35
T-9	35	Disorganized, pebble-cobble-gravle, clast supported, matrix filled	0.9
T-10	10	Disorganize, pebble-cobble gravel	0.3
T-11	15	Massive, clast supporte boulder-pebble-cobble gravel	0.3
T-12	5	Massive, green grey, boulder, cobble gravel	1
T-13	10	Cobble-pebble gravle, coarsens slightly to base	0.75
T-14	10	Pebble-cobble gravel, grades downward	1.4
T-15	5	Grey-green, clast supported, matrix filled, pebble-cobble gravel, moderate to poorly sorte	0.55
T-16	5	Massive, grey-green, cobble-pebble, planar bedding, clast supported, rounded clasts	1

APPENDIX B

TOTAL SAMPLE WEIGHTS

(Grams)

			SAMPLE NUMBER - A															
		Microns	1	2	3	4	5	6	7	8	9	10	11	12	13	14	15	16
1	+10	2000	2083.90	2165.94	2430.69	2273.90	2622.30	1302.80	1721.59	1666.04	904.96	1233.50	1275.56	1524.72	1195.30	2622.26	2377.65	2087.38
2	+12	1680	156.97	208.16	193.29	154.76	244.45	103.11	131.23	172.16	100.04	146.90	142.78	135.59	113.52	254.83	263.55	205.97
3	+16	1190	298.95	251.63	338.98	230.74	431.03	240.75	279.95	368.28	122.48	196.58	230.66	276.25	305.21	482.44	531.62	300.74
4	+20	841	218.83	223.08	276.15	215.90	400.36	196.44	219.54	310.32	108.57	192.09	181.21	224.02	356.08	409.76	232.02	257.01
5	+30	595	194.28	184.77	227.72	204.55	217.52	179.44	154.04	281.64	96.16	159.59	185.64	185.21	466.96	335.62	352.35	185.62
6	+40	425	422.70	220.54	289.63	429.06	273.24	192.95	188.65	300.33	108.82	198.12	216.76	221.47	546.41	508.85	283.80	236.24
7	+70	212	799.84	553.84	635.91	636.97	801.00	613.89	528.18	839.79	231.41	490.76	360.32	511.40	514.82	891.79	616.99	538.61
8	+100	150	243.59	769.09	317.39	267.13	374.14	242.21	185.87	474.57	101.23	144.82	122.72	153.28	137.15	247.10	317.73	117.42
9	+140	106	68.47	61.44	143.95	89.75	277.59	143.89	65.82	274.96	99.74	136.04	110.52	57.19	43.09	113.18	132.89	128.14
10	+200	75	56.69	126.18	78.71	149.25	180.76	102.81	47.14	204.18	77.14	76.04	69.46	46.09	34.99	78.43	60.57	57.85
11	>270	53	38.15	25.84	60.39	75.67	116.19	83.28	56.50	170.32	87.49	66.21	66.91	41.47	39.54	70.46	30.44	52.11
12	<270	<53	218.65	294.59	238.24	246.82	285.09	347.87	216.00	424.18	246.84	179.62	238.54	168.63	185.28	302.07	179.87	149.22
		Total	4801.02	5085.10	5231.05	4974.50	6223.67	3749.44	3794.51	5486.77	2284.88	3220.27	3201.08	3545.32	3938.35	6316.79	5379.48	4316.31

TOTAL SAMPLE PERCENTAGES

			SAMPLE NUMBER - A															
		Microns	1	2	3	4	5	6	7	8	9	10	11	12	13	14	15	16
1	+10	2000	43.41	42.59	46.47	45.71	42.13	34.75	45.37	30.36	39.61	38.30	39.85	43.01	30.35	41.51	17.42	48.36
2	+12	1680	3.27	4.09	3.70	3.11	3.93	2.75	3.46	3.14	4.38	4.56	4.46	3.82	2.88	4.03	1.69	4.77
3	+16	1190	6.23	4.95	6.48	4.64	6.93	6.42	7.38	6.71	5.36	6.10	7.21	7.79	7.75	7.64	3.21	6.97
4	+20	841	4.56	4.39	5.28	4.34	6.43	5.24	5.79	5.66	4.75	5.97	5.66	6.32	9.04	6.49	2.72	5.95
5	+30	595	4.05	3.63	4.35	4.11	3.50	4.79	4.06	5.13	4.21	4.96	5.80	5.22	11.86	5.31	2.23	4.30
6	+40	425	8.80	4.34	5.54	8.63	4.39	5.15	4.97	5.47	4.76	6.15	6.77	6.25	13.87	8.06	3.38	5.47
7	+70	212	16.66	10.89	12.16	12.80	12.87	16.37	13.92	15.31	10.13	15.24	11.26	14.42	13.07	14.12	5.93	12.48
8	+100	150	5.07	15.12	6.07	5.37	6.01	6.46	4.90	8.65	4.43	4.50	3.83	4.32	3.48	3.91	1.64	2.72
9	+140	106	1.43	1.21	2.75	1.80	4.46	3.84	1.73	5.01	4.37	4.22	3.45	1.61	1.09	1.79	0.75	2.97
10	+200	75	1.18	2.48	1.50	3.00	2.90	2.74	1.24	3.72	3.38	2.36	2.17	1.30	0.89	1.24	0.52	1.34
11	>270	53	0.79	0.51	1.15	1.52	1.87	2.22	1.49	3.10	3.83	2.06	2.09	1.17	1.00	1.12	0.47	1.21
12	<270	<53	4.55	5.79	4.55	4.96	4.58	9.28	5.69	7.73	10.80	5.58	7.45	4.76	4.70	4.78	2.01	3.46
		Total	100.00	100.00	100.00	100.00	100.00	100.00	100.00	100.00	100.00	100.00	100.00	100.00	100.00	100.00	100.00	100.00

Weights and Percentages of Size Fractions in **Long-Tom Concentrate** Samples

TOTAL SAMPLE WEIGHTS

(Grams)

	Sieve	Microns	SAMPLE NUMBER - B 1	2	3	4	5	6	7	8	9	10	11	12	13	14	15	16
1	+10	2000	91.81	48.04	32.80	67.24	217.64	143.89	199.74	140.84	37.74	79.57	85.37	157.59	68.12	25.79	67.08	42.82
2	+12	1680	201.6	221.74	165.74	344.74	352.81	359.98	225.40	257.44	235.14	212.11	309.77	307.84	197.27	170.36	480.39	213.67
3	+16	1190	358.07	351.82	438.92	468.15	644.17	596.81	455.05	361.21	477.53	462.06	571.45	483.21	365.80	436.56	801.56	517.56
4	+20	841	361.7	305.75	377.68	465.81	501.97	684.39	528.78	465.81	474.60	387.89	835.08	759.06	549.97	357.65	664.31	415.45
5	+30	595	226.42	274.05	290.76	452.44	801.62	659.65	512.70	397.54	415.77	449.06	1051.78	336.61	479.84	280.37	585.16	411.91
6	+40	425	660.3	620.15	455.99	820.45	681.45	828.42	563.94	525.60	486.09	679.59	998.28	591.15	698.52	441.55	628.26	440.24
7	+70	212	957.87	350.47	1008.55	1171.46	547.09	1120.46	329.24	961.47	1100.02	1199.38	227.94	770.76	229.41	705.67	837.56	630.10
8	+100	150	332.21	267.15	270.75	382.61	355.33	697.37	223.23	501.81	172.74	448.25	57.86	336.47	319.87	239.30	314.90	252.18
9	+140	106	36.58	15.55	14.98	15.18	39.34	24.12	46.43	3.99	108.06	45.35	17.94	13.54	14.35	11.01	18.42	9.00
10	+200	75	8.67	11.29	9.77	10.02	25.96	26.96	21.24	6.15	59.44	21.57	11.70	15.04	9.52	8.18	30.22	6.63
11	>270	53	8.61	2.82	3.55	5.69	11.27	17.08	11.27	2.92	37.05	9.87	9.59	4.99	3.67	4.63	9.92	3.28
12	<270	<53	17.84	6.69	10.82	14.13	16.96	34.04	21.84	11.42	46.82	16.17	15.60	13.16	12.62	11.39	29.23	12.41
	Total		3261.68	2475.52	3080.31	4217.92	4195.61	5193.17	3138.86	3636.20	3651.00	4010.87	4192.36	3789.42	2948.96	2692.46	4467.01	2955.25

TOTAL SAMPLE PERCENTAGES

	Sieve	Microns	SAMPLE NUMBER - B 1	2	3	4	5	6	7	8	9	10	11	12	13	14	15	16
1	+10	2000	2.81	1.94	1.06	1.59	5.19	2.77	6.36	3.87	1.03	1.98	2.04	4.16	2.31	0.96	1.50	1.45
2	+12	1680	6.18	8.96	5.38	8.17	8.41	6.93	7.18	7.08	6.44	5.29	7.39	8.12	6.69	6.33	10.75	7.23
3	+16	1190	10.98	14.21	14.25	11.10	15.35	11.49	14.50	9.93	13.08	11.52	13.63	12.75	12.40	16.21	17.94	17.51
4	+20	841	11.09	12.35	12.26	11.04	11.96	13.18	16.85	12.81	13.00	9.67	19.92	20.03	18.65	13.28	14.87	14.06
5	+30	595	6.94	11.07	9.44	10.73	19.11	12.70	16.33	10.93	11.39	11.20	25.09	8.88	16.27	10.41	13.10	13.94
6	+40	425	20.24	25.05	14.80	19.45	16.24	15.95	17.97	14.45	13.31	16.94	23.81	15.60	23.69	16.40	14.06	14.90
7	+70	212	29.37	14.16	32.74	27.77	13.04	21.58	10.49	26.44	30.13	29.90	5.44	20.34	7.78	26.21	18.75	21.32
8	+100	150	10.19	10.79	8.79	9.07	8.47	13.43	7.11	13.80	4.73	11.18	1.38	8.88	10.85	8.89	7.05	8.53
9	+140	106	1.12	0.63	0.49	0.36	0.94	0.46	1.48	0.11	2.96	1.13	0.43	0.36	0.49	0.41	0.41	0.30
10	+200	75	0.27	0.46	0.32	0.24	0.62	0.52	0.68	0.17	1.63	0.54	0.28	0.40	0.32	0.30	0.68	0.22
11	>270	53	0.26	0.11	0.12	0.13	0.27	0.33	0.36	0.08	1.01	0.25	0.23	0.13	0.12	0.17	0.22	0.11
12	<270	<53	0.55	0.27	0.35	0.33	0.40	0.66	0.70	0.31	1.28	0.40	0.37	0.35	0.43	0.42	0.65	0.42
	Total		100.00	100.00	100	100.00	100.00	100.00	100.00	100.00	100.00	100.00	100.00	100.00	100.00	100.00	100.00	100.00

Weights and Percentages of Size Fractions in **Long-Tom Concentrate** Samples

TOTAL SAMPLE WEIGHTS

(grams)

	Sieve	Microns	SAMPLE NUMBER - C 1	2	3	4	5	6	7	8	9	10	11	12	13	14	15	16
1	+10	2000	1913.39	1617.95	1310.52	1457.98	1540.64	2054.55	1352.41	1498.40	2439.33	1198.90	1336.40	1612.06	1022.54	1355.15	1264.40	1769.95
2	+12	1680	330.85	330.32	379.36	405.88	343.32	426.29	293.04	363.11	643.95	302.41	363.11	361.21	229.22	371.45	385.21	454.00
3	+16	1190	60.90	667.17	527.02	625.48	648.13	916.95	509.20	741.77	1063.98	578.61	619.37	829.40	543.55	660.26	795.23	750.81
4	+20	841	790.23	739.83	695.73	826.00	692.33	1132.26	679.01	652.89	1135.90	774.06	785.97	799.19	615.95	662.24	873.34	915.32
5	+30	595	604.72	581.47	682.63	793.03	662.61	890.29	511.03	750.40	972.64	746.96	660.44	684.87	749.93	683.62	722.04	652.65
6	+40	425	1184.42	1294.64	1067.06	1330.58	1444.32	1598.23	887.64	988.44	1425.23	1248.14	1343.34	922.03	737.27	806.81	955.41	1164.96
7	+70	212	1788.51	1213.18	1478.60	1334.41	1401.71	1579.43	1356.77	1250.70	1322.76	1659.15	1135.92	1378.82	1029.66	992.52	1264.84	1410.56
8	+100	150	672.92	498.72	513.59	589.42	666.68	733.74	790.94	718.32	816.63	465.66	471.34	802.86	706.51	252.97	863.70	432.91
9	+140	106	130.75	158.26	130.22	69.65	90.10	333.94	175.85	82.47	150.99	89.29	137.95	154.00	163.38	102.73	98.13	89.20
10	+200	75	68.55	44.41	54.73	57.08	49.57	90.10	97.70	44.41	69.70	40.61	61.90	72.16	60.34	52.68	66.26	66.78
11	>270	53	31.73	20.98	16.22	21.79	18.09	47.86	42.50	18.77	30.97	11.90	31.48	22.55	35.18	25.54	24.38	27.51
12	<270	<53	77.91	73.73	65.52	77.60	73.74	92.38	134.96	83.55	105.18	36.73	66.41	54.18	68.32	42.24	93.96	77.43
		Total	7654.88	7240.66	6921.20	7588.90	7631.24	9896.02	6831.05	7193.23	10177.26	7152.42	7013.63	7693.33	5961.85	6008.21	7406.90	7812.08

TOTAL SAMPLE PERCENTAGES

	Sieve	Microns	SAMPLE NUMBER - C 1	2	3	4	5	6	7	8	9	10	11	12	13	14	15	16
1	+10	2000	25.00	22.35	18.93	19.21	20.19	20.76	19.80	20.83	31.52	16.76	19.05	20.95	17.15	22.55	17.07	22.66
2	+12	1680	4.32	4.56	5.48	5.35	4.50	4.31	4.29	5.05	8.32	4.23	5.18	4.70	3.84	6.18	5.20	5.81
3	+16	1190	0.80	9.21	7.61	8.24	8.49	9.27	7.45	10.31	13.75	8.09	8.83	10.78	9.12	10.99	10.74	9.61
4	+20	841	10.32	10.22	10.05	10.88	9.07	11.44	9.94	9.08	14.68	10.82	11.21	10.39	10.33	11.02	11.79	11.72
5	+30	595	7.90	8.03	9.86	10.45	8.68	9.00	7.48	10.43	12.57	10.44	9.42	8.90	12.58	11.38	9.75	8.35
6	+40	425	15.47	17.88	15.42	17.53	18.93	16.15	12.99	13.74	18.42	17.45	19.15	11.98	12.37	13.43	12.90	14.91
7	+70	212	23.36	16.76	21.36	17.58	18.37	15.96	19.86	17.39	17.09	23.20	16.20	17.92	17.27	16.52	17.08	18.06
8	+100	150	8.79	6.89	7.42	7.77	8.74	7.41	11.58	9.99	10.55	6.51	6.72	10.44	11.85	4.21	11.66	5.54
9	+140	106	1.71	2.19	1.88	0.92	1.18	3.37	2.57	1.15	1.95	1.25	1.97	2.00	2.74	1.71	1.32	1.14
10	+200	75	0.90	0.61	0.79	0.75	0.65	0.91	1.43	0.62	0.90	0.57	0.88	0.94	1.01	0.88	0.89	0.85
11	>270	53	0.41	0.29	0.23	0.29	0.24	0.48	0.62	0.26	0.40	0.17	0.45	0.29	0.59	0.43	0.33	0.35
12	<270	<53	1.02	1.02	0.95	1.02	0.97	0.93	1.98	1.16	1.36	0.51	0.95	0.70	1.15	0.70	1.27	0.99
		Total	100.00	100.00	100.00	100.00	100.00	100.00	100.00	100.00	131.52	100.00	100.00	100.00	100.00	100.00	100.00	100.00

Weights and Percentages of Size Fractions in **Long-Tom Concentrate** Samples

			Sample #													
	1	2	3	4	5	6	7	8	9	10	11	12	13	14	15	16
Mass of material in Catch Tub (kg)	168.4	125.6	174.35	170.9	157.05	149.25	139.9	125.55	148.95	133.2	146.17	157	155.05	155.6	153.2	152.2
Mass of Concentrate (kg)	7.65	7.24	6.92	7.59	7.63	9.90	6.83	7.19	10.18	7.15	7.01	7.69	5.96	6.01	7.41	7.81
Total Sample Mass (kg)	176.05	132.84	181.27	178.49	164.68	159.15	146.73	132.74	159.13	140.35	153.18	164.69	161.01	161.61	160.61	160.01
Mass of Coarse Fractions																
millimeters	kilograms															
(+200)	22.70	0.00	16.90	35.70	5.20	13.60	0.00	2.10	6.80	0.00	15.00	11.60	13.20	6.40	0.00	0.00
91 - 200	2.20	3.70	10.55	3.15	5.70	4.55	4.80	6.55	19.50	3.80	5.70	2.70	6.10	5.70	3.30	10.50
64 - 91	10.55	5.40	12.60	6.65	6.50	16.40	5.50	5.70	10.05	11.30	9.10	9.80	6.95	14.15	7.60	8.30
45 - 64	11.60	3.20	12.50	13.50	9.70	16.55	8.90	11.80	12.40	19.00	15.97	11.55	10.05	20.90	18.70	15.90
32 - 45	11.20	14.20	17.50	14.95	13.60	13.30	11.60	9.95	9.90	12.70	9.60	12.05	13.10	16.60	12.20	12.35
16 - 32	22.90	21.40	22.20	24.05	24.50	18.55	18.95	19.95	22.40	23.00	17.20	23.40	14.60	18.10	17.20	16.40
(8 - 16)	19.70	20.20	17.30	18.80	20.00	14.10	18.55	15.50	18.95	19.60	18.00	18.40	12.25	14.65	18.55	16.40
(4 - 8)	17.35	21.20	16.00	16.80	19.00	11.40	18.25	14.60	15.20	12.40	7.90	18.20	12.10	18.60	17.80	28.80
(2 - 4)	13.00	13.90	13.90	10.20	13.75	9.00	15.90	11.50	9.75	0.00	4.30	10.60	15.30	2.10	17.75	13.30
<2	37.20	22.40	34.90	27.10	39.10	31.80	37.45	27.90	24.00	31.40	43.40	38.70	51.40	38.40	40.10	30.25
Mass of Fine Fractions Wet Sieved in Lab																
millimeters	Mass in Kilograms															
+2	2.0839	2.16594	2.43069	2.2739	2.6223	1.3028	1.7216	1.666	0.905	1.2335	1.2756	1.5247	1.1953	2.6223	2.3777	2.08738
1.68-2	0.15697	0.20816	0.19329	0.15476	0.24445	0.1031	0.1312	0.1722	. 0.1	0.1469	0.1428	0.1356	0.1135	0.2548	0.2636	0.20597
1.19-1.68	0.29895	0.25163	0.33898	0.23074	0.43103	0.2408	0.28	0.3683	0.1225	0.1966	0.2307	0.2763	0.3052	0.4824	0.5316	0.30074
.841-1.19	0.21883	0.22308	0.27615	0.2159	0.40036	0.1964	0.2195	0.3103	0.1086	0.1921	0.1812	0.224	0.3561	0.4098	0.232	0.25701
.595-.841	0.19428	0.18477	0.22772	0.20455	0.21752	0.1794	0.154	0.2816	0.0962	0.1596	0.1856	0.1852	0.467	0.3356	0.3524	0.18562
.425-.595	0.4227	0.22054	0.28963	0.42906	0.27324	0.193	0.1887	0.3003	0.1088	0.1981	0.2168	0.2215	0.5464	0.5089	0.2838	0.23624
.212-.425	0.79984	0.55384	0.63591	0.63697	0.801	0.6139	0.5282	0.8398	0.2314	0.4908	0.3603	0.5114	0.5148	0.8918	0.617	0.53861
.15-.212	0.24359	0.76909	0.31739	0.26713	0.37414	0.2422	0.1859	0.4746	0.1012	0.1448	0.1227	0.1533	0.1372	0.2471	0.3177	0.11742
.106-.212	0.06847	0.06144	0.14395	0.08975	0.27759	0.1439	0.0658	0.275	0.0997	0.136	0.1105	0.0572	0.0431	0.1132	0.1329	0.12814
.075-.106	0.05669	0.12618	0.07871	0.14925	0.18076	0.1028	0.0471	0.2042	0.0771	0.076	0.0695	0.0461	0.035	0.0784	0.0606	0.05785
.053-.075	0.03815	0.02584	0.06039	0.07567	0.11619	0.0833	0.0565	0.1703	0.0875	0.0662	0.0669	0.0415	0.0395	0.0705	0.0304	0.05211
0-.053	0.21865	0.29459	0.23824	0.24682	0.28509	0.3479	0.216	0.4242	0.2468	0.1796	0.2385	0.1686	0.1853	0.3021	0.1799	0.14922
Total Mass of Fines	4.80102	5.0851	5.23105	4.9745	6.22367	3.7494	3.7945	5.4868	2.2849	3.2203	3.2011	3.5453	3.9384	6.3168	5.3795	4.31631
Mass of Fines ranging in size to 2 mm	2.71712	2.91916	2.80036	2.7006	3.60137	2.4466	2.0729	3.8207	1.3799	1.9868	1.9255	2.0206	2.7431	3.6945	3.0018	2.22893

Total Mass Distribution In Catch Tub																
millimeters	Kilograms															
(+200)	22.70	0.00	16.900	35.70	5.20	13.60	0.00	2.10	6.80	0.00	15.00	11.60	13.20	6.40	0.00	0.00
91 - 200	2.20	3.70	10.550	3.15	5.70	4.55	4.80	6.55	19.50	3.80	5.70	2.70	6.10	5.70	3.30	10.50
64 - 91	10.55	5.40	12.600	6.65	6.50	16.40	5.50	5.70	10.05	11.30	9.10	9.80	6.95	14.15	7.60	8.30
45 - 64	11.60	3.20	12.500	13.50	9.70	16.55	8.90	11.80	12.40	19.00	15.97	11.55	10.05	20.90	18.70	15.90
32 - 45	11.20	14.20	17.500	14.95	13.60	13.30	11.60	9.95	9.90	12.70	9.60	12.05	13.10	16.60	12.20	12.35
16 - 32	22.90	21.40	22.200	24.05	24.50	18.55	18.95	19.95	22.40	23.00	17.20	23.40	14.60	18.10	17.20	16.40
(8 - 16)	19.70	20.20	17.300	18.80	20.00	14.10	18.55	15.50	18.95	19.60	18.00	18.40	12.25	14.65	18.55	16.40
(4 - 8)	17.35	21.20	16.000	16.80	19.00	11.40	18.25	14.60	15.20	12.40	7.90	18.20	12.10	18.60	17.80	28.80
(2 - 4)	13.00	13.90	13.900	10.20	13.75	9.00	15.90	11.50	9.75	0.00	4.30	10.60	15.30	2.10	17.75	13.30
1.68-2	2.149	1.597	2.409	1.553	2.654	1.340	2.371	1.257	1.740	2.322	3.218	2.597	2.127	2.649	3.521	2.795
1.19-1.68	4.093	1.931	4.225	2.315	4.680	3.129	5.058	2.689	2.130	3.107	5.199	5.291	5.719	5.014	7.102	4.082
.841-1.19	2.996	1.712	3.442	2.167	4.347	2.553	3.966	2.266	1.888	3.036	4.084	4.291	6.672	4.259	3.099	3.488
.595-.841	2.660	1.418	2.838	2.053	2.362	2.332	2.783	2.057	1.672	2.522	4.184	3.547	8.750	3.488	4.707	2.519
.425-.595	5.787	1.692	3.610	4.306	2.967	2.508	3.408	2.193	1.893	3.131	4.886	4.242	10.239	5.289	3.791	3.206
.212-.425	10.951	4.250	7.925	6.392	8.696	7.979	9.542	6.132	4.025	7.756	8.121	9.795	9.647	9.269	8.242	7.310
.15-.212	3.335	5.902	3.956	2.681	4.062	3.148	3.358	3.465	1.761	2.289	2.766	2.936	2.570	2.568	4.244	1.594
.106-.212	0.937	0.471	1.794	0.901	3.014	1.870	1.189	2.008	1.735	2.150	2.491	1.095	0.807	1.176	1.775	1.739
.075-.106	0.776	0.968	0.981	1.498	1.963	1.336	0.852	1.491	1.342	1.202	1.566	0.883	0.656	0.815	0.809	0.785
.053-.075	0.522	0.198	0.753	0.759	1.261	1.082	1.021	1.244	1.522	1.046	1.508	0.794	0.741	0.732	0.407	0.707
0-.053	2.994	2.261	2.969	2.477	3.095	4.521	3.902	3.097	4.293	2.839	5.377	3.230	3.472	3.140	2.403	2.025
Total	168.400	125.600	174.350	170.900	157.050	149.250	139.900	125.550	148.950	133.200	146.170	157.000	155.050	155.600	153.200	152.200

Mass Distribution in Concentrate	Sample #		Grams													
millimeters	1	2	3	4	5	6	7	8	9	10	11	12	13	14	15	16
(8 - 16)	44.41	41.92	0.00	46.94	57.46	6.94	158.70	42.74	25.24	35.00	25.19	49.22	32.22	13.05	0.00	99.04
(4 - 8)	435.63	434.96	328.38	404.80	382.60	643.77	412.84	430.33	833.55	310.73	363.21	402.44	305.49	375.67	337.03	484.94
(2 - 4)	1433.35	1141.07	982.14	1006.24	1100.58	1403.84	780.86	1025.33	1580.53	853.18	948.00	1160.39	684.83	966.43	927.37	1185.98
1.68-2	330.85	330.32	379.36	405.88	343.32	426.29	293.04	363.11	643.95	302.41	363.11	361.21	229.22	371.45	385.21	454
1.19-1.68	60.9	667.17	527.02	625.48	648.13	916.95	509.2	741.77	1064	578.61	619.37	829.4	543.55	660.26	795.23	750.81
.841-1.19	790.23	739.83	695.73	826	692.33	1132.3	679.01	652.89	1135.9	774.06	785.97	799.19	615.95	662.24	873.34	915.32
.595-.841	604.72	581.47	682.63	793.03	662.61	890.29	511.03	750.4	972.64	746.96	660.44	684.87	749.93	683.62	722.04	652.65
.425-.595	1184.42	1294.64	1067.06	1330.58	1444.32	1598.2	887.64	988.44	1425.2	1248.1	1343.3	922.03	737.27	806.81	955.41	1164.96
.212-.425	1788.51	1213.18	1478.6	1334.41	1401.71	1579.4	1356.8	1250.7	1322.8	1659.2	1135.9	1378.8	1029.7	992.52	1264.8	1410.56
.15-.212	672.92	498.72	513.59	589.42	666.68	733.74	790.94	718.32	816.63	465.66	471.34	802.86	706.51	252.97	863.7	432.91
.106-.212	130.75	158.26	130.22	69.65	90.1	333.94	175.85	82.47	150.99	89.29	137.95	154	163.38	102.73	98.13	89.2
.075-.106	68.55	44.41	54.73	57.08	49.57	90.1	97.7	44.41	69.7	40.61	61.9	72.16	60.34	52.68	66.26	66.78
.053-.075	31.73	20.98	16.22	21.79	18.09	47.86	42.5	18.77	30.97	11.9	31.48	22.55	35.18	25.54	24.38	27.51
0-.053	77.91	73.73	65.52	77.6	73.74	92.38	134.96	83.55	105.18	36.73	66.41	54.18	68.32	42.24	93.96	77.43
Total	7654.88	7240.66	6921.2	7588.9	7631.24	9896	6831.1	7193.2	10177	7152.4	7013.6	7693.3	5961.9	6008.2	7406.9	7812.08

APPENDIX C

Total Mass Distribution		Sample #		Mass in Kilograms													
millimeters	PHI	1	2	3	4	5	6	7	8	9	10	11	12	13	14	15	16
(+200)	-8.00	22.700	0.000	16.900	35.700	5.200	13.600	0.000	2.100	6.800	0.000	15.000	11.600	13.200	6.400	0.000	0.000
91 - 200	-7.00	2.200	3.700	10.550	3.150	5.700	4.550	4.800	6.550	19.500	3.800	5.700	2.700	6.100	5.700	3.300	10.500
64 - 91	-6.51	10.550	5.400	12.600	6.650	6.500	16.400	5.500	5.700	10.050	11.300	9.100	9.800	6.950	14.150	7.600	8.300
45 - 64	-6.00	11.600	3.200	12.500	13.500	9.700	16.550	8.900	11.800	12.400	19.000	15.970	11.550	10.050	20.900	18.700	15.900
32 - 45	-5.49	11.200	14.200	17.500	14.950	13.600	13.300	11.600	9.950	9.900	12.700	9.600	12.050	13.100	16.600	12.200	12.350
16 - 32	-5.00	22.900	21.400	22.200	24.050	24.500	18.550	18.950	19.950	22.400	23.000	17.200	23.400	14.600	18.100	17.200	16.400
(8 - 16)	-4.00	19.744	20.242	17.300	18.847	20.057	14.107	18.709	15.543	18.975	19.635	18.025	18.449	12.282	14.663	18.550	16.499
(4 - 8)	-3.00	17.786	21.635	16.328	17.205	19.383	12.044	18.663	15.030	16.034	12.711	8.263	18.602	12.405	18.976	18.137	29.285
(2 - 4)	-2.00	14.433	15.041	14.882	11.206	14.851	10.404	16.681	12.525	11.331	0.853	5.248	11.760	15.985	3.066	18.677	14.486
1.68-2	-1.00	2.480	1.928	2.788	1.959	2.997	1.766	2.664	1.620	2.384	2.624	3.581	2.958	2.356	3.020	3.906	3.249
1.19-1.68	-0.75	4.154	2.598	4.752	2.941	5.328	4.046	5.567	3.431	3.194	3.685	5.818	6.120	6.263	5.675	7.897	4.832
.841-1.19	-0.25	3.786	2.452	4.137	2.993	5.039	3.685	4.645	2.919	3.024	3.810	4.870	5.090	7.288	4.921	3.973	4.403
.595-.841	0.25	3.265	1.999	3.521	2.846	3.024	3.223	3.294	2.807	2.645	3.269	4.845	4.232	9.500	4.172	5.429	3.172
.425-.595	0.75	6.972	2.987	4.677	5.636	4.411	4.106	4.296	3.182	3.318	4.379	6.229	5.164	10.976	6.096	4.747	4.371
.212-.425	1.23	12.739	5.463	9.404	7.726	10.098	9.558	10.899	7.383	5.348	9.415	9.257	11.174	10.676	10.262	9.507	8.720
.15-.212	2.24	4.008	6.400	4.469	3.270	4.729	3.882	4.149	4.184	2.577	2.754	3.237	3.739	3.276	2.821	5.108	2.026
.106-.212	2.74	1.068	0.630	1.924	0.970	3.104	2.204	1.365	2.090	1.886	2.239	2.629	1.249	0.971	1.279	1.873	1.828
.075-.106	3.24	0.845	1.013	1.036	1.555	2.012	1.426	0.949	1.535	1.411	1.242	1.627	0.955	0.716	0.868	0.875	0.852
.053-.075	3.74	0.554	0.219	0.769	0.781	1.280	1.130	1.063	1.262	1.553	1.058	1.540	0.817	0.776	0.758	0.431	0.735
0-.053	4.24	3.071	2.334	3.035	2.554	3.169	4.614	4.037	3.181	4.398	2.876	5.443	3.284	3.540	3.182	2.497	2.103
Total		176.055	132.841	181.271	178.489	164.681	159.146	146.731	132.743	159.127	140.352	153.184	164.693	161.012	161.608	160.607	160.012

Percentages of Mass		Sample #															
millimeters	PHI	1	2	3	4	5	6	7	8	9	10	11	12	13	14	15	16
(+200)	-8.00	12.89	0.00	9.32	20.00	3.16	8.55	0.00	1.58	4.27	0.00	9.79	7.04	8.20	3.96	0.00	0.00
91 - 200	-7.00	1.25	2.79	5.82	1.76	3.46	2.86	3.27	4.93	12.25	2.71	3.72	1.64	3.79	3.53	2.05	6.56
64 - 91	-6.51	5.99	4.07	6.95	3.73	3.95	10.31	3.75	4.29	6.32	8.05	5.94	5.95	4.32	8.76	4.73	5.19
45 - 64	-6.00	6.59	2.41	6.90	7.56	5.89	10.40	6.07	8.89	7.79	13.54	10.43	7.01	6.24	12.93	11.64	9.94
32 - 45	-5.49	6.36	10.69	9.65	8.38	8.26	8.36	7.91	7.50	6.22	9.05	6.27	7.32	8.14	10.27	7.60	7.72
16 - 32	-5.00	13.01	16.11	12.25	13.47	14.88	11.66	12.91	15.03	14.08	16.39	11.23	14.21	9.07	11.20	10.71	10.25
(8 - 16)	-4.00	11.21	15.24	9.54	10.56	12.18	8.86	12.75	11.71	11.92	13.99	11.77	11.20	7.63	9.07	11.55	10.31
(4 - 8)	-3.00	10.10	16.29	9.01	9.64	11.77	7.57	12.72	11.32	10.08	9.06	5.39	11.30	7.70	11.74	11.29	18.30
(2 - 4)	-2.00	8.20	11.32	8.21	6.28	9.02	6.54	11.37	9.44	7.12	0.61	3.43	7.14	9.93	1.90	11.63	9.05
1.68-2	-1.00	1.41	1.45	1.54	1.10	1.82	1.11	1.82	1.22	1.50	1.87	2.34	1.80	1.46	1.87	2.43	2.03
1.19-1.68	-0.75	2.36	1.96	2.62	1.65	3.24	2.54	3.79	2.58	2.01	2.63	3.80	3.72	3.89	3.51	4.92	3.02
.841-1.19	-0.25	2.15	1.85	2.28	1.68	3.06	2.32	3.17	2.20	1.90	2.71	3.18	3.09	4.53	3.05	2.47	2.75
.595-.841	0.25	1.85	1.51	1.94	1.59	1.84	2.02	2.24	2.11	1.66	2.33	3.16	2.57	5.90	2.58	3.38	1.98
.425-.595	0.75	3.96	2.25	2.58	3.16	2.68	2.58	2.93	2.40	2.09	3.12	4.07	3.14	6.82	3.77	2.96	2.73
.212-.425	1.23	7.24	4.11	5.19	4.33	6.13	6.01	7.43	5.56	3.36	6.71	6.04	6.78	6.63	6.35	5.92	5.45
.15-.212	2.24	2.28	4.82	2.47	1.83	2.87	2.44	2.83	3.15	1.62	1.96	2.11	2.27	2.03	1.75	3.18	1.27
.106-.212	2.74	0.61	0.47	1.06	0.54	1.88	1.38	0.93	1.57	1.19	1.60	1.72	0.76	0.60	0.79	1.17	1.14
.075-.106	3.24	0.48	0.76	0.57	0.87	1.22	0.90	0.65	1.16	0.89	0.89	1.06	0.58	0.44	0.54	0.55	0.53
.053-.075	3.74	0.31	0.17	0.42	0.44	0.78	0.71	0.72	0.95	0.98	0.75	1.01	0.50	0.48	0.47	0.27	0.46
0-.053	4.24	1.74	1.76	1.67	1.43	1.92	2.90	2.75	2.40	2.76	2.05	3.55	1.99	2.20	1.97	1.55	1.31
Total		100	100	100	100	100	100	100	100	100	100	100	100	100	100	100	100

Cummulative Percentages		Sample #																
millimeters	PHI	1	2	3	4	5	6	7	8	9	10	11	12	13	14	15	16	
(+200)	-8.00	100.00	100.00	100.00	100.00	100.00	100.00	100.00	100.00	100.00	100.00	100.00	100.00	100.00	100.00	100.00	100.00	
91 - 200	-7.00	87.11	100.00	90.68	80.00	96.84	91.45	100.00	98.42	95.73	100.00	90.21	92.96	91.80	96.04	100.00	100.00	
64 - 91	-6.51	85.86	97.21	84.86	78.23	93.38	88.60	96.73	93.48	83.47	97.29	86.49	91.32	88.01	92.51	97.95	93.44	
45 - 64	-6.00	79.86	93.15	77.91	74.51	89.43	78.29	92.98	89.19	77.16	89.24	80.55	85.37	83.70	83.76	93.21	88.25	
32 - 45	-5.49	73.28	90.74	71.01	66.94	83.54	67.89	86.91	80.30	69.36	75.70	70.12	78.35	77.46	70.82	81.57	78.31	
16 - 32	-5.00	66.91	80.05	61.36	58.57	75.29	59.53	79.01	72.80	63.14	66.66	63.85	71.04	69.32	60.55	73.97	70.60	
(8 - 16)	-4.00	53.91	63.94	49.11	45.09	60.41	47.88	66.09	57.78	49.07	50.27	52.63	56.83	60.25	49.35	63.26	60.35	
(4 - 8)	-3.00	42.69	48.70	39.57	34.54	48.23	39.01	53.34	46.07	37.14	36.28	40.86	45.63	52.62	40.28	51.71	50.04	
(2 - 4)	-2.00	32.59	32.42	30.56	24.90	36.46	31.45	40.63	34.74	27.07	27.22	35.46	34.33	44.92	28.54	40.42	31.73	
1.68-2	-1.00	24.39	21.09	22.35	18.62	27.44	24.91	29.26	25.31	19.94	26.61	32.04	27.19	34.99	26.64	28.79	22.68	
1.19-1.68	-0.75	22.98	19.64	20.81	17.52	25.62	23.80	27.44	24.09	18.45	24.74	29.70	25.39	33.53	24.77	26.36	20.65	
.841-1.19	-0.25	20.62	17.69	18.19	15.87	22.39	21.26	23.65	21.50	16.44	22.12	25.90	21.68	29.64	21.26	21.44	17.63	
.595-.841	0.25	18.47	15.84	15.91	14.20	19.33	18.94	20.48	19.30	14.54	19.40	22.72	18.59	25.11	18.22	18.97	14.88	
.425-.595	0.75	16.62	14.34	13.96	12.60	17.49	16.92	18.24	17.19	12.88	17.07	19.56	16.02	19.21	15.63	15.59	12.90	
.212-.425	1.23	12.66	12.09	11.38	9.44	14.81	14.34	15.31	14.79	10.79	13.95	15.49	12.88	12.39	11.86	12.63	10.16	
.15-.212	2.24	5.42	7.98	6.20	5.12	8.68	8.33	7.88	9.23	7.43	7.25	9.45	6.10	5.76	5.51	6.71	4.71	
.106-.212	2.74	3.15	3.16	3.73	3.28	5.81	5.89	5.05	6.08	5.81	5.28	7.34	3.83	3.73	3.77	3.53	3.45	
.075-.106	3.24	2.54	2.68	2.67	2.74	3.92	4.51	4.12	4.50	4.63	3.69	5.62	3.07	3.13	2.97	2.37	2.31	
.053-.075	3.74	2.06	1.92	2.10	1.87	2.70	3.61	3.48	3.35	3.74	2.80	4.56	2.49	2.68	2.44	1.82	1.77	
0-.053	4.24	1.74	1.76	1.67	1.43	1.92	2.90	2.75	2.40	2.76	2.05	3.55	1.99	2.20	1.97	1.55	1.31	

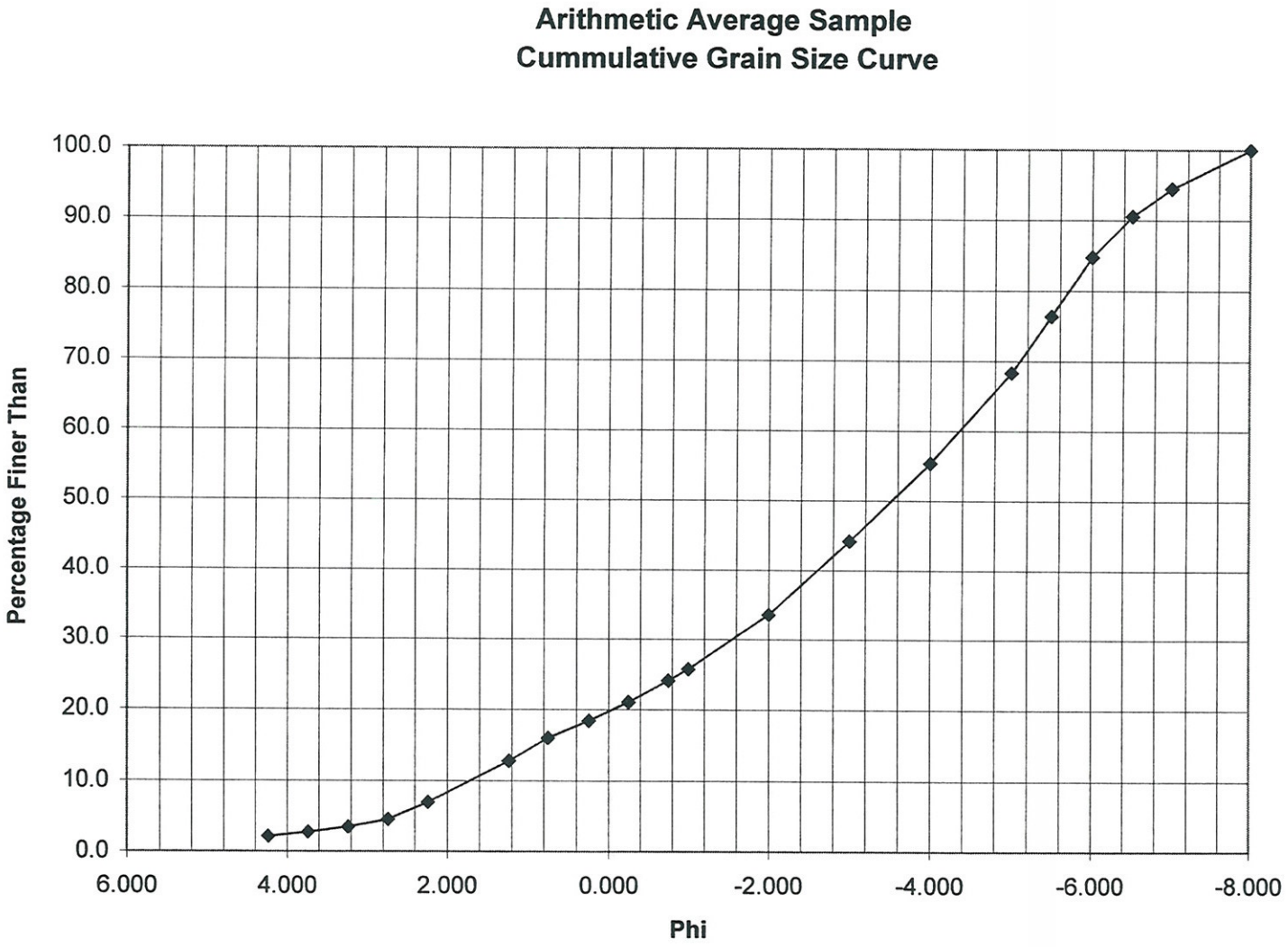
Arithmetic Average Sample
Cummulative Grain Size Curve
Percentage Finer Than
100.0
90.0
80.0
70.0
60.0
50.0
40.0
30.0
20.0
10.0
0.0
6.000
4.000
2.000
0.000
-2.000
-4.000
-6.000
-8.000
Phi

Sample T - 1
Cummulative Grain Size Curve

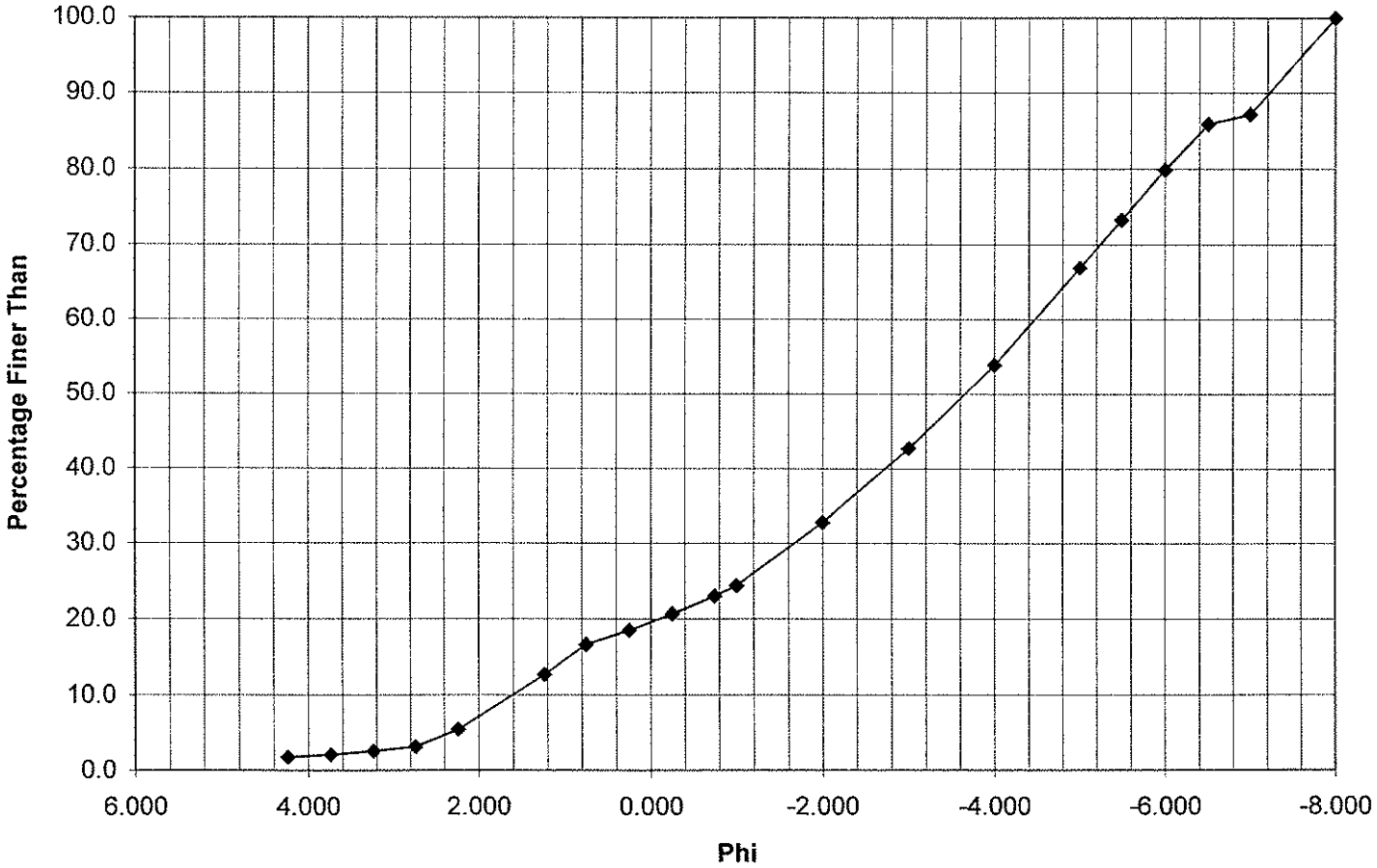

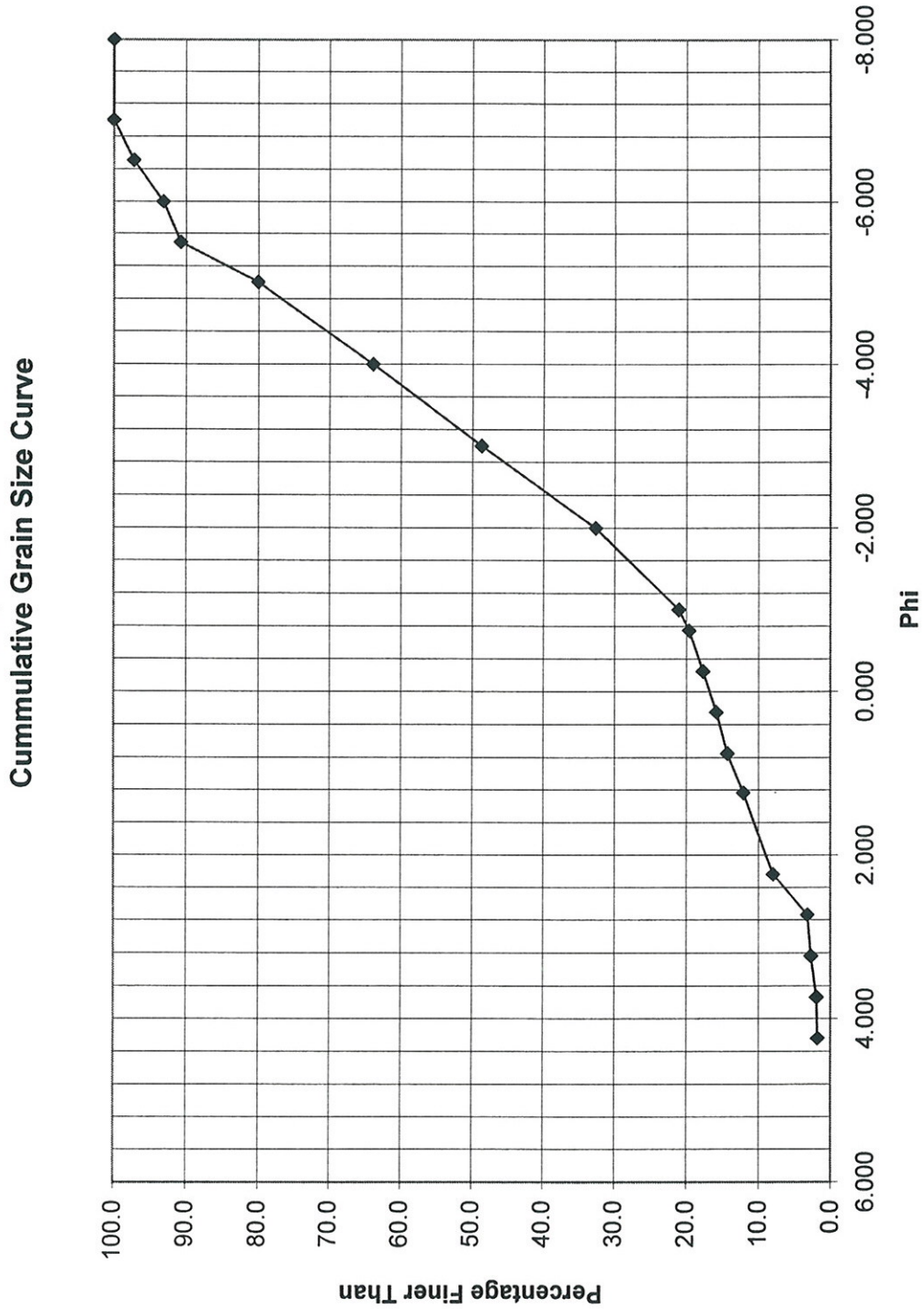
Sample T - 2
Cummulative Grain Size Curve
Percentage Finer Than
100.0
90.0
80.0
70.0
60.0
50.0
40.0
30.0
20.0
10.0
0.0
6.000
4.000
2.000
0.000
-2.000
-4.000
-6.000
-8.000
Phi

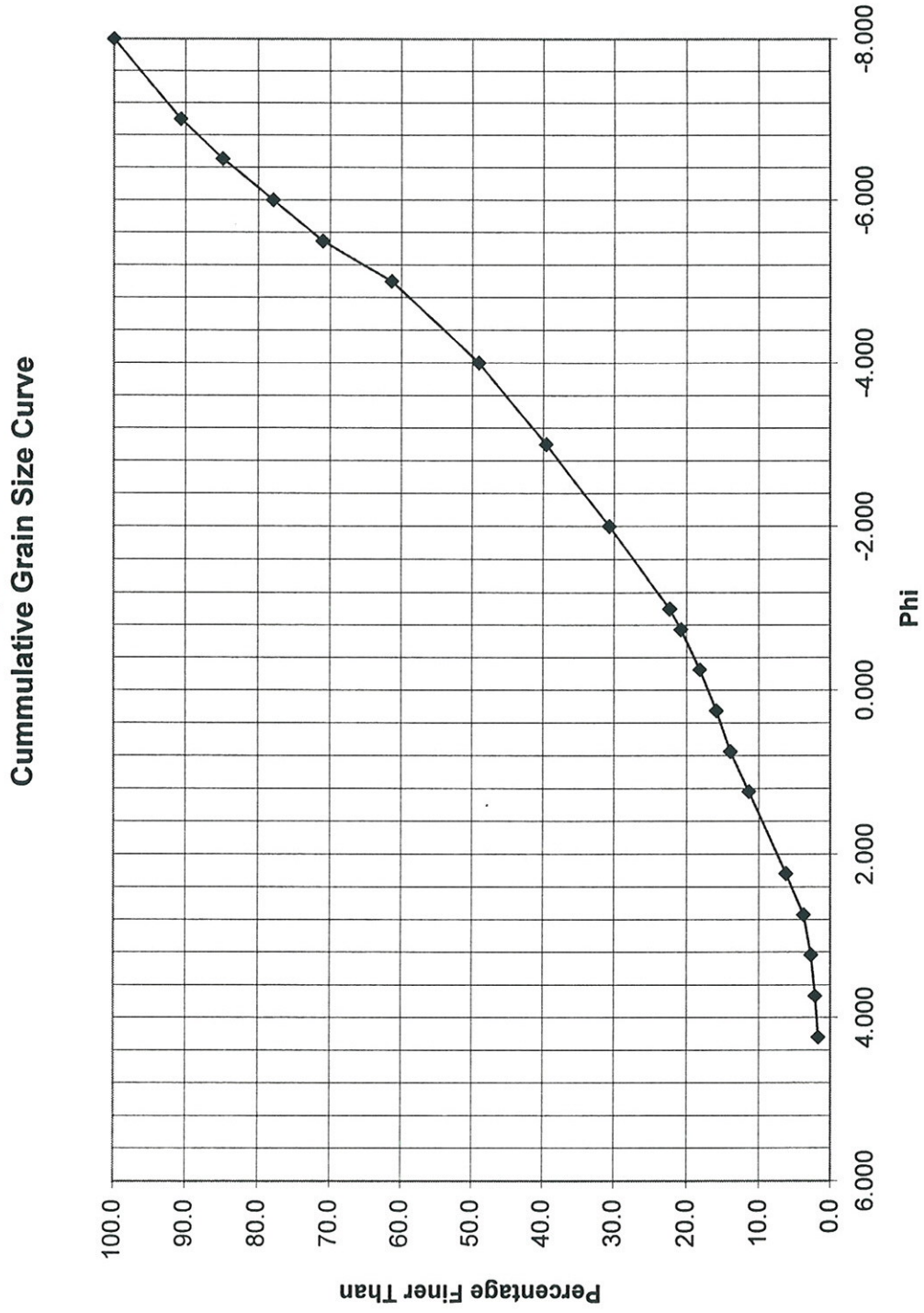
Sample T - 3
Cummulative Grain Size Curve
Percentage Finer Than
100.0
90.0
80.0
70.0
60.0
50.0
40.0
30.0
20.0
10.0
0.0
6.000
4.000
2.000
0.000
-2.000
-4.000
-6.000
-8.000
Phi

APPENDIX D

Cummulative Percentages

Grain Size		Sample #																
mm	Phi	1	2	3	4	5	6	7	8	9	10	11	12	13	14	29	30	Average
200	-8.000	100.0	100.0	100.0	100.0	100.0	100.0	100.0	100.0	100.0	100.0	100.0	100.0	100.0	100.0	100.0	100.0	100.0
128	-7.000	90.7	80.0	96.8	91.5	100.0	98.4	95.7	100.0	90.2	93.0	91.8	96.0	100.0	100.0	87.1	100.0	94.5
91	-6.508	84.9	78.2	93.4	88.6	96.7	93.5	83.5	97.3	86.5	91.3	88.0	92.5	97.9	93.4	85.9	97.2	90.6
64	-6.000	77.9	74.5	89.4	78.3	93.0	89.2	77.2	89.2	80.5	85.4	83.7	83.8	93.2	88.3	79.9	93.1	84.8
45	-5.492	71.0	66.9	83.5	67.9	86.9	80.3	69.4	75.7	70.1	78.4	77.5	70.8	81.6	78.3	73.3	90.7	76.4
32	-5.000	61.4	58.6	75.3	59.5	79.0	72.8	63.1	66.7	63.9	71.0	69.3	60.6	74.0	70.6	66.9	80.1	68.3
16	-4.000	49.1	45.1	60.4	47.9	66.1	57.8	49.1	50.3	52.6	56.8	60.3	49.4	63.3	60.3	53.9	63.9	55.4
8	-3.000	39.6	34.6	48.3	39.0	53.5	46.1	37.2	36.3	40.9	45.7	52.6	40.3	51.7	50.1	42.7	48.7	44.2
4	-2.000	30.7	25.1	36.6	31.7	40.9	35.0	27.5	27.4	35.6	34.5	45.1	28.7	40.6	32.0	32.8	32.7	33.5
2	-1.000	22.3	18.6	27.4	24.9	29.3	25.3	19.9	26.6	32.0	27.2	35.0	26.6	28.8	22.7	24.4	21.1	25.8
1.68	-0.748	20.8	17.5	25.6	23.8	27.4	24.1	18.4	24.7	29.7	25.4	33.5	24.8	26.4	20.7	23.0	19.6	24.1
1.19	-0.251	18.2	15.9	22.4	21.3	23.6	21.5	16.4	22.1	25.9	21.7	29.6	21.3	21.4	17.6	20.6	17.7	21.1
0.841	0.250	15.9	14.2	19.3	18.9	20.5	19.3	14.5	19.4	22.7	18.6	25.1	18.2	19.0	14.9	18.5	15.8	18.4
0.595	0.749	14.0	12.6	17.5	16.9	18.2	17.2	12.9	17.1	19.6	16.0	19.2	15.6	15.6	12.9	16.6	14.3	16.0
0.425	1.234	11.4	9.4	14.8	14.3	15.3	14.8	10.8	14.0	15.5	12.9	12.4	11.9	12.6	10.2	12.7	12.1	12.8
0.212	2.238	6.2	5.1	8.7	8.3	7.9	9.2	7.4	7.2	9.5	6.1	5.8	5.5	6.7	4.7	5.4	8.0	7.0
0.15	2.737	3.7	3.3	5.8	5.9	5.1	6.1	5.8	5.3	7.3	3.8	3.7	3.8	3.5	3.4	3.1	3.2	4.6
0.106	3.238	2.7	2.7	3.9	4.5	4.1	4.5	4.6	3.7	5.6	3.1	3.1	3.0	2.4	2.3	2.5	2.7	3.5
0.075	3.737	2.1	1.9	2.7	3.6	3.5	3.3	3.7	2.8	4.6	2.5	2.7	2.4	1.8	1.8	2.1	1.9	2.7
0.053	4.238	1.7	1.4	1.9	2.9	2.8	2.4	2.8	2.0	3.6	2.0	2.2	2.0	1.6	1.3	1.7	1.8	2.1

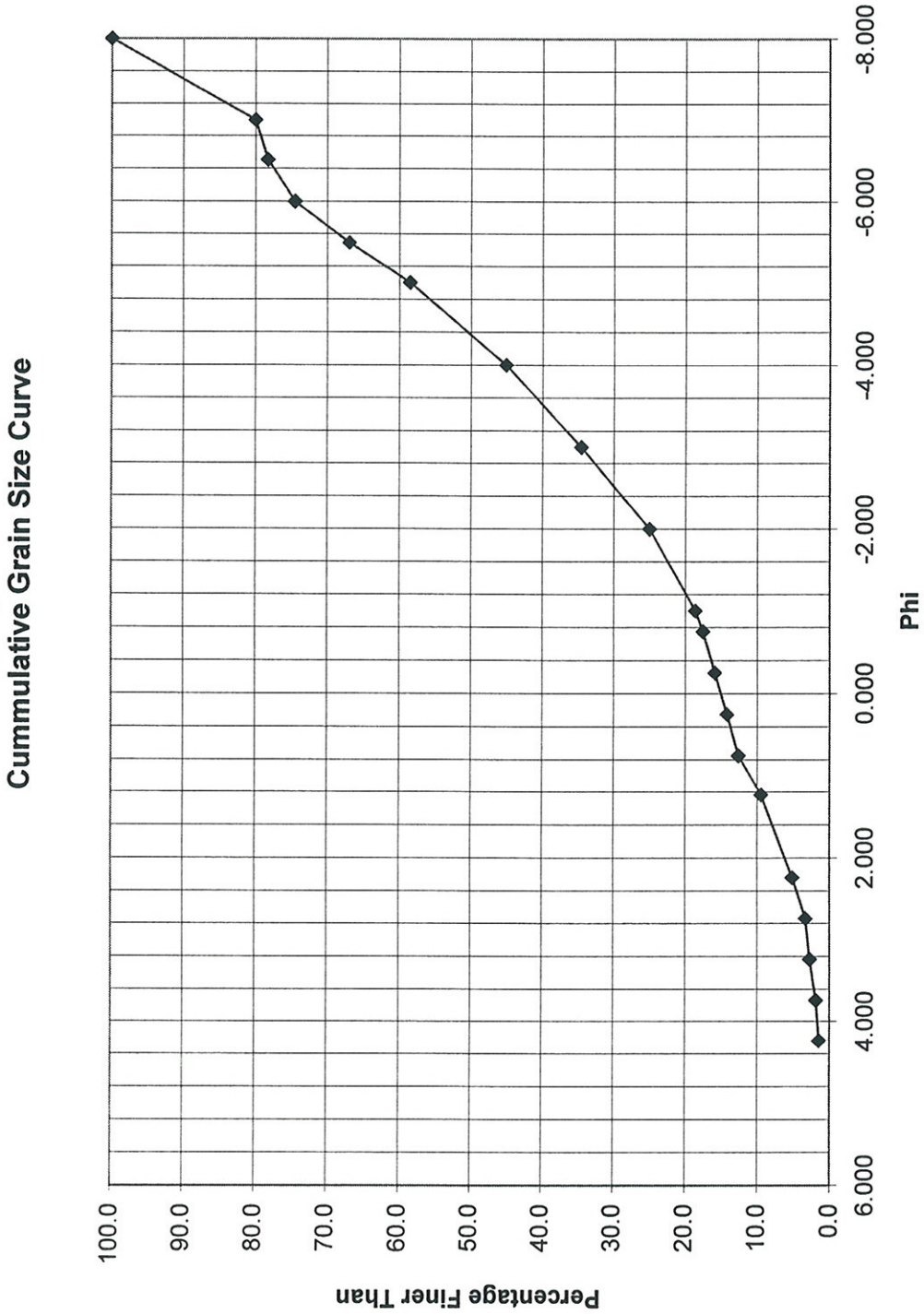
Sample T - 4
Cummulative Grain Size Curve
Percentage Finer Than
100.0
90.0
80.0
70.0
60.0
50.0
40.0
30.0
20.0
10.0
0.0
6.000
4.000
2.000
0.000
-2.000
-4.000
-6.000
-8.000
Phi

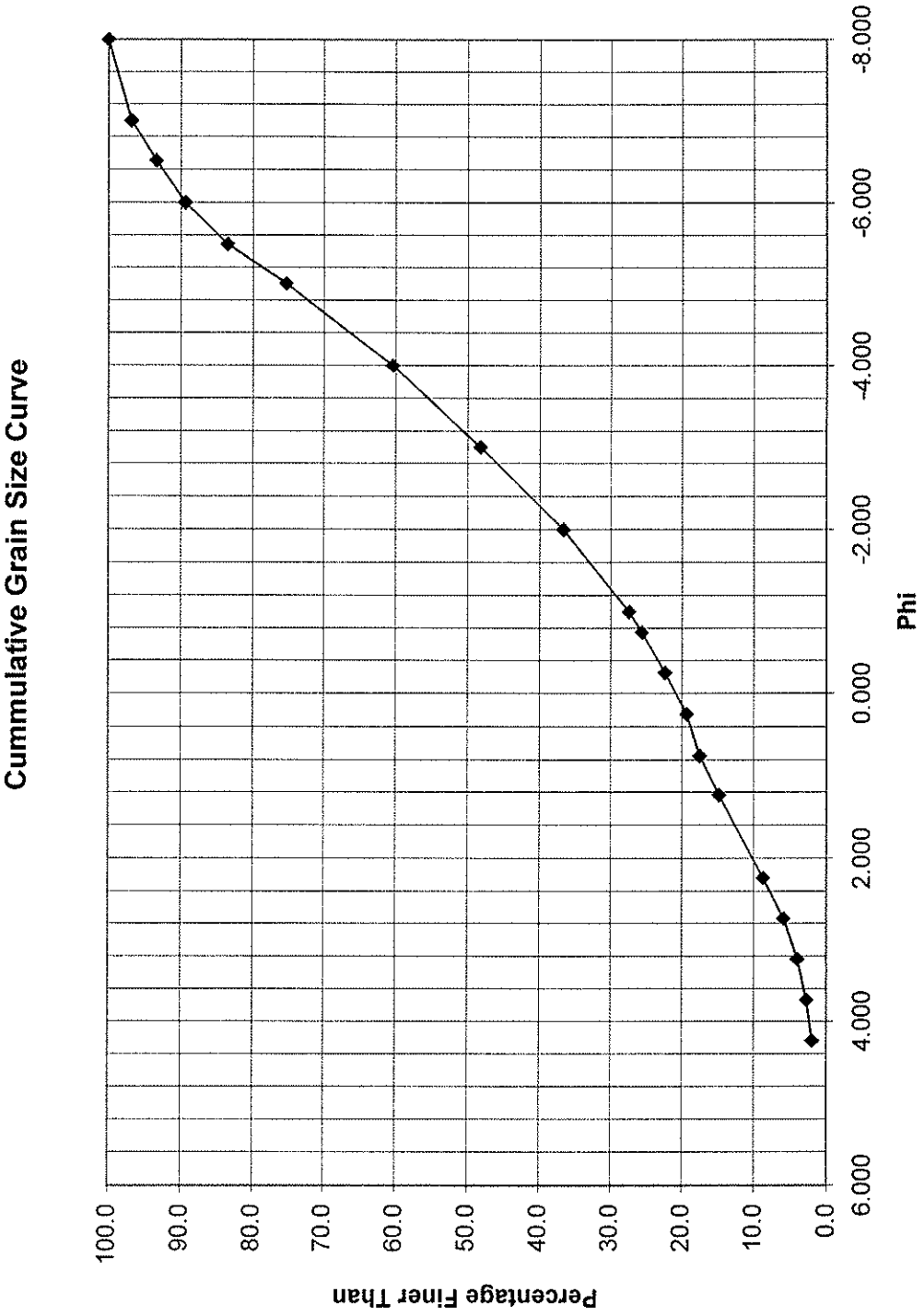
Sample T - 5
Cummulative Grain Size Curve
Percentage Finer Than
100.0
90.0
80.0
70.0
60.0
50.0
40.0
30.0
20.0
10.0
0.0
6.000
4.000
2.000
0.000
-2.000
-4.000
-6.000
-8.000
Phi

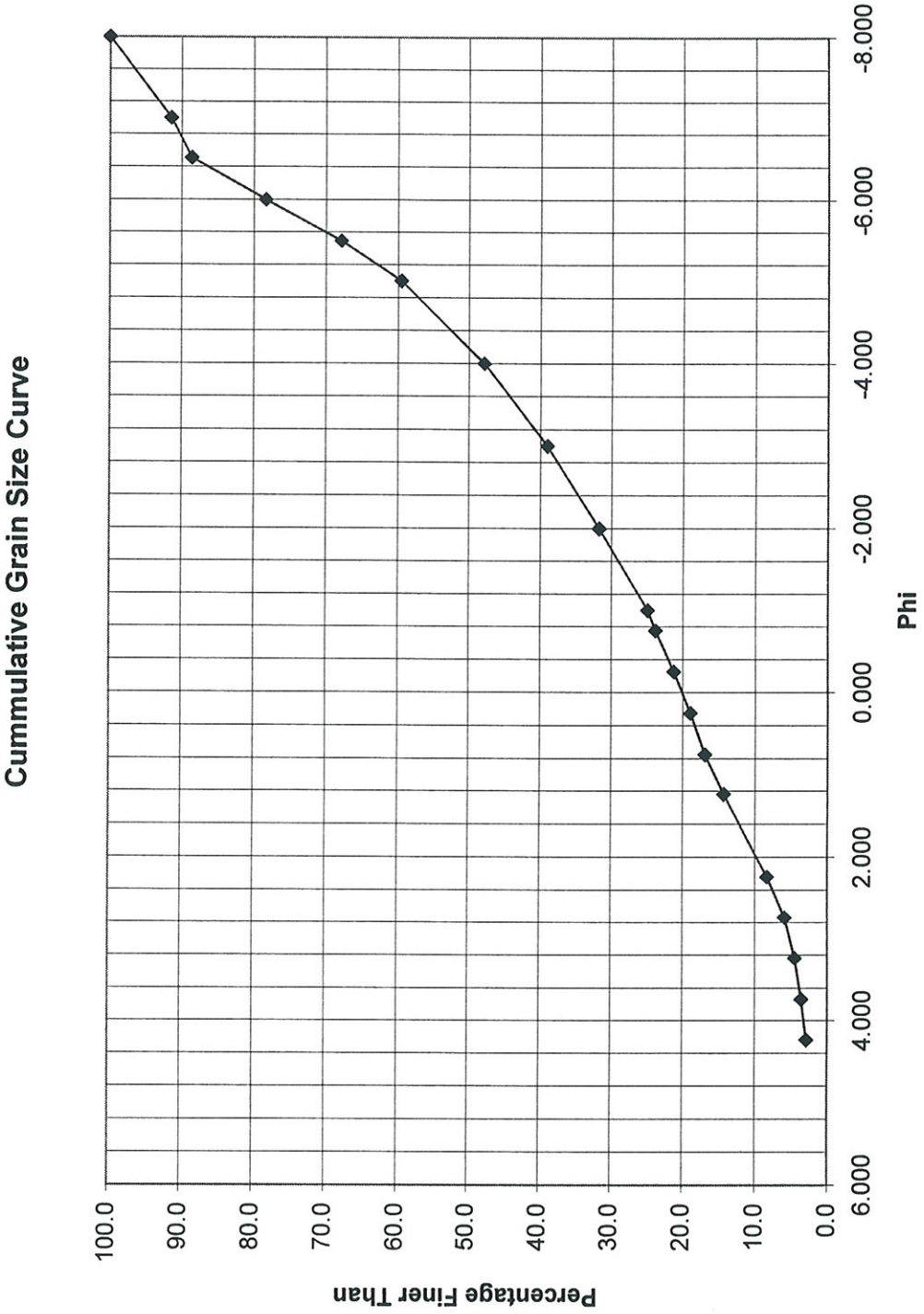
Sample T - 6
Cummulative Grain Size Curve
Percentage Finer Than
100.0
90.0
80.0
70.0
60.0
50.0
40.0
30.0
20.0
10.0
0.0
6.000
4.000
2.000
0.000
-2.000
-4.000
-6.000
-8.000
Phi

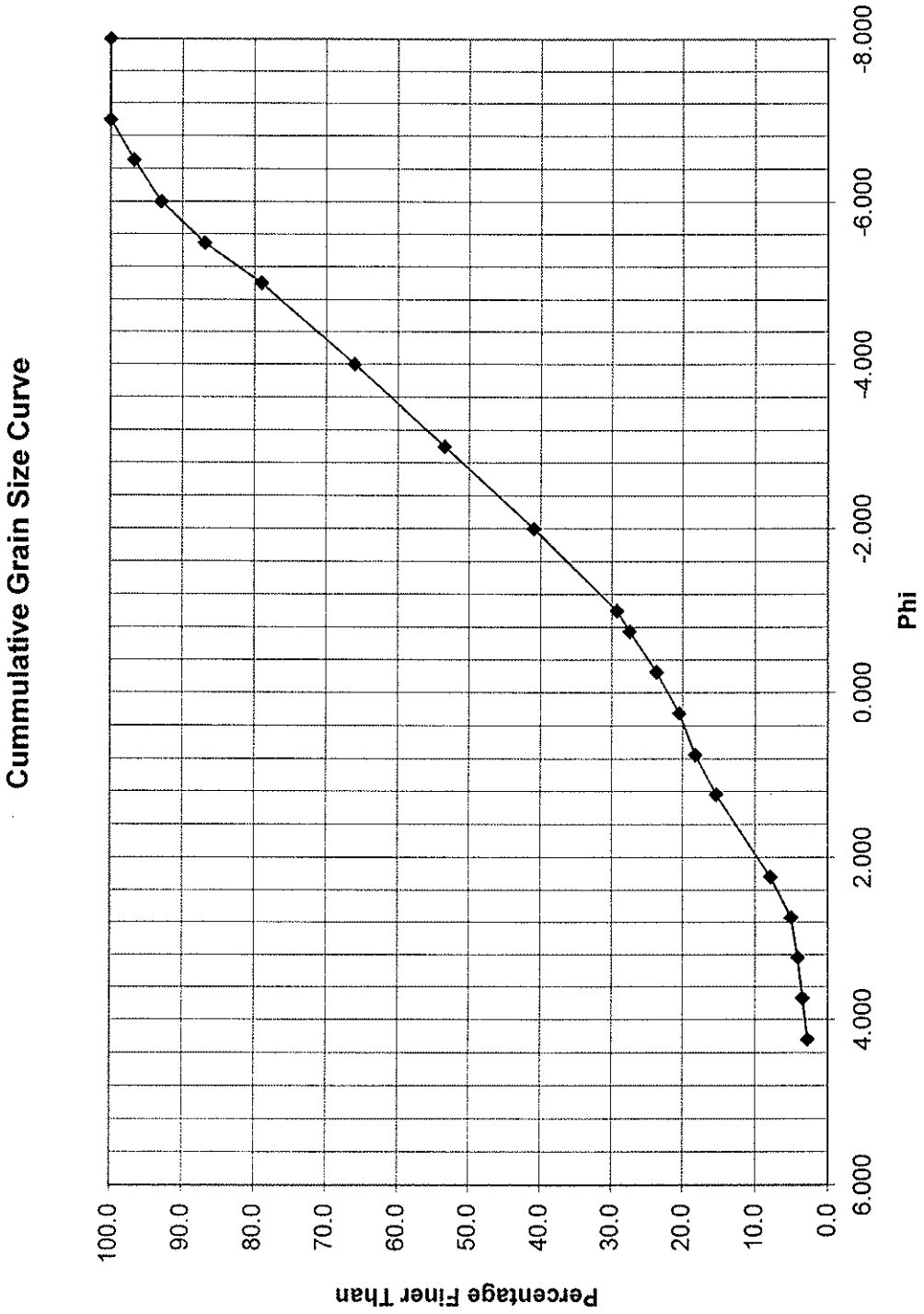
Sample T - 7
Cummulative Grain Size Curve
Percentage Finer Than
100.0
90.0
80.0
70.0
60.0
50.0
40.0
30.0
20.0
10.0
0.0
6.000
4.000
2.000
0.000
-2.000
-4.000
-6.000
-8.000
Phi

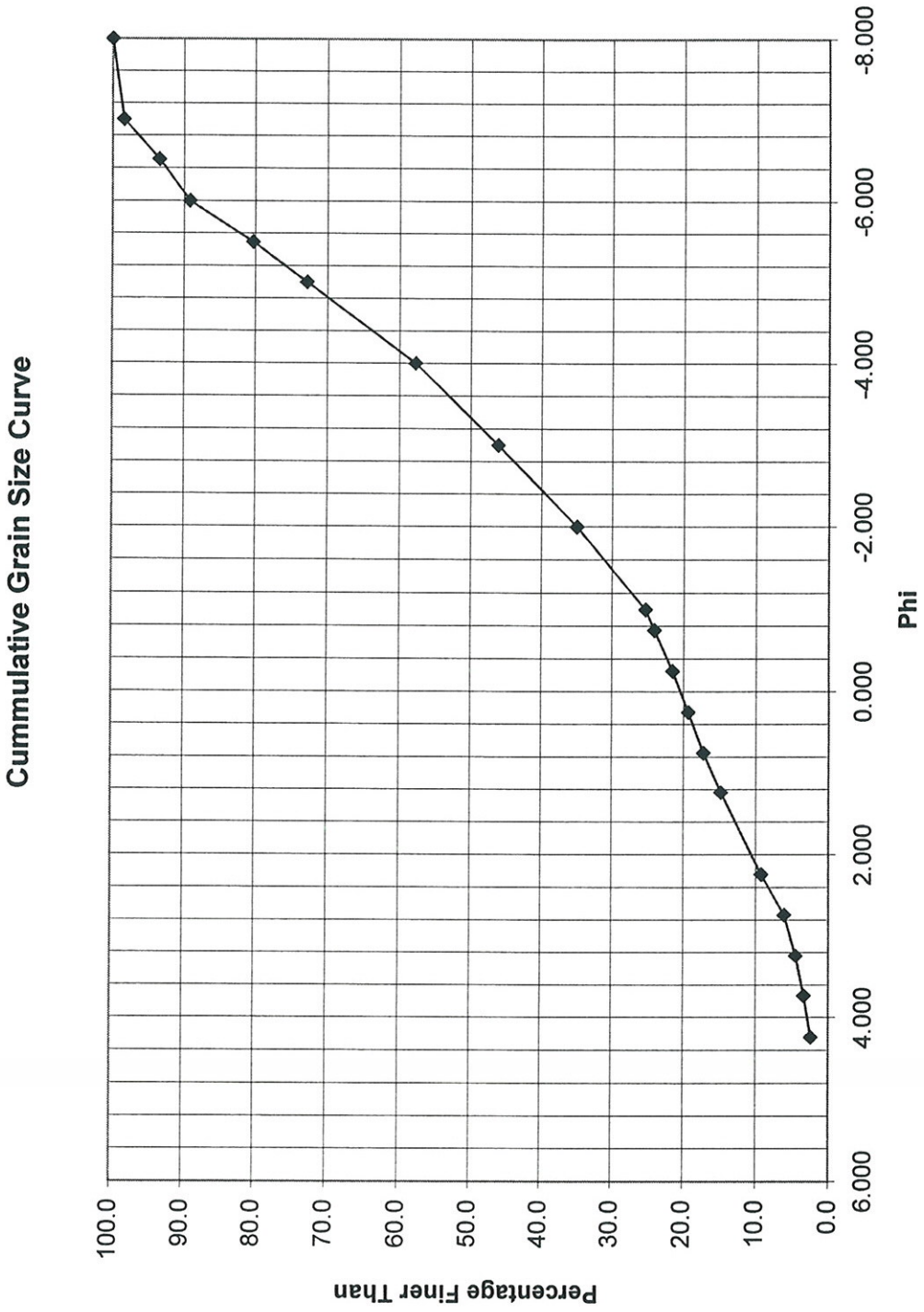
Sample T - 8
Cummulative Grain Size Curve
Percentage Finer Than
100.0
90.0
80.0
70.0
60.0
50.0
40.0
30.0
20.0
10.0
0.0
6.000
4.000
2.000
0.000
-2.000
-4.000
-6.000
-8.000
Phi

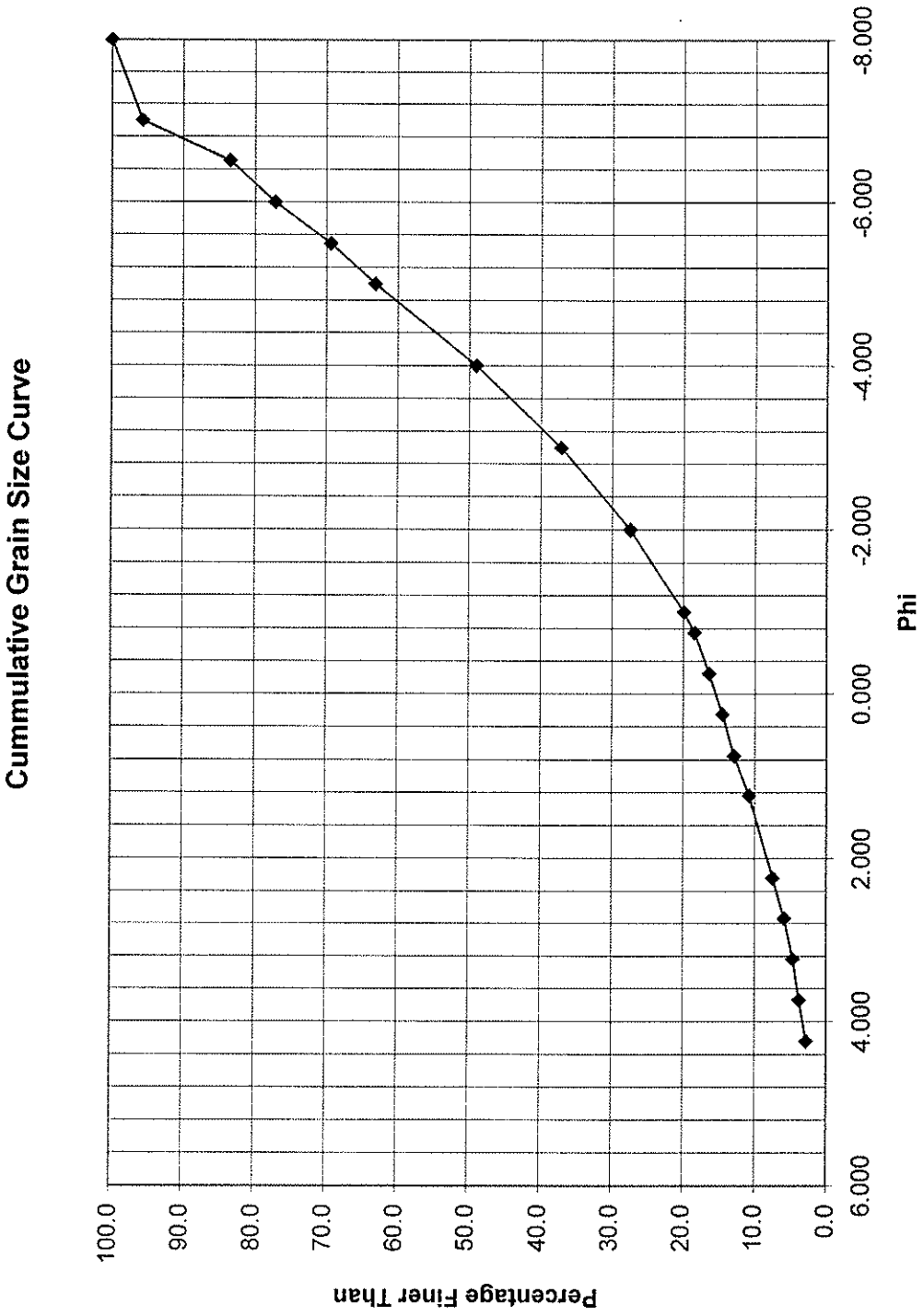
Sample T - 9
Cummulative Grain Size Curve
Percentage Finer Than
100.0
90.0
80.0
70.0
60.0
50.0
40.0
30.0
20.0
10.0
0.0
6.000
4.000
2.000
0.000
-2.000
-4.000
-6.000
-8.000
Phi

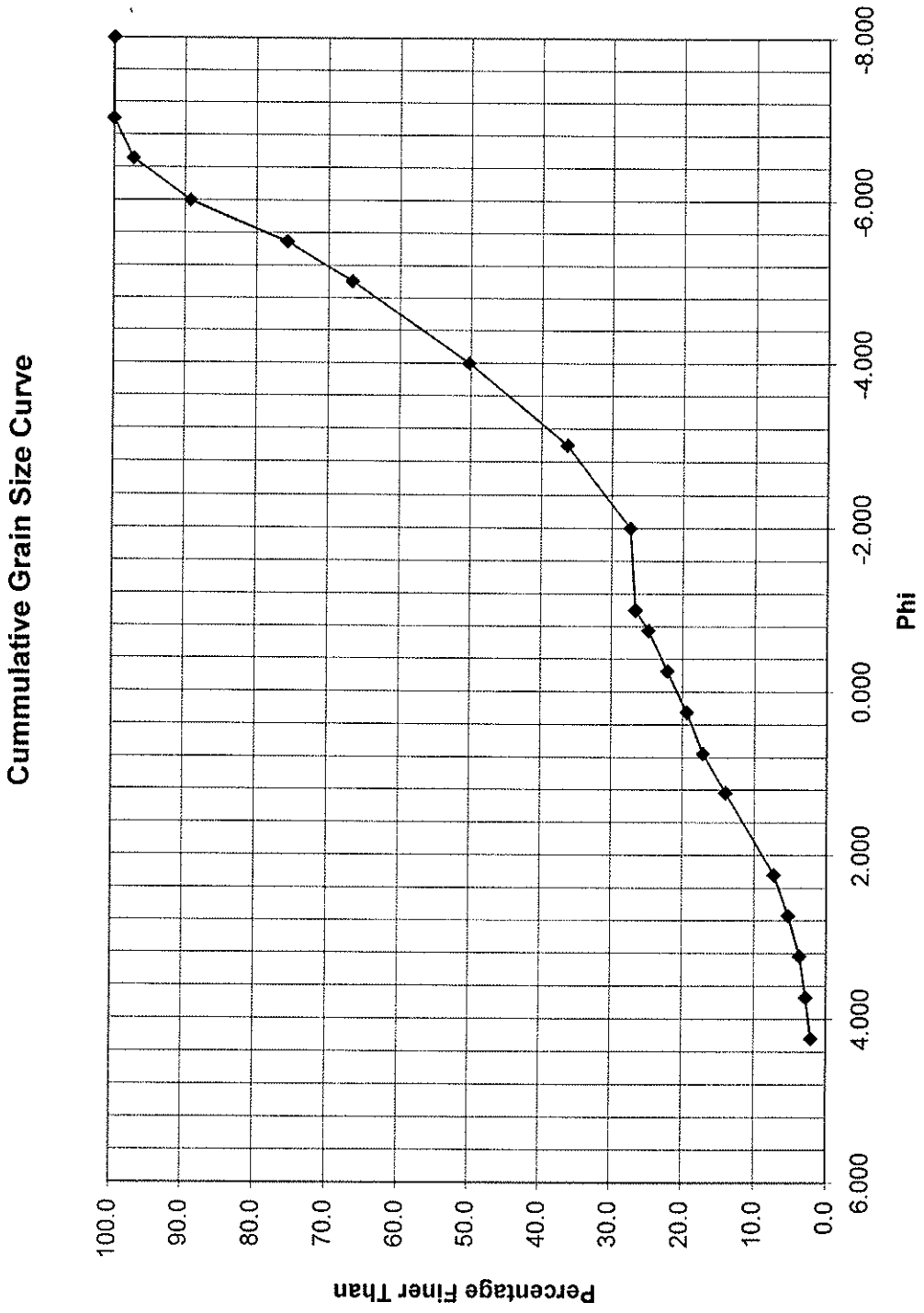
Sample T - 10
Cummulative Grain Size Curve
Percentage Finer Than
100.0
90.0
80.0
70.0
60.0
50.0
40.0
30.0
20.0
10.0
0.0
6.000
4.000
2.000
0.000
-2.000
-4.000
-6.000
-8.000
Phi

Sample T - 11
Cummulative Grain Size Curve

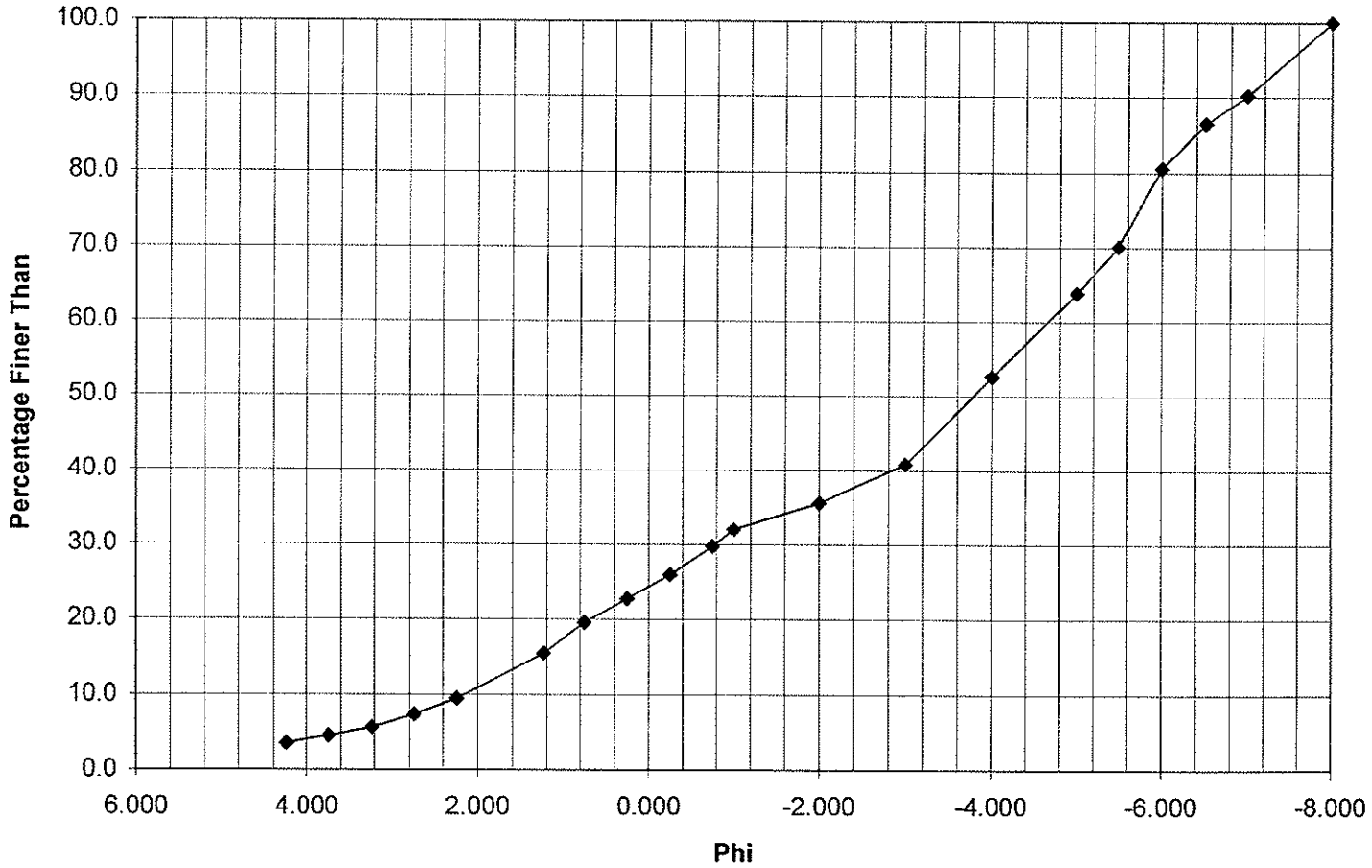

Sample T - 12
Cummulative Grain Size Curve

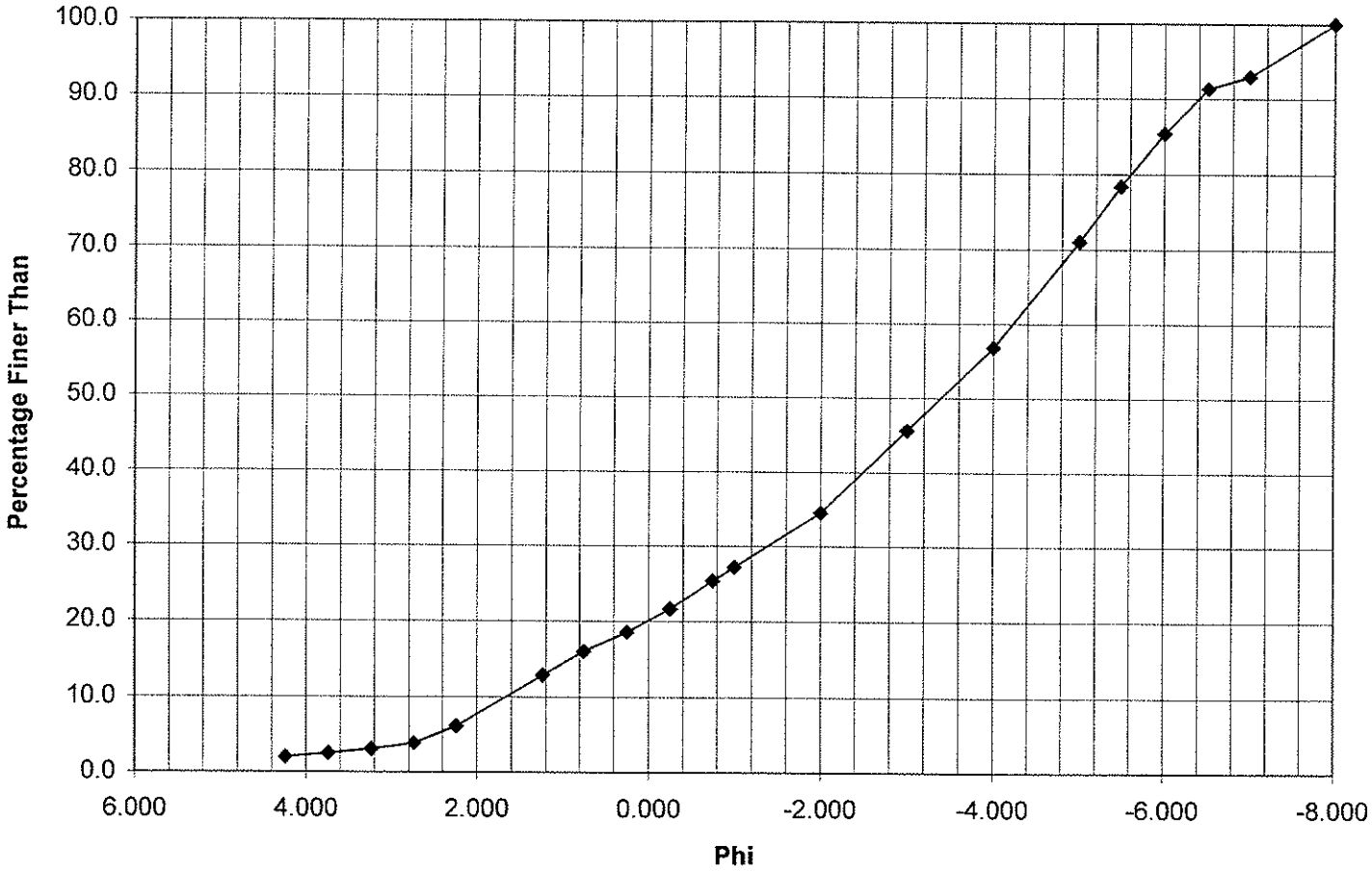

Sample T - 13
Cummulative Grain Size Curve

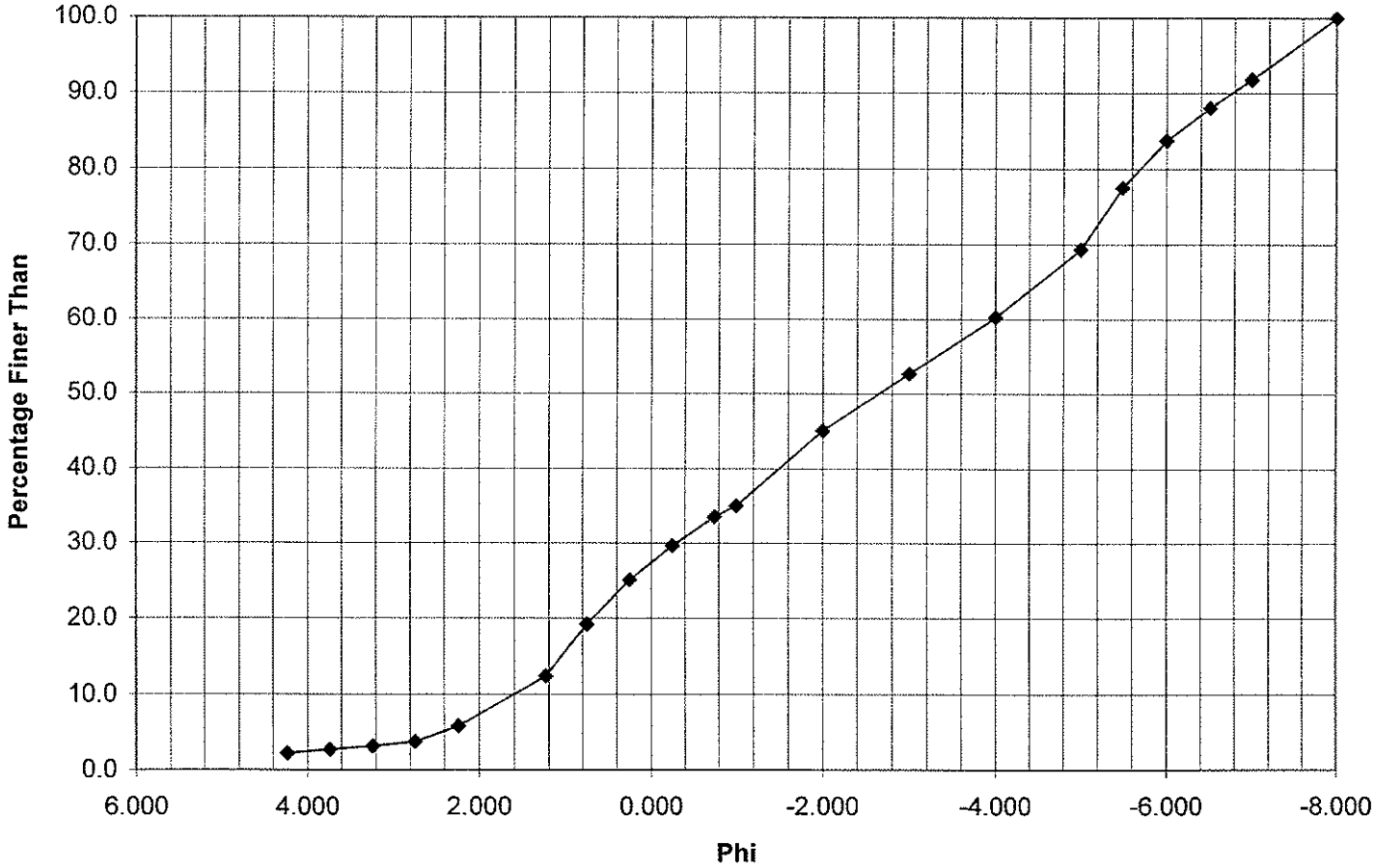

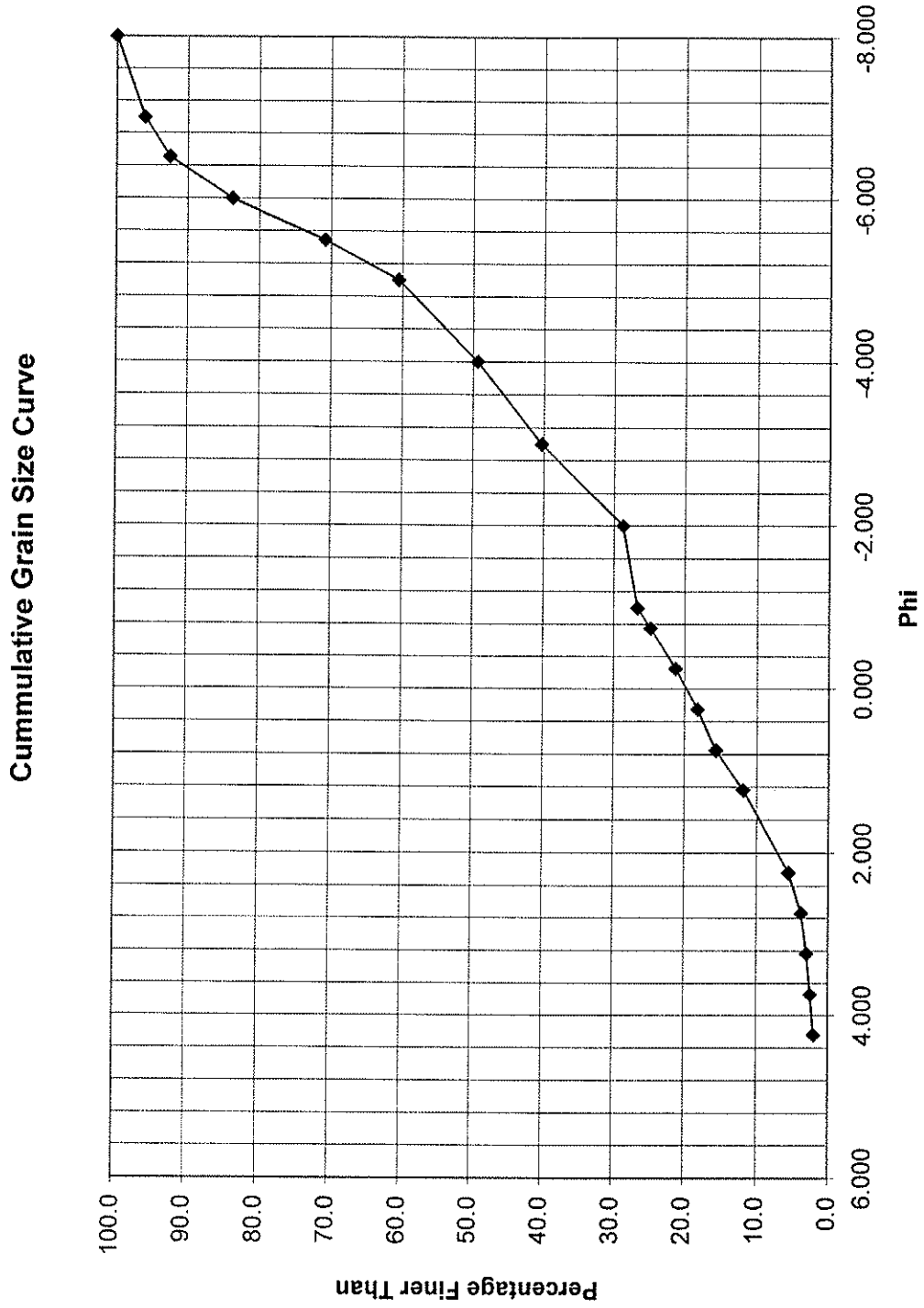
Sample T - 14
Cummulative Grain Size Curve
Percentage Finer Than
100.0
90.0
80.0
70.0
60.0
50.0
40.0
30.0
20.0
10.0
0.0
6.000
4.000
2.000
0.000
-2.000
-4.000
-6.000
-8.000
Phi

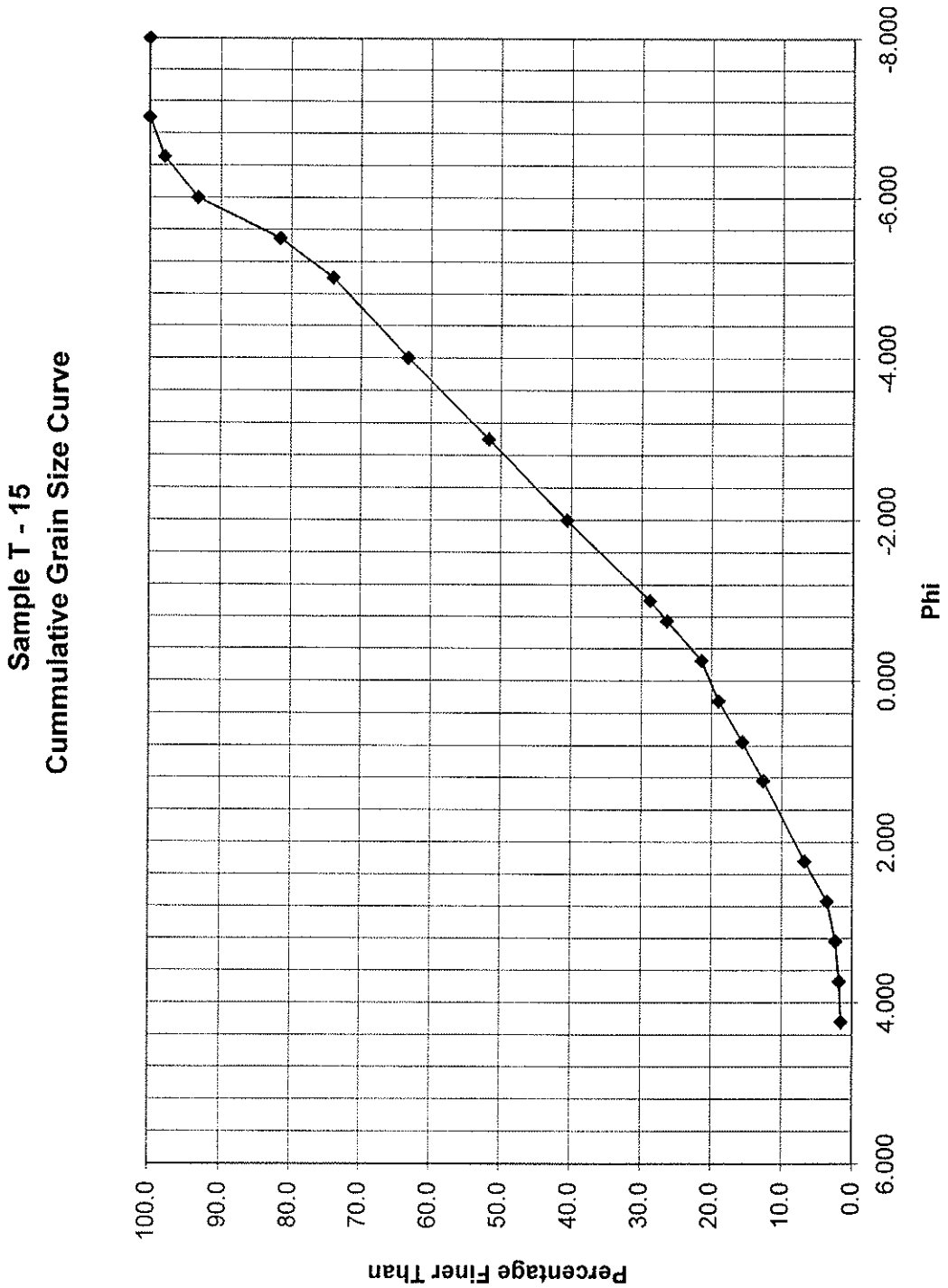
Sample T - 15
Cummulative Grain Size Curve
Percentage Finer Than
100.0
90.0
80.0
70.0
60.0
50.0
40.0
30.0
20.0
10.0
0.0
6.000
4.000
2.000
0.000
-2.000
-4.000
-6.000
-8.000
Phi

Sample T - 16
Cummulative Grain Size Curve

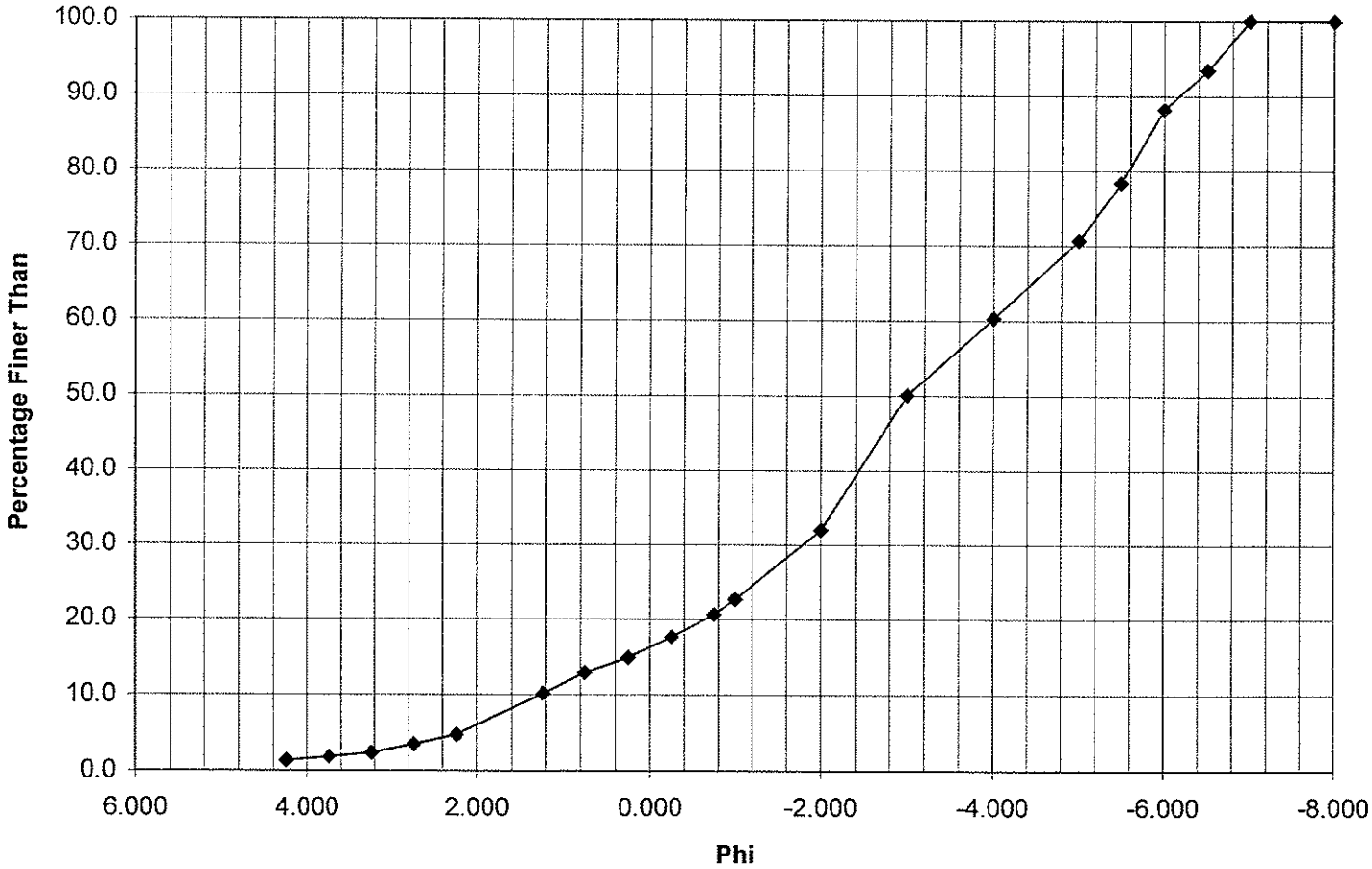

APPENDIX E

PROBABILITY GRAPH DATA

POPULATION A

Sample Number	% of popluation in sample	Phi 50	Sigma (std. dev)	Phi 95	Phi 5	Phi 84	Phi 16	-Binormal -Trinormal
T-1	16	1.8	-1.2	0.9	2.8	1.2	5.0	T
T-2	11	3.1	-1.1	1.3	5.0	2.1	4.2	T
T-3	16	1.6	-1.4	0.8	5.2	1.6	4.5	T
T-4	12	2.0	-0.5	0.8	3.4	0.9	1.1	T
T-5	22	2.0	-1.3	0.3	4.3	0.5	3.4	B
T-6	30	2.2	-2.4	-3.8	4.6	-1.3	3.4	B
T-7	14	2.6	-0.6	3.0	4.0	1.6	3.4	T
T-8	26	1.4	-2.1	-2.2	4.8	-0.8	3.6	B
T-9	20	1.5	-2.0	-2.0	4.7	-0.5	3.5	B
T-10	27	1.2	-1.8	-1.8	4.3	-0.6	3.0	B
T-11	42	0.4	-1.8	-3.4	4.2	-1.8	0.8	B
T-12	27	1.1	-1.7	-1.8	3.7	-0.6	2.8	T
T-13	42	0.4	-2.6	-6.5	4.4	-1.6	2.2	T
T-14	50	-1.8	-3.1	-7.0	3.2	-5.0	1.2	B
T-15	33	0.6	-2.0	-2.0	2.4	-1.2	4.0	T
T-16	12	1.7	-1.1	0.8	2.8	1.1	4.2	T
Average	25	1.4	-1.7	-1.4	4.0	-0.3	3.1	
Max	50	3	0	3	5	2	5	
Min	11	-2	-3	-7	2	-5	1	

Average Grain Diameter (mm): 0.4

POPULTATION B

Sample Number	% of popluation in sample	Phi 50	Sigma (std. dev)	Phi 95	Phi 5	Phi 84	Phi 16	-Binormal -Trinormal
T-1	78	-4.8	-2.4	-8.6	-0.8	-7.2	-2.4	T
T-2	83	-3.6	-1.9	-6.8	-0.4	-5.6	-1.7	T
T-3	78	-5.1	-1.6	-7.8	-2.4	-6.8	-3.5	T
T-4	83	-4.9	-1.9	-8.0	-1.8	-6.8	-3.0	T
T-5	78	-3.8	-2.0	-7.0	-0.4	-5.8	-1.8	B
T-6	70	-5.3	-1.5	-7.9	-2.7	-6.8	-3.8	B
T-7	78	-3.6	-2.3	-7.3	0.3	-5.9	-1.4	T
T-8	74	-4.2	-2.1	-7.6	-0.8	-6.2	-2.0	B
T-9	80	-5.0	-2.2	-8.8	-1.4	-7.2	-2.7	B
T-10	73	-4.9	-1.9	-8.0	-1.6	-6.8	-3.0	B
T-11	58	-5.7	-1.3	-7.8	-3.5	-7.0	-4.4	B
T-12	70	-4.8	-1.8	-7.8	-1.8	-6.5	-2.9	T
T-13	55	-5.2	-1.5	-7.6	-2.6	-6.8	-3.7	T
T-14	50	-5.8	-0.9	-7.4	-4.3	-6.7	-4.9	B
T-15	60	-5.7	-2.0	-8.0	-1.3	-6.8	-2.7	T
T-16	82	-4.1	-2.2	-7.7	-0.6	-6.3	-2.0	T
Average	72	-5	-2	-8	-2	-7	-3	
max	83	-4	-1	-7	0	-6	-1	
min	50	-6	-2	-9	-4	-7	-5	

Average grain diameter (mm)= 27.4

POPULTATION C

Sample Number	% of popluation in sample	Phi 50	Sigma (std. dev)	Phi 95	Phi 5	Phi 84	Phi 16	-Binormal -Trinormal
T-1	7	3.4	-1.6	0.8	6.0	1.8	5.0	T
T-2	6	3.1	-1.1	1.3	5.0	2.1	4.2	T
T-3	6	2.9	-0.9	-0.3	5.9	1	3.8	T
T-4	5	3.0	-1.8	0.0	5.8	1.3	4.8	T
T-5			0.0					B
T-6			0.0					B
T-7	8	5.2	-1.6	0.8	7.3	3.2	5.8	T
T-8			0.0					B
T-9			0.0					B
T-10			0.0					B
T-11			0.0					B
T-12	3	4.2	-0.3	3.4	3.5	4.2	5.1	T
T-13	4	4.6	-2.7	0.1	9.0	1.8	7.2	T
T-14			0.0					B
T-15	7	1.8	-1.9	-1.4	4.9	-0.3	3.6	T
T-16	6	2.0	-2.3	-1.8	5.6	-0.4	4.2	T
Average	6	3.4	-0.9	0.3	5.9	1.6	4.9	
max	8	5.2	0.0	3.4	9.0	4.2	7.2	
min	3	1.8	-2.7	-1.8	3.5	-0.4	3.6	

Average grain size mm) = 0.10

PROBABILITY GRAPH DATA

POPULATION A

Sample Number	% of popluation in sample	Phi 50	Sigma (std. dev)	Phi 95	Phi 5	Phi 84	Phi 16	B-Binormal T-Trinormal
T-5	22	2.0	-1.3	0.3	4.3	0.5	3.4	B
T-6	30	2.2	-2.4	-3.8	4.6	-1.3	3.4	B
T-8	26	1.4	-2.1	-2.2	4.8	-0.8	3.6	B
T-9	20	1.5	-2.0	-2.0	4.7	-0.5	3.5	B
T-10	27	1.2	-1.8	-1.8	4.3	-0.6	3.0	B
T-11	42	0.4	-1.8	-3.4	4.2	-1.8	0.8	B
T-14	50	-1.8	-3.1	-7.0	3.2	-5.0	1.2	B
Average	31	1.0	-2.1	-2.8	4.3	-1.3	2.7	
Max	50	2	-1	0	5	1	4	
Min	20	-2	-3	-7	3	-5	1	

Average Grain Diameter (mm): 0.5

POPULTATION B

Sample Number	% of popluation in sample	Phi 50	Sigma (std. dev)	Phi 95	Phi 5	Phi 84	Phi 16	B-Binormal T-Trinormal
T-5	78	-3.8	-2.0	-7.0	-0.4	-5.8	-1.8	B
T-6	70	-5.3	-1.5	-7.9	-2.7	-6.8	-3.8	B
T-8	74	-4.2	-2.1	-7.6	-0.8	-6.2	-2.0	B
T-9	80	-5.0	-2.2	-8.8	-1.4	-7.2	-2.7	B
T-10	73	-4.9	-1.9	-8.0	-1.6	-6.8	-3.0	B
T-11	58	-5.7	-1.3	-7.8	-3.5	-7.0	-4.4	B
T-14	50	-5.8	-0.9	-7.4	-4.3	-6.7	-4.9	B
Average	69	-5.0	-1.7	-7.8	-2.1	-6.6	-3.2	
max	80	-3.8	-0.9	-7.0	-0.4	-5.8	-1.8	
min	50	-5.8	-2.2	-8.8	-4.3	-7.2	-4.9	

Average grain diameter (mm)= 31.1

PROBABILITY GRAPH DATA

POPULATION A

Sample Number	% of popluation in sample	Phi 50	Sigma (std. dev)	Phi 95	Phi 5	Phi 84	Phi 16	B-Binormal T-Trinormal
T-1	16	1.8	-1.2	0.9	2.8	1.2	5.0	T
T-2	11	3.1	-1.1	1.3	5.0	2.1	4.2	T
T-3	16	1.6	-1.4	0.8	5.2	1.6	4.5	T
T-4	12	2.0	-0.5	0.8	3.4	0.9	1.1	T
T-7	14	2.6	-0.6	3.0	4.0	1.6	3.4	T
T-12	27	1.1	-1.7	-1.8	3.7	-0.6	2.8	T
T-13	42	0.4	-2.6	-6.5	4.4	-1.6	2.2	T
T-15	33	0.6	-2.0	-2.0	2.4	-1.2	4.0	T
T-16	12	1.7	-1.1	0.8	2.8	1.1	4.2	T
Average	20	1.7	-1.3	-0.3	3.7	0.6	3.5	
Max	42	3	0	3	5	2	5	
Min	11	0	-3	-7	2	-2	1	

Average Grain Diameter (mm): 0.3

POPULTATION B

Sample Number	% of popluation in sample	Phi 50	Sigma (std. dev)	Phi 95	Phi 5	Phi 84	Phi 16	B-Binormal T-Trinormal
T-1	78	-4.8	-2.4	-8.6	-0.8	-7.2	-2.4	T
T-2	83	-3.6	-1.9	-6.8	-0.4	-5.6	-1.7	T
T-3	78	-5.1	-1.6	-7.8	-2.4	-6.8	-3.5	T
T-4	83	-4.9	-1.9	-8.0	-1.8	-6.8	-3.0	T
T-7	78	-3.6	-2.3	-7.3	0.3	-5.9	-1.4	T
T-12	70	-4.8	-1.8	-7.8	-1.8	-6.5	-2.9	T
T-13	55	-5.2	-1.5	-7.6	-2.6	-6.8	-3.7	T
T-15	60	-5.7	-2.0	-8.0	-1.3	-6.8	-2.7	T
T-16	82	-4.1	-2.2	-7.7	-0.6	-6.3	-2.0	T
Average	74	-4.6	-2.0	-7.7	-1.3	-6.5	-2.6	
max	83	-3.6	-1.5	-6.8	0.3	-5.6	-1.4	
min	55	-5.7	-2.4	-8.6	-2.6	-7.2	-3.7	

Average grain diameter (mm)= 24.9

POPULTATION C

Sample Number	% of popluation in sample	Phi 50	Sigma (std. dev)	Phi 95	Phi 5	Phi 84	Phi 16	B-Binormal T-Trinormal
T-1	7	2.0	-2.4	-3.0	7.0	-1.2	2.3	T
T-2	6	2.8	-1.2	0.5	6.1	0.8	2.2	T
T-3	6	3.0	-0.4	0.4	3.0	1.6	4.5	T
T-4	5	3.2	-1.2		3.8	1.8	4.4	T
T-7	8	3.4	-2.4	-0.3	8.0	1.2	5.6	T
T-12	3	4.2	-0.3	3.4	3.5	4.2	5.1	T
T-13	4	-1.3	-1.8	2.5	3.4	-4.4	2.4	T
T-15	7	2.8	-1.2	0.8	4.8	1.6	4.1	T
T-16	6	2.4	-1.6	-0.1	5.4	1.1	4.3	T
Average	6	2.5	-1.4	0.5	5.0	0.7	3.9	
max	8	4.2	-0.3	3.4	8.0	4.2	5.6	
min	3	-1.3	-2.4	-3.0	3.0	-4.4	2.2	

Average grain size mm) = 0.18

Partitioned Cumulative Log Probability Plot
For Sediment Size Distribution
Sample T-1

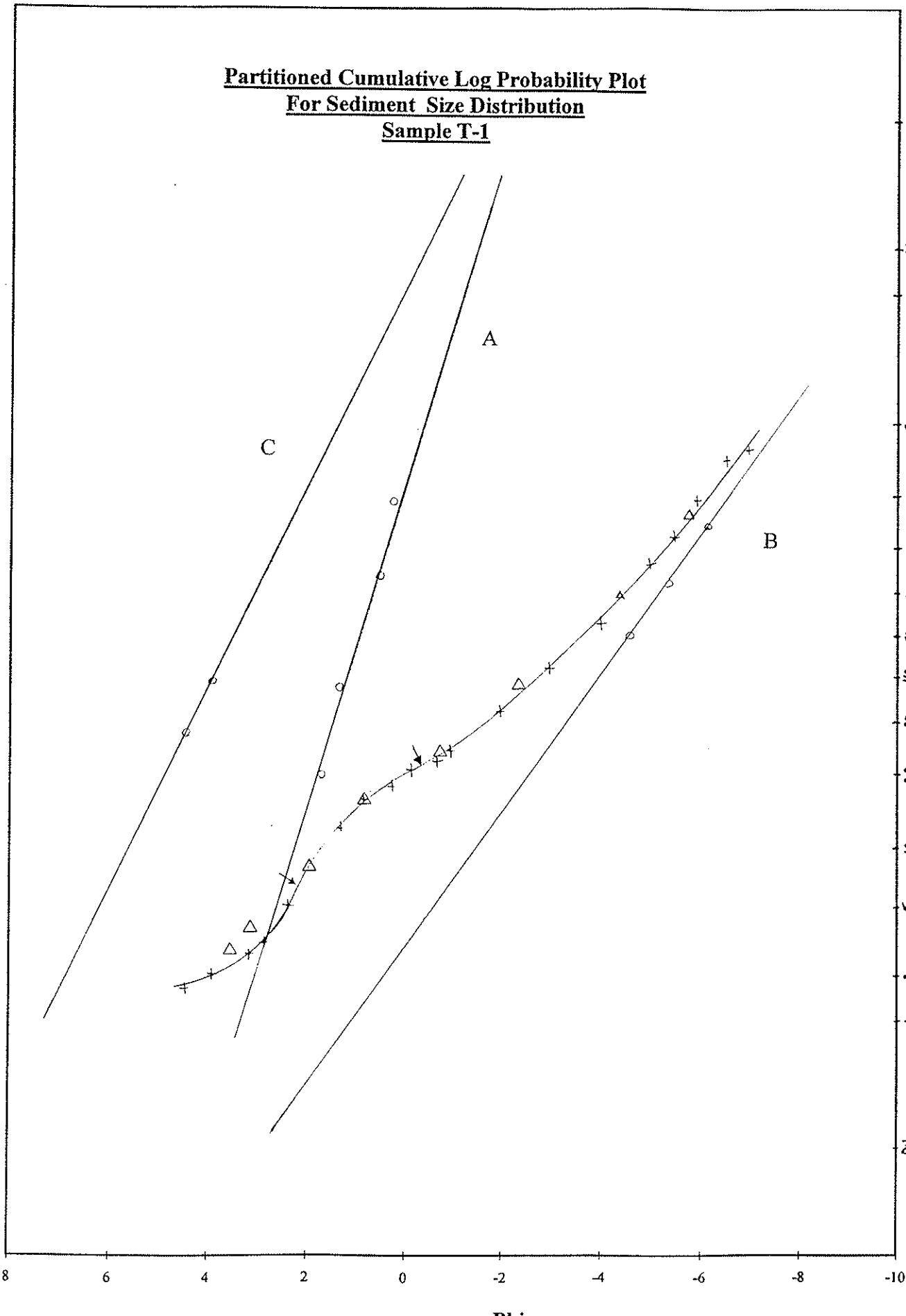

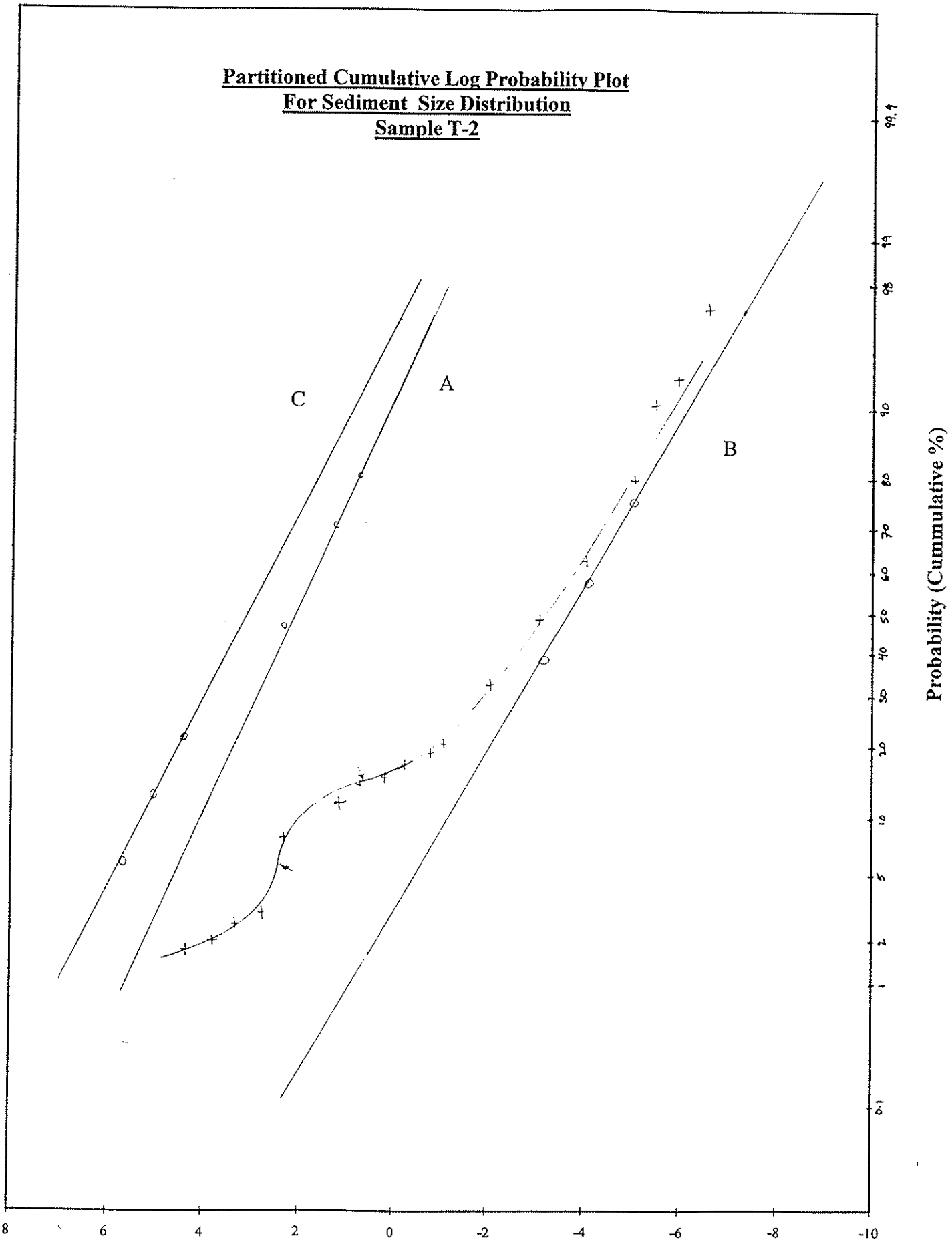
Partitioned Cumulative Log Probability Plot
For Sediment Size Distribution
Sample T-2
C
A
B
99.9
99
98
90
80
70
60
50
40
30
20
10
5
2
1
0.1
Probability (Cummulative %)
8
6
4
2
0
-2
-4
-6
-8
-10
Phi

Partitioned Cumulative Log Probability Plot
For Sediment Size Distribution
Sample T-3

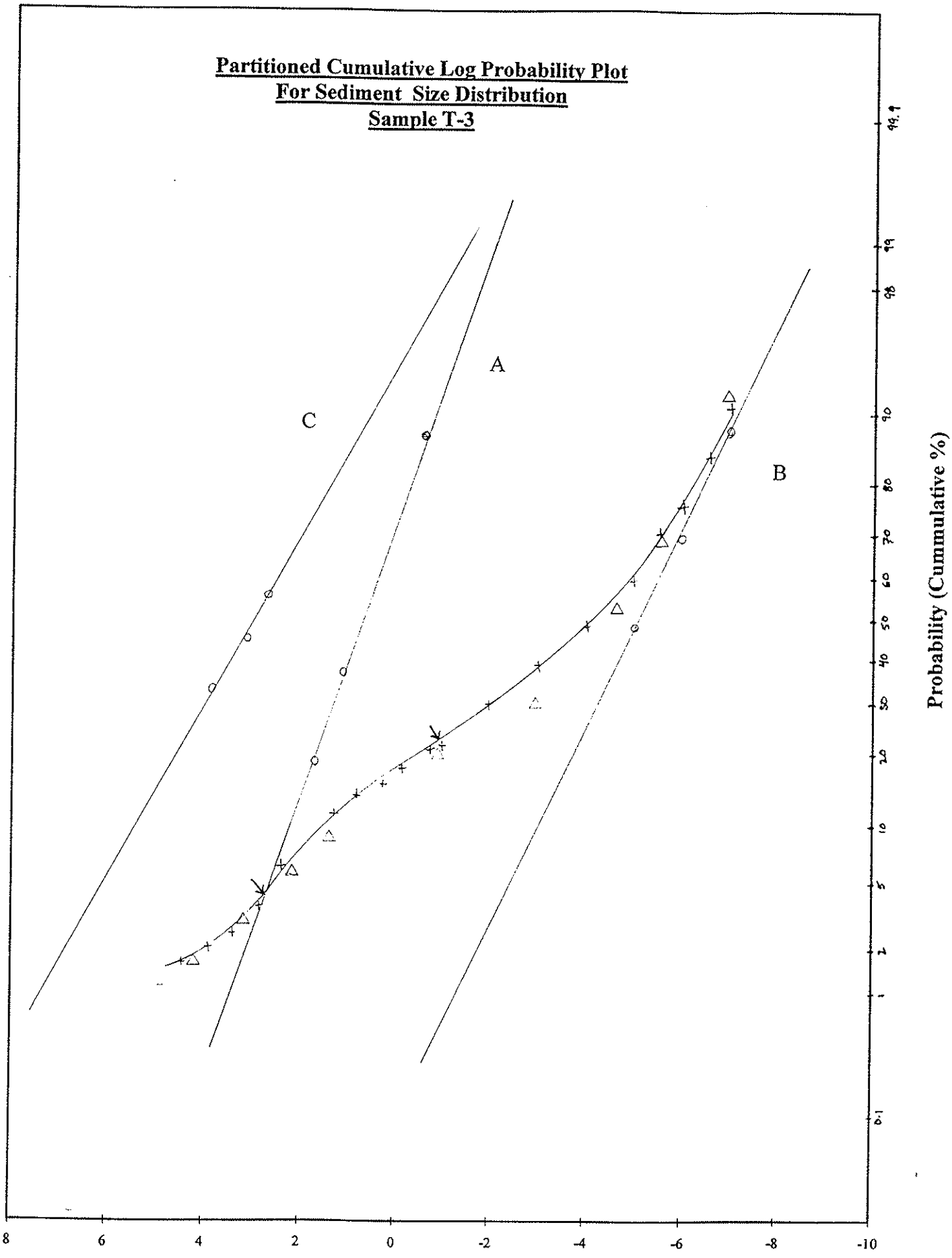

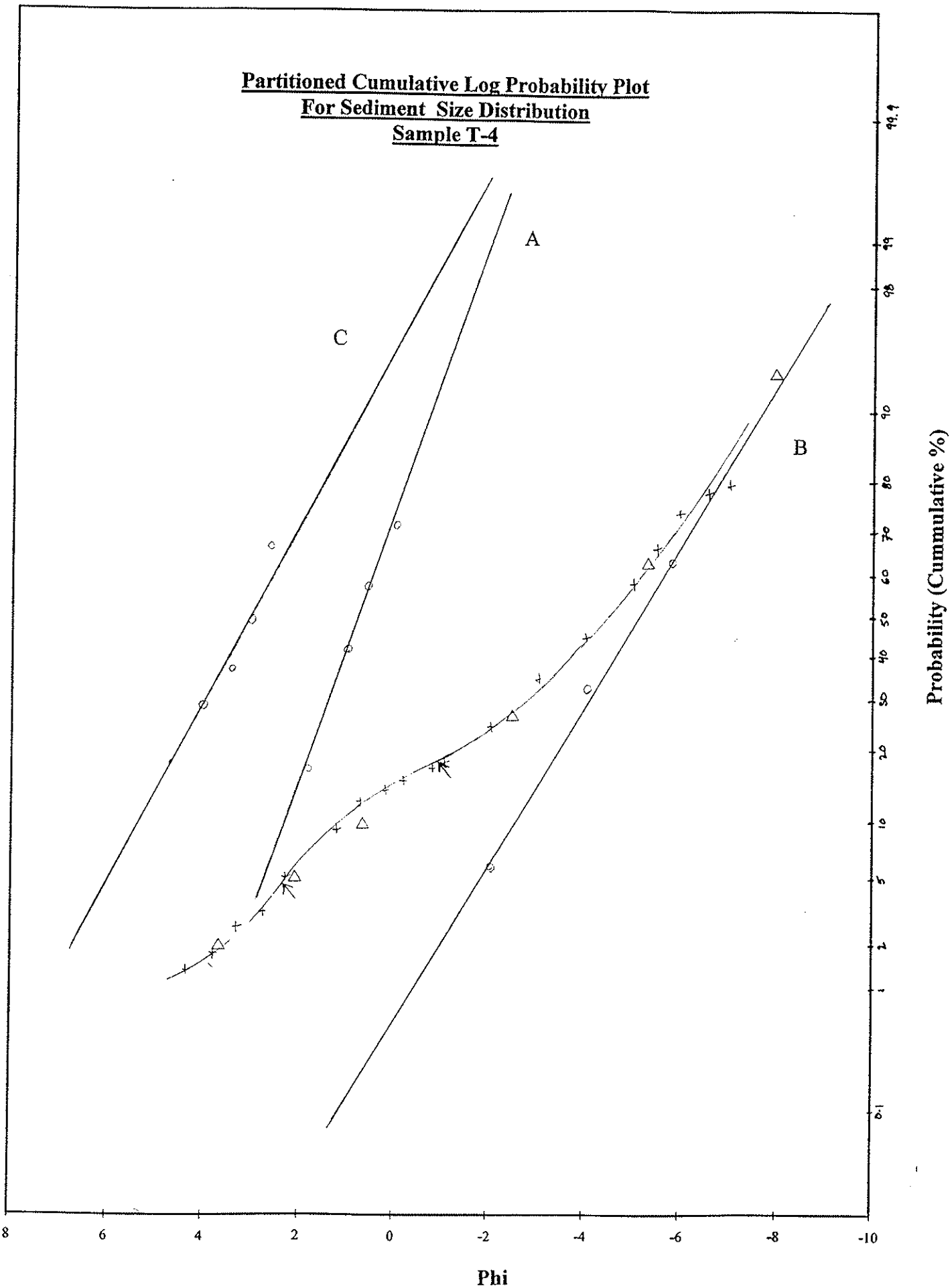
Partitioned Cumulative Log Probability Plot
For Sediment Size Distribution
Sample T-4
A
B
C
99.9
99
98
90
80
70
60
50
40
30
20
10
5
2
1
0.1
Probability (Cummulative %)
8
6
4
2
0
-2
-4
-6
-8
-10
Phi

Partitioned Cumulative Log Probability Plot
For Sediment Size Distribution
Sample T-5

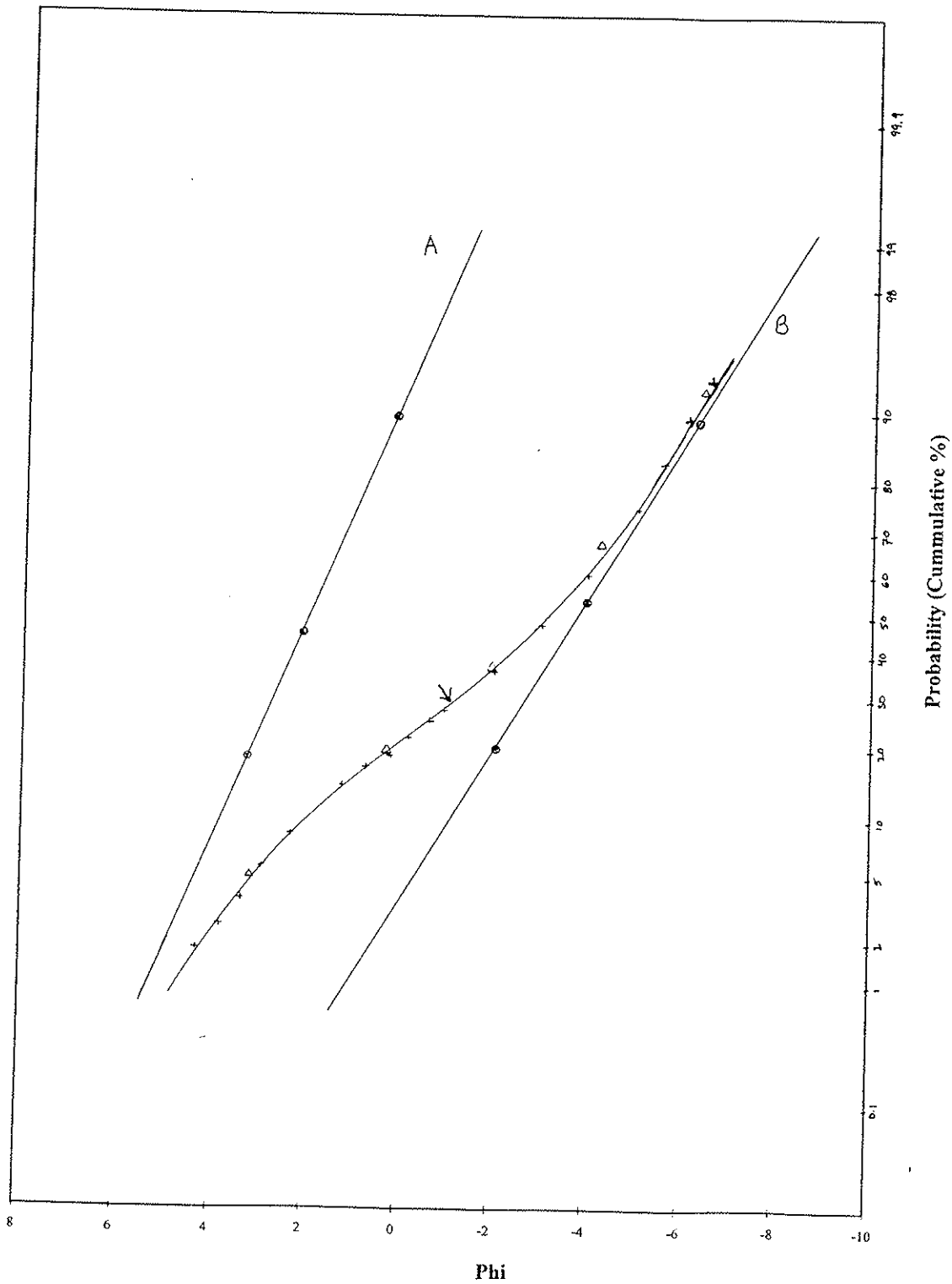

Partitioned Cumulative Log Probability Plot
For Sediment Size Distribution
Sample T-6

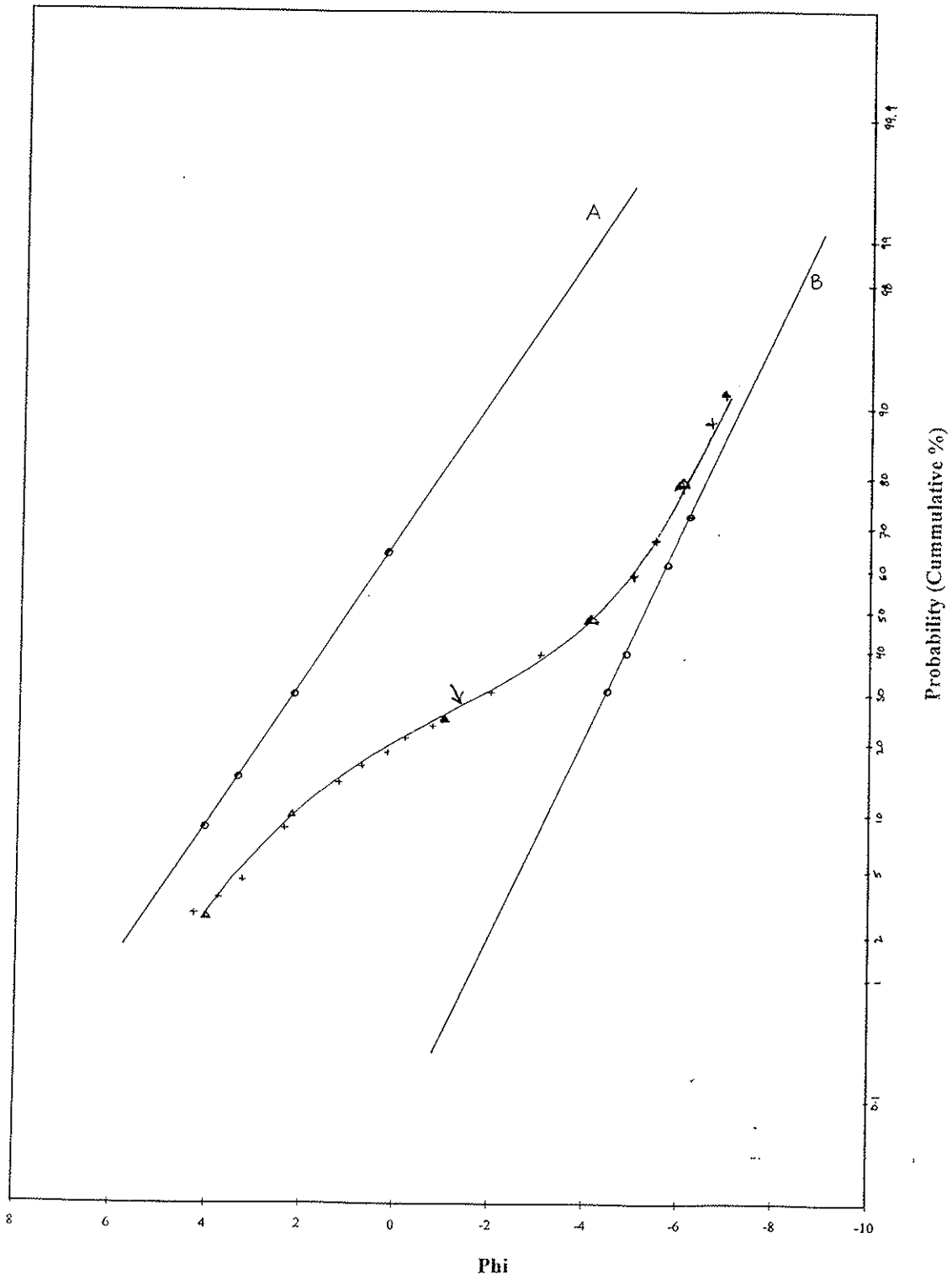

Partitioned Cumulative Log Probability Plot
For Sediment Size Distribution
Sample T-9

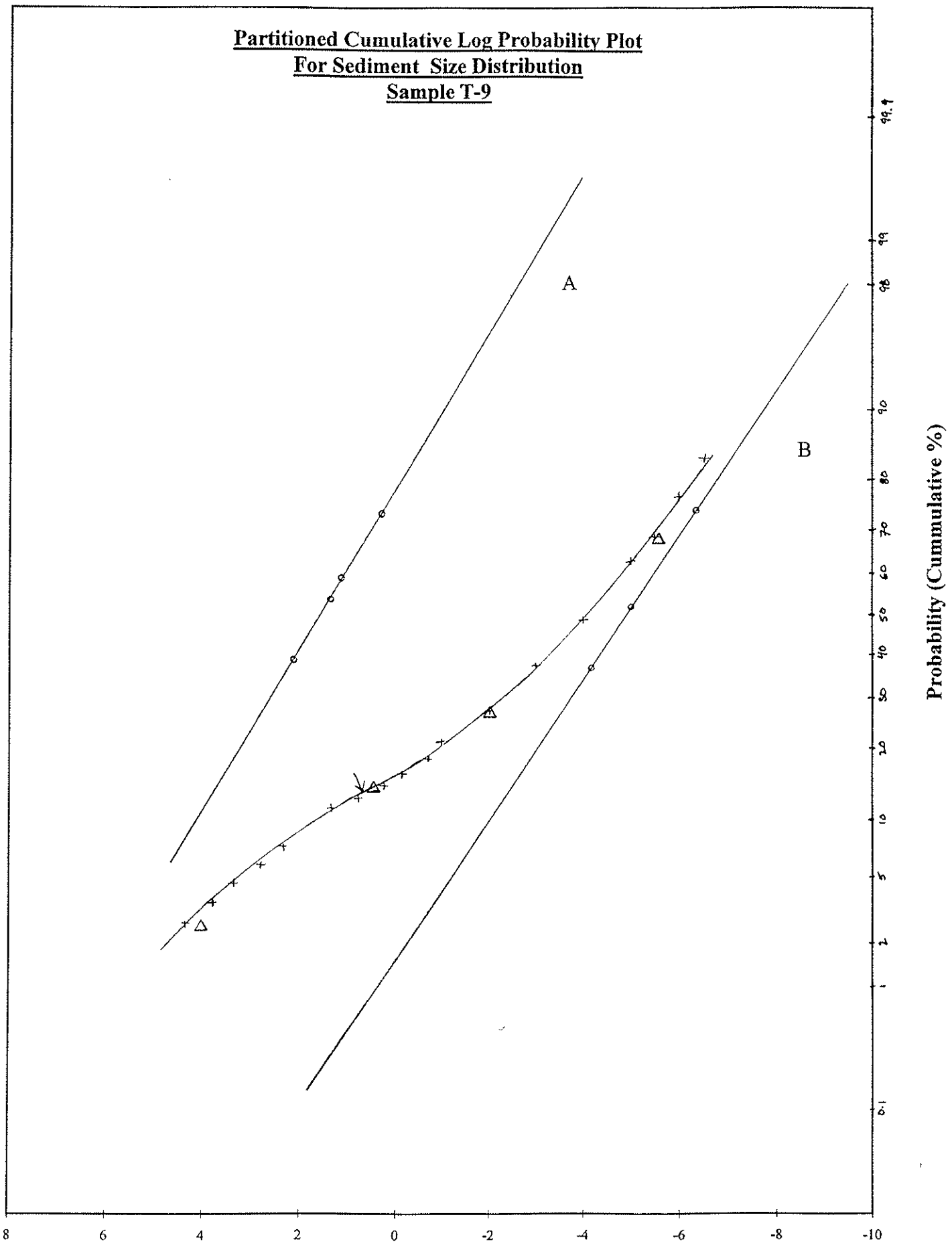

Partitioned Cumulative Log Probability Plot
For Sediment Size Distribution
Sample T-10

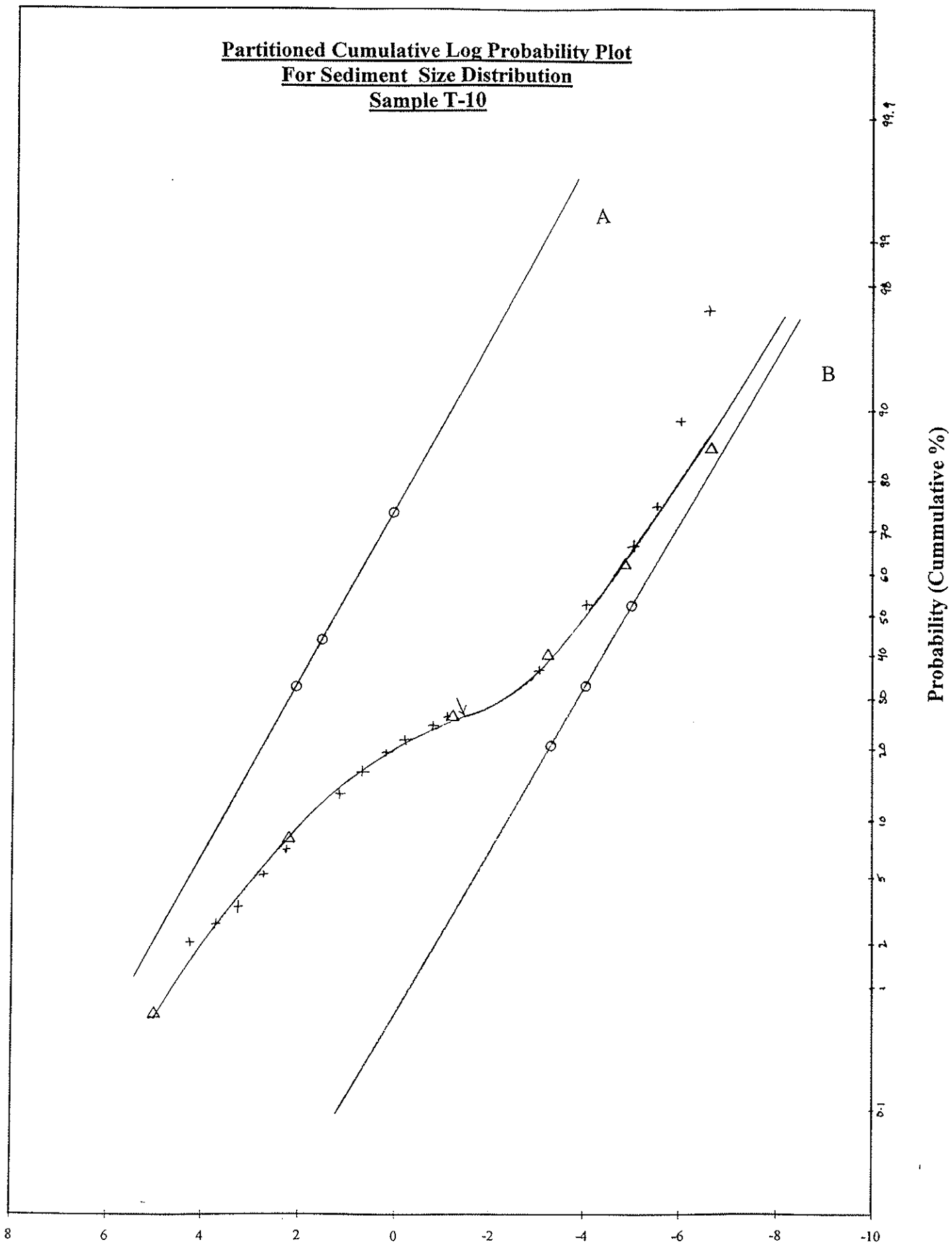

Partitioned Cumulative Log Probability Plot
For Sediment Size Distribution
Sample T-11

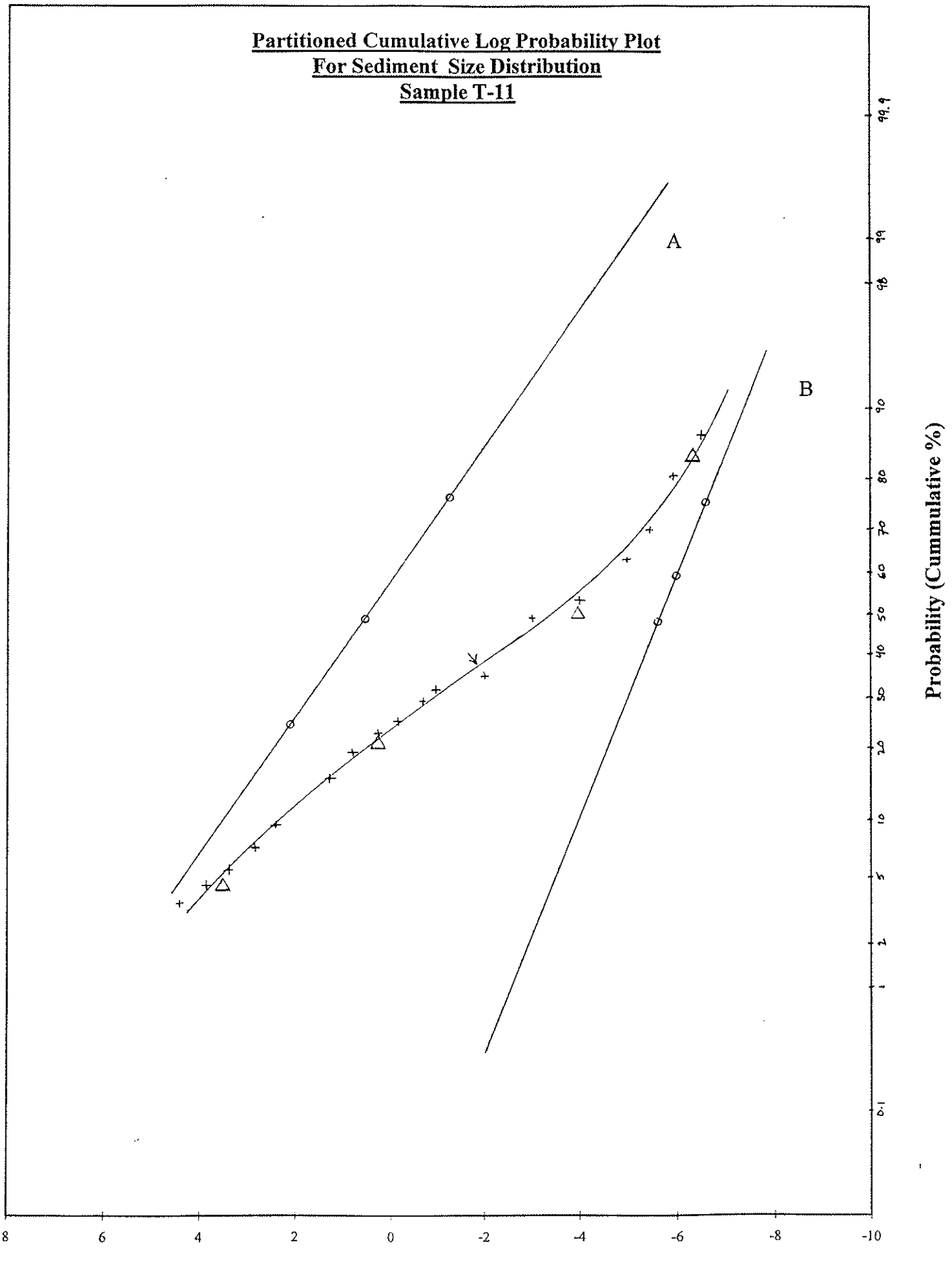

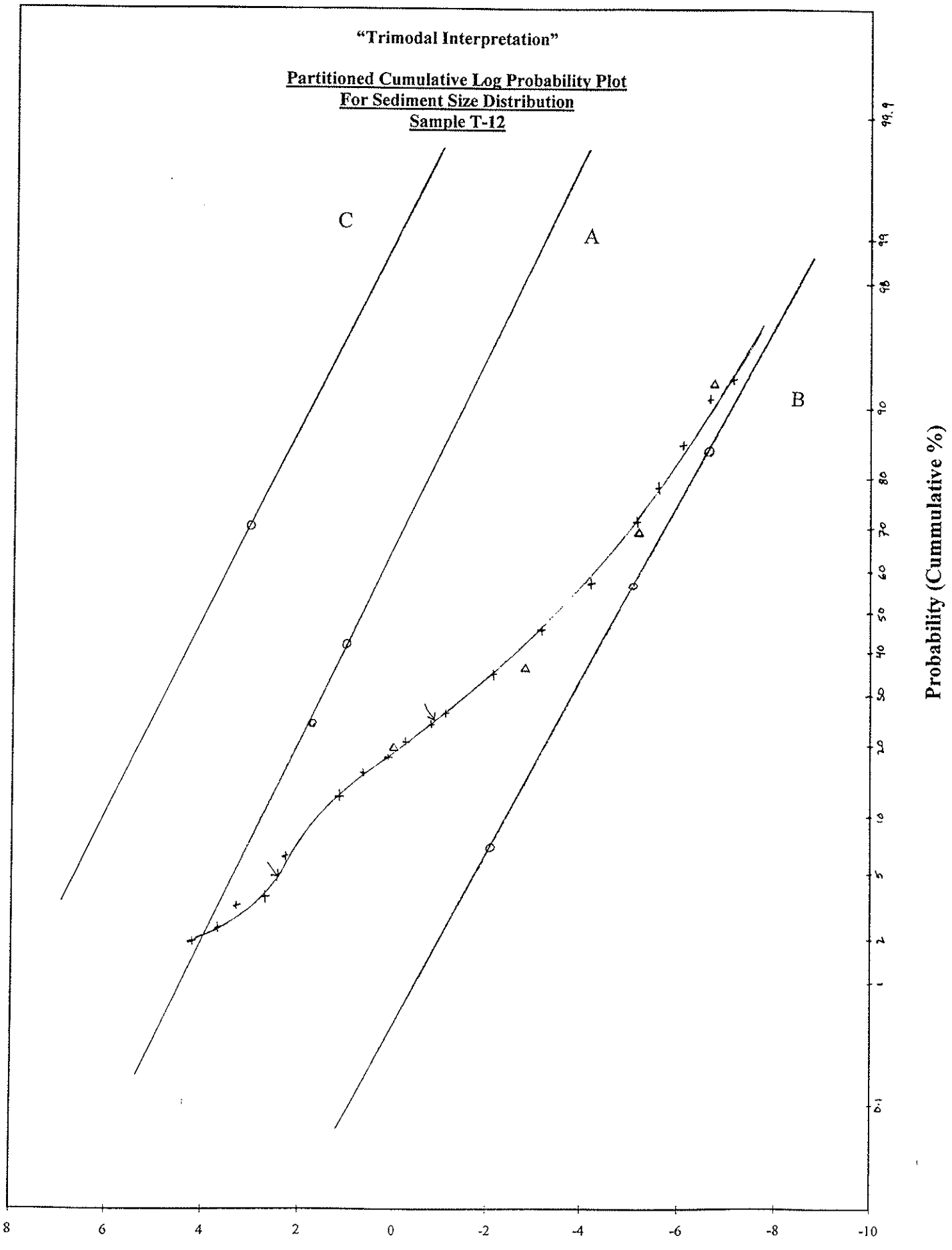
"Trimodal Interpretation"
Partitioned Cumulative Log Probability Plot
For Sediment Size Distribution
Sample T-12
C
A
B
99.9
99
98
90
80
70
60
50
40
30
20
10
5
2
1
0.1
Probability (Cummulative %)
8
6
4
2
0
-2
-4
-6
-8
-10
Phi

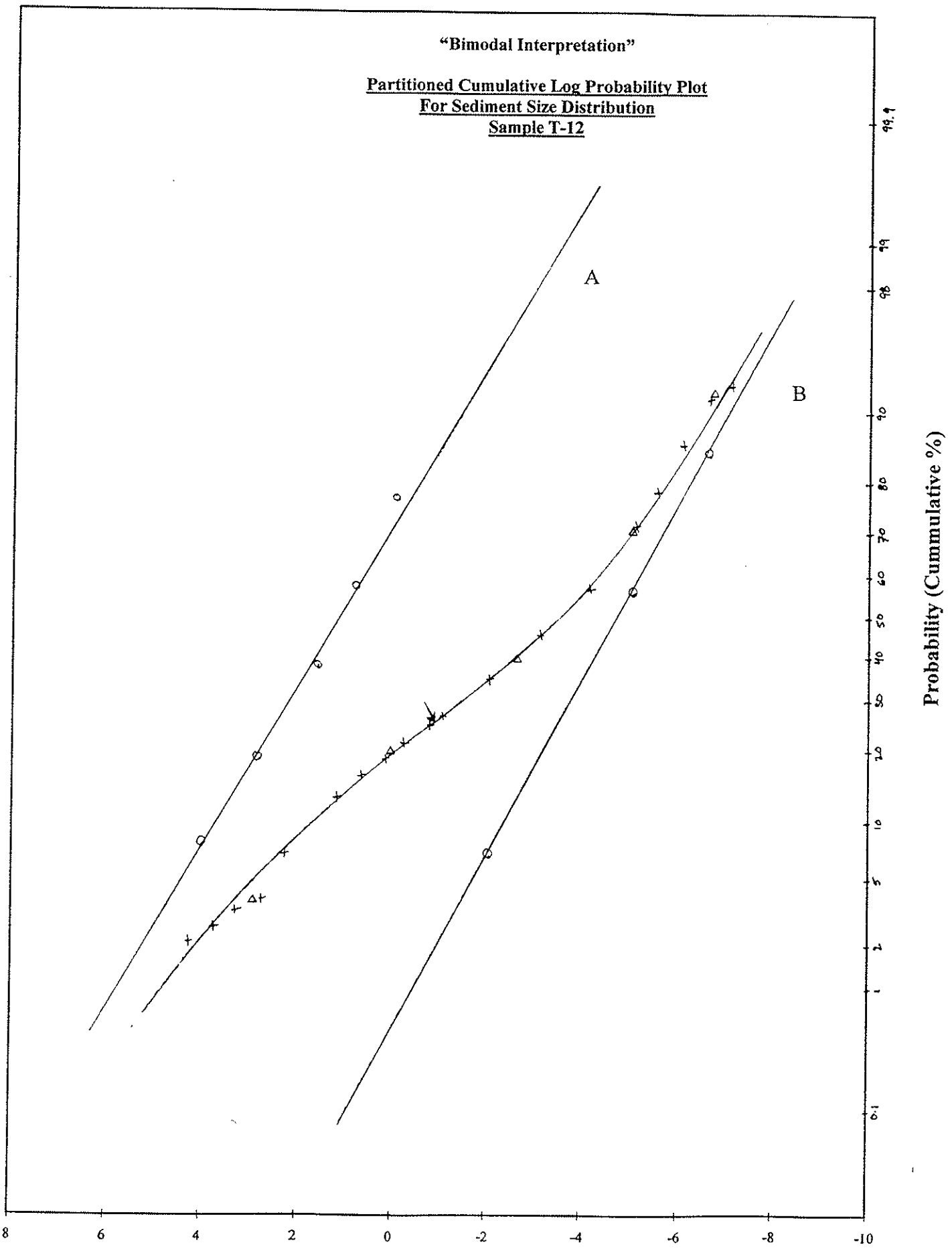
"Bimodal Interpretation"
Partitioned Cumulative Log Probability Plot
For Sediment Size Distribution
Sample T-12
A
B
99.9
99
98
90
80
70
60
50
40
30
20
10
5
2
1
0.1
Probability (Cummulative %)
8
6
4
2
0
-2
-4
-6
-8
-10
Phi

Partitioned Cumulative Log Probability Plot
For Sediment Size Distribution
Sample T-13

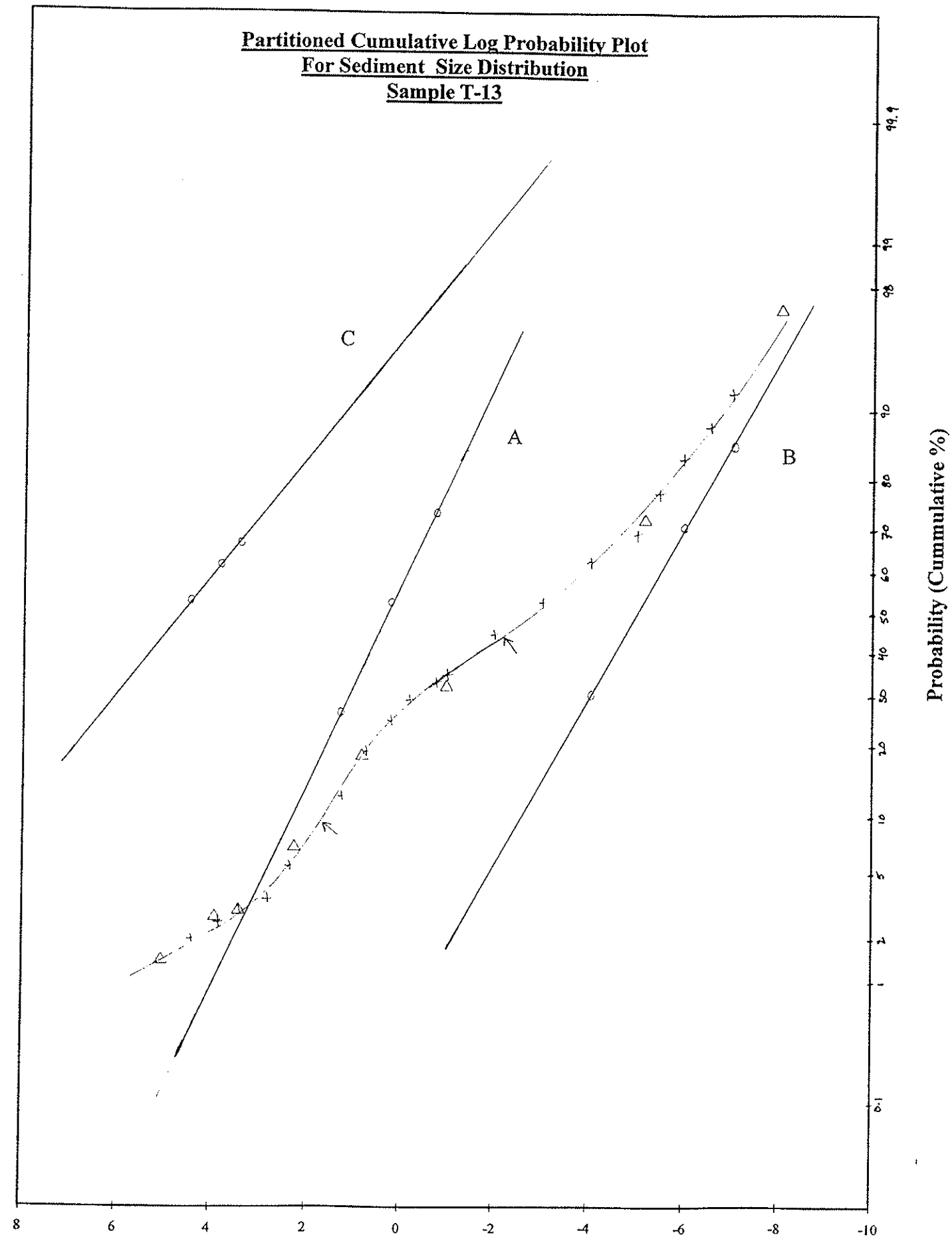

Partitioned Cumulative Log Probability Plot
For Sediment Size Distribution
Sample T-14

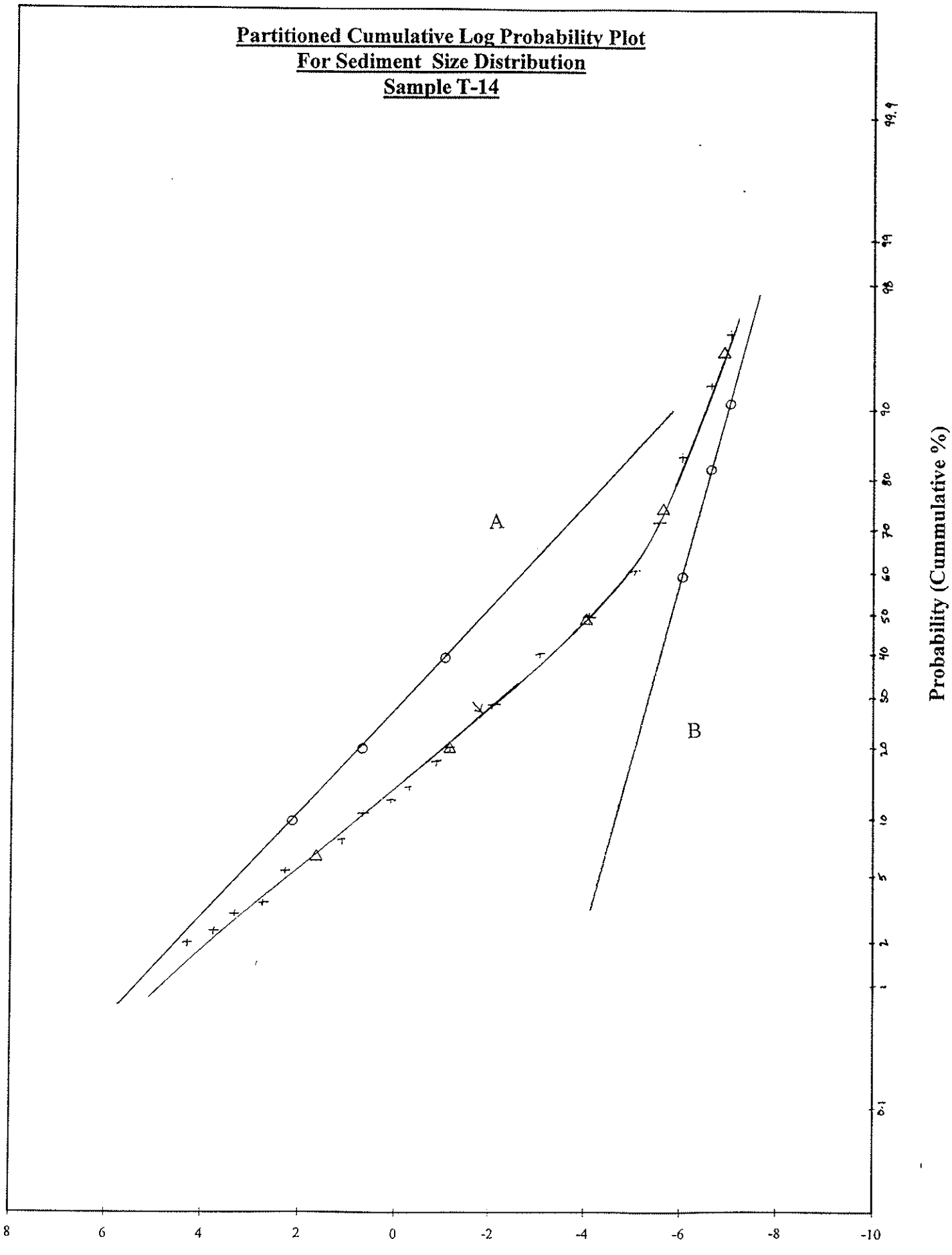

Partitioned Cumulative Log Probability Plot
For Sediment Size Distribution
Sample T-15

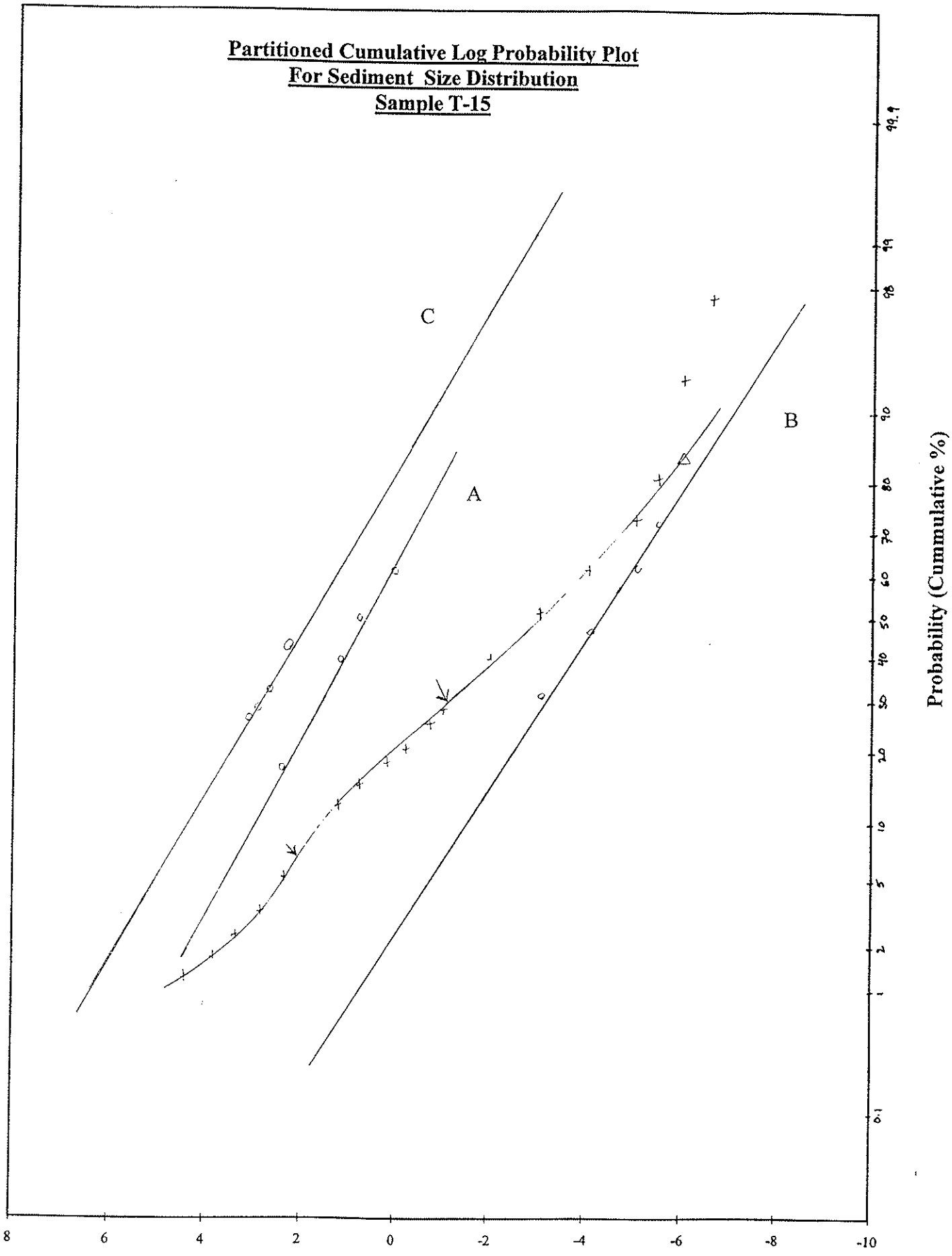

Partitioned Cumulative Log Probability Plot
For Sediment Size Distribution
Sample T-16

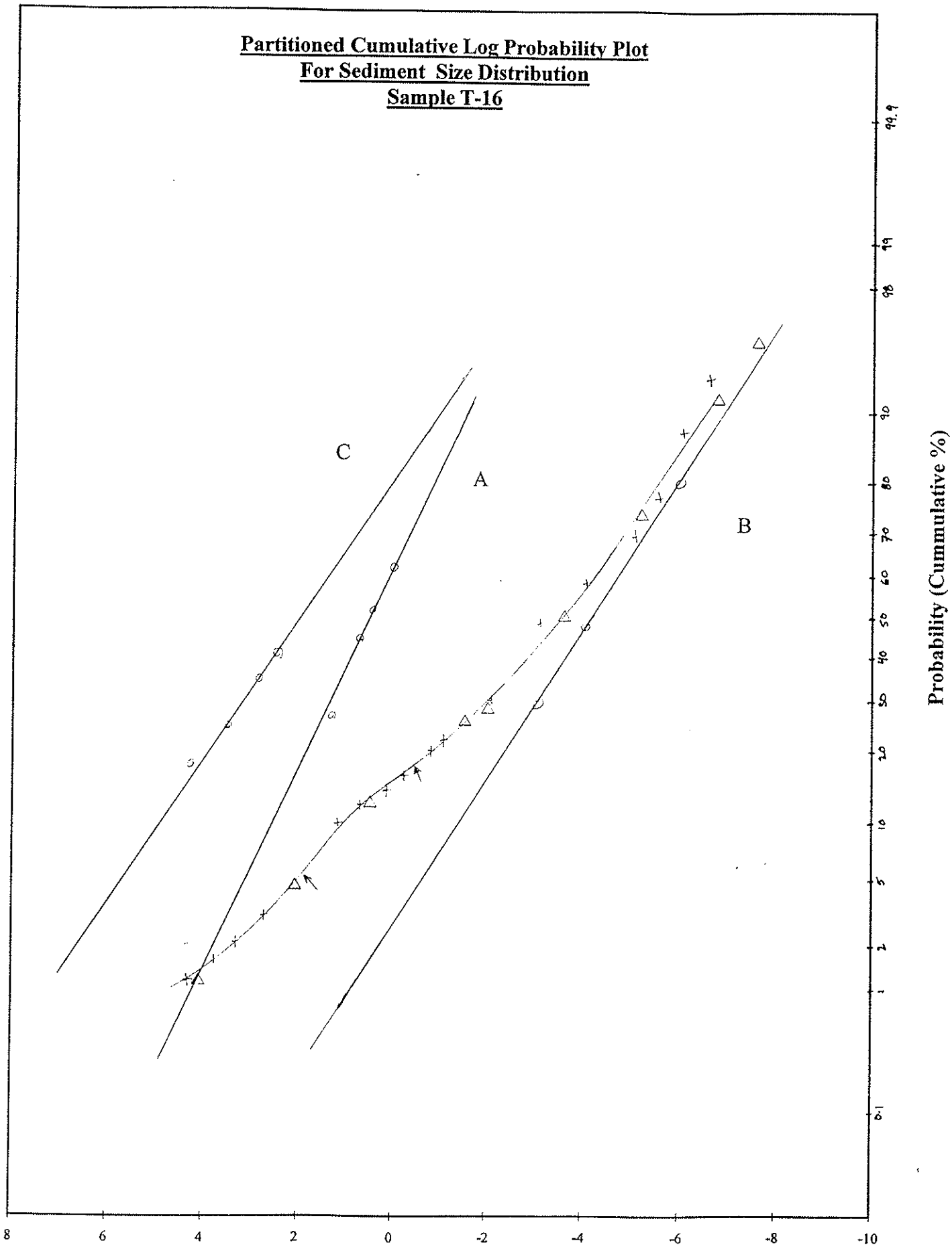

APPENDIX F

ANALYTICAL RESULTS

VIAL #	Sample # 95-TMC		Sieve #	Sieve Size microns	Au ppb FA + AA
TMC26	1	B	9	106	2
TMC27	11	C	8	150	6050
TMC28	14	B	9	106	5
TMC29	6	C	8	150	3290
TMC30	4	B	10	75	20
TMC31	30	B	9	106	35
TMC32	30	C	8	150	95
TMC33	29	B	12	<53	75
TMC34	2	C	9	106	1610
TMC35	30	B	8	150	505
TMC36	9	B	7	212	525
TMC37	8	B	9	106	70
TMC38	2	B	11	53	20
TMC39	7	B	10	75	30
TMC40	12	C	8	150	2280
TMC41	2	B	8	150	35
TMC42	8	C	8	150	10400
TMC43	1	B	7	212	5
TMC44	7	B	7	212	2
TMC45	29	B	8	150	2340
TMC46	12	C	7	212	26700
TMC47	4	C	12	<53	585
TMC48	9	C	12	<53	1230
TMC49	1	C	7	212	5360
TMC50	9	C	10	75	1610
TMC51	2	C	7	212	16200
TMC52	1	B	11	53	115
TMC53	8	B	10	75	15
TMC54	30	B	10	75	20
TMC55	13	B	8	150	15
TMC56	29	C	8	150	7060
TMC57	4	B	7	212	5
TMC58	12	B	11	53	2
TMC59	10	C	7	212	51400
TMC60	4	C	9	106	9150
TMC61	2	C	11	53	1910
TMC62	29	C	10	75	14200
TMC63	13	C	12	<53	515
TMC64	10	C	12	<53	2040
TMC65	11	B	8	150	25
TMC66	30	B	12	<53	75

ANALYTICAL RESULTS

VIAL #	Sample # 95-TMC		Sieve #	Sieve Size microns	Au ppb FA + AA
TMC67	14	C	8	150	5390
TMC68	6	B	7	212	2
TMC69	5	B	10	75	145
TMC70	30	C	7	212	13800
TMC71	5	B	11	53	210
TMC72	2	B	7	212	2
TMC73	12	B	12	<53	60
TMC74	9	C	11	53	1410
TMC75	7	B	11	53	175
TMC76	2	C	10	75	935
TMC77	8	B	7	212	10
TMC78	14	B	11	53	60
TMC79	12	C	9	106	5820
TMC80	7	B	8	150	10
TMC81	6	B	12	<53	80
TMC82	14	C	9	106	5370
TMC83	14	C	11	53	6930
TMC84	10	B	10	75	65
TMC85	11	C	9	106	8190
TMC86	6	C	9	106	7070
TMC87	7	B	9	106	190
TMC88	4	C	10	75	3710
TMC89	4	B	8	150	95
TMC90	9	B	8	150	2140
TMC91	13	C	10	75	395
TMC92	30	B	7	212	5
TMC93	12	B	10	75	2
TMC94	10	C	11	53	2820
TMC95	7	C	11	53	1860
TMC96	14	C	12	<53	7100
TMC97	10	C	8	150	1720
TMC98	7	C	8	150	1750
TMC99	2	C	12	<53	570
TMC100	11	C	9	106	8040
TMC101	10	B	8	150	25
TMC102	1	C	9	106	4630
TMC103	6	B	8	150	165
TMC104	2	B	12	<53	80
TMC105	2	B	7	212	2
TMC106	5	C	10	75	1000
TMC107	4	C	9	106	4380

ANALYTICAL RESULTS

VIAL #	Sample # 95-TMC		Sieve #	Sieve Size microns	Au ppb FA + AA
TMC108	4	C	7	212	10900
TMC109	6	B	10	75	2
TMC110	13	C	7	212	760
TMC111	30	C	12	<53	790
TMC112	1	C	12	<53	625
TMC113	7	C	7	212	3920
TMC114	10	B	8	150	70
TMC115	11	B	12	<53	10
TMC116	29	C	7	212	10600
TMC117	13	C	9	106	2860
TMC118	11	B	10	75	40
TMC119	4	B	11	53	50
TMC120	13	B	7	212	25
TMC121	14	B	12	<53	145
TMC122	10	C	9	106	2320
TMC123	1	B	12	<53	80
TMC124	4	B	9	106	10
TMC125	7	C	7	212	19400
TMC126	9	C	8	150	9500
TMC127	10	C	10	75	2060
TMC128	s3			<53	8320
TMC129	6	B	7	212	2
TMC130	29	C	11	53	6930
TMC131	13	B	11	53	65
TMC132	29	C	9	106	14500
TMC133	4	B	8	150	345
TMC134	11	C	10	75	6220
TMC135	6	B	9	106	2
TMC136	5	C	10	75	2710
TMC137	30	C	10	75	2060
TMC138	14	C	8	150	2080
TMC139	10	B	9	106	25
TMC140	9	B	11	53	230
TMC141	8	B	11	53	130
TMC142	13	C	7	212	5800
TMC143	9	C	7	212	22400
TMC144	4	B	12	<53	250
TMC145	14	B	8	150	640
TMC146	12	C	11	53	3810
TMC147	10	C	8	150	3430
TMC148	14	C	10	75	5280

ANALYTICAL RESULTS

VIAL #	Sample # 95-TMC		Sieve #	Sieve Size microns	Au ppb FA + AA
TMC149	30	C	11	53	1640
TMC150	5	C	8	150	1270
TMC151	6	C	12	<53	1020
TMC152	6	B	11	53	2
TMC153	4	C	8	150	2490
TMC154	12	B	9	106	5
TMC155	7	C	10	75	1990
TMC156	5	C	9	106	1520
TMC157	12	C	12	<53	2590
TMC158	5	C	12	<53	1490
TMC159	10	B	7	212	2
TMC160	5	C	11	53	2570
TMC161	11	C	7	212	10000
TMC162	4	C	7	212	9890
TMC163	29	B	9	106	45
TMC164	6	C	10	75	4170
TMC165	9	B	12	<53	125
TMC166	14	C	7	212	8570
TMC167	11	B	7	212	2
TMC168	5	B	7	212	2
TMC169	30	B	11	53	680
TMC170	2	C	8	150	7280
TMC171	29	C	10	75	17000
TMC172	8	C	11	53	20000
TMC173	29	B	7	212	25
TMC174	12	C	10	75	4880
TMC175	8	C	12	<53	31700
TMC176	11	C	11	53	5820
TMC177	14	B	10	75	25
TMC178	1	C	10	75	1360
TMC179	2	B	9	106	2
TMC180	14	B	7	212	2
TMC181	5	B	12	<53	165
TMC182	12	B	8	150	755
TMC183	6	C	11	53	1830
TMC184	8	C	9	106	20900
TMC185	1	C	11	53	2600
TMC186	5	B	9	106	660
TMC187	5	C	7	212	2940
TMC188	8	B	8	150	10
TMC189	1	B	10	75	55

ANALYTICAL RESULTS

VIAL #	Sample # 95-TMC		Sieve #	Sieve Size microns	Au ppb FA + AA
TMC190	8	C	7	212	9140
TMC191	11	C	12	<53	2330
TMC192	10	B	11	53	10
TMC193	13	C	8	150	990
TMC194	6	C	7	212	17800
TMC195	7	C	9	106	2890
TMC196	1	B	8	150	25
TMC197	29	B	10	75	250
TMC198	s1			<53	17600
TMC199	12	B	8	150	380
TMC200	9	B	10	75	515
TMC201	9	C	9	106	2180
TMC202	30	C	9	106	2230
TMC203	29	C	12	<53	675
TMC204	13	B	9	106	30
TMC205	9	B	9	106	740
TMC206	4	C	11	53	5850
TMC207	1	C	7	212	2
TMC208	13	C	11	53	1450
TMC209	13	B	10	75	75
TMC210	29	B	11	53	10
TMC211	6	B	8	150	25
TMC212	12	B	7	212	2
TMC213	7	B	9	106	10
TMC214	7	C	12	<53	930
TMC215	13	C	12	<53	555
TMC216	2	B	10	75	10
TMC217	8	C	10	75	21300
TMC218	1	C	8	150	625
TMC219	11	B	9	106	15
TMC220	5	C	12	<53	1320
TMC221	5	B	8	150	75
TMC222	8	B	12	<53	285
TMC223	11	B	11	53	2
TMC224	13	B	12	<53	165
TMC225	10	B	12	<53	125
TMC226	7	B	12	<53	240
TMC227	s2			<53	1730
TMC228	10	C	7	212	14000

RESULTS OF LABORATORY ANALYSIS OF DUPLICATES									
VIAL #	Sample #		Sieve	Sieve Size	Au ppb				
	95-TMC		#	microns	FA + AA	Ordinal	Duplicate	Mean	Deviation
TMC49	1	C	7	212	5360	170	1	2680	5360
TMC207	1	C	7	212	0	169	1		
TMC72	2	B	7	212	0	186	2	0	0
TMC105	2	B	7	212	0	185	2		
TMC89	4	B	8	150	95	187	3	220	250
TMC133	4	B	8	150	345	188	3		
TMC108	4	C	7	212	10900	196	4	10395	1010
TMC162	4	C	7	212	9890	195	4		
TMC60	4	C	9	106	9150	199	5	6765	4770
TMC107	4	C	9	106	4380	200	5		
TMC106	5	C	10	75	1000	197	6	1855	1710
TMC136	5	C	10	75	2710	198	6		
TMC158	5	C	12	<53	1490	164	7	1405	170
TMC220	5	C	12	<53	1320	163	7		
TMC68	6	B	7	212	0	175	8	0	0
TMC129	6	B	7	212	0	176	8		
TMC103	6	B	8	150	165	177	9	95	140
TMC211	6	B	8	150	25	178	9		
TMC87	7	B	9	106	190	183	10	100	180
TMC213	7	B	9	106	10	184	10		
TMC113	7	C	7	212	3920	171	11	11660	15480
TMC125	7	C	7	212	19400	172	11		
TMC101	10	B	8	150	25	180	12	47.5	45
TMC114	10	B	8	150	70	179	12		
TMC59	10	C	7	212	51400	189	13	32700	37400
TMC228	10	C	7	212	14000	190	13		
TMC97	10	C	8	150	1720	191	14	2575	1710
TMC147	10	C	8	150	3430	192	14		
TMC85	11	C	9	106	8190	168	15	8115	150
TMC100	11	C	9	106	8040	167	15		
TMC182	12	B	8	150	755	182	16	567.5	375
TMC199	12	B	8	150	380	181	16		
TMC110	13	C	7	212	760	166	17	3280	5040
TMC142	13	C	7	212	5800	165	17		
TMC63	13	C	12	<53	515	162	18	535	40
TMC215	13	C	12	<53	555	161	18		
TMC67	14	C	8	150	5390	173	19	3735	3310
TMC138	14	C	8	150	2080	174	19		
TMC62	29	C	10	75	14200	193	20	15600	2800
TMC171	29	C	10	75	17000	194	20		

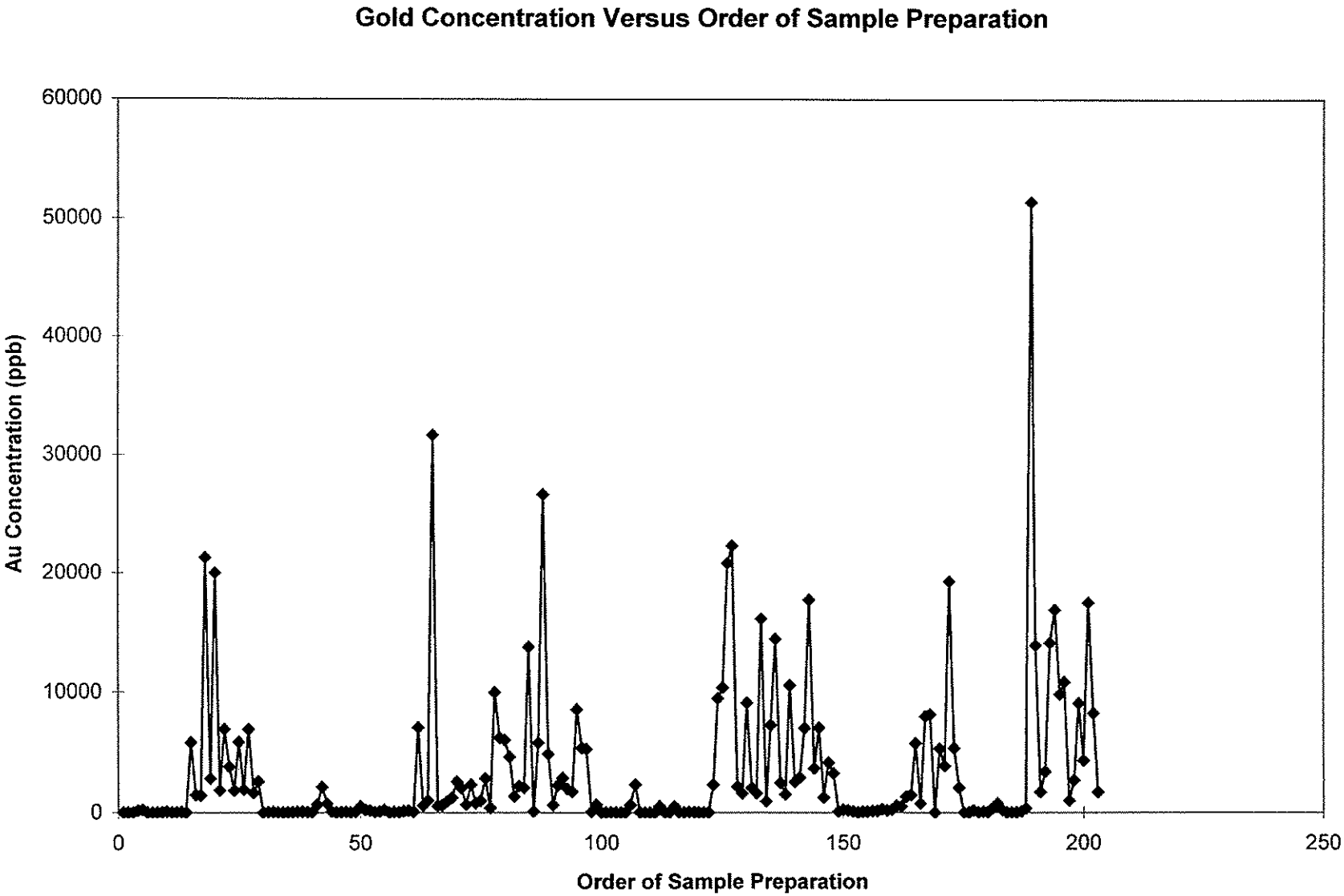
Gold Concentration Versus Order of Sample Preparation
Au Concentration (ppb)
60000
50000
40000
30000
20000
10000
0
0
50
100
150
200
250
Order of Sample Preparation

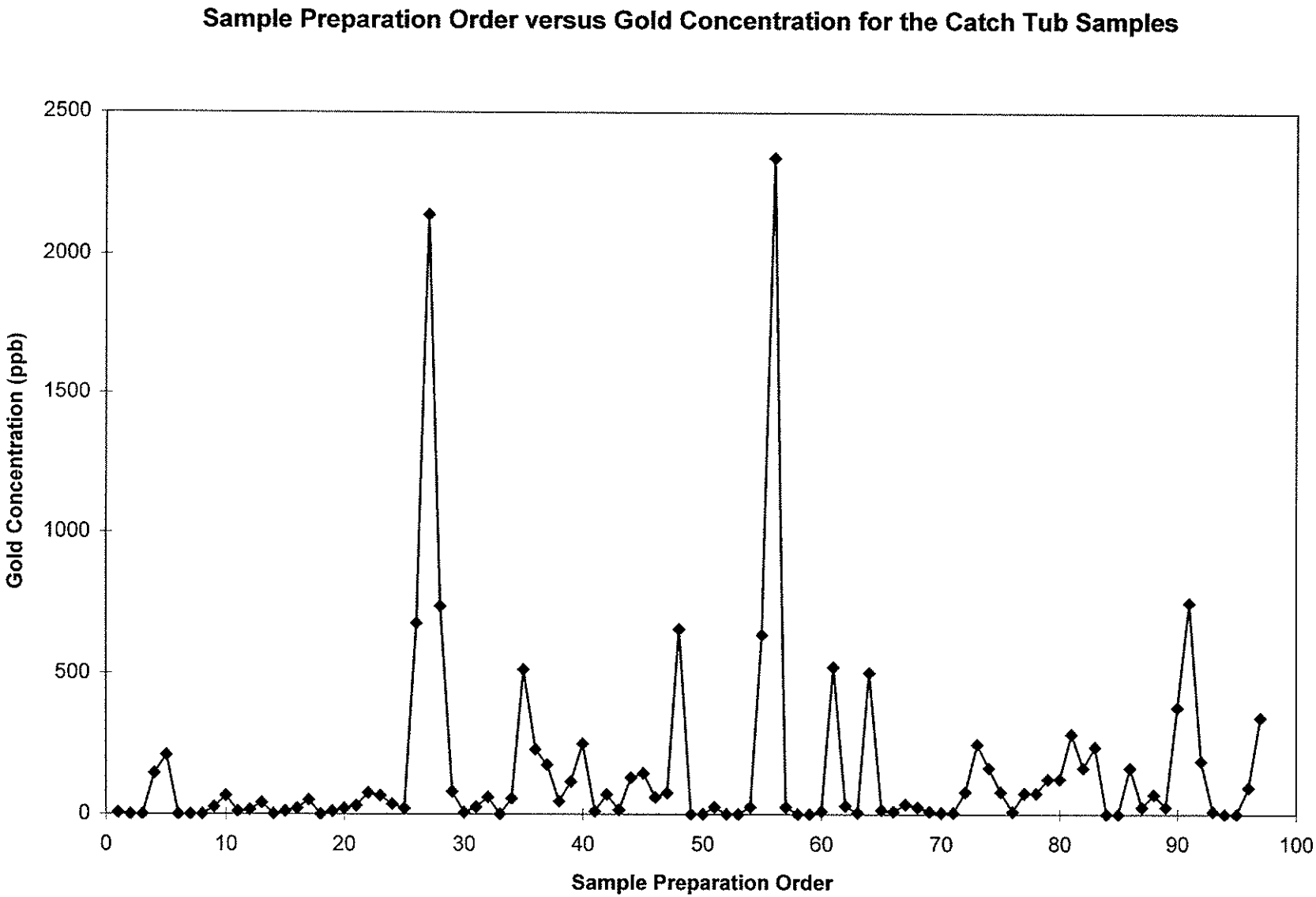
Sample Preparation Order versus Gold Concentration for the Catch Tub Samples
Gold Concentration (ppb)
2500
2000
1500
1000
500
0
0
10
20
30
40
50
60
70
80
90
100
Sample Preparation Order

Sample Preparation Order Versus Gold Concentration For Long-Tom Concentrate Samples

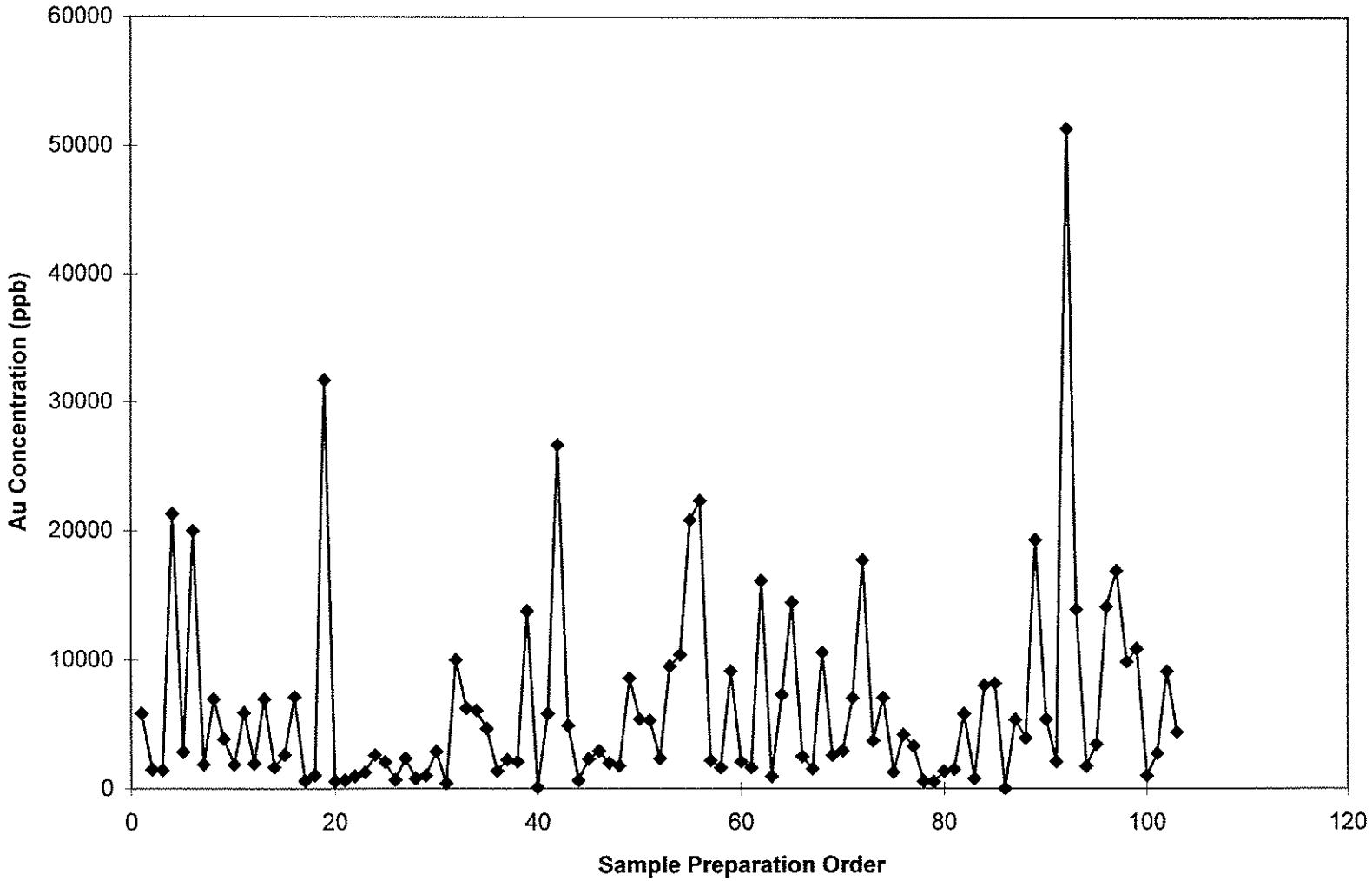

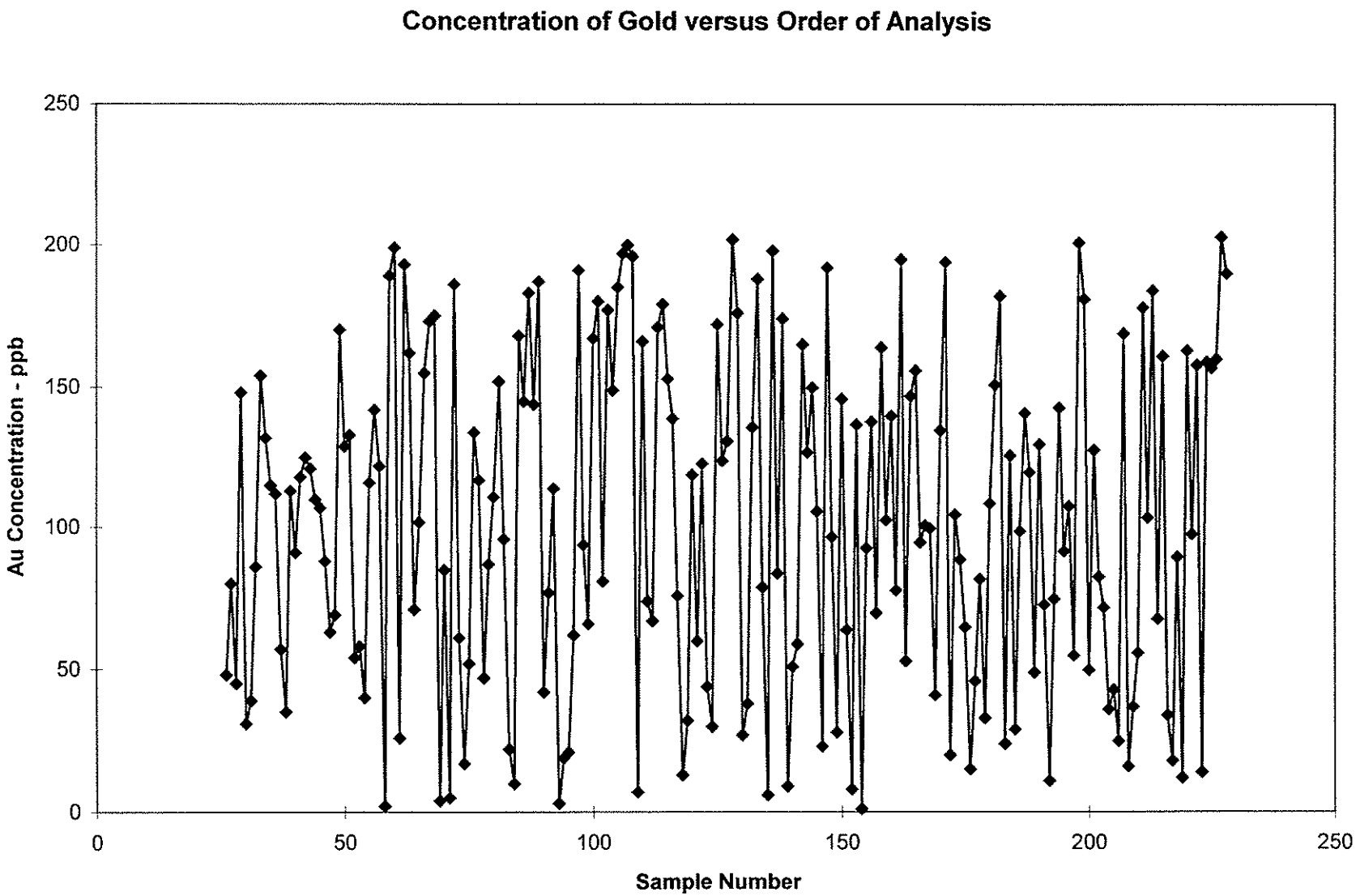
Concentration of Gold versus Order of Analysis
Au Concentration - ppb
Sample Number
0
50
100
150
200
250

APPENDIX G

DETEMINATION OF TOTAL GOLD IN THE SAMPLE

TOTAL GOLD IN CONCETRATE

	Sample #																
Size Fraction	1	2	3	4	5	6	7	8	9	10	11	12	13	14	15	16	AVERAGE
(microns)	MILLIGRAMS																
212-425	18.958206	16.741884	3.962648	21.6174	5.4106	16.4182	3.9889	22.2625	15.4234	15.1646	25.4446	45.0874	10.2966	26.5003	8.29735	12.0885	17.2300987
150-212	4.750815	0.047378	0.320994	4.29098	1.5267	1.82701	1.00449	2.36327	1.4291	4.84286	4.47773	2.06736	4.27439	0.57677	0.85506	1.61692	2.45509105
106-150	1.895875	0.352920	0.602919	0.11214	0.0009	2.2591	0.26729	0.58306	0.43636	1.86616	0.30073	0.35728	1.32583	0.59789	0.28065	0.479	0.68673915
75-106	1.069380	0.091485	0.074433	0.05337	0.08972	0.33427	0.18123	0.18519	0.1387	0.86499	0.09966	0.14865	0.37531	0.25708	0.02617	0.3526	0.25968088
53-75	0.219889	0.034407	0.042172	0.04162	0.03238	0.27998	0.10923	0.03435	0.0576	0.238	0.04439	0.06359	0.20475	0.09731	0.03535	0.19064	0.11595909
<53	0.052589	0.058247	0.040950	0.04423	0.03761	0.05404	0.18962	0.08522	0.09782	1.16434	0.08168	0.11053	0.15919	0.1094	0.05027	0.54975	0.2908616
Total	26.946754	17.326321	5.044115	26.1598	7.09791	21.1726	5.74077	25.5136	17.583	24.141	30.4488	47.8348	16.6361	28.1387	9.54486	15.2774	21.0384304

TOTAL GOLD IN CATCH TUB

	Sample #																
Size Fraction	1	2	3	4	5	6	7	8	9	10	11	12	13	14	15	16	AVERAGE
(microns)	MILLIGRAMS																
212-425	0.27376	0.02125	0.03963	0.01278	0.04348	0.01596	0.01908	0.01226	0.00805	0.07756	4.26372	0.01959	0.01929	0	0.20605	0.01462	0.33136464
150-212	7.80386	2.98029	0.09889	0.09382	0.89365	0.20463	0.25185	0.32922	0.01761	0.02289	5.9193	0.14092	0.06425	1.45622	0.06367	1.01988	0.83850253
106-150	0.04218	0.01650	0.00359	0.0018	0.03014	0.0187	0.78482	0.00402	0.17347	0.1505	1.84338	0.02738	0.01211	0.00588	0.05326	0.0087	0.20304218
75-106	0.19404	0.01936	0.05395	0.01498	0.03925	0.02673	0.12349	0.00298	0.04025	0.01803	0.80628	0.05738	0.02623	0.00163	0.06068	0.01963	0.08410313
53-75	0.00522	0.13483	0.08655	0.01519	0.06307	0.02165	0.21436	0.00249	0.26629	0.13603	0.34687	0.00794	0.00148	0.00146	0.02643	0.04243	0.07557896
<53	0.22451	0.16954	0.23753	0.19814	0.7738	0.22607	0.64388	0.2478	1.03035	0.80906	0.67207	0.40372	0.03472	0.18838	0.39646	0.29365	0.44450133
TOTAL			0.52013	0.33671	1.84339	0.51373	2.03748	0.59876	1.53601	1.21408	13.8516	0.65692	0.15808	1.65358	0.80655	1.39891	1.97709277

TOTAL GOLD < 425 MICRONS IN SAMPLE

	Sample #																
Size Fraction	1	2	3	4	5	6	7	8	9	10	11	12	13	14	15	16	AVERAGE
(microns)	MILLIGRAMS																
212-425	19.23197057	16.76313329	4.00227	21.6302	5.45408	16.4341	4.00799	22.2747	15.4314	15.2422	29.7083	45.107	10.3159	26.5003	8.5034	12.1031	17.5614633
150-212	12.55467455	3.027669333	0.41988	4.3848	2.42034	2.03164	1.25634	2.69249	1.44671	4.86575	10.397	2.20828	4.33863	2.03299	0.91873	2.6368	3.29359358
106-150	1.938058923	0.369420766	0.60651	0.11394	0.03104	2.27781	1.05211	0.58708	0.60983	2.01666	2.14411	0.38466	1.33794	0.60377	0.33391	0.4877	0.88978134
75-106	1.263415228	0.110849294	0.12838	0.06835	0.12897	0.361	0.30472	0.18817	0.17895	0.88302	0.90593	0.20603	0.40154	0.25871	0.08686	0.37223	0.343784
53-75	0.225112004	0.169238754	0.12872	0.05681	0.09545	0.30163	0.32358	0.03684	0.32389	0.37403	0.39126	0.07153	0.20623	0.09877	0.06178	0.23308	0.19153805
<53	0.277103994	0.227785608	0.27848	0.24238	0.81141	0.28011	0.8335	0.33302	1.12817	1.9734	0.75375	0.51424	0.1939	0.29778	0.44673	0.8434	0.73536293
TOTAL	35.49033527	20.66809705	5.56425	26.4965	8.9413	21.6863	7.77825	26.1123	19.119	25.3551	44.3004	48.4918	16.7941	29.7923	10.3514	16.6763	23.0155232

CONCENTRATION OF GOLD IN SAMPLE

	ppb																
Size Fraction	1	2	3	4	5	6	7	8	9	10	11	12	13	14	15	16	AVERAGE
(microns)																	
212-425	1510	3068	426	2800	540	1719	368	3017	2886	1619	3209	4037	966	2582	894	1388	1889
150-212	3132	473	94	1341	512	523	303	644	561	1766	3212	591	1324	721	180	1301	934
106-150	1814	587	315	117	10	1033	771	281	323	901	816	308	1378	472	178	267	512
75-106	1496	109	124	44	64	253	321	123	127	711	557	216	561	298	99	437	281
53-75	406	772	167	73	75	267	304	29	209	353	254	88	266	130	143	317	191
<53	90	98	92	95	256	61	206	105	257	686	138	157	55	94	179	401	199

Concentration of Au < 425 microns in the Total Sample (ppb)

202	156	31	148	54	136	53	197	120	181	289	294	104	184	64	104	140

Concentraion of Au < 425 Microns in Portion of Sample less than 425 microns (ppb)

1593	1287	270	1572	367	951	346	1330	1113	1295	1867	2286	842	1554	510	1025	1095

DETERMINATION OF GOLD CONTENT IN LOG-TOM CONCENTRATE																		
	Sample #	1	2	3	4	5	6	7	8	9	10	11	12	13	14	15	16	AVERAGE
TOTAL MASS OF EACH SIZE FRACTION IN CONCENTRATE																		
Microns	Phi	grams																
212-425	1.25 - 2.25	1788.51	1213.18	1478.60	1334.41	1401.71	1579.43	1356.77	1250.70	1322.76	1659.15	1135.92	1378.82	1029.66	992.52	1264.84	1410.56	1328.28
150-212	2.25 - 2.75	672.92	498.72	513.59	589.42	666.68	733.74	790.94	718.32	816.63	465.66	471.34	802.86	706.51	252.97	863.70	432.91	630.38
106-150	2.75 - 3.25	130.75	158.26	130.22	69.65	90.10	333.94	175.85	82.47	150.99	89.29	137.95	154.00	163.38	102.73	98.13	89.20	133.42
75-106	3.25 - 3.75	68.55	44.41	54.73	57.08	49.57	90.10	97.70	44.41	69.70	40.61	61.90	72.16	60.34	52.68	66.26	66.78	63.14
53-75	3.75 - 4.25	31.73	20.98	16.22	21.79	18.09	47.86	42.50	18.77	30.97	11.90	31.48	22.55	35.18	25.54	24.38	27.51	26.77
<53	+4.25	77.91	73.73	65.52	77.60	73.74	92.38	134.96	83.55	105.18	36.73	66.41	54.18	68.32	42.24	93.96	77.43	76.59
Total mass of < 425 um		2770.37	2009.28	2258.88	2149.95	2299.89	2877.45	2598.72	2198.22	2496.23	2303.34	1905.00	2484.57	2063.39	1468.68	2411.27	2104.39	2258.57
Total Mass of Concentrate		7654.88	7240.66	6921.20	7588.90	7631.24	9896.02	6831.05	7193.23	10177.26	7152.42	7013.63	7693.33	5961.85	6008.21	7406.90	7812.08	7520.52
CONCENTRATION OF GOLD IN EACH SIZE FRACTION IN THE ANALYTICAL PORTION (ppb)																		
Microns	Phi																	
212-425	1.25 - 2.25	10600	13800	2680	16200	3860	10395	2940	17800	11660	9140	22400	32700	10000	26700	6560	8570	12972
150-212	2.25 - 2.75	7060	95	625	7280	2290	2490	1270	3290	1750	10400	9500	2575	6050	2280	990	3735	3895
106-150	2.75 - 3.25	14500	2230	4630	1610	10	6765	1520	7070	2890	20900	2180	2320	8115	5820	2860	5370	5147
75-106	3.25 - 3.75	15600	2060	1360	935	1810	3710	1855	4170	1990	21300	1610	2060	6220	4880	395	5280	4113
53-75	3.75 - 4.25	6930	1640	2600	1910	1790	5850	2570	1830	1860	20000	1410	2820	5820	3810	1450	6930	4332
<53	+4.25	675	790	625	570	510	585	1405	1020	930	31700	1230	2040	2330	2590	535	7100	3798
MASS OF GOLD IN THE CONCENTRATE																		
		MILLIGRAMS																
Microns	Phi																	
212-425	1.25 - 2.25	18.958206	16.741884	3.962648	21.61744	5.410601	16.41817	3.988904	22.26246	15.42338	15.16463	25.44461	45.08741	10.2966	26.50028	8.29735	12.0885	17.23010
150-212	2.25 - 2.75	4.7508152	0.0473784	0.320994	4.290978	1.526697	1.827013	1.004494	2.363273	1.429103	4.842864	4.47773	2.067365	4.274386	0.576772	0.855063	1.616919	2.45509
106-150	2.75 - 3.25	1.895875	0.3529198	0.602919	0.112137	0.000901	2.259104	0.267292	0.583063	0.436361	1.866161	0.300731	0.35728	1.325829	0.597889	0.280652	0.479004	0.68674
75-106	3.25 - 3.75	1.06938	0.0914846	0.074433	0.05337	0.089722	0.334271	0.181234	0.18519	0.138703	0.864993	0.099659	0.14865	0.375315	0.257078	0.026173	0.352598	0.25968
53-75	3.75 - 4.25	0.2198889	0.0344072	0.042172	0.041619	0.032381	0.279981	0.109225	0.034349	0.057604	0.238	0.044387	0.063591	0.204748	0.097307	0.035351	0.190644	0.11596
<53	+4.25	0.05258925	0.0582467	0.04095	0.044232	0.037607	0.054042	0.189619	0.085221	0.097817	1.164341	0.081684	0.110527	0.159186	0.109402	0.050269	0.549753	0.29086
		MILLIGRAMS																
Total Mass of Au		26.9467544	17.3263207	5.044115	26.15978	7.097909	21.17259	5.740767	25.51356	17.58297	24.14099	30.4488	47.83483	16.63606	28.13873	9.544858	15.27742	20.02381
in Size fractions Less																		
Than 425 mincrons																		
		ppb																
Overall Grade for		9727	8623	2233	12168	3086	7358	2209	11606	7044	10481	15984	19253	8062	19159	3958	7260	8866
Fraction Less than																		
425 microns																		

MASS OF EACH SIZE FRACTION IN THE TOTAL CATCH TUB SAMPLE																		
		KILOGRAMS																
Microns	Phi	1	2	3	4	5	6	7	8	9	10	11	12	13	14	15	16	AVERAGE
212-425	1.25 - 2.25	10.9506	4.2499	7.9251	6.3919	8.6964	7.9790	9.5423	6.1324	4.0248	7.7562	8.1214	9.7947	9.6468	9.2690	8.2421	7.3098	7.9166
150-212	2.25 - 2.75	3.3350	5.9016	3.9555	2.6806	4.0620	3.1481	3.3580	3.4654	1.7606	2.2888	2.7660	2.9357	2.5700	2.5683	4.2444	1.5936	2.9569
106-150	2.75 - 3.25	0.9374	0.4715	1.7940	0.9006	3.0138	1.8702	1.1891	2.0078	1.7347	2.1501	2.4910	1.0953	0.8074	1.1764	1.7752	1.7391	1.6961
75-106	3.25 - 3.75	0.7761	0.9682	0.9809	1.4977	1.9625	1.3363	0.8516	1.4910	1.3416	1.2018	1.5656	0.8827	0.6557	0.8152	0.8091	0.7851	1.1555
53-75	3.75 - 4.25	0.5223	0.1983	0.7526	0.7593	1.2615	1.0824	1.0207	1.2437	1.5217	1.0464	1.5081	0.7943	0.7409	0.7323	0.4066	0.7072	0.9698
<53	+4.25	2.9935	2.2605	2.9691	2.4768	3.0952	4.5214	3.9023	3.0975	4.2931	2.8388	5.3765	3.2297	3.4718	3.1396	2.4028	2.0251	3.3457
Total Mass <425 um		19.5150	14.0499	18.3773	14.7069	22.0915	19.9374	19.8641	17.4378	14.6765	17.2821	21.8287	18.7325	17.8926	17.7009	17.8802	14.1599	18.0406
Total Catch tub Sample mass		168.4000	125.6000	174.3500	170.9000	157.0500	149.2500	139.9000	125.5500	148.9500	133.2000	146.1700	157.0000	155.0500	155.6000	153.2000	152.2000	151.3121
CONCENTRATION OF GOLD IN EACH SIZE FRACTION IN THE ANALYTICAL PORTION (ppb)																		
Microns	Phi																	
212-425	1.25 - 2.25	25	5	5	2	5	2	2	2	2	10	525	2	2	0	25	2	42
150-212	2.25 - 2.75	2340	505	25	35	220	65	75	95	10	10	2140	48	25	567	15	640	284
106-150	2.75 - 3.25	45	35	2	2	10	10	660	2	100	70	740	25	15	5	30	5	120
75-106	3.25 - 3.75	250	20	55	10	20	20	145	2	30	15	515	65	40	2	75	25	73
53-75	3.75 - 4.25	10	680	115	20	50	20	210	2	175	130	230	10	2	2	65	60	78
<53	+4.25	75	75	80	80	250	50	165	80	240	285	125	125	10	60	165	145	133
MASS OF GOLD IN TOTAL CATCH TUB SAMPLE																		
		milligrams																
Microns	Phi																	
212-425	1.25 - 2.25	0.273764574	0.021249291	0.03962572	0.012784	0.043482	0.015958	0.0190845	0.0122647	0.00805	0.0775624	4.2637246	0.0195894	0.0192937	0	0.2060518	0.01462	0.3313646
150-212	2.25 - 2.75	7.803859351	2.980290933	0.09888828	0.093821	0.893647	0.204627	0.2518488	0.3292166	0.017606	0.0228881	5.9193033	0.140915	0.0642488	1.4562228	0.063666	1.019885	0.8385025
106-150	2.75 - 3.25	0.042183923	0.016500966	0.00358801	0.001801	0.030138	0.018702	0.7848219	0.0040157	0.173471	0.1505035	1.8433766	0.0273836	0.0121115	0.0058818	0.0532564	0.008695	0.2030422
75-106	3.25 - 3.75	0.194035228	0.019364694	0.05395158	0.014977	0.03925	0.026725	0.1234886	0.002982	0.040249	0.0180267	0.8062755	0.0573787	0.0262261	0.0016304	0.0606844	0.019628	0.0841031
53-75	3.75 - 4.25	0.005223104	0.134831554	0.08655147	0.015187	0.063074	0.021648	0.2143567	0.0024874	0.266289	0.1360345	0.3468701	0.0079426	0.0014818	0.0014647	0.0264312	0.042433	0.075579
<53	+4.25	0.224514744	0.169538908	0.23752877	0.198143	0.773804	0.226071	0.643883	0.2477981	1.030348	0.8090616	0.6720672	0.4037155	0.0347183	0.1883783	0.3964614	0.293646	0.4445013
		milligrams																
Total Mass of Au		8.543580924	3.341776347	0.52013383	0.336713	1.843395	0.513731	2.0374835	0.5987646	1.536014	1.2140769	13.851617	0.6569249	0.1580801	1.653578	0.8065512	1.398906	1.93757
in Size fractions Less																		
Than 425 mincrons																		
		ppb																
Overall Grade of Au <425 um		438	238	28	23	83	26	103	34	105	70	635	35	9	93	45	99	107
in the portion of the catch tub																		
< 425 microns																		
		ppb																
Overall grade of Au < 425 um																		
in the catch tub		51	27	3	2	12	3	15	5	10	9	95	4	1	11	5	9	13

CALCULATION OF NUMBER OF PARTICLES IN A 30 GRAM SUBSAMPLE FOR THE 75-106 MICRON SIZE FRACTION IN THE LONG-TOM CONCENTRATE																	
assumption: density of gold 17 g/cubic cm																	
assumption: Corey Grain Shape Factor for this size Fraction is .2																	
Volume of a particle of shits size fraction	5.94E-07	cubic cm															
Logarithmic average diameter of grain	89.16	microns															
Mass of one particle of Gold	1.01E-05	grams															
Sample #	1	2	3	4	5	6	7	8	9	10	11	12	13	14	15	16	Average
Concentration of gold in Analytical Portion (ppb)	15600	2060	1360	935	1810	3710	1855	4170	1990	21300	1610	2060	6220	4880	395	5280	4112.5
Mass of Analytical Portion (grams)	30	30	30	29.76	30	30	30	30	30	30	30	30	30	30	30	30	30
Mass of Gold in Analytical Portion (GRAMS)	0.000468	6.18E-05	4.08E-05	2.78E-05	5.43E-05	0.000111	5.57E-05	0.000125	5.97E-05	0.000639	4.83E-05	6.18E-05	0.000187	0.000146	1.19E-05	0.000158	0.000123
Number of Particles of Au in sample	46.36264	6.122246	4.041871	2.756556	5.379255	11.02599	5.512993	12.39309	5.914208	63.30283	4.784862	6.122246	18.48562	14.50318	1.173926	15.69197	12.2222
CALCULATION OF NUMBER OF PARTICLES IN A 30 GRAM SUBSAMPLE FOR THE 53-75 MICRON SIZE FRACTION IN THE LONG-TOM CONCENTRATE																	
assumption: density of gold 17 g/cubic cm																	
assumption: Corey Grain Shape Factor for this size Fraction is .2																	
Volume of a particle of shits size fraction	2.1E-07	cubic cm															
Logarithmic average diameter of grain	63.05	microns															
Mass of one particle of Gold	3.57E-06	grams															
Sample #	1	2	3	4	5	6	7	8	9	10	11	12	13	14	15	16	Average
Concentration of gold in Analytical Portion (ppb)	6930	1640	2600	1910	1790	5850	2570	1830	1860	20000	1410	2820	5820	3810	1450	6930	4332.143
Mass of Analytical Portion (grams)	30	20.72	16.04	21.52	17.79	30	30	30	18.57	11.76	27.47	22.29	30	30	30	30	30
Mass of Gold in Analytical Portion (GRAMS)	0.000208	3.4E-05	4.17E-05	4.11E-05	3.18E-05	0.000176	7.71E-05	5.49E-05	3.45E-05	0.000235	3.87E-05	6.29E-05	0.000175	0.000114	4.35E-05	0.000208	0.00013
Number of Particles of Au in sample	58.24138	9.519427	11.68301	11.51471	8.920849	49.16481	21.5989	15.37976	9.676138	65.88924	10.85063	17.60907	48.91268	32.02016	12.18615	58.24138	36.40837
CALCULATION OF NUMBER OF PARTICLES IN A 30 GRAM SUBSAMPLE FOR THE -53 MICRON SIZE FRACTION IN THE LONG-TOM CONCENTRATE																	
assumption: density of gold 17 g/cubic cm																	
assumption: Corey Grain Shape Factor for this size Fraction is .2																	
Volume of a particle of shits size fraction	6.7E-09	cubic cm															
Logarithmic average diameter of grain	20	microns															
Mass of one particle of Gold	1.14E-07	grams															
Sample #	1	2	3	4	5	6	7	8	9	10	11	12	13	14	15	16	Average
Concentration of gold in Analytical Portion (ppb)	675	790	625	570	510	585	1405	1020	930	31700	1230	2040	2330	2590	535	7100	3797.857
Mass of Analytical Portion (grams)	30	30	30	30	27.02	30	30	30	30	30	30	30	25.3	24.23	24.23	20.72	30
Mass of Gold in Analytical Portion (GRAMS)	2.0E-05	2.4E-05	1.9E-05	1.7E-05	1.4E-05	1.8E-05	4.2E-05	3.1E-05	2.8E-05	9.5E-04	3.7E-05	6.1E-05	5.9E-05	6.3E-05	1.3E-05	1.5E-04	1.1E-04
Number of Particles of Au in sample	1.8E+02	2.1E+02	1.6E+02	1.5E+02	1.2E+02	1.5E+02	3.7E+02	2.7E+02	2.4E+02	8.3E+03	3.2E+02	5.4E+02	5.2E+02	5.5E+02	1.1E+02	1.3E+03	1.0E+03

CALCULATION OF NUMBER OF PARTICLES INTHE ANALYTICAL PORTION FOR THE 212-425 MICRON SIZE FRACTION IN THE LONG-TOM CONCENTRATE																	
assumption: density of gold 17 g/cubic cm																	
assumption: Corey Grain Shape Factor for this size Fraction is .2																	
Volume of a particle of this size fraction	2.27E-05	cubic cm															
Logarithmic average diameter of grain	300.17	microns															
Mass of one particle of Gold	0.000385	grams															
Sample #	1	2	3	4	5	6	7	8	9	10	11	12	13	14	15	16	Average
Concentration of gold in Analytical Portion (ppb)	10600	13800	2680	16200	3860	10395	2940	17800	11660	9140	22400	32700	10000	26700	6560	8570	12875.31
Mass of Analytical Portion (grams)	30	30	30	30	30	30	30	30	30	30	30	30	30	30	30	30	30
Mass of Gold in Analytical Portion (GRAMS)	0.000318	0.000414	8.04E-05	0.000486	0.000116	0.000312	8.82E-05	0.000534	0.00035	0.000274	0.000672	0.000981	0.0003	0.000801	0.000197	0.000257	0.000386
Number of Particles of Au in sample	0.825577	1.074808	0.208731	1.261731	0.300635	0.809611	0.228981	1.386347	0.908135	0.711866	1.744616	2.546828	0.778847	2.07952	0.510923	0.667471	1.002789
CALCULATION OF NUMBER OF PARTICLES IN A 30 GRAM SUBSAMPLE FOR THE 150-212 MICRON SIZE FRACTION IN THE LONG-TOM CONCENTRATE																	
assumption: density of gold 17 g/cubic cm																	
assumption: Corey Grain Shape Factor for this size Fraction is .2																	
Volume of a particle of shits size fraction	4.75E-06	cubic cm															
Logarithmic average diameter of grain	178.33	microns															
Mass of one particle of Gold	8.08E-05	grams															
Sample #	1	2	3	4	5	6	7	8	9	10	11	12	13	14	15	16	Average
Concentration of gold in Analytical Portion (ppb)	7060	95	625	7280	2290	2490	1270	3290	1750	10400	9500	2575	6050	2280	990	3735	3855
Mass of Analytical Portion (grams)	30	30	30	30	30	30	30	30	30	30	30	30	30	30	30	30	30
Mass of Gold in Analytical Portion (GRAMS)	0.000212	2.85E-06	1.88E-05	0.000218	6.87E-05	7.47E-05	3.81E-05	9.87E-05	5.25E-05	0.000312	0.000285	7.73E-05	0.000182	6.84E-05	2.97E-05	0.000112	0.000116
Number of Particles of Au in sample	2.622317	0.035286	0.232146	2.704032	0.850582	0.924868	0.47172	1.222015	0.650008	3.862903	3.528614	0.95644	2.24717	0.846867	0.367719	1.387302	1.431874
CALCULATION OF NUMBER OF PARTICLES IN A 30 GRAM SUBSAMPLE FOR THE 106-150 MICRON SIZE FRACTION IN THE LONG-TOM CONCENTRATE																	
assumption: density of gold 17 g/cubic cm																	
assumption: Corey Grain Shape Factor for this size Fraction is .2																	
Volume of a particle of shits size fraction	1.68E-06	cubic cm															
Logarithmic average diameter of grain	126.1	microns															
Mass of one particle of Gold	2.86E-05	grams															
Sample #	1	2	3	4	5	6	7	8	9	10	11	12	13	14	15	16	Average
Concentration of gold in Analytical Portion (ppb)																	
Mass of Analytical Portion (grams)	14500	2230	4630	1610	10	6765	1520	7070	2890	20900	2180	2320	8115	5820	2860	5370	5147.143
Mass of Gold in Analytical Portion (GRAMS)	30	30	30	30	30	30	30	30	30	30	30	30	30	30	30	30	30
Number of Particles of Au in sample	0.000435	6.69E-05	0.000139	4.83E-05	3E-07	0.000203	4.56E-05	0.000212	8.67E-05	0.000627	6.54E-05	6.96E-05	0.000243	0.000175	8.58E-05	0.000161	0.000154
	15.23269	2.342682	4.863954	1.691353	0.010505	7.106836	1.596806	7.427247	3.036032	21.95608	2.290155	2.43723	8.525051	6.114085	3.004516	5.641346	5.407228

Total Number of Particles in both portions

CALCULATION OF LOWER LIMIT OF POISSON DISTRIBUTION

Sample	212-425				150-212				106-150				75-106				53-75				<53			
Number	LT+CT	v	LL	st.dev	LT+CT	v	LL	st.dev	LT+CT	v	LL	st.dev	LT+CT	v	LL	st.dev	LT+CT	v	LL	st.dev	LT+CT	v	LL	st.dev
1	0.83	1.66	1.92	1.39	3.49	6.98	6.30	2.51	2.36	4.72	0.36	0.60	6.14	12.29	2.61	1.62	10.03	20.06	5.43	2.33	212.28	424.56	377.26	19.42
2	1.08	2.15	3.00	1.73	0.04	1.00	1.92	1.39	4.86	9.73	1.66	1.29	4.09	8.19	1.37	1.17	11.79	23.58	6.55	2.56	172.03	344.06	302.02	17.38
3	0.21	1.00	1.92	1.39	0.24	1.00	1.92	1.39	1.69	3.38	0.18	0.42	2.77	5.53	0.57	0.76	11.55	23.09	6.55	2.56	159.79	319.58	278.62	16.69
4	1.26	2.52	3.00	1.73	2.72	5.43	5.54	2.35	0.02	1.00	0.00	0.04	5.43	10.86	1.97	1.40	9.08	18.15	4.70	2.17	157.55	315.10	274.88	16.58
5	0.30	1.00	1.92	1.39	0.93	1.86	1.92	1.39	7.12	14.23	3.29	1.81	11.07	22.15	6.17	2.48	49.31	98.63	38.08	6.17	161.48	322.93	281.43	16.78
6	0.81	1.62	1.92	1.39	0.95	1.90	1.92	1.39	2.29	4.58	0.36	0.60	11.03	22.05	6.17	2.48	11.43	22.85	6.17	2.48	11.03	22.05	12.34	3.51
7	0.23	1.00	1.92	1.39	0.50	1.00	1.92	1.39	7.43	14.86	3.29	1.81	12.39	24.79	6.92	2.63	21.60	43.20	14.48	3.81	276.51	553.02	499.46	22.35
8	1.39	2.77	3.00	1.73	1.26	2.51	3.00	1.73	3.14	6.28	0.82	0.90	5.98	11.96	2.29	1.51	10.15	20.31	5.43	2.33	278.60	557.20	503.26	22.43
9	0.91	1.82	1.92	1.39	0.65	1.31	1.92	1.39	22.00	44.00	14.48	3.81	63.32	126.64	50.54	7.11	66.24	132.47	53.23	7.30	8385.13	16770.26	#NUM!	32.00 *
10	0.71	1.43	1.92	1.39	3.87	7.73	7.03	2.65	2.63	5.25	0.57	0.76	5.55	11.09	2.29	1.51	11.17	22.33	6.17	2.48	338.11	676.22	616.68	24.83
11	1.79	3.57	3.91	1.98	4.32	8.65	7.75	2.78	2.45	4.90	0.36	0.60	6.18	12.37	2.61	1.62	17.62	35.24	11.23	3.35	550.54	1101.09	1024.97	32.02
12	2.55	5.09	5.54	2.35	0.97	1.95	1.92	1.39	8.53	17.06	4.34	2.08	18.52	37.03	12.04	3.47	48.92	97.83	37.64	6.14	518.38	1036.75	962.28	31.02
13	0.78	1.56	1.92	1.39	2.26	4.51	4.74	2.18	6.12	12.23	2.61	1.62	14.51	29.02	8.85	2.98	32.03	64.05	23.30	4.83	566.06	1132.13	#NUM!	32.00 *
14	2.08	4.16	4.74	2.18	1.06	2.11	3.00	1.73	3.01	6.03	0.82	0.90	1.22	2.44	0.05	0.23	12.24	24.49	6.92	2.63	131.82	263.64	226.45	15.05
15	0.51	1.03	1.92	1.39	0.37	1.00	1.92	1.39	5.65	11.29	2.29	1.51	15.71	31.43	9.64	3.10	58.38	116.77	46.07	6.79	1313.60	2627.21	#NUM!	45.00 *
16	0.67	1.34	1.92	1.39	1.63	3.25	3.91	1.98	5.53	11.07	2.29	1.51	12.44	24.88	6.92	2.63	37.06	74.13	27.59	5.25	1034.99	2069.98	#NUM!	32.00
Average	1.01	2.01	3.00	1.73	1.58	3.16	3.91	1.98	5.30	10.60	1.97	1.40	12.27	24.54	6.92	2.63	26.16	52.32	18.22	4.27	891.74	1783.48	#NUM!	32.00

CALCULATION OF UPPER LIMIT OF POISSON DISTRIBUTION

Sample	212-425				150-212				106-150				75-106				53-75				<53			
Number	LT+CT	v	UL	st.dev	LT+CT	v	UL	st.dev	LT+CT	v	UL	st.dev	LT+CT	v	UL	st.dev	LT+CT	v	UL	st.dev	LT+CT	v	UL	st.dev
1	0.83	3.66	3.91	2.178041	3.49	8.98	7.75	2.784539	2.36	6.72	6.30	2.509141	6.14	14.29	11.84	3.441278	10.03	22.06	16.96	4.118523	212.28	426.56	237.56078	15.41301
2	1.08	4.15	4.74	1.73082	0.04	2.07	3.00	1.73082	4.86	11.73	9.84	3.136491	4.09	10.19	9.15	3.025478	11.79	25.58	18.83	4.338922	172.03	346.06	195.18813	13.97097
3	0.21	2.42	3.00	2.178041	0.24	2.48	3.00	1.73082	1.69	5.38	5.54	2.352709	2.77	7.53	7.03	2.652087	11.55	25.09	18.83	4.338922	159.79	321.58	181.89124	13.48671
4	1.26	4.52	4.74	1.73082	2.72	7.43	7.03	2.652087	0.02	2.04	3.00	1.73082	5.43	12.86	10.51	3.24238	9.08	20.15	15.71	3.96298	157.55	317.10	179.76089	13.40749
5	0.30	2.60	3.00	1.976705	0.93	3.86	3.91	1.976705	7.12	16.23	13.15	3.626032	11.07	24.15	18.21	4.267026	49.31	100.63	62.17	7.884862	161.46	324.93	183.48848	13.54579
6	0.81	3.62	3.91	1.73082	0.95	3.90	3.91	1.976705	2.29	6.58	6.30	2.509141	11.03	24.05	18.21	4.267026	11.43	24.85	18.21	4.267026	11.03	24.05	18.207513	4.267026
7	0.23	2.46	3.00	2.178041	0.50	3.00	3.00	1.73082	7.43	16.86	13.15	3.626032	12.39	26.79	19.44	4.409372	21.60	45.20	30.83	5.552307	276.51	555.02	305.45713	17.47733
8	1.39	4.77	4.74	1.976705	1.26	4.51	4.74	2.178041	3.14	8.28	7.75	2.784539	5.98	13.96	11.18	3.343802	10.15	22.31	16.96	4.118523	278.60	559.20	307.55579	17.53727
9	0.91	3.82	3.91	1.976705	0.65	3.31	3.91	1.976705	22.00	46.00	30.83	5.552307	63.32	128.64	77.70	8.814895	66.24	134.47	81.01	9.000434	8385.13	16772.26	#NUM!	32
10	0.71	3.43	3.91	2.352709	3.87	9.73	8.46	2.908519	2.63	7.25	7.03	2.652087	5.55	13.09	11.18	3.343802	11.17	24.33	18.21	4.267026	338.11	678.22	369.8427	19.23129
11	1.79	5.57	5.54	2.652087	4.32	10.65	9.15	3.025478	2.45	6.90	6.30	2.509141	6.18	14.37	11.84	3.441278	17.62	37.24	26.10	5.108439	550.54	1103.09	590.68793	24.30407
12	2.55	7.09	7.03	1.976705	0.97	3.95	3.91	1.976705	8.53	19.06	15.07	3.882236	18.52	39.03	27.29	5.223612	48.92	99.83	61.61	7.84937	518.38	1038.75	#NUM!	32
13	0.78	3.56	3.91	2.509141	2.26	6.51	6.30	2.509141	6.12	14.23	11.84	3.441278	14.51	31.02	22.49	4.742644	32.03	66.05	42.98	6.556102	566.06	1134.13	#NUM!	32
14	2.08	6.16	6.30	1.976705	1.06	4.11	4.74	2.178041	3.01	8.03	7.75	2.784539	1.22	4.44	4.74	2.178041	12.24	26.49	19.44	4.409372	131.82	265.64	151.9849	12.32822
15	0.51	3.03	3.91	1.976705	0.37	2.75	3.00	1.73082	5.65	13.29	11.18	3.343802	15.71	33.43	23.70	4.868259	58.38	118.77	72.18	8.495694	1313.60	2629.21	#NUM!	32
16	0.67	3.34	3.91	2.178041	1.63	5.25	5.54	2.352709	5.53	13.07	11.18	3.343802	12.44	26.88	19.44	4.409372	37.06	76.13	48.68	6.976782	1034.99	2071.98	1088.9925	32.99989
Average	1.01	4.01	4.74	0	1.58	5.16	5.54	2.352709	5.30	12.60	10.51	3.24238	12.27	26.54	19.44	4.409372	26.16	54.32	36.08	6.00638	891.74	1785.48	942.20145	30.6953

APPENDIX H

APPENDIX H - LONG-TOM CONCENTRATION OF GOLD

A long-tom is a scaled down version of a sluice, which has been used by miners in North America for over a century to recover gold and other precious minerals. The principle behind the sluice is that heavy minerals will be trapped in the riffles and matting of the run, while less dense minerals will be washed through. The percentage of gold which a long-tom or sluice can recover is an important factor in determining whether mining can be successful. It is also important in determining whether processing through a long-tom is an effective tool for producing a heavy mineral (gold) concentrate for use in sedimentological studies.

LONG-TOM (SLUICE) SETUP

A sluice consists of a metal or wood trough with matting on the bottom which is covered by metal riffles or expanded metal. There are many types of sluices and long-toms, however, the principle variables in any sluice system which have and effect upon gold recovery are:

1. Dimensions of sluice run: length, width, height of sides
2. Type of matting used to catch concentrate: principle types are Cocoanut matting and rubber matting (primarily 3M Nomad matting)
3. Type of riffles or expanded metal: weight, orientation, position sitting.
4. Screen or grading device to restrict grain size passing through sluice
5. Volume of water used
6. Method used to clean long-tom
7. Slope (influences velocity of water and sediments transported)
8. Water/ Solids ratio

Refer to section 3 for figures showing the long-tom configuration used in this sampling program. The run, which was eight feet long and 1 ft wide and had 6 inch high sides, was placed on a 1(vertical) to 2 (horizontal) slope. The run was lined with 8 12"X12" pieces of unbacked, green, 1/4 inch thick, 3M (nomad) matting. Four pieces of light-weight expanded metal were placed over the matting. The expanded metal was held tight to the matting by wooden 1x2's placed along the sides of the sluice run and forced down by wooden wedges under metal plates welded onto the side of the sluice run.

Boulders, cobbles and large pebbles have been found to create turbulence and plug up sluice runs and decrease the effectiveness in recovering gold particles. To prevent the build up of large materials in the sluice run, a screen was used at the top of the long-tom to manually remove larger materials. The metal screen had approximately 1"X 2" mesh, was 36 inch long, by 24 inch wide and was laid on a moderate incline. When a sample was poured out of the buckets over the screen, rock could be selectively removed. Any rocks which became logged in the sluice during processing were removed by hand.

The amount of water used to wash the sample in this program was regulated by valves at a 2" four horse-power Honda pump and was kept as constant as the equipment and operators could manage. Two 1/2 inch garden hoses were used to wash the material through the screen at the top of the sluice. Material then passed into a smaller dump box of the sluice run where a spray bar further washed the material and held back excess material to prevent surges. The amount of water in the sluice run must be sufficient to create adequate vortices over the expanded metal (or riffles) and to prevent concentrated slurries of sediments from passing over the expanded metal. Slurries are similar to debris flows, and prevent heavy minerals from becoming trapped in the expanded metal and matting.

Once a sample was completely sluiced, the entire contents of the sluice concentrate were washed into a 24 inch by 12 inch aluminum bin placed under the end of the sluice. This concentrate was then bagged and saved for later processing.

LONG-TOM RECOVERY

There are many potential reasons why gold may be lost during sluicing, including:

-the floatation of gold particles due to the hydrophobicity of gold

-the large surface area of gold to weight and high turbidity in sluice run preventing flakes of gold from being trapped in the matting and riffles of the long-tom.

-gold trapped in clays adhering to cobbles which are not adequately washed in the sluicing process

- large cobbles, pebbles and angular rocks which knock gold out of the riffles

In Figures H.1A and H.1B the total concentration of gold for each size fraction has been plotted against the percentage of gold in that size fraction recovered in the long-tom. Simple linear regression was used to fit the data. There is insufficient data to determine if statistically significant trends are present or to fit to more complex models. From these plots the following preliminary, but inconclusive, observations can be made:

1. The percentage of gold recovered by the long-tom increases with increasing gold grain size and is erratic for all size fractions less than 212 microns. Table H.1 shows the average and median recoveries of gold for each size fraction.

Figure H.2A: Graphs of Total Concentration in Sample Versus Percentage of Gold Recovered in the Long Tom for Different Size Fractions. Note the change in concentration scale. Lines represent linear regression lines. Insufficient data is available for statistical analysis.

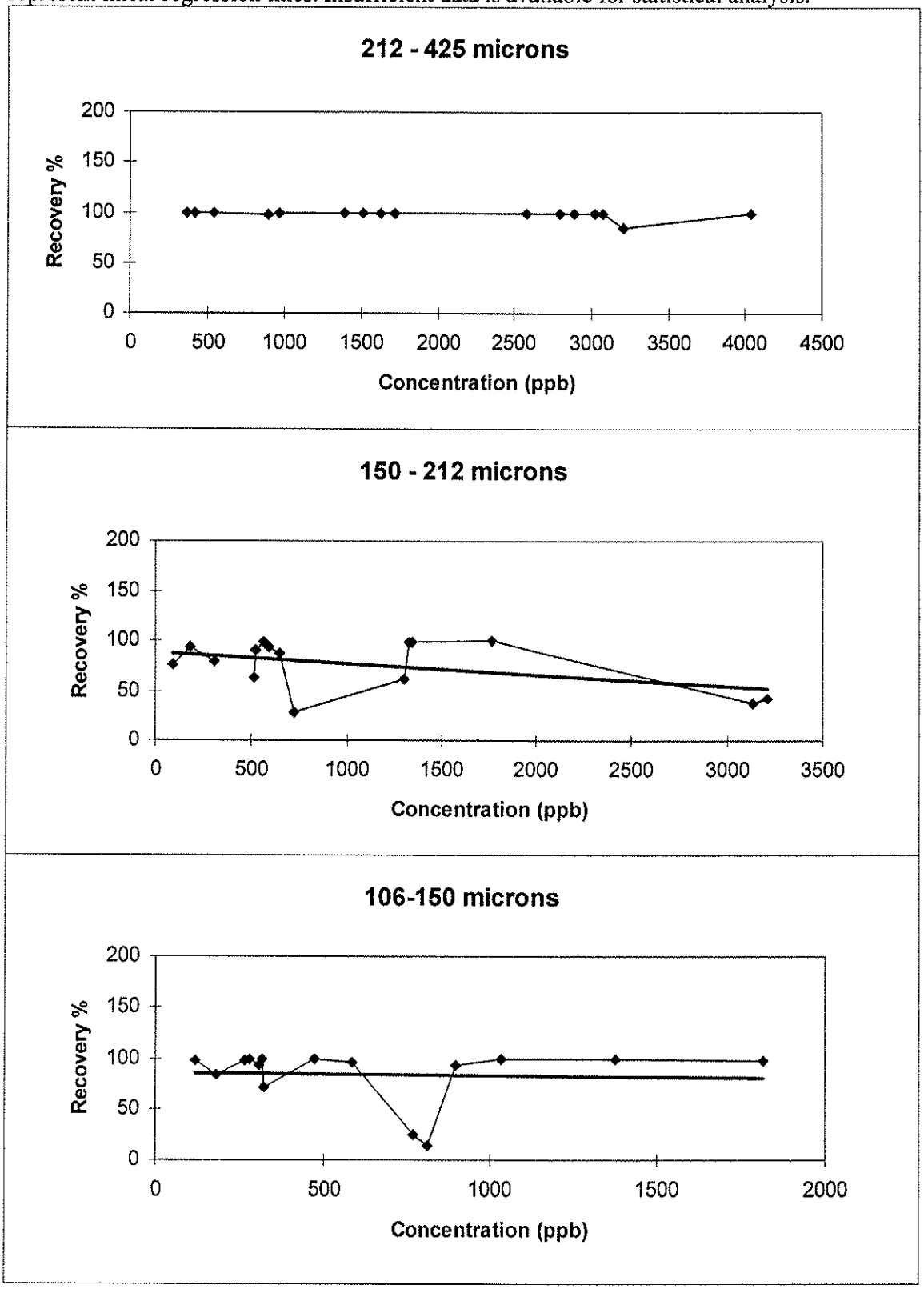

Figure H.2B: Graphs of Total Concentration in Sample Versus Percentage of Gold Recovered in the Long Tom for Different Size Fractions. Note the change in concentration scale. Lines represent linear regression lines. Insufficient data is available for statistical analysis.

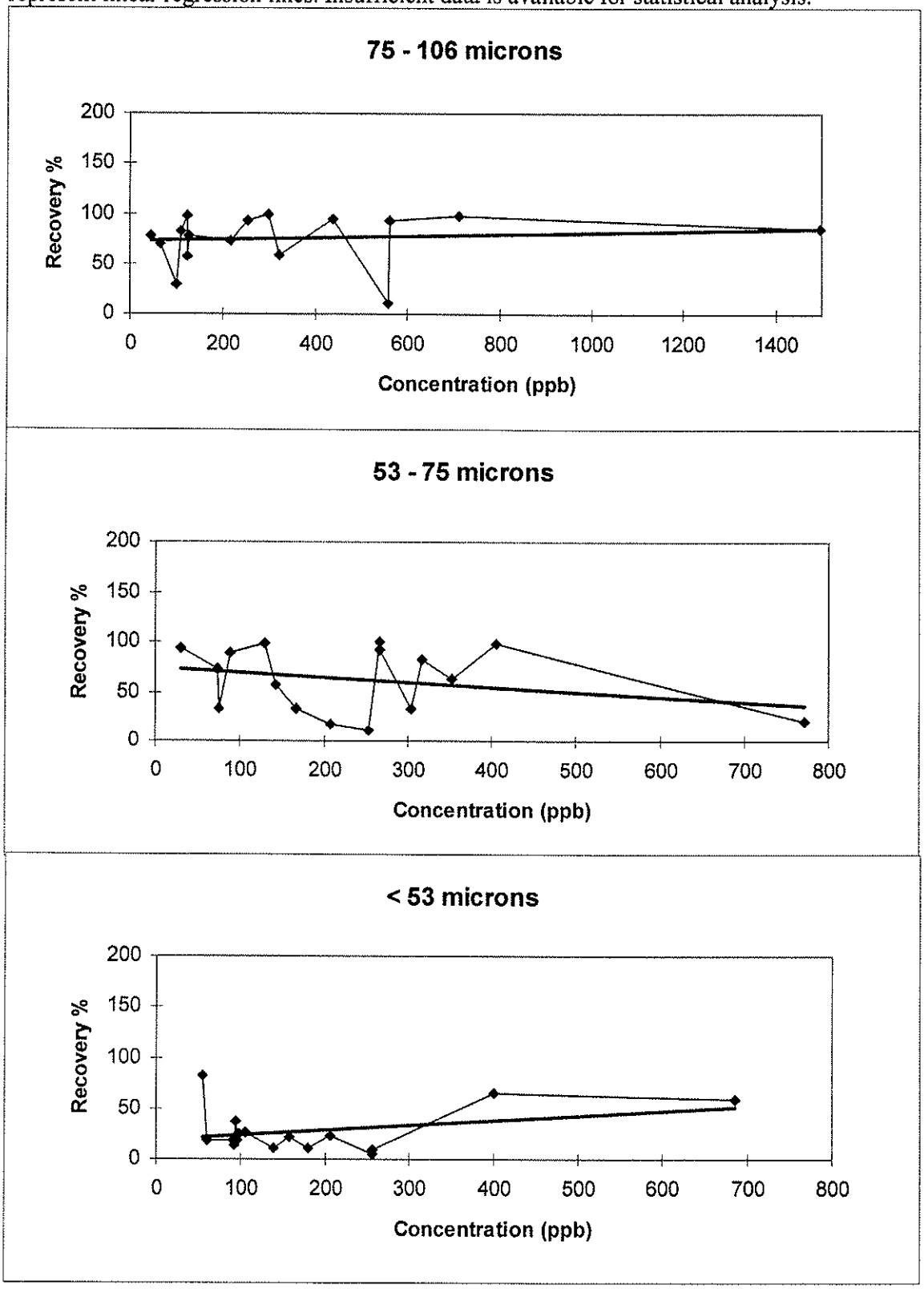

2. The percentage of gold recovered by the long-tom decreases with increasing concentration of gold in the respective size fractions of the total sample. Exceptions are:

- The 212-425 μm size for which the percentage recovery of gold remain relatively constant at an average value of 99 %.
- The <53 μm size fraction, for which recovery appears to increase slightly with increasing concentration; however, the regression line, seen in Figure H.1B (c), shows that this increase is based on two samples only. The other samples have considerably lower percentages of gold recovery and thus this increase is likely due to the erratic nature of the <53 micron sample and does not actually represent and increase in recovery with increasing concentration.
- Plots of recovery versus volume of sample were erratic and showed no obvious changes in recovery with changing volume of sample. Sample sizes were all within 130-185 kilograms and thus there may not be enough range to determine any potential relationships between volume. As a larger sample would also take longer to sluice there is also no obvious relationship between amount of time to process sample.
- No relationship between total gold in the sample and recovery for various size fractions is evident.

IMPLICATIONS

A principle concern in any mining operation is the efficiency of the gold recovery system. If losses are significant, the economic implications are equally significant and in terms of the dollar value, a small percentage of gold lost can mean a great monetary loss. An operating mine should

Using a pre-concentration method, such as the long-tom also has limitations. With this method we must account for the gold which is lost from the long-tom and ends up in the tailings in order to reconstruct the total gold concentration and grain size distribution in the deposit. Considerably higher expense for geochemical analysis and lab preparation of samples is incurred. Also, the variance due to sampling and analysis for the catch-tub and long-tom samples must be added to determine representative error bounds around the calculated gold concentrations. Table H.2 shows the number of particles in the long tom and the catch tub. Error arises from many sources including: sampling the tailings, lab preparation, geochemical analysis, and gold concentrations. Also, the gold which escapes the long-tom tends to be the "flaky" gold, while more spherical and rod shaped particles are trapped. This leads to errors in assumptions that must be made about the shape of particles and the average diameter of particles. For this study, it was assumed that particles in both the catch tub and long-tom concentrate could be approximated by a disc shaped particle (5 thickness : 1 diameter) with a diameter which equaled the logarithmic average of the bounding grain size. This is likely not a valid assumption since particles which escape the long-tom into the catch-tub tend to be a different shape from those which are caught by the long-tom.

In summary, while the use of the long-tom is effective as preconcentration method, the user should be aware of the limitations and potential errors which may arise from any mechanical processing method. The effects of these errors should be considered and , if possible, quantified, when reconstructing gold concentrations in the original sample.